# *Perturbative and non-perturbative studies in low dimensional quantum field theory*

Anna Rebecca Lishman

# Perturbative and Non-Perturbative Studies in Low Dimensional Quantum Field Theory

Anna Rebecca Lishman



A Thesis presented for the degree of
Doctor of Philosophy

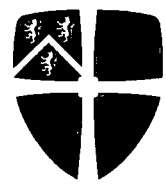

Centre for Particle Theory
Department of Mathematical Sciences
University of Durham
England

September 2007

*Dedicated to*

Mum and Dad

# Perturbative and Non-Perturbative Studies in Low Dimensional Quantum Field Theory

**Anna Rebecca Lishman**

Submitted for the degree of Doctor of Philosophy
September 2007

## Abstract

A relevant perturbation of a conformal field theory (CFT) on the half-plane, by both a bulk and boundary operator, often leads to a massive theory with a particle description in terms of the bulk $S$-matrix and boundary reflection factor $R$. The link between the particle basis and the CFT in the bulk is usually made with the thermodynamic Bethe ansatz effective central charge $c_{\text{eff}}$. This allows a conjectured $S$-matrix to be identified with a specific perturbed CFT. Less is known about the links between the reflection factors and conformal boundary conditions, but it has been proposed that an exact, off-critical version of Affleck and Ludwig's $g$-function could be used, analogously to $c_{\text{eff}}$, to identify the physically realised reflection factors and to match them with the corresponding boundary conditions. In the first part of this thesis, this exact $g$-function is tested for the purely elastic scattering theories related to the $ADET$ Lie algebras. Minimal reflection factors are given, and a method to incorporate a boundary parameter is proposed. This enables the prediction of several new flows between conformal boundary conditions to be made.

The second part of this thesis concerns the three-parameter family of $\mathcal{PT}$-symmetric Hamiltonians $H_{M,\alpha,l} = p^2 - (ix)^{2M} - \alpha(ix)^{M-1} + \frac{l(l+1)}{x^2}$. The positions where the eigenvalues merge and become complex correspond to quadratic and cubic exceptional points. The quasi-exact solvability of the models for $M = 3$ is exploited to explore the Jordan block structure of the Hamiltonian at these points, and the phase diagram away from $M = 3$ is investigated using both numerical and perturbative approaches.

# Declaration

The work in this thesis is based on research carried out at the Department of Mathematical Sciences, the University of Durham, England. No part of this thesis has been submitted elsewhere for any other degree or qualification.

Chapters 1, 2, 3 and Sections 4.1, 4.2, and 5.1-5.4 all contain necessary background material and no claim of originality is made. The remaining work is believed to be original, unless stated otherwise. The work in Chapter 4, apart from the final section, is published in collaboration with Patrick Dorey, Chaiho Rim and Roberto Tateo in [1]. The work in Chapter 5 is done in collaboration with Patrick Dorey, Clare Dunning and Roberto Tateo, and will form a paper currently in preparation [2].

# Acknowledgements

I would like to thank Patrick Dorey for his help and support during my studies. Thanks also to Clare Dunning and Roberto Tateo for helpful explanations, and to Daniel Roggenkamp for useful discussions. I thank EPSRC for financial support and EUCLID for making it possible for me to attend various schools and conferences.

Thanks to my office mates: Mark Goodsell, David Leonard, Lisa Muller, Jen Richardson and Gina Titchener for our many coffee breaks and lunch trips that made my time pass a little quicker than it should. Thanks to my parents, Robert and Jenni, and my sister, Emma, for their support and encouragement over the years. Finally I thank my husband, James, for keeping me sane and making me laugh.

# Contents

# List of Figures

# List of Tables

# Chapter 1

# Introduction

This thesis is concerned with problems in two areas of low dimensional quantum field theory which at first sight seem quite disconnected. The aim of this section is to give a brief outline of the thesis and details of the topics mentioned will be elaborated on in later chapters

The first part of this thesis looks into two dimensional integrable quantum field theory. A question one might ask is why should one study quantum field theory in two dimensions when the real world lives in four? The first reason is that many interesting quantum field theories can only be solved perturbatively and so some information is lost. In two dimensions, there is a special class of theories which have enough symmetry to enable them to be solved exactly (non-perturbatively) and so there is a trade off: the complete picture in two dimensions versus the incomplete picture in four. The hope is to gain an insight into the non-perturbative aspects of the realistic four dimensional theories by studying these exactly solvable (integrable) two dimensional theories.

The prototypes of two dimensional integrable field theories are the conformal field theories (CFTs). These are very interesting theories in their own right as they can be applied to many areas of physics. In string theory, for example, the strings live on a two dimensional world sheet which is described by a CFT. The application of interest in this thesis, however, is statistical lattice models at criticality. Conformal field theories are scale invariant and hence massless, but by perturbing the theory by a relevant perturbation a mass can be introduced. This can also be used to study the statistical models away from the critical point. Far away from this point (in



the infrared, or IR), the massive theory has a particle description in terms of the two dimensional scattering matrices, $S$. These $S$ matrices have a set of constraints imposed by integrability which can be solved for $S$, up to some ambiguity known as the 'CDD factor'. The link between this IR particle description and the UV (short distance) CFT is often made by the thermodynamic Bethe ansatz (TBA) effective central charge $c_{\text{eff}}$, which allows the $S$-matrix conjecture to be identified with a specific perturbed CFT. This is all discussed in Chapter 2.

In many cases it is interesting to study integrable theories on a half plane. This corresponds to open string problems, where different conformal boundary conditions are thought to correspond to different possible branes. There are also quantum impurity problems (for example, the Kondo problem) where the quantum defect can be modelled as a boundary. For statistical models, experimentally it is impossible to produce an infinite lattice so it is important to know the effects of the boundary. Chapter 3 discusses the boundary conditions consistent with conformal symmetry. The discussion of perturbed CFT is then extended to the boundary case, where the theory can now be perturbed by both a relevant bulk and boundary operator. In the IR there is once again a particle description, now with both the bulk $S$-matrices and the boundary scattering matrices, known as reflection factors $R$, in play. The contraints imposed on $R$ by integrability are similar to those on $S$, however there are many more ambiguities in the boundary case, which is to be expected since each bulk theory can have many different integrable boundary conditions. The question, which the first part of this thesis aims to answer, is which of the infinite number of possible reflection factors for a given bulk theory are physically realised, and to which boundary conditions do they correspond?

It is argued, in Chapter 3, that in order to answer this question one needs a boundary analogue of the TBA effective central charge. It is shown that the obvious candidate for this is the $g$-function, defined by Affleck and Ludwig in [3], and the origin of the exact off-critical version of this, recently proposed in [4], is discussed. This exact $g$-function is tested in Chapter 4 for the purely elastic theories related to the $ADET$ Lie algebras.

Chapter 5 is concerned with the second main topic of this thesis, namely one dimensional $\mathcal{PT}$-symmetric quantum mechanics. In conventional quantum mechanics, the Hamiltonian is Hermitian and it is this property that guarantees the reality of the

spectrum. Here, this is weakened to invariance under parity $\mathcal{P}$ and time reversal $\mathcal{T}$. Although this doesn't necessarily lead to an entirely real spectrum, it can be used to prove that all eigenvalues must either be real or appear in complex conjugate pairs. The main focus of Chapter 5 is on the three-parameter family of Hamiltonians

$$H_{M,\alpha,l} = p^2 - (ix)^{2M} - \alpha(ix)^{M-1} + \frac{l(l+1)}{x^2} \tag{1.0.1}$$

and in particular, on the exceptional points which occur when complex eigenvalues are formed in the spectrum.

The connection between these two seemingly very different topics is made with the ODE/IM correspondence. This provides a link between functional relations in integrable models and spectral problems in ordinary differential equations and, as shown in Chapter 5, it can be used to prove the reality of the spectrum of $H_{M,\alpha,l}$ for certain regions of the parameter space.

# Chapter 2

# Techniques in Integrability

The integrable quantum field theories of interest in this thesis are given by certain perturbations of two dimensional conformal field theories. In this chapter, conformal field theory is introduced and the effect of perturbing the theory by a relevant field is examined. Such a perturbation can result in a massive integrable theory in certain cases. These theories have an $S$ matrix description and the method which allows the $S$ matrix of a perturbed theory to be linked to the original CFT is described. Finally, a curious link between functional relations of integrable models and spectral problems of ODEs is presented, which will be used, in the context of spectral problems, in Chapter 5.

As mentioned in Chapter 1, conformal field theories have applications in many areas of physics, but it is the area of statistical lattice models, near criticality, that is particularly relevant here. This chapter therefore begins with a brief overview of statistical mechanics which follows the presentation given by Di Francesco et. al. in [5] and Cardy in [6].

## 2.1 Statistical Mechanics

Statistical mechanics is the study of complex physical systems where the exact states cannot be specified. The so called macrostate of the system is characterised by physical observables such as temperature and magnetisation, whereas the microstate is specified by the quantum numbers of the particles, or spin configuration on the lattice for discrete models. There will be several microstates corresponding to each

macrostate and the basic idea of statistical mechanics is that any physical property can be thought of as a statistical average over the relevant collection of microstates.

The statistical models of interest in this thesis are the discrete lattice models, the most famous of which is the two-dimensional Ising model. This can be defined on an $N$ site square lattice of spacing $a$, with a spin $\sigma_i$, taking the value $\pm 1$, assigned to each site. The energy of a specific configuration of spins is given by the Hamiltonian

$$H = -J \sum_{\langle ij \rangle} \sigma_i \sigma_j - h \sum_i \sigma_i \,. \tag{2.1.1}$$

The notation $\langle ij \rangle$ indicates that the summation is taken over pairs of nearest-neighbour lattice sites. The first term, with coupling $J$, represents a ferromagnetic interaction between neighbouring spins and the second term represents the interaction with an external magnetic field $h$.

The probability of a particular configuration with energy $E_i$ at temperature $T$ is given by the Boltzmann distribution:

$$P_i = \frac{1}{Z} e^{-E_i/k_B T} \tag{2.1.2}$$

where $k_B$ is the Boltzmann constant. The normalisation, $Z$, is called the partition function and is given by the sum over all configurations:

$$Z = \sum_i e^{-E_i/k_B T} \,. \tag{2.1.3}$$

This is a key function in statistical mechanics as it encodes many of the thermodynamic quantities. For example, the free energy of the system, $F$, is given by

$$F = -k_B T \ln Z \,. \tag{2.1.4}$$

The magnetisation $M$, which is the mean value of a single spin, is

$$M = -\frac{1}{N} \frac{\partial F}{\partial h} \tag{2.1.5}$$

and the magnetic susceptibility, which indicates how the magnetisation responds to a small external field is

$$\chi = \left. \frac{\partial M}{\partial h} \right|_{h=0} \,. \tag{2.1.6}$$

The heat capacity at constant volume is also related to the free energy:

$$C = -k_B T \frac{\partial^2 F}{\partial T^2} \tag{2.1.7}$$

and the specific heat is defined as the heat capacity per unit volume. These properties will all vary with the Boltzmann distribution, the fluctuations being of order $1/\sqrt{N}$. To avoid any problems that may arise with the finite lattice, the *thermodynamic limit*, $N \to \infty$ will be taken, in which these fluctuations disappear and the quantities above can be considered as exact variables.

### 2.1.1 Critical Phenomena

Consider the Ising model with no external magnetic field, i.e. with $h = 0$. At low temperatures, it is energetically favourable for the spins to align and so the material is said to be spontaneously magnetised. The lowest energy configuration, at zero temperature, will be doubly degenerate: the spins will either all point up $(+1)$ or all point down $(-1)$. Assume for now that all the spins are pointing up. As the temperature increases some of the spins will use the additional energy to change direction so pockets of down spins will occur. The overall dominating spin will still be up but the spontaneous magnetisation will be reduced. Domains of down spin of all sizes will occur, up to some maximum size. The average domain size is known as the correlation length $\xi$.

As the temperature increases the domains of down spin, and hence the correlation length, continue to grow. At a specific temperature, known as the critical temperature $T_c$, the correlation length becomes infinite. At this point, although the magnetisation is continuous, its derivative with respect to the magnetic field, the susceptibility $\chi$, diverges. The system therefore undergoes a second order phase transition at this point. As the temperature is increased above $T_c$ there will be domains of both up and down spin, but neither will dominate overall and the spontaneous magnetisation will be lost.

Close to this critical point, many of the properties of the model simplify greatly. Instead of depending on the spin configurations they have a power law dependence on the distance from the critical point in the phase space, i.e. on $|T - T_c|$ or $h$. This is the case for the magnetisation, susceptibility and heat capacity. The pair correlation function, $\Gamma(i - j) = \langle \sigma_i \sigma_j \rangle - \langle \sigma_i \rangle \langle \sigma_j \rangle$, near this critical temperature, has a power law dependence on the distance between each pair of spins. The exponents of these power laws, known as critical exponents, are given in table 2.1.

| Critical Exponent | Property | Exponent Value |
|---|---|---|
| $\alpha$ | $C \propto (T - T_c)^{-\alpha}$ | 0 |
| $\beta$ | $M \propto (T_c - T)^{\beta}$ | 1/8 |
| $\gamma$ | $\chi \propto (T - T_c)^{-\gamma}$ | 7/4 |
| $\delta$ | $M \propto h^{1/\delta}$ | 15 |
| $\nu$ | $\xi \propto (T - T_c)^{-\nu}$ | 1 |
| $\eta$ | $\Gamma(i - j) \propto \lvert i - j \rvert^{-\eta}$ | 1/4 |

Table 2.1: Critical exponents for the two-dimensional Ising model

### 2.1.2 Renormalisation Group

A remarkable fact in statistical mechanics is that all models fall into relatively few universality classes, which are characterised by their critical exponents. One of the main aims is therefore to find the critical exponents of a model and so determine its universality class. The renormalisation group provides a method of doing this by exploring the model close to the critical point.

Here the real space, or block-spin, renormalisation of the Ising model will be discussed, following [6]. The general idea is that the physical properties of the system described above are long ranging, so if some of the microscopic detail of the model is lost, through coarse-graining, these properties should remain unchanged.

To implement this coarse-graining one can perform a block spin transformation: group the lattice into $3 \times 3$ blocks and assign to each a block spin $\sigma' = \pm 1$ to indicate whether the spins are predominantly up or down, as shown in the figure 2.1. The resulting lattice must now be rescaled by a factor of 3 so that the blocks are the size of the original lattice spacing. The result of this is that the correlation length reduces by a factor of the lattice spacing. At the critical point, since the correlation length is infinite, no matter how many times this transformation is applied, the physical properties will remain unchanged. This, however, is not the case away from this point. For $T < T_c$, this procedure acts to decrease the size of the domains of down spin so the system becomes more ordered. Similarly, for $T > T_c$, this reduces the domain size of both the up and down spins so neither dominates. This critical point is therefore an unstable fixed point of the renormalisation group.

This procedure of coarse-graining can be described in a more mathematical way

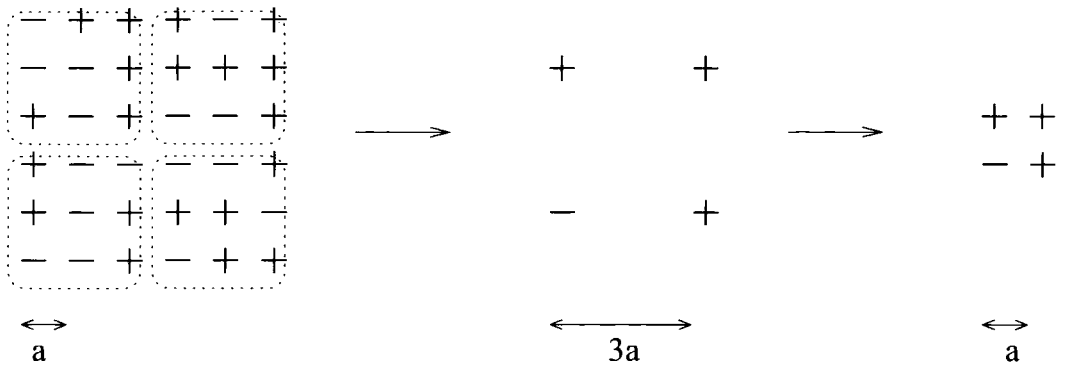


Figure 2.1: A block spin transformation

using the following operator, defined for each block as

$$T(\sigma';\sigma_1,\ldots,\sigma_9) = \begin{cases} 1 & \text{if } \sigma' \sum_i \sigma_i > 0 \\ 0 & \text{otherwise}. \end{cases} \tag{2.1.8}$$

After a block spin transformation, the new Hamiltonian is defined by

$$e^{-\mathcal{H}'(\sigma')} = \sum_{\sigma} \prod_{\text{blocks}} T(\sigma';\sigma_i) e^{-\mathcal{H}(\sigma)} \tag{2.1.9}$$

where $\mathcal{H}$ is the *reduced* Hamiltonian, related to the usual Hamiltonian by $\mathcal{H} = H/k_BT$. Since the sum $\sum_{\sigma'} T(\sigma';\sigma_i) = 1$, the partition function is not altered by this transformation. The physical properties described above are therefore also left unchanged; the only difference is that they should be expressed in terms of the blocked spins $\sigma'$, rather than the original $\sigma$.

Although the original Hamiltonian consists of only nearest neighbour interactions, this block-spin transformation could generate next-to-nearest neighbour interactions, denoted by $\sum^{(2)}_{\langle ij \rangle}$, and so on. The most general form of the new Hamiltonian is therefore

$$\mathcal{H}'(\sigma') = -J'_1 \sum_{\langle ij \rangle} \sigma_i\sigma_j - J'_2 \sum^{(2)}_{\langle ij \rangle} \sigma_i\sigma_j - J'_3 \sum^{(3)}_{\langle ij \rangle} \sigma_i\sigma_j \ldots - h' \sum_i \sigma_i \tag{2.1.10}$$

and it is useful to think of the couplings, $J'_i$ as forming a vector $\mathbf{J}' = (J'_1, J'_2, \ldots)$. The original Hamiltonian $\mathcal{H}$ can also be considered to depend on a similar vector $\mathbf{J} = (J_1, J_2, \ldots)$, although in this case $J_i = 0$ for $i \geq 2$. Since the partition functions of the two Hamiltonians, $\mathcal{H}$ and $\mathcal{H}'$, are equal there must be a relation between the vectors $\mathbf{J}$ and $\mathbf{J}'$. The map between the two is given by the renormalisation group

transformation:

$$\mathbf{J}' = \mathcal{R}\mathbf{J}\,. \tag{2.1.11}$$

Successive iterations of this map generate a sequence of points in the space of couplings, which is known as an RG trajectory. As mentioned earlier, critical points which have infinite correlation length correspond to stationary points of an RG trajectory, and so are called fixed points of the renormalisation group.

The renormalisation group can be used to find the critical exponents by linearising the RG transformation at a fixed point. Assuming a fixed point exists at $\mathbf{J}^*$, and that $\mathcal{R}$ is differentiable at this point, then the following approximation can be made:

$$J'_a - J^*_a \approx \sum_b T_{ab}(J_b - J^*_b)\,, \tag{2.1.12}$$

where $T_{ab} = \partial J'_a/\partial J_b|_{J=J*}$. The matrix $\mathbf{T}$ can be diagonalised, with eigenvalues $\lambda^i$ and corresponding eigenvectors $\nu^i$, so

$$\sum_a \nu^i_a T_{ab} = \lambda^i \nu^i_b\,. \tag{2.1.13}$$

These eigenvectors are used to define the scaling variables as $u_i = \sum_a \nu^i_a (J_a - J^*_a)$ which transform multiplicatively near the fixed point:

$$\begin{aligned} u'_i &= \sum_a \nu^i_a (J'_a - J^*_a) = \sum_{a,b} \nu^i_a T_{ab}(J_b - J^*_b) \\ &= \sum_b \lambda^i \nu^i_b (J_b - J^*_b) = \lambda^i u_i\,. \end{aligned} \tag{2.1.14}$$

The so called 'renormalisation group eigenvalues', $y_i$, are defined by $\lambda^i = a^{y_i}$, where $a$ is the lattice spacing. The behaviour of the scaling variable under an RG transformation depends on the sign of $y_i$:

- If $y_i > 0$, $u_i$ is *relevant*: the RG trajectory flows away from the critical point
- If $y_i < 0$, $u_i$ is *irrelevant*: the RG trajectory flows towards the critical point
- If $y_i = 0$, $u_i$ is *marginal*: in this case the linear approximation around $\mathbf{J}^*$ is not valid.

The Ising model has two relevant scaling variables, $u_t$ and $u_h$, with the respective RG eigenvalues $y_t$ and $y_h$. These variables are related to the only two free parameters

in the model: the reduced temperature $t = (T - T_c)/T_c$ and the external magnetic field $h$. Since the partition function is invariant under a RG transformation, the free energy must also remain the same. To ensure this, the free energy per unit site must increase

$$f(t', h') = a^2 f(t, h). \tag{2.1.15}$$

Close to the critical point, the scaling variables can be taken to be proportional to the parameters $t$ and $h$, so under the renormalisation group, $t$ and $h$ will transform according to (2.1.14). This leads to the scaling hypothesis

$$f(t, h) = a^{-2} f(a^{y_t} t, a^{y_h} h) \tag{2.1.16}$$

which can be used to find relations between the critical exponents. The first observation to make, as mentioned in [5], is that $t^{-2/y_t} f(t, h)$ is invariant under the scalings $t \to a^{y_t} t$ and $h \to a^{y_h} h$ and so it must depend only on the scale invariant variable $h/t^{y_h/y_t}$. The free energy per unit site can therefore be expressed as

$$f(t, h) = t^{2/y_t} g(h/t^{y_h/y_t}) \tag{2.1.17}$$

for some function $g$. The critical exponents can now be found, in terms of the RG eigenvalues $y_t$ and $y_h$, by differentiating $f$ as follows:

- The specific heat $C = -T \left.\frac{\partial^2 f}{\partial T^2}\right|_{h=0} = -\frac{1}{T_c} t^{2/y_t - 2} g''(0)$ so $\alpha = 2 - 2/y_t$
- The spontaneous magnetisation $M = -\left.\frac{\partial f}{\partial h}\right|_{h=0} = t^{(2-y_h)/y_t} g'(0)$ so $\beta = \frac{2-y_h}{y_t}$
- The susceptibility $\chi = \left.\frac{\partial^2 f}{\partial h^2}\right|_{h=0} = t^{(2-2y_h)/y_t} g''(0)$ so $\gamma = \frac{2y_h - 2}{y_t}$

Other critical exponents can be found in a similar manner.

### 2.1.3 Transfer Matrix

The transfer matrix method is the analogue, in statistical mechanics, of the operator formalism in quantum field theory. It will be described here in terms of the Ising model, following the discussion presented in [5]. Taking the Ising model on a square lattice with $m$ rows and $n$ columns, the spin, $\sigma_{ij}$ at each site is now indexed by two integers, for the row and column numbers. Imposing periodic boundary conditions (and so defining the lattice on a torus):

$$\sigma_{i,j+n} = \sigma_{ij} \ , \ \sigma_{i+m,j} = \sigma_{ij} \ . \tag{2.1.18}$$

Let $\mu_i$ denote the configuration of spins on the $i^{th}$ row: $\mu_i = \{\sigma_{i1}, \sigma_{i2}, \ldots, \sigma_{in}\}$. Each row configuration has its own energy

$$E[\mu_i] = -J \sum_{k=1}^{n} \sigma_{ik}\sigma_{i,k+1} \,, \tag{2.1.19}$$

along with an interaction energy with neighbouring rows:

$$E[\mu_i, \mu_j] = -J \sum_{k=1}^{n} \sigma_{ik}\sigma_{jk} \,. \tag{2.1.20}$$

Now, by defining a formal vector space of row configurations spanned by the states $|\mu_i\rangle$, the action of the transfer matrix $T$ can be defined by its matrix elements

$$\langle \mu | T | \mu' \rangle = e^{-\frac{1}{k_B T}(E[\mu,\mu'] + \frac{1}{2}E[\mu] + \frac{1}{2}E[\mu'])} \,. \tag{2.1.21}$$

The partition function has a very simple form in terms of this operator $T$:

$$\begin{aligned} Z &= \sum_{\mu_1,\ldots,\mu_m} \langle \mu_1 | T | \mu_2 \rangle \langle \mu_2 | T | \mu_3 \rangle \ldots \langle \mu_m | T | \mu_1 \rangle \\ &= Tr\, T^m \,. \end{aligned} \tag{2.1.22}$$

In Euclidean quantum field theory, the analogue of the partition function is the generating function

$$Z = \int \mathcal{D}\phi \, e^{-S[\phi]} \,, \tag{2.1.23}$$

where $S$ is the action which depends on a set of local fields $[\phi]$. To move from this description to the operator formalism, constant time surfaces are specified and the operator $U(t) = \exp(-iHt)$ evolves states from time $t_0$ to $t + t_0$. The transfer matrix plays the role of this operator, evolving states over a 'distance of time' equal to the lattice spacing $a$, and so one can define a Hamiltonian operator $\widehat{H}$ by

$$T = e^{-a\widehat{H}} \,. \tag{2.1.24}$$

There is also a relation between the correlation length and the mass of the corresponding lattice quantum field theory:

$$\xi = \frac{1}{ma} \,. \tag{2.1.25}$$

Close to a critical point the correlation functions are insensitive to the fine details of the underlying theory, i.e. to whether it is a discrete statistical model or a lattice

quantum field theory. They are also identical to the correlation functions of the corresponding continuum quantum field theory, so one can describe statistical models, near criticality, by quantum field theories. At the critical point, $\xi \to \infty$ and the corresponding quantum field theory is massless.

So far it is clear that a statistical model, at a critical point, is scale invariant. However, for a system with only local interactions Polyakov showed [7] that it is also invariant under the larger symmetry of conformal transformations, and so can be described in terms of a conformal field theory, which will be discussed in the next section. The idea is that information about all the possible universality classes can be gained by studying all possible conformal field theories. There are two advantages of this description: firstly, conformal invariance in two dimensions puts heavy constraints on the model, so it should be more tractable than the corresponding statistical model, and secondly, by perturbing the conformal field theory it is possible to study the statistical model away from criticality. This is of particular interest in this thesis and will be discussed in more detail in section 2.3.

## 2.2 Conformal Field Theory

The connection between a statistical model at a critical point and a CFT was first made by Polykov in [7], but it was some years before the detailed structure of CFT was studied by Belavin, Polyakov and Zamolodchikov in [8], which paved the way for the large volume of work which subsequently followed. A brief outline of some of the main points is presented here, based on the reviews by Di Francesco et. al. [5] and Ginsparg [9]. More detail can be found in these texts and, for example, in [10].

A theory has conformal symmetry if it is invariant under transformations which leave the metric unchanged, up to a local scale factor

$$\eta_{\mu\nu}(x) \to \eta'_{\mu\nu}(x') = \Omega(x)\eta_{\mu\nu}(x)\,. \tag{2.2.1}$$

This means that the angle between vectors is preserved. Under an infinitesimal coordinate transformation, $x^\mu \to x'^\mu = x^\mu + \epsilon^\mu$, the metric transforms as

$$\eta_{\mu\nu} \to \eta'_{\mu\nu} = \eta_{\mu\nu} - (\partial_\mu \epsilon_\nu + \partial_\nu \epsilon_\mu)\,. \tag{2.2.2}$$

For this to be a conformal transformation

$$\partial_\mu \epsilon_\nu + \partial_\nu \epsilon_\mu = f(x)\eta_{\mu\nu} \tag{2.2.3}$$

where $\Omega(x) = 1 - f(x)$. Acting with $\eta^{\mu\nu}$ on both sides, assuming the theory is $d$ dimensional, $f(x)$ can be found to be

$$\frac{2}{d}(\partial_\rho \epsilon^\rho) . \tag{2.2.4}$$

In $d \geq 3$ dimensions, the possible transformations are given by the Poincaré group

$$x'^\mu = x^\mu + a^\mu \tag{2.2.5}$$

$$x'^\mu = \Lambda^\mu_\nu x^\nu , \tag{2.2.6}$$

the dilations

$$x'^\mu = \lambda x^\mu \tag{2.2.7}$$

and the special conformal transformations

$$x'^\mu = \frac{x^\mu + b^\mu \boldsymbol{x}^2}{1 - 2\boldsymbol{b}.\boldsymbol{x} + b^2\boldsymbol{x}^2} . \tag{2.2.8}$$

The two-dimensional case is somewhat special, due to the fact that the global transformations given here are supplemented by an infinite number of local transformations, which provide powerful constraints for the theory. Restricting to two dimensional Euclidean space, the metric becomes $\eta_{\mu\nu} = \delta_{\mu\nu}$, and the constraint in (2.2.3) reduces to the Cauchy-Riemann equations

$$\partial_1 \epsilon_1 = \partial_2 \epsilon_2 , \partial_1 \epsilon_2 = -\partial_2 \epsilon_1 . \tag{2.2.9}$$

This provides motivation to introduce the complex coordinates $z$ and $\bar{z}$ with the relations

$$z = x^1 + ix^2 \quad , \quad \bar{z} = x^1 - ix^2 \tag{2.2.10}$$

$$\partial_z = \frac{1}{2}(\partial_1 - i\partial_2) \quad , \quad \partial_{\bar{z}} = \frac{1}{2}(\partial_1 + i\partial_2) . \tag{2.2.11}$$

With this change of coordinates the Cauchy-Riemann equations become $\partial_{\bar{z}}\epsilon = 0$, $\partial_z \bar{\epsilon} = 0$, where $\epsilon = \epsilon^1 + i\epsilon^2$ and $\bar{\epsilon} = \epsilon^1 - i\epsilon^2$, so in two dimensions, the group of conformal transformations is isomorphic to the infinite dimensional group of analytic transformations

$$z \to f(z) , \bar{z} \to \bar{f}(\bar{z}) . \tag{2.2.12}$$

The infinitesimal mappings $z \to z + \epsilon$ and $\bar{z} \to \bar{z} + \bar{\epsilon}$ admit the Laurent expansions

$$\epsilon(z) = \sum_{n=-\infty}^{\infty} c_n z^{n+1} , \bar{\epsilon}(\bar{z}) = \sum_{n=-\infty}^{\infty} c'_n \bar{z}^{n+1} \tag{2.2.13}$$

around $z = 0$, so the infinitesimal conformal transformations can be locally generated by

$$l_n = -z^{n+1}\partial_z\,,\ \bar{l}_n = -\bar{z}^{n+1}\partial_{\bar{z}}\,, \tag{2.2.14}$$

which satisfy the commutation relations

$$\begin{aligned} [l_n, l_m] &= (n-m)l_{n+m} \\ [\bar{l}_n, \bar{l}_m] &= (n-m)\bar{l}_{n+m} \\ [l_n, \bar{l}_m] &= 0\,. \end{aligned} \tag{2.2.15}$$

This algebra is generally known as the Witt algebra. Following the presentation of [9], since $l_n$ and $\bar{l}_m$ commute, the algebra splits into a direct sum of two isomorphic subalgebras, generated by the holomorphic ($l_n$) and anti-holomorphic ($\bar{l}_n$) generators respectively. Consequently, $z$ and $\bar{z}$ can be thought of as independent coordinates, each taking values over the whole complex plane. Of course, to return to the physical case one must impose the condition $\bar{z} = z^*$. The physical theory is therefore invariant under transformations generated by $(l_n + \bar{l}_n)$ and $i(l_n - \bar{l}_n)$.

The only infinitesimal generators to be globally well-defined on the Riemann sphere $\mathcal{S}^2 = \mathbb{C} \cup \infty$, are $\{l_{-1}, l_0, l_1\} \cup \{\bar{l}_{-1}, \bar{l}_0, \bar{l}_1\}$, and so the subalgebra they generate is associated with the global conformal group. From the definition above one can see that $l_{-1}$ and $\bar{l}_{-1}$ generate translations, $(l_0 + \bar{l}_0)$ and $i(l_0 - \bar{l}_0)$ generate dilations and rotations respectively, while $l_1$ and $\bar{l}_1$ produce special conformal transformations. The finite transformations corresponding to the generators $\{l_{-1}, l_0, l_1\}$ form the group of projective conformal transformations $SL(2,\mathbb{C})/\mathbb{Z}_2$, which can be written as

$$z \to \frac{az+b}{cz+d}\,, \tag{2.2.16}$$

where $a, b, c, d \in \mathbb{C}$ and $ad - bc = 1$. The same holds for the anti-holomorphic generators $\{\bar{l}_{-1}, \bar{l}_0, \bar{l}_1\}$. The global conformal algebra can be used to characterise the physical states. In fact, it will be useful to work in the basis of the eigenstates $l_0$ and $\bar{l}_0$, with the real eigenvalues $h$ and $\bar{h}$ respectively. Since $(l_0 + \bar{l}_0)$ generates dilations and $i(l_0 - \bar{l}_0)$ rotations, the scaling dimension $y$ and the spin $s$ of the state can be defined as $y = h + \bar{h}$ and $s = h - \bar{h}$.

The classical action of a field theory, under an infinitesimal conformal transformation $x^\mu \to x^\mu + \epsilon^\mu(x)$, will have variation

$$\delta S = \frac{1}{2}\int d^2x\, T^{\mu\nu}(\partial_\mu\epsilon_\nu + \partial_\nu\epsilon_\mu) = \frac{1}{2}\int d^2x\, T^\mu_\mu \partial_\nu \epsilon^\nu \tag{2.2.17}$$

where $T^{\mu\nu} = T^{\nu\mu}$ is the canonical energy-momentum tensor, which can always be made symmetric (see [5]). The theory is scale invariant if this tensor is traceless, and in turn this guarantees conformal invariance since $\delta S = 0$. In terms of the complex coordinates $z$ and $\bar{z}$, $T^{\mu}_{\nu}$ has the form

$$T_{zz} = \frac{1}{4}(T_{11} - 2iT_{12} - T_{22}) \tag{2.2.18}$$

$$T_{\bar{z}\bar{z}} = \frac{1}{4}(T_{11} + 2iT_{12} - T_{22}) \tag{2.2.19}$$

$$T_{z\bar{z}} = \frac{1}{4}(T_{11} + T_{22}) = 0\,; \tag{2.2.20}$$

the final equality results from the fact that $T^{\mu}_{\mu} = 0$. Translation and rotation invariance requires that $\partial_\mu T^{\mu\nu} = 0$, which in terms of the complex coordinates is

$$\partial_{\bar{z}} T_{zz} = 0\,,\ \partial_z T_{\bar{z}\bar{z}} = 0\,. \tag{2.2.21}$$

Since $\partial_{\bar{z}} T_{zz} = 0$, $T_{zz}$ is a function of $z$ alone (similarly $T_{\bar{z}\bar{z}}$ is a function of $\bar{z}$) and so the energy-momentum tensor splits into an holomorphic and an anti-holomorphic part, often denoted $T(z) = -2\pi T_{zz}$ and $\bar{T}(\bar{z}) = -2\pi T_{\bar{z}\bar{z}}$ respectively. This property is assumed to hold when the theory is quantised.

This quantum theory is expected to contain fields known as primary fields, which transform covariantly under any conformal transformation

$$\phi_j(z,\bar{z}) \to (\partial_z f)^h (\partial_{\bar{z}} \bar{f})^{\bar{h}} \phi_j(z,\bar{z})\,. \tag{2.2.22}$$

The real exponents $h$ and $\bar{h}$ are the conformal weights of the primary field $\phi_j$. Quasi-primary fields are those which transform as above for the *global* conformal transformations only. The energy momentum tensor is one example of a quasi-primary field.

Under the local transformation $z \to z + \epsilon(z)$, the holomorphic part of a primary field transforms as

$$\begin{aligned} \phi(z) &\to [\partial_z(z+\epsilon(z))]^h \phi(z+\epsilon(z)) \\ &= (1 + h\partial_z\epsilon(z) + \epsilon(z)\partial_z + O(\epsilon(z)^2))\phi(z)\,, \end{aligned} \tag{2.2.23}$$

so the variation of $\phi(z)$ (ignoring the anti-holomorphic part, which is equivalent) is

$$\delta\phi(z) = h\partial_z\epsilon(z)\phi(z) + \epsilon(z)\partial_z\phi(z)\,. \tag{2.2.24}$$

This transformation can be used to restrict the form taken by the correlation functions, as described in [9]. The two-point function $G_2(z_1, \bar{z}_1, z_2, \bar{z}_2) = \langle \phi(z_1, \bar{z}_1), \phi(z_2, \bar{z}_2) \rangle$ must be invariant under conformal transformations, so it must satisfy

$$\begin{aligned} \delta_{\epsilon,\bar{\epsilon}} G_2(z_1, \bar{z}_1, z_2, \bar{z}_2) &= \langle \delta\phi(z_1, \bar{z}_1), \phi(z_2, \bar{z}_2) \rangle + \langle \phi(z_1, \bar{z}_1), \delta\phi(z_2, \bar{z}_2) \rangle \,. \\ &= 0 \end{aligned} \tag{2.2.25}$$

This leads to

$$\begin{aligned} &(h_1 \partial_{z_1} \epsilon(z_1) + \epsilon(z_1)\partial_{z_1} + h_2 \partial_{z_2} \epsilon(z_2) + \epsilon(z_2)\partial_{z_2}) G_2(z_1, \bar{z}_1, z_2, \bar{z}_2) \\ &+ (\bar{h}_1 \partial_{\bar{z}_1} \bar{\epsilon}(\bar{z}_1) + \bar{\epsilon}(\bar{z}_1)\partial_{\bar{z}_1} + \bar{h}_2 \partial_{\bar{z}_2} \bar{\epsilon}(\bar{z}_2) + \bar{\epsilon}(\bar{z}_2)\partial_{\bar{z}_2}) G_2(z_1, \bar{z}_1, z_2, \bar{z}_2) = 0 \,. \end{aligned} \tag{2.2.26}$$

Taking the holomorphic part alone, the infinitesimal transformations generated by $l_{-1}$, $l_0$ and $l_1$ lead to the following constraints on $G_2(z_1, z_2)$:

$$\begin{aligned} \epsilon = 1 \;&\Rightarrow\; (\partial_{z_1} + \partial_{z_2}) G_2(z_1, z_2) = 0 \\ &\Rightarrow\; G_2 \text{ depends only on } z_{12} = z_1 - z_2 \\ \epsilon = z \;&\Rightarrow\; (h_1 + h_2) G_2(z_{12}) = -z_{12} \partial_z G_2(z_{12}) \\ &\Rightarrow\; G_2(z_{12}) = \frac{C_{12}}{z_{12}^{(h_1+h_2)}} \\ \epsilon = z^2 \;&\Rightarrow\; 2(h_1 z_1 + h_2 z_2) \frac{C_{12}}{z_{12}^{(h_1+h_2)}} = (h_1 + h_2) \frac{C_{12}(z_1^2 - z_2^2)}{z_{12}^{(h_1+h_2+1)}} \\ &\Rightarrow\; C_{12}(h_1 - h_2)(z_1 - z_2) = 0 \Rightarrow C_{12} = 0 \text{ unless } h_1 = h_2 \,. \end{aligned}$$

The anti-holomorphic part can be examined in the same way. The two-point functions of primary and quasi-primary fields must therefore have the form

$$G_2(z_1, \bar{z}_1, z_2, \bar{z}_2) = \frac{\delta_{12}}{z_{12}^{2h} \bar{z}_{12}^{2\bar{h}}} \,, \tag{2.2.27}$$

where $h_1 = h_2 = h$, $\bar{h}_1 = \bar{h}_2 = \bar{h}$, and the normalisation $C_{12}$ has been set to $\delta_{12}$. The three-point correlation function $G_3 = \langle \phi_1(z_1, \bar{z}_1), \phi_2(z_2, \bar{z}_2), \phi_3(z_3, \bar{z}_3) \rangle$ will be constrained in a similar way, and it can be shown that it must have the form

$$G_3 = C_{123} \frac{1}{z_{12}^{h_1+h_2-h_3} z_{23}^{h_2+h_3-h_1} z_{31}^{h_3+h_1-h_2}} \frac{1}{\bar{z}_{12}^{\bar{h}_1+\bar{h}_2-\bar{h}_3} \bar{z}_{23}^{\bar{h}_2+\bar{h}_3-\bar{h}_1} \bar{z}_{31}^{\bar{h}_3+\bar{h}_1-\bar{h}_2}} \,. \tag{2.2.28}$$

Higher correlation functions are not so simple to determine, and further conditions must be imposed in order to fix their forms.

For a general field theory, the effect of an infinitesimal transformation on the correlation functions is given by the Ward identity. In a conformal field theory,

the three Ward identities corresponding to the translation, rotation and dilation transformations can be combined into one identity known as the conformal Ward identity: for the transformation $x^\nu \to x^\nu + \epsilon^\nu(x)$ acting on a string of primary fields $\phi(x_1)\dots\phi(x_n)$, denoted here by $X$, this is given by

$$\delta_\epsilon\langle X\rangle = \int_M d^2x\, \partial_\mu\langle T^{\mu\nu}(x)\epsilon_\nu(x)X\rangle\,, \tag{2.2.29}$$

where the domain $M$ contains the positions of all the fields in the string $X$. This can also be written in terms of the complex variables $z, \bar{z}$ and $T, \bar{T}$ as

$$\delta_{\epsilon,\bar{\epsilon}}\langle X\rangle = \frac{1}{2\pi i}\oint_C dz\,\epsilon(z)\langle T(z)X\rangle - \frac{1}{2\pi i}\oint_C d\bar{z}\,\bar{\epsilon}(\bar{z})\langle\bar{T}(\bar{z})X\rangle\,. \tag{2.2.30}$$

The integration contour, $C$, must enclose the positions of all the fields in $X$.

In order to introduce an operator formalism, following [5], it is necessary to distinguish between the time and space directions. In the statistical mechanics lattice models described earlier, one direction of the lattice was chosen to be 'space' and the orthogonal direction was taken as 'time'. In the continuum limit, there is more freedom in the choice of space and time directions. The usual choice, known as 'radial quantisation' is described here: first, define the theory on an infinite cylinder of radius $L$, with the time coordinate $x^1$ running along the length of the cylinder and the space coordinate $x^2$ compactified. In Euclidean space this cylinder is described by a single complex coordinate $\xi = x^1 + ix^2$. Now consider the conformal map $\xi \to z = \exp(2\pi\xi/L)$. This maps the cylinder to the complex plane, as shown in figure 2.2. The infinite past and future on the cylinder, $x^1 = \mp\infty$, are mapped to

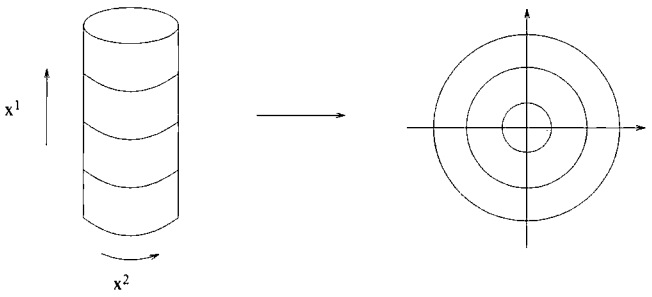


Figure 2.2: Radial quantisation. The concentric circles are surfaces of equal time.

the points $z = 0, \infty$ on the plane respectively and equal time surfaces, $x^1 = \text{const}$, become circles of constant radius on the $z$-plane.

Concentrating on the holomorphic part of the primary field $\phi(w)$, the conformal Ward identity for this field, within the radial quantisation scheme is

$$\langle \delta\phi(w) \rangle = \oint_{|z|>|w|} \frac{dz}{2\pi i} \epsilon(z) \langle T(z)\phi(w) \rangle. \tag{2.2.31}$$

The variation of $\phi(w)$ was found in (2.2.24), and using this in the Ward identity, the short distance operator product expansion (OPE) of the $T(z)$ with $\phi(w)$ is found to be

$$T(z)\phi(w) = \frac{h\phi(w)}{(z-w)^2} + \frac{\partial_z \phi(w)}{(z-w)} + \dots \tag{2.2.32}$$

with the dots representing regular terms. The energy momentum tensor represents an energy density, so it should have scaling dimension 2 and spin 2. One would therefore expect $T(z)$ to have conformal weights $h = 2$, $\bar{h} = 0$, and $\bar{T}(\bar{z})$ to have $h = 0$, $\bar{h} = 2$ [5]. The OPE of $T(z)$ with itself will have a similar form to (2.2.32), with $h = 2$, but since $T(z)$ is a quasi-primary field, not a primary field, an extra term should be added:

$$T(z)T(w) = \frac{2T(w)}{(z-w)^2} + \frac{\partial_z T(w)}{(z-w)} + f(z,w) + \dots \tag{2.2.33}$$

Now $T$ is expected to transform as $T' = (\partial_z g)^{-2} T(z)$ under the global transformation $z \to g(z)$, so the transformation $z \to w = 1/z$ will produce

$$T'(w) = (\partial_z w)^{-2} T(z) = z^4 T(z)\,. \tag{2.2.34}$$

$T(0)$ should always be finite and since $T'(1/z)$ must be just as regular as $T(z)$ this implies that $T(z)$ must decay as $z^{-4}$ as $z \to \infty$ [5]. The extra term in the OPE must therefore have the form

$$f(z,w) = \frac{c/2}{(z-w)^4}\,, \tag{2.2.35}$$

where $c$ is a constant and the factor $1/2$ is just convention.

Using the OPE of $T(z)T(w)$ in the conformal Ward identity, the variation of $T$ under a local conformal transformation is given by

$$\begin{aligned} \delta_\epsilon T(w) &= -\frac{1}{2\pi i} \oint_C dz \epsilon(z) T(z) T(w) \\ &= -\frac{1}{2\pi i} \oint_C dz \epsilon(z) \left( 2\frac{T(w)}{(z-w)^2} + \frac{\partial_z T(w)}{(z-w)} + \frac{c/2}{(z-w)^4} \right) \\ &= -2T(w)\partial_w \epsilon(w) - \epsilon(w)\partial_w T(w) - \frac{c}{12}\partial_w^3 \epsilon(w)\,. \end{aligned} \tag{2.2.36}$$

As shown in [5], this corresponds to sending $T(z) \to T'(w)$ under the finite transformation $z \to w(z)$ where

$$T'(w) = \left(\frac{dw}{dz}\right)^{-2} \left(T(z) - \frac{c}{12}\{w; z\}\right), \tag{2.2.37}$$

and $\{w; z\}$ is the Schwarzian derivative given by

$$\{w; z\} = \frac{(d^3w/dz^3)}{(dw/dz)} - \frac{3}{2}\left(\frac{d^2w/dz^2}{dw/dz}\right)^2. \tag{2.2.38}$$

$T(z)$ (equivalently $\bar{T}(\bar{z})$) admits the mode expansion

$$T(z) = \sum_{n\in\mathbb{Z}} z^{-n-2} L_n\,,\; L_n = \frac{1}{2\pi i}\oint dz z^{n+1} T(z)\,. \tag{2.2.39}$$

The commutator $[L_m, \phi(w)]$ can be found using this mode expansion and the OPE $T(z)\phi(w)$ given in (2.2.32) as

$$\begin{aligned}[L_m, \phi(w)] &= \frac{1}{2\pi i}\oint_{|z|>|w|} dz z^{m+1} T(z)\phi(w) - \frac{1}{2\pi i}\oint_{0<|z|<|w|} dz z^{m+1}\phi(w)T(z) \\ &= \frac{1}{2\pi i}\oint_C dz z^{m+1}\left(\frac{h\phi(w)}{(z-w)^2} + \frac{\partial_z\phi(w)}{(z-w)}\right)\end{aligned} \tag{2.2.40}$$

where $C$ is the contour enclosing $w$, as shown in figure 2.3. Using the mode expansion

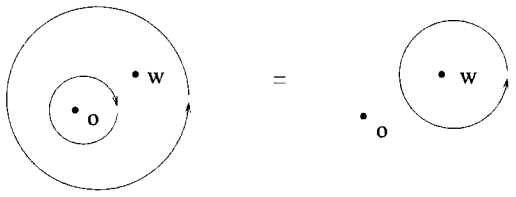


Figure 2.3: The contour $C$

and the OPE of $T(z)T(w)$, the commutation relations for $L_n$ (and $\bar{L}_n$) can be derived in a similar way (see [5] for details). The result is

$$\begin{aligned}[L_n, L_m] &= (n-m)L_{n+m} + \frac{c}{12}n(n^2-1)\delta_{n+m,0} \\ [\bar{L}_n, \bar{L}_m] &= (n-m)\bar{L}_{n+m} + \frac{c}{12}n(n^2-1)\delta_{n+m,0} \\ [L_n, \bar{L}_m] &= 0\,.\end{aligned} \tag{2.2.41}$$

This is known as the Virasoro algebra and it is the central extension of the classical Witt algebra. For this reason, the constant $c$ is often referred to as the central charge.

Notice that for the global symmetry generators $L_{-1}$, $L_0$ and $L_1$, this central extension disappears and the algebra reverts to the classical one.

The theory is assumed to have a unique vacuum state, $|0\rangle$, which is invariant under global symmetries, so

$$L_n|0\rangle = 0\,,\; n \geq -1\,. \tag{2.2.42}$$

A state, $|\phi\rangle$, can then be associated to each primary field $\phi(z)$ with the definition $|\phi\rangle = \lim_{z\to 0}\phi(z)|0\rangle$. Using the commutator $[L_n, \phi(z)]$ from (2.2.40) and the relation (2.2.42) it is easy to show (see [5]) that

$$\begin{aligned} L_0|\phi\rangle &= \lim_{z\to 0} L_0\phi(z)|0\rangle = h|\phi\rangle \\ L_n|\phi\rangle &= 0\,,\; n > 0\,, \end{aligned} \tag{2.2.43}$$

with equivalent relations holding for $\bar{L}_0|\phi\rangle$ and $\bar{L}_n|\phi\rangle$. This is a highest weight state of the Virasoro algebra and representations of this algebra can be built from these states in the following way: acting on $|\phi\rangle$ with the generators $L_n$, $n < 0$, produces an infinite tower of states $L_{-n_1}\ldots L_{-n_m}|\phi\rangle$, $1 \leq n_1 \leq \ldots \leq n_m$, known as left descendants. They are eigenstates of $L_0$ with eigenvalues $h' = h + n_1 + \ldots + n_m = h + l$, where $l$ is known as the level of the descendant. An equivalent tower of right descendants is generated from $|\phi\rangle$ with the application of $\bar{L}_n$, $n < 0$. The subset of the Hilbert space, spanned by the primary state $|\phi\rangle$ and its descendants, is closed under the action of the Virasoro generators and so it forms a representation of the Virasoro algebra known as a Verma module.

The set of fields containing the primary field $\phi$ and its descendants is called a conformal family, denoted by $[\phi]$. Since the generators $L_n$ and $\bar{L}_n$ commute, each conformal family can be considered as a direct product of the space of left descendants, $\Phi$, and right descendants, $\bar{\Phi}$, so any discussions can be restricted to the 'left' (holomorphic) sector with the understanding that equivalent statements will hold for the 'right' (anti-holomorphic) sector.

The objects of interest in these theories are the correlation functions as these are the physically measurable quantities. Correlation functions between descendant fields can be expressed in terms of those between the primary fields only, so in order to solve the theory one needs to know all the correlation functions between the primary fields. For this it is necessary to know the operator algebra: the complete OPE (including

all regular terms) of all primary fields with each other. Applying this OPE within a correlation function reduces it to two-point functions which are known.

By taking the limit as any two fields approach one another in the three-point correlation function (2.2.28), the OPE for primary fields can be expressed as

$$\phi_i(z_i,\bar{z}_i)\phi_j(z_j,\bar{z}_j) = \sum_k C_{ijk}\frac{1}{(z_i-z_j)^{h_k-h_i-h_j}}\frac{1}{(\bar{z}_i-\bar{z}_j)^{\bar{h}_k-\bar{h}_i-\bar{h}_j}}\phi_k(z_k,\bar{z}_k)+\ldots \tag{2.2.44}$$

The complete operator algebra of primary fields can be obtained from conformal symmetry once the central charge, $c$, the conformal dimensions of the primary fields, and the 3-point function coefficients $C_{ijk}$ are known. Out of these quantities, only the $C_{ijk}$ require some dynamical input to find; one often imposes crossing symmetry which, as described in [9], comes from the observation that the four point function

$$\langle\phi_i(z_1,\bar{z}_1)\phi_j(z_2,\bar{z}_2)\phi_l(z_3,\bar{z}_3)\phi_m(z_4,\bar{z}_4)\rangle$$

can be evaluated in two ways. One can take $z_1 \to z_2$ and $z_3 \to z_4$, shown pictorially on the left of figure 2.4. Alternatively, one could take $z_1 \to z_3$ and $z_2 \to z_4$, shown on the right of figure 2.4. The equivalence of these two approaches puts constraints on the coefficients $C_{ijk}$ which, at least for the minimal models, introduced below, can be solved completely for $C$.

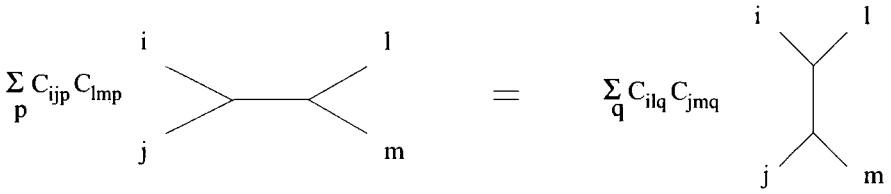


Figure 2.4: Crossing symmetry

## 2.2.1 Null states and minimal models

In some cases, a representation of the Virasoro algebra comprising some highest weight state $|\phi\rangle$ and its descendants is reducible. This means that there exists a subspace that is itself a representation of the Virasoro algebra, generated by a descendant $|\chi\rangle$ of $|\phi\rangle$ that is also a highest weight state: $L_n|\chi\rangle = 0$, $n > 0$. The state

$|\chi\rangle$ is known as a singular or null vector. It is orthogonal to the whole Verma module as

$$\langle\chi|L_{-k_1}L_{-k_2}\dots L_{-k_n}|\phi\rangle = \langle\phi|L_{k_n}\dots L_{k_2}L_{k_1}|\chi\rangle^* = 0\,, \tag{2.2.45}$$

using Hermitian conjugation, and its norm $\langle\chi|\chi\rangle = 0$. In fact, all descendants of $|\chi\rangle$ also have zero norm and are orthogonal to all states in the Verma module of the same level. An irreducible representation may be constructed by quotienting out of the Verma module the null submodule, i.e. by identifying states that differ only by a state of zero norm.

To each Verma module, one can associate a function $\chi_{(c,h)}(\tau)$ called the character of the module:

$$\chi_{(c,h)}(\tau) = Tr\, q^{L_0-c/24} = \sum_{l=0}^{\infty} \dim(l) q^{l+h-c/24} \tag{2.2.46}$$

where $\dim(l)$ is the number of linearly independent states at level $l$, $\tau$ is a complex variable such that $\Im m\,\tau > 0$ and $q = e^{2\pi i\tau}$. These characters are generating functions for the level degeneracy $\dim(l)$, so knowing the character amounts to knowing how many states there are at each level.

Another quantity to determine the number of linearly independent vectors in the Verma module at level $l$ is the Gram matrix, $M^{(l)}(c,h)$, built of inner products between all basis states:

$$M^{(l)}(c,h) = \langle\phi_h|L_{m_1}\dots L_{m_j}L_{-n_1}\dots L_{-n_k}|\phi_h\rangle \tag{2.2.47}$$

with $n_i, m_i \geq 0$ and $\sum_{i=1}^{k} n_i = \sum_{i=1}^{j} m_i = l$. If $\det M^{(l)}(c,h)$ vanishes then one can conclude that there are null vectors at level $l$. If the determinant is negative there must be states with a negative norm present so the representation is not unitary. A general formula for this determinant was found by Kac [11] (and proven by Feigin and Fuchs in [12]):

$$\det M^{(l)} = \alpha_l \prod_{\substack{r,s\geq 1 \\ rs\leq l}} [h - h_{r,s}]^{P(l-rs)}\,. \tag{2.2.48}$$

$P(l-rs)$ is the number of partitions of the integer $l-rs$ and $\alpha_l$ is a positive constant independent of $h$ and $c$

$$\alpha_l = \prod_{\substack{r,s\geq 1 \\ rs\leq l}} [(2r)^s s!]^{m(r,s)} \tag{2.2.49}$$

with $m(r,s) = P(l - rs) - P(l - r(s+1))$. The roots of this determinant can be expressed by first reparametrising $c$ in terms of the (possibly complex) quantity

$$m = -\frac{1}{2} \pm \frac{1}{2}\sqrt{\frac{25-c}{1-c}}\,. \tag{2.2.50}$$

The $h_{r,s}(m)$ are then given by

$$h_{r,s}(m) = \frac{[(m+1)r - ms]^2 - 1}{4m(m+1)}\,, \tag{2.2.51}$$

and, in this notation, the central charge becomes

$$c = 1 - \frac{6}{m(m+1)}\,. \tag{2.2.52}$$

The existence of null states also puts a constraint on the operator algebra which becomes

$$\phi_{(r_1,s_1)} \times \phi_{(r_2,s_2)} = \sum_{\substack{k=1+|r_1-r_2| \\ k+r_1+r_2=1 \bmod 2 \\ \text{step } 2}}^{k=r_1+r_2-1} \sum_{\substack{l=1+|s_1-s_2| \\ l+s_1+s_2=1 \bmod 2 \\ \text{step } 2}}^{l=s_1+s_2-1} \phi_{(k,l)}\,. \tag{2.2.53}$$

These are known as fusion rules. This notation means that the OPE of $\phi_{(r_1,s_1)}$ with $\phi_{(r_2,s_2)}$ (or their descendant fields) may contain terms belonging to the conformal families of $\phi_{(k,l)}$ on the RHS. In general, a conformal family $[\phi_{(r,s)}]$, with $r, s$ arbitrarily large, can be generated by repeatedly applying (2.2.53) which implies that there are an infinite number of conformal families in the theory. However, if the central charge can be expressed in terms of two coprime integers $p$, $p'$ as

$$c = 1 - 6\frac{(p-p')^2}{pp'}\,, \tag{2.2.54}$$

then the conformal weights become

$$h_{r,s} = \frac{(pr - p's)^2 - (p-p')^2}{4pp'}\,, \tag{2.2.55}$$

which has the periodicity properties

$$h_{r+p',s+p} = h_{r,s}\,,\; h_{r,s} = h_{p'-r,p-s}. \tag{2.2.56}$$

The integers $p$ and $p'$ can be taken to be positive and without a loss of generality it can be assumed that $p > p'$. They are related to the parameter $m$ by

$$m = \frac{p'}{p-p'} \tag{2.2.57}$$

where the positive branch of $m$ in (2.2.50) has been chosen. It can easily be shown that $h_{r,s}$ also satisfies the identities:

$$\begin{aligned} h_{r,s} + rs &= h_{p'+r,p-s} = h_{p'-r,p+s} \\ h_{r,s} + (p'-r)(p-s) &= h_{r,2p-s} = h_{2p'-r,s}. \end{aligned} \tag{2.2.58}$$

From (2.2.58) it is clear that the null vectors at levels $rs$ and $(p'-r)(p-s)$ are themselves highest weights of degenerate Verma modules. These two null vectors will give rise to submodules that also contain null vectors of the same form, and so on. There will therefore be an infinite number of null vectors within the Verma module. The existence of each of these null vectors imposes a constraint on the operator algebra and the result is a Verma module consisting of a *finite* number of conformal families. The corresponding conformal weights are $h_{r,s}$ with $1 \leq r \leq p'-1$ and $1 \leq s \leq p-1$, but because of the symmetry $h_{r,s} = h_{p'-r,p-s}$, there are only $(p-1)(p'-1)/2$ fields in the theory with $\phi_{(r,s)} = \phi_{(p'-r,p-s)}$. To avoid double counting one often takes $p's < pr$. The pairs $(r,s)$ are known as Kac labels and $E_{p,p'}$ denotes the set of such pairs in the range described here. These theories are the minimal models, usually denoted by $\mathcal{M}_{(p,p')}$.

The fusion rules given in (2.2.53) can be expressed in the form of the fusion *algebra*

$$\phi_i \times \phi_j = \sum_k N_{ij}^k \phi_k \tag{2.2.59}$$

where the $N_{ij}^k$ are integers. Here the indices $i,j,k$ label the primary fields. For the minimal models, they can be replaced by the Kac labels $(r,s)$ but the concept of the fusion algebra can be applied to more general models which will be discussed later. This algebra is commutative and associative, with the identity element $\phi_1 = I$ the identity field, so $N_{i1}^k = \delta_{ik}$. Commutativity implies that $N_{ij}^k$ is symmetric in $i$ and $j$. Using this, along with the associativity $\phi_i \times (\phi_j \times \phi_k) = (\phi_i \times \phi_j) \times \phi_k$ leads to the expression

$$\sum_l N_{kj}^l N_{il}^m = \sum_l N_{ij}^l N_{lk}^m . \tag{2.2.60}$$

By defining a matrix with the entries $(N_i)_j^k = N_{ij}^k$, this condition can be rephrased as

$$N_i N_k = \sum_l N_{ik}^l N_l \tag{2.2.61}$$

so the $N_i$ form a matrix representation of the fusion rules. They can be simultaneously diagonalised and their eigenvalues then form one dimensional representations of the fusion rules.

The full Hilbert space of the CFT is given by

$$\mathcal{H} = \bigoplus_{h,\bar{h}} n_{h,\bar{h}} \mathcal{V}_h \otimes \mathcal{V}_{\bar{h}} \tag{2.2.62}$$

where the non-negative integers $n_{h,\bar{h}}$ specify how many distinct primary fields of weight $(h, \bar{h})$ there are in the CFT. The fusion algebra, shown above, indicates which values of $(h, \bar{h})$ are consistent with the CFT, but not which ones actually occur. For this one needs the extra constraints imposed when the theory is required to be modular invariant on the torus. This was first suggested by Cardy in [13].

### 2.2.2 Finite size effects

Now, consider a CFT on a complex plane and map this to a cylinder of circumference $L$ with the transformation $z \to w = \frac{L}{2\pi} \ln z$. The Schwarzian derivative is $\{w; z\} = 1/2z^2$ and using (2.2.37), the energy-momentum tensor on the cylinder $T_{cyl}(w)$ can be related to that on the plane, $T_{plane}$ by

$$T_{cyl}(w) = \left(\frac{2\pi}{L}\right)^2 \left(T_{plane}(z)z^2 - \frac{c}{24}\right). \tag{2.2.63}$$

Assuming that the vacuum energy density $\langle T_{plane} \rangle$ vanishes on the plane, taking the expectation value of the above gives a nonzero vacuum energy density on the cylinder

$$\langle T_{cyl}(w) \rangle = -\frac{c\pi^2}{6L^2}. \tag{2.2.64}$$

The change in energy brought about by imposing these boundary conditions is known as the Casimir energy. The relation between this and the central charge can now be used to show that $c$ is also related to the free energy. When the metric tensor is changed the free energy $F$ varies as

$$\delta F = -\frac{1}{2} \int d^2x \sqrt{\det g} \delta g_{\mu\nu} \langle T^{\mu\nu} \rangle. \tag{2.2.65}$$

In this cylindrical geometry, an infinitesimal scaling of the circumference $\delta L = \epsilon L$ corresponds to the coordinate variation $\delta z^0 = \epsilon z^0$ and $\delta z^1 = 0$, where $z^0$ runs around the cylinder and $z^1$ along it. The metric tensor then varies as $\delta g_{\mu\nu} = -2\epsilon \delta_{\mu 0} \delta_{\nu 0}$. Now

$$\langle T^{00} \rangle = \langle T_{zz} \rangle + \langle T_{\bar{z}\bar{z}} \rangle = -\frac{1}{\pi} \langle T(z) \rangle = \frac{\pi c}{6L^2} \tag{2.2.66}$$

so the variation of the free energy is

$$\delta F = \int dz^0 dz^1 \frac{\pi c}{6L^2} \frac{\delta L}{L} . \tag{2.2.67}$$

The integration over $z^0$ introduces a factor of $L$, whereas the integration over $z^1$ can be avoided by considering the free energy per unit length, $F_L$, which varies as

$$\delta F_L = \frac{\pi c}{6L^2} \delta L . \tag{2.2.68}$$

Integrating this then leads to

$$F_L = -\frac{\pi c}{6L} . \tag{2.2.69}$$

The central charge also appears in the Hamiltonian for the CFT on the cylinder, where $z = \exp(x^1 + ix^2)$. Here dilations $z \to e^a z$ become time translations $x^1 \to x^1 + a$ therefore the dilation generator on the conformal plane can be regarded as the Hamiltonian for the system:

$$H = \frac{2\pi}{L} \left( (L_0)_{cyl} + (\bar{L}_0)_{cyl} \right) . \tag{2.2.70}$$

Substituting the mode expansion $T_{plane}(z) = \sum z^{-n-2} L_n$ into the relation (2.2.63) gives

$$T_{cyl} = \left( \frac{2\pi}{L} \right)^2 \left( \sum_{n \in \mathbb{Z}} z^{-n} L_n - \frac{c}{24} \right) = \left( \frac{2\pi}{L} \right)^2 \sum_{n \in \mathbb{Z}} \left( L_n - \frac{c}{24} \delta_{n0} \right) e^{-2\pi n \omega / L} \tag{2.2.71}$$

where $\omega = \frac{L}{2\pi} \ln z$. Therefore the translation generator $(L_0)_{cyl}$ on the cylinder, in terms of the dilation generator $L_0$ on the plane is

$$(L_0)_{cyl} = L_0 - \frac{c}{24} , \tag{2.2.72}$$

so the Hamiltonian is

$$H = \frac{2\pi}{L} \left( L_0 + \bar{L}_0 - \frac{c}{12} \right) , \tag{2.2.73}$$

where the constant term $c/12$ ensures that the vacuum energy vanishes in the $L \to \infty$ limit. The momentum generates translations along the circumference of the cylinder so this can be written as

$$P = \frac{2\pi i}{L} \left( (L_0)_{cyl} - (\bar{L}_0)_{cyl} \right) = \frac{2\pi i}{L} \left( L_0 - \bar{L}_0 \right) . \tag{2.2.74}$$

For a CFT on the entire complex plane the holomorphic and anti-holomorphic sectors completely decouple and can be studied separately. However requiring the

theory to be consistent on a torus puts useful constraints theory which will now be discussed. This follows closely the presentation given in [5].

Define a torus by specifying two linearly independent vectors on the complex plane, and identify points which differ by an integer combination of these vectors. These vectors can be represented by two complex numbers $\omega_1$ and $\omega_2$, which are the periods of the torus. Next the space and time directions must be defined. Here space is taken along the real axis, and time along the imaginary axis. The Hamiltonian, $H$, and total momentum, $P$, of the theory generate translations along the time and space directions respectively so the operator which translates the system parallel to the period $\omega_2$, over a distance $a$ in Euclidean space-time is given by

$$e^{-\frac{a}{|\omega_2|}(H\, Im\omega_2 - iP\, Re\omega_2)} . \tag{2.2.75}$$

If $a$ is the lattice spacing in a statistical mechanics problem then this translation will go from one row of the lattice to the next, parallel to $\omega_2$. If a complete period contains $m$ lattice spacings, so $|\omega_2| = ma$, then the partition function is obtained by taking the trace of the translation operator to the $m^{th}$ power:

$$Z(\omega_1, \omega_2) = Tr\, e^{-(H\, Im\omega_2 - iP\, Re\omega_2)} . \tag{2.2.76}$$

Now to express $H$ and $P$ in terms of the Virasoro generators $L_0$ and $\bar{L}_0$ it is useful to consider the torus as cylinder of finite length with the ends identified. Recall that on a cylinder of circumference $L$ the Hamiltonian is $H = (2\pi/L)(L_0 + \bar{L}_0 - c/12)$ and the momentum is $P = (2\pi i/L)(L_0 - \bar{L}_0)$. Here $\omega_1 = L$, so in terms of the ratio of periods $\tau = \omega_2/\omega_1$, known as the modular parameter, the partition functions is

$$\begin{aligned} Z(\tau) &= Tr\, \exp[\pi i\{(\tau - \bar{\tau})(L_0 + \bar{L}_0 - c/12) + (\tau + \bar{\tau})(L_0 - \bar{L}_0)\}] \\ &= Tr\, \exp[2\pi i\{\tau(L_0 - c/24) - \bar{\tau}(\bar{L}_0 - c/24)\}] . \end{aligned} \tag{2.2.77}$$

Defining the parameters

$$q = e^{2\pi i\tau} , \; \bar{q} = e^{-2\pi i\bar{\tau}} , \tag{2.2.78}$$

the partition function can be expressed as

$$Z(\tau) = Tr\left(q^{L_0 - c/24}\bar{q}^{\bar{L}_0 - c/24}\right) , \tag{2.2.79}$$

which involves the characters described in (2.2.46).

For a CFT to be sensible on a torus its partition function must be independent of the choice of periods $\omega_{1,2}$ of the torus. Let $\omega'_{1,2}$ be two periods, describing the same lattice as $\omega_{1,2}$. Since $\omega'_{1,2}$ are points on the lattice they must be integer combinations of $\omega_{1,2}$:

$$\begin{pmatrix} \omega'_1 \\ \omega'_2 \end{pmatrix} = \begin{pmatrix} a & b \\ c & d \end{pmatrix} \begin{pmatrix} \omega_1 \\ \omega_2 \end{pmatrix} \tag{2.2.80}$$

with $a, b, c, d \in \mathbb{Z}$ and $ad - bc = 1$. This matrix should have an inverse with integer entries, since $\omega_{1,2}$ must also be expressed in terms of $\omega'_{1,2}$ in the same way. Also, as the unit cell of the lattice must have the same area, regardless of the choice of periods, this matrix must have unit determinant and so these matrices form the group $SL(2,\mathbb{Z})$. Under this change of period, the modular parameter transforms as

$$\tau \rightarrow \frac{a\tau + b}{c\tau + d}, \; ad - bc = 1\,. \tag{2.2.81}$$

Since this is invariant under a sign change of all the parameters $a, b, c$ and $d$, the relevant symmetry, known as the modular group, is $PSL(2,\mathbb{Z}) = SL(2,\mathbb{Z})/\mathbb{Z}_2$.

The generators of this group can be considered geometrically as the cutting of the torus along one of the non-trivial cycles and gluing back, after a twist by $2\pi$, as described in [9]. Cutting along a line of constant time, $x^1$, and re-gluing corresponds to transformation $\mathcal{T} : \tau \rightarrow \tau + 1$. A similar operation performed along a line of fixed $x^2$ is equivalent to the transformation $\mathcal{U} : \tau \rightarrow \tau/(\tau + 1)$. The generators that are usually considered are

$$\mathcal{T} \;\; : \;\; \tau \rightarrow \tau + 1 \tag{2.2.82}$$

$$\mathcal{S} = \mathcal{T}^{-1}\mathcal{U}\mathcal{T}^{-1} \;\; : \;\; \tau \rightarrow -\frac{1}{\tau} \tag{2.2.83}$$

which satisfy $\mathcal{S}^2 = (\mathcal{S}\mathcal{T})^3 = 1$.

Recall that the Hilbert space of a minimal model with central charge $c$ can be decomposed into left and right Virasoro modules:

$$\mathcal{H} = \bigoplus_{h,\bar{h}} n_{h,\bar{h}} \mathcal{V}_h \otimes \mathcal{V}_{\bar{h}}\,. \tag{2.2.84}$$

The torus partition function is given by

$$Z(\tau) = \sum_{h,\bar{h}} n_{h,\bar{h}} \chi_h(\tau) \bar{\chi}_{\bar{h}}(\bar{\tau}) \tag{2.2.85}$$

in terms of the Virasoro characters

$$\chi_h(\tau) = Tr_{\mathcal{V}_h}(q^{L_0-c/24}) = q^{h-c/24}\sum_{n\geq 0} d(n)q^n\,. \tag{2.2.86}$$

The action of $\mathcal{T}$ on the minimal characters is

$$\chi_{r,s}(\tau+1) = \sum_{(\rho,\sigma)\in E_{p,p'}} \mathcal{T}_{rs,\rho\sigma}\chi_{\rho,\sigma}(\tau) \tag{2.2.87}$$

where

$$\mathcal{T}_{rs,\rho\sigma} = \delta_{r,\rho}\delta_{s,\sigma}e^{2i\pi(h_{r,s}-c/24)} \tag{2.2.88}$$

with the conformal dimensions given by the Kac formula (2.2.55). The modular transformation $\mathcal{S}$ acts on the characters as

$$\chi_{r,s}(-1/\tau) = \sum_{(\rho,\sigma)\in E_{p,p'}} \mathcal{S}_{rs,\rho\sigma}\chi_{\rho,\sigma} \tag{2.2.89}$$

where

$$\mathcal{S}_{rs,\rho\sigma} = 2\sqrt{\frac{2}{pp'}}(-1)^{1+s\rho+r\sigma}\sin\left(\pi\frac{p}{p'}r\rho\right)\sin\left(\pi\frac{p'}{p}s\sigma\right) \tag{2.2.90}$$

is known as the modular $\mathcal{S}$ matrix [13][14].

The requirement that the partition function be invariant under the transformations generated by $\mathcal{T}$ and $\mathcal{S}$ puts constraints on the multiplicities $n_{h,\bar{h}}$, which are described below following [5]. There is also an additional requirement (at least for a unitary theory) that the $n_{h,\bar{h}}$ be non-negative integers, and that the identity operator appear just once, so $n_{0,0} = 1$.

The $\mathcal{T}$ invariance is the weakest condition. This restricts the left-right association of modules by

$$h - \bar{h} = 0\,, \mathrm{mod}\ 1\,. \tag{2.2.91}$$

An obvious solution to this is $h = \bar{h}$ which leads to a 'diagonal' partition function

$$Z = \sum_{(r,s)\in E_{p,p'}} |\chi_{r,s}|^2\,. \tag{2.2.92}$$

Since $\mathcal{S}$ is unitary this is modular invariant. The operator content of this theory can be read off from the partition function: each field in the Kac table $E(p,p')$ appears exactly once in the combination $\Phi_{(r,s)} = \phi_{(r,s)} \otimes \bar{\phi}_{(r,s)}$. This is known as the minimal model $\mathcal{M}(p,p')$. The simplest such unitary minimal model is $\mathcal{M}(4,3)$, with central

charge $c = 1/2$ and this can be shown to correspond to the critical Ising model. The continuum version of the critical Ising model has three operators: the identity $\mathbb{1}$ with conformal dimension $(0,0)$, the spin $\sigma$ (the continuum version of the lattice spin $\sigma_i$) and the energy density, or thermal operator, $\varepsilon$ (the continuum version of the interaction energy $\sigma_i\sigma_{i+1}$). The exponents $\eta$ and $\nu$ can be defined in terms of the critical correlators

$$\langle\sigma_i\sigma_{i+n}\rangle = \frac{1}{|n|^\eta}\,,\ \langle\varepsilon_i\varepsilon_{i+n}\rangle = \frac{1}{|n|^{4-2/\nu}}\,. \tag{2.2.93}$$

In table 2.1, these exponents are given as $\eta = 1/4$ and $\nu = 1$ and with the form of the two point function for primary fields (2.2.27), assuming that the fields $\sigma$ and $\varepsilon$ have no spin ($h = \bar{h}$), their conformal dimensions must be

$$(h,\bar{h})_\sigma = \left(\frac{1}{16},\frac{1}{16}\right)\,,\ (h,\bar{h})_\varepsilon = \left(\frac{1}{2},\frac{1}{2}\right)\,. \tag{2.2.94}$$

The operator-field correspondence is given in table 2.2 restricting to the holomorphic part for simplicity.

| Kac labels $(r,s)$ | Conformal Dimension $h$ | Operator |
|---|---|---|
| $(1,1)$ or $(2,3)$ | $0$ | $\mathbb{1}$ Identity |
| $(2,2)$ or $(1,2)$ | $\frac{1}{16}$ | $\sigma$ Spin |
| $(2,1)$ or $(1,3)$ | $\frac{1}{2}$ | $\varepsilon$ Thermal operator |

Table 2.2: Operator-field correspondence for the critical Ising model

Minimal models also exist where not all of the possible fields from the Kac table are present. One example of this is the three-state Potts model. This is related to the $\mathcal{M}(6,5)$ model, but only the fields $\phi_{(r,s)}$ with $s = 1,3,5$ are present in the theory. In order to find modular invariants one can group the fields into blocks which have the required transformation properties. It can be shown that the characters for the relevant blocks are

$$\begin{aligned} \mathcal{C}_{r,1}(\tau) &= \chi_{r,1}(\tau) + \chi_{r,5}(\tau) \\ \mathcal{C}_{r,3}(\tau) &= \chi_{r,3}(\tau) \end{aligned} \tag{2.2.95}$$

and the modular invariant partition function [14] is

$$\begin{aligned} Z(\tau) &= \sum_{r=1,2} \left\{ |\mathcal{C}_{r,1}(\tau)|^2 + 2|\mathcal{C}_{r,3}(\tau)|^2 \right\} \\ &= \sum_{r=1,2} \left\{ |\chi_{r,1} + \chi_{r,5}|^2 + 2|\chi_{r,3}|^2 \right\} . \end{aligned} \tag{2.2.96}$$

This shows that only the operators $\phi_{(r,s)}$ with $s = 1, 5$ and $r = 1, 2$ are present in the theory along with two copies of $\phi_{(r,3)}$ with $r = 1, 2$. This multiplicity 2 indicates that the three-state Potts model is not a subtheory of the $\mathcal{M}(6, 5)$ model but actually has a larger symmetry algebra, known as the $W_3$ algebra, of which the Virasoro algebra is a subalgebra. The block-characters given above are the characters with respect to this extended algebra and the partition function is 'diagonal' when written in terms of these. Theories of this form are therefore known as block-diagonal. Further discussion of extended algebras will be given in Section 4.2. The search for these modular invariant partition functions began in [14]. A full 'ADE' classification for the minimal models was conjectured by Cappelli, Itzykson and Zuber in [15] , which was later proved in [16] [17].

There is an important relation between the modular $\mathcal{S}$ matrices and the fusion algebra which was first proposed by Verlinde in [18], and later proven in [19],[20]. This states that $\mathcal{S}$ diagonalises the fusion rules, i.e. $N_{ij}^k = \sum_n \mathcal{S}_{jn} \lambda_i^{(n)} \bar{\mathcal{S}}_{nk}$, where $\lambda_i^{(n)}$ are the eigenvalues of the matrix $N_i$. This relation can be used to solve for the $N_{ij}^k$, in terms of the matrix $\mathcal{S}$: first label the identity by $i = 0$ so $N_{0j}^k = \delta_j^k$, then the eigenvalues $\lambda_i^{(n)}$ must satisfy $\lambda_i^{(n)} = \mathcal{S}_{in}/\mathcal{S}_{0n}$. The Verlinde formula then follows:

$$N_{ij}^k = \sum_n \frac{\mathcal{S}_{in} \mathcal{S}_{jn} \bar{\mathcal{S}}_{nk}}{\mathcal{S}_{0n}} . \tag{2.2.97}$$

This will be of use later on.

## 2.3 Perturbed CFT

As mentioned earlier, conformal field theories can be used to describe statistical models at their critical points. One advantage to this description is that it is possible to perturb a CFT in such a way that it remains integrable, which allows the statistical model to be studied away from criticality. Such integrable perturbations were first shown to exist by Zamolodchikov in [21]. This section contains a brief review of this work.

Integrability of conformal field theory is guaranteed by the existence of an infinite number of conserved charges provided by the holomorphic and anti-holomorphic components of the stress energy tensor and other descendants of the identity. The identity operator $I$ is the unique primary field with weights $(0,0)$. Its conformal family can be split into holomorphic and antiholomorphic sectors and the space of left descendants of $I$ will be denoted by $\Lambda$. The operator $L_0$ can be used to decompose this into subspaces $\Lambda_s$, labelled by spin $s$

$$L_0\Lambda_s = s\Lambda_s \tag{2.3.1}$$

$$\bar{L}_0\Lambda_s = 0 \tag{2.3.2}$$

$$\Lambda = \bigoplus_{s=0}^{\infty} \Lambda_s \,. \tag{2.3.3}$$

Each field $T_s \in \Lambda_s$ has conformal weight $(s,0)$ and so spin $s$. Since it is holomorphic it follows that

$$\partial_{\bar{z}} T_s = 0 \tag{2.3.4}$$

so an infinite number of conserved charges can be defined:

$$\oint T_s(\varsigma)(\varsigma - z)^{n+s-1} d\varsigma \,, \; n = 0, \pm 1, \pm 2, \ldots \tag{2.3.5}$$

Not all of these conserved charges will be linearly independent as some of the fields $T_s$ may be total derivatives, but these fields can be avoided by considering the factor space

$$\widehat{\Lambda} = \Lambda / L_{-1}\Lambda \,, \tag{2.3.6}$$

which can be decomposed as before

$$\widehat{\Lambda} = \bigoplus_{s=0}^{\infty} \widehat{\Lambda}_s \tag{2.3.7}$$

$$L_0\widehat{\Lambda}_s = s\widehat{\Lambda}_s \tag{2.3.8}$$

$$\bar{L}_0\widehat{\Lambda}_s = 0 \,. \tag{2.3.9}$$

Once conformal symmetry is broken one would expect these conserved charges to no longer exist and integrability to be lost. However, Zamolodchikov [21] has argued that for certain perturbations of conformal field theory, a sufficient number of conserved charges remain to allow all the states in the theory to be identified and

hence the theory to still be considered integrable. An outline of his argument is provided here. Consider a perturbation of a conformal field theory with an action related to that of the CFT by

$$\mathcal{A} = \mathcal{A}_{CFT} + \lambda \int \phi(z, \bar{z})\, d^2z \tag{2.3.10}$$

where $\phi$ is a field in the CFT with conformal weight $(h, h)$, and so scaling dimension $2h$. The coupling constant, $\lambda$, has conformal dimension $(1-h, 1-h)$ (scaling dimension $y = 2(1-h)$). For a relevant perturbation, $y > 0$ so $\phi$ is a relevant operator if $h < 1$. When $\lambda \neq 0$, $T_s$ will no longer satisfy (2.3.4). Instead $\partial_{\bar{z}} T_s$ can be expanded in a Taylor series

$$\partial_{\bar{z}} T_s = \lambda R^{(1)}_{s-1} + \lambda^2 R^{(2)}_{s-1} + \ldots \tag{2.3.11}$$

where the $R^{(n)}_{s-1}$ are assumed to be fields belonging to the CFT. The dimensions of $\partial_{\bar{z}} T_s$ and $\lambda$ are $(s, 1)$ and $(1-h, 1-h)$ respectively, so by comparing dimensions it is clear that the fields $R^{(n)}_{s-1}$ must have dimension

$$[R^{(n)}_{s-1}] = (s - n(1-h), 1 - n(1-h)). \tag{2.3.12}$$

For $n$ large enough, $1 - n(1-h) < 0$. However, all fields in unitary theories have positive conformal dimensions, so this series must terminate. This argument can clearly be extended to any non-unitary theories where the conformal dimensions of the fields are bounded from below. The only possible terms in the series are those fields in the CFT with conformal dimension

$$1 - n(1-h) = \Delta \tag{2.3.13}$$

which are easily identified as the dimensions of all the fields are known. In many cases, only the first term, with $n = 1$, is possible in which case

$$\partial_{\bar{z}} T_s = \lambda R^{(1)}_{s-1} \tag{2.3.14}$$

where $R^{(1)}_{s-1}$ has dimension $(h + s - 1, h)$ and so is a left descendant of the perturbing field $\phi$. The space, $\Phi$, of all left descendants of $\phi$ can be decomposed in the same way as $\Lambda$:

$$\Phi = \bigoplus_{s=0}^{\infty} \Phi_s\,, \tag{2.3.15}$$

where

$$L_0\Phi_s = (\Delta + s)\Phi_s \tag{2.3.16}$$

$$\bar{L}_0\Phi_s = \Delta\Phi_s\,, \tag{2.3.17}$$

so $\partial_{\bar{z}}$ can be considered as the linear map

$$\partial_{\bar{z}} : \Lambda_s \to \Phi_{s-1}. \tag{2.3.18}$$

For $T_s$ to be non-trivial, it must be non-zero in $\widehat{\Lambda} = \Lambda/L_{-1}\Lambda$ and for it to be a conserved charge, $R^{(1)}_{s-1}$ must be a total $z$-derivative, i.e. it must lie in $L_{-1}\Phi$. Its projection onto $\widehat{\Phi} = \Phi/L_{-1}\Phi$ must then be zero, so it must therefore lie in the kernel of the map

$$\partial_{\bar{z}} : \widehat{\Lambda}_s \to \widehat{\Phi}_{s-1}. \tag{2.3.19}$$

Conversely, if the kernel of this mapping is nonzero then a conserved charge must exist. This problem then boils down to checking the dimensions of the spaces $\widehat{\Lambda}_s$ and $\widehat{\Phi}_{s-1}$: the kernel will be nonzero, and so a conserved charge will exist, provided

$$\dim \widehat{\Lambda}_s > \dim \widehat{\Phi}_{s-1}. \tag{2.3.20}$$

Using this method, Zamolodchikov demonstrated the existence of a whole series of conserved charges for the minimal models perturbed by the operators $\phi_{13}$, $\phi_{12}$ and $\phi_{21}$ and so conjectured that these perturbations are integrable.

The continuity equation $\partial_\mu T^{\mu\nu} = 0$ for the stress energy tensor, written in coordinates $z$, $\bar{z}$ is

$$\partial_{\bar{z}} T = \partial_z \Theta \tag{2.3.21}$$

where $\Theta = -T_{z\bar{z}}$. This ensures the conservation of momentum of the theory, with IM

$$P_1 = \oint [T\,dz + \Theta\,d\bar{z}]\,. \tag{2.3.22}$$

Following this notation, the higher spin integrals of motion of the perturbed theory are

$$P_s = \oint [T_{s+1}dz + \Theta_{s-1}d\bar{z}] \tag{2.3.23}$$

where the local fields $T_{s+1}$ and $\Theta_{s-1}$ satisfy the relation

$$\partial_{\bar{z}} T_{s+1} = \partial_z \Theta_{s-1}. \tag{2.3.24}$$

A priori there is no reason why one cannot perturb a CFT by two or more relevant operators simultaneously. However, for the models of interest in this thesis, such a perturbation will not result in an integrable theory.

## 2.4 S matrices

For many cases, perturbing a CFT will result in a massive theory which, in the infrared region, can be described in terms of an S-matrix. In this section the constraints on this S-matrix, due to integrability, will be described and the method of building an S-matrix using the knowledge of the conserved charges of the theory will be discussed. Note that this S-matrix approach is naturally described in (1+1) Minkowski space, while the CFT description above was given in 2 dimensional Euclidean space. This discussion is based on the original paper by Zamolodchikov and Zamolodchikov [22], but mainly follows the review by Dorey [23].

Consider a theory with $n$ particles, each with a different mass $m_a$, $a = 1, \ldots, n$. These particles are on-shell when their light-cone momenta $p_a$, $\bar{p}_a$ satisfy the condition $p_a\bar{p}_a = m_a^2$. It will be convenient to parametrise these momenta in terms of the rapidity $\theta_a$

$$(p_a, \bar{p}_a) = (m_a e^{\theta_a}, m_a e^{-\theta_a}). \tag{2.4.1}$$

Denoting a particle of type $a_i$, moving with rapidity $\theta_i$, by $A_{a_i}(\theta_i)$, an n-particle asymptotic state can be written as

$$|A_{a_1}(\theta_1)A_{a_2}(\theta_2)\ldots A_{a_n}(\theta_n)\rangle. \tag{2.4.2}$$

An *in* state, is a state where there are no further interactions as $t \to -\infty$ so the particles must be ordered by rapidity, with the fastest on the left and the slowest on the right. Similarly, if there are no more interactions as $t \to \infty$, then the state is known as an *out* state, with the order of rapidities reversed. By considering the $A_{a_i}(\theta_i)$ as non-commuting symbols, the notation can be simplified and the *in* and *out* states can be written as

$$A_{a_1}(\theta_1)A_{a_2}(\theta_2)\ldots A_{a_n}(\theta_n) \tag{2.4.3}$$

with $\theta_1 > \theta_2 > \ldots \theta_n$ and $\theta_1 < \theta_2 < \ldots \theta_n$ respectively.

The S-matrix is a mapping between the *in*-state basis and the *out*-state basis. Given a 2-particle *in* state this is

$$A_{a_1}(\theta_1)A_{a_2}(\theta_2) = \sum_{n=2}^{\infty} \sum_{\theta'_1 < \ldots < \theta'_n} S_{a_1 a_2}^{b_1 \ldots b_n}(\theta_1, \theta_2; \theta'_1, \ldots, \theta_n) A_{b_1}(\theta'_1)\ldots A_{b_n}(\theta'_n) \tag{2.4.4}$$

where a sum on $b_1 \ldots b_n$ is implied and the sum on the $\theta'_i$ will, in general, involve a number of integrals. The rapidities are also constrained by momentum conservation.

A conserved charge, $Q_s$ of spin $s$ acts on a one-particle state as

$$Q_s|A_a(\theta)\rangle = q_a^{(s)} e^{s\theta}|A_a(\theta)\rangle. \tag{2.4.5}$$

Considering only local conserved charges, which are integrals of local densities, their action on multiparticle wavepackets is additive:

$$Q_s|A_{a_1}(\theta_1)\dots A_{a_n}(\theta_n)\rangle = (q_{a_1}^{(s)} e^{s\theta_1} + \dots + q_{a_n}^{(s)} e^{s\theta_n})|A_{a_1}(\theta_1)\dots A_{a_n}(\theta_n)\rangle. \tag{2.4.6}$$

The momentum operator ($Q_1$) will act on a state by shifting all the particles by a fixed amount. However, in general, the higher spin operators will shift particles by an amount dependent on their initial rapidity. Parke [24], using this argument, found that provided there exists a couple of conserved charges with spin $s > 1$, then the scattering matrix for a $1+1$ dimensional theory has several constraints placed upon it:

- there is no particle production
- the initial and final sets of momenta are equal
- the S-matrix factorises into a product of $2 \to 2$ S-matrices.

These constraints are particular to $1+1$ dimensions; for higher dimensions, the Coleman-Mandula theorem [25] states that the existence of a conserved charge of spin $s \geq 2$ leads to a trivial S-matrix.

From these constraints, it is clear that the fundamental object is the $2 \to 2$ S-matrix, $A_{a_1}(\theta_1)A_{a_2}(\theta_2) = S_{a_1 a_2}^{b_1 b_2}(\theta_1 - \theta_2)A_{b_1}(\theta_1)A_{b_2}(\theta_2)$. Once this is known for all particles then the full S-matrix is known. As a Lorentz boost shifts the rapidities by a constant, the S-matrix will depend on rapidity difference, $\theta_{12} = \theta_1 - \theta_2$, only.

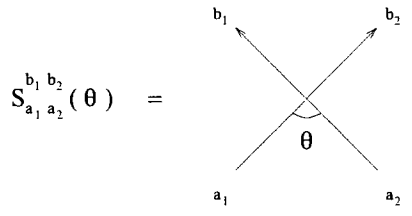


Figure 2.5: The two particle S-matrix

In a theory with $n$ particles, there are $n^4$ functions $S_{a_1 a_2}^{b_1 b_2}$, however not all of these will be independent. Firstly, momentum conservation demands that $m_{a_1} = m_{b_1}$ and

$m_{a_2} = m_{b_2}$, so unless there is a degenerate mass spectrum $a_1 = b_1$ and $a_2 = b_2$. It is also assumed that $P$, $C$ and $T$ symmetries hold which impose the condition

$$S_{a_1 a_2}^{b_1 b_2}(\theta) = S_{\bar{a}_1 \bar{a}_2}^{\bar{b}_1 \bar{b}_2}(\theta) = S_{b_2 b_1}^{a_2 a_1}(\theta). \tag{2.4.7}$$

The analytic properties of the S-matrix are most easily understood when described in terms of the Mandelstam variables

$$s = (p_1 + p_2)^2\,,\; t = (p_1 - p_3)^2\,,\; u = (p_1 - p_4)^2 \tag{2.4.8}$$

where $s+t+u = \sum_{i=1}^{4} m_i^2$. Here $p_1$ and $p_2$ are the momenta of the incoming particles and $p_3$ and $p_4$ that of the outgoers. In $1+1$ dimensions only one of these variables is independent, so choosing $s$ and writing it in terms of the rapidities

$$s = m_i^2 + m_j^2 + 2m_i m_j \cosh(\theta_1 - \theta_2). \tag{2.4.9}$$

For a physical process, the rapidities are real and so $s$ must be real and $s \geq (m_i + m_j)^2$. Continuing S into the complex plane it is single valued, once suitable cuts, as shown in figure 2.6, have been made. $S(s)$ is real for real $s$ satisfying $(m_i - m_j)^2 \leq s \leq (m_i + m_j)^2$ and physical values occur for $s = s^+$ just above the right hand cut, as shown in figure 2.6. $S(s)$ is also real-analytic, i.e. $S_{ij}^{kl}(s^*) = \left(S_{ij}^{kl}(s)\right)^*$ holds,

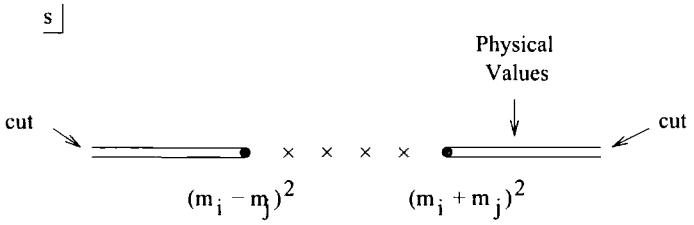


Figure 2.6: Cuts in the complex plane

where $*$ denotes complex-conjugate. Unitarity requires that for physical values of $s$ ($s^+ = s + i\epsilon$, $\epsilon \to 0$, $s > (m_i + m_j)^2$), $S(s)S^\dagger(s) = 1$. Since there is no particle production in this case this corresponds to

$$S_{ij}^{kl}(s^+)\left(S_{kl}^{nm}(s^+)\right)^* = \delta_i^n \delta_l^m \tag{2.4.10}$$

and using the real-analycity property this becomes

$$S_{ij}^{kl}(s^+) S_{kl}^{nm}(s^-) = \delta_i^n \delta_l^m \tag{2.4.11}$$

where $s^- = s - i\epsilon$, $\epsilon \to 0$.

Having so far discussed only the right hand cut, the left hand can be understood using the relativistic property of crossing. This involves taking particles involved in an interaction and inverting their paths in time so that incoming particles become outgoing and vice versa. If one incoming particle and one outgoing particle are simultaneously "crossed" then the result should be another physical process. Here this corresponds to looking at the diagram 2.5 from the side, so the forward channel momenta is $t = (p_1 - p_3)^2$, rather than $s$. Since $p_2 = p_3$ here, there is a simple relation between $s$ and $t$

$$t = (p_1 - p_2)^2 = 2m_i^2 + 2m_j^2 - s. \tag{2.4.12}$$

The amplitude for this process can be obtained from the previous amplitude by analytic continuation into a region where $t$ is now physical. This is where $t$ is real and $t \geq (m_i + m_j)^2$ which corresponds to $s \leq (m_i - m_j)^2$. Physical amplitudes correspond to approaching this from above in $t$, and so from below in $s$, therefore they occur on the lower edge of the left hand cut in figure 2.6. So this is just

$$S_{ij}^{kl}(s^+) = S_{i\bar{l}}^{k\bar{j}}(2m_i^2 + 2m_j^2 - s^+) \tag{2.4.13}$$

which simplifies when written in terms of the rapidity $\theta$, using the transformation

$$\begin{aligned} \theta &= \cosh^{-1}\left(\frac{s - m_i^2 - m_j^2}{2m_i m_j}\right) \qquad (2.4.14) \\ &= \log\left(\frac{1}{2m_i m_j}\left(s - m_i^2 - m_j^2 + \sqrt{(s - (m_i + m_j)^2)(s - (m_i - m_j)^2)}\right)\right). \end{aligned}$$

This maps the physical sheet into the physical strip $0 \leq \Im m\,\theta \leq \pi$, with the unphysical sheets mapped into the strips $n\pi \leq \Im m\,\theta \leq (n+1)\pi$. The cuts open up and the branch points go to 0 and $\pi$. Rewriting the constaints in terms of $\theta$:

- Real analycity: $S(\theta)$ is real for $\theta$ purely imaginary
- Unitarity: $S_{ij}^{nm}(\theta)S_{nm}^{kl}(-\theta) = \delta_i^k \delta_j^l$
- Crossing: $S_{ij}^{kl}(\theta) = S_{i\bar{l}}^{k\bar{j}}(i\pi - \theta)$.

The factorisation property also gives rise to the Yang-Baxter equation

$$S_{ij}^{\beta\alpha}(\theta_{12})S_{\beta\gamma}^{n\gamma}(\theta_{13})S_{\alpha\gamma}^{ml}(\theta_{23}) = S_{jk}^{\beta\gamma}(\theta_{23})S_{i\gamma}^{\alpha l}(\theta_{13})S_{\alpha\beta}^{nm}(\theta_{12}) \tag{2.4.15}$$

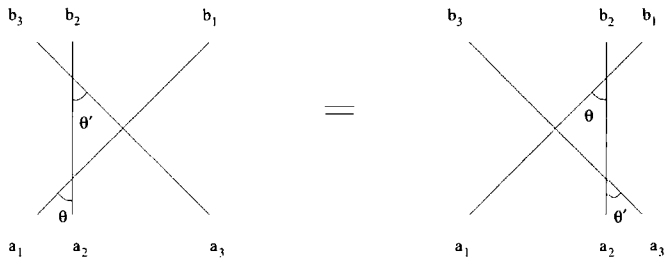


Figure 2.7: The Yang-Baxter equation

shown diagrammatically in figure 2.7. This constraint, along with the properties above usually allow the S-matrix to be fixed, up to the "CDD" ambiguity

$$S_{ij}^{kl}(\theta) \to S_{ij}^{kl}(\theta)\Phi(\theta) \tag{2.4.16}$$

where the CDD factor must satisfy

$$\Phi(\theta) = \Phi(i\pi - \theta)\,,\ \Phi(\theta)\Phi(-\theta) = 1. \tag{2.4.17}$$

Further restrictions come from the bootstrap. The discussion of this will be restricted to the purely elastic scattering theories (PEST) as they are the only theories of concern in the remainder of this thesis. These are theories with no degeneracy in the spectrum so the scattering is diagonal. The S matrix for these theories needs only two indices and the unitarity condition becomes

$$S_{ij}(\theta)S_{ij}(-\theta) = 1 \tag{2.4.18}$$

and the crossing symmetry is

$$S_{ij}(\theta) = S_{i\bar{j}}(i\pi - \theta). \tag{2.4.19}$$

Combining these two constraints reveals the periodicity of the S-matrix

$$S_{ij}(\theta + 2\pi i) = S_{ij}(\theta). \tag{2.4.20}$$

The Yang-Baxter equation is trivially satisfied for these theories.

Simple poles in the physical strip of an S-matrix element are often associated with bound states in the spectrum. This is not always the case; exceptions will be mentioned later. A bound state occurring in the forward (s) channel, with fusing

angle $U_{ij}^k$ will correspond to a simple pole in the physical strip, at $\theta_{ij} = iU_{ij}^k$. Around this pole the S-matrix can be considered as

$$S_{ij}(\theta) \approx i\frac{C^{ijk}C^{ijk}}{\theta - iU_{ij}^k} \tag{2.4.21}$$

where $C^{ijk}$ is the three point coupling associated with the bound state. For unitary theories this three point coupling is real and so this pole will have a positive residue and will always be paired with another simple pole, at $\theta_{ij} = \pi - iU_{ij}^k$, with negative residue, corresponding to the same bound state in the crossed (t) channel, see figure 2.8. For non-unitary theories, the distinction between the forward and crossed

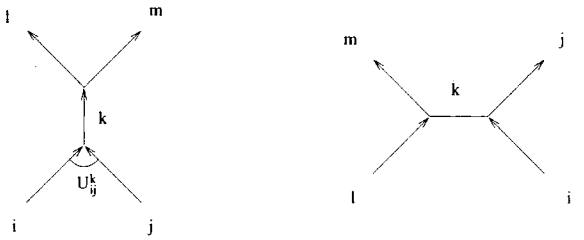


Figure 2.8: A bound state, shown in the forward and crossed channels

channels is not so clear as the residues will not necessarily be positive and negative respectively since $C^{ijk}$ will not always be real. The intermediate particle $k$ is on-shell, so should be long-lived, and by the boostrap principle, is expected to be one of the other asymptotic one-particle states of the model. For the forward channel process, since the internal particle $k$ is on-shell, $s = m_k^2$ and so

$$m_k^2 = m_i^2 + m_j^2 + 2m_i m_j \cos U_{ij}^k. \tag{2.4.22}$$

This implies that $U_{ij}^k$ is the exterior angle of a 'mass triangle' of sides $m_i$, $m_j$ and $m_k$, shown in figure 2.9. Therefore the fusing angles satisfy

$$U_{ij}^k + U_{jk}^i + U_{ki}^j = 2\pi \tag{2.4.23}$$

as one might expect from figure 2.8.

If a third particle interacts with a bound state, this interaction could occur before or after the bound state is formed. However, the factorisation condition implies that these cases cannot be distinguished, which leads to the bootstrap equation

$$S_{l\bar{k}}(\theta) = S_{li}(\theta - i\bar{U}_{ki}^j)S_{lj}(\theta + i\bar{U}_{jk}^i) \tag{2.4.24}$$

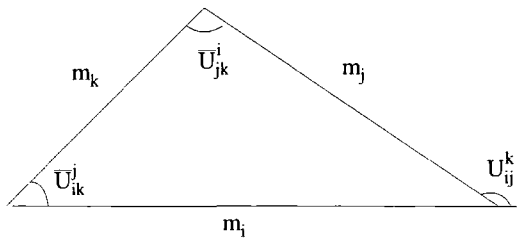


Figure 2.9: The mass triangle

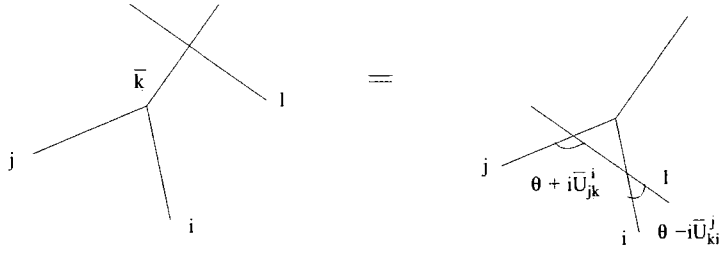


Figure 2.10: The bootstrap

where $\bar{U} = \pi - U$. This is shown pictorially in figure 2.10. There is an equivalent constraint for the conserved charges which comes about when one considers the action of one of the conserved charges, given by (2.4.6), on the state before and after fusing. Equating these leads to the conserved charge bootstrap

$$q_{\bar{k}}^{(s)} = q_i^{(s)} e^{is\bar{U}_{ki}^j} + q_j^{(s)} e^{-is\bar{U}_{kj}^i} \tag{2.4.25}$$

which can be put into a symmetrical form, using $q_{\bar{k}}^{(s)} = (-1)^{s+1} q_k^{(s)}$

$$q_i^{(s)} + q_j^{(s)} e^{isU_{ij}^k} + q_k^{(s)} e^{is(U_{ij}^k + U_{jk}^i)} = 0. \tag{2.4.26}$$

So far only simple poles have been discussed, but higher order poles also occur in S-matrix elements. The explanation for these poles is given by the Coleman-Thun mechanism [26]; the discussion of this presented here follows [27]. For a given Feynman diagram, if the external momenta are such that one or more of the internal propagators are on-shell then the loop integrals will give rise to a singularity in the amplitude. The bound states described here are examples of this, where one propagator, the bound state particle, is on-shell. In three or more dimensions, all singularities which do not correspond to bound states appear as branch points, but in $1 + 1$ dimensions they are poles. These poles correspond to more complicated diagrams composed of entirely on-shell particles (known as Landau diagrams). An

example of such a diagram, which would produce a double pole in the relevant S-matrix element, is shown in figure 2.11. For a diagram with $P$ propagators and $L$

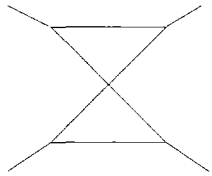

Figure 2.11: Example of a Landau diagram

loops, the corresponding pole has order $p = P - 2L$. This, however, is not yet the whole story as not every simple pole corresponds to a bound state, so one needs to find a way to reduce the order of a second order diagram to explain such simple poles. An obvious way that this can occur is if one of the 'internal' S-matrix elements has a zero at the necessary rapidity. Alternatively, if more than one diagram can be drawn, for fixed external lines, then these diagrams must be added together with appropriate relative weights. If cancellation occurs between the different diagrams then the overall order of the pole is lower than would be expected from the individual diagrams.

To illustrate how one can build an S-matrix the example of the Ising model in a magnetic field will be discussed. Zamolodchikov [28] showed that, for this theory, local conserved charges exist with the spins

$$s = 1,\ 7,\ 11,\ 13,\ 17,\ 19, \tag{2.4.27}$$

and so conjectured that this model is integrable. Zamolodchikov's $c$-theorem [29] states that for a perturbed CFT there is a function of the coupling constants which decreases along the RG flow and is stationary only at fixed points. At these points it is equal to the central charge of the corresponding theory. Physically one can think of this as some kind of entropy function which measures the loss of information in the coarse-graining procedure of the renormalisation group. Since the central charge of the Ising model is $c = 1/2$ and there is no unitary CFT with $c$ less than this, by this $c$-theorem the perturbed theory must be massive and so an $S$-matrix will exist.

The search for the $S$-matrix begins by assuming the existence of a particle of mass $m_1$, and for simplicity take the model to have diagonal scattering. Since the $\mathbb{Z}_2$ symmetry of the model is broken by the perturbation, a $\phi^3$ type interaction is not

ruled out so one can assume that the 3-point coupling $C^{111} \neq 0$. The mass triangle is then an equilateral, with all the fusing angles equal to $2\pi/3$. The conserved charge bootstrap equation is

$$q_1^{(s)} + q_1^{(s)} e^{2\pi i s/3} + q_1^{(s)} e^{4\pi i s/3} = 0. \tag{2.4.28}$$

This has a non-trivial solution whenever $s$ has no common divisor with 6

$$s = 1, 5, 7, 11, 13, 17, \ldots \tag{2.4.29}$$

This is close to the spin 'fingerprint' of the model, however there are still too many spins so Zamolodchikov introduced a second particle with mass $m_2$ and nonzero coupling $C^{112}$ and $C^{122}$, so $A_2$ can be interpreted as the 'bound state' $A_1 A_1$ and vice versa. Let $y_1 = \exp(iU_{21}^1)$ and $y_2 = \exp(iU_{12}^2)$ then the conserved charge bootstap equations are

$$C^{121} \neq 0 \quad \Rightarrow \quad q_1^{(s)} + q_2^{(s)} y_1^s + q_1^{(s)} y_1^{2s} = 0 \tag{2.4.30}$$

$$C^{212} \neq 0 \quad \Rightarrow \quad q_2^{(s)} + q_1^{(s)} y_2^s + q_2^{(s)} y_2^{2s} = 0. \tag{2.4.31}$$

Eliminating $q_1^{(s)}$ and $q_2^{(s)}$ from the above gives

$$(y_1^s + y_1^{-s})(y_2^s + y_2^{-s}) = 1. \tag{2.4.32}$$

This is satisfied by $y_1 = \exp(4\pi i/5)$ and $y_2 = \exp(3\pi i/5)$, for any odd $s$ which is not a multiple of 5, which corresponds to the following set of fusing angles

$$U_{12}^1 = U_{21}^1 = 4\pi/5 \quad , \quad U_{11}^2 = 2\pi/5 \tag{2.4.33}$$

$$U_{21}^2 = U_{12}^2 = 3\pi/5 \quad , \quad U_{22}^1 = 4\pi/5 \tag{2.4.34}$$

and the mass ratio

$$m_2 = 2\cos(\pi/5) m_1. \tag{2.4.35}$$

By introducing this second particle the unwanted spins are eliminated and attention can now be turned to the S-matrix. This will be built from the blocks

$$(x)(\theta) = \frac{\sinh(\frac{\theta}{2} + \frac{i\pi x}{60})}{\sinh(\frac{\theta}{2} - \frac{i\pi x}{60})} \tag{2.4.36}$$

which are unitary, and when combined with the blocks $(30 - x)$, also satisfy the crossing symmetry property. The choice of 60 here is to ensure that the $x$ is always an integer. Each block has a single physical-strip pole at $i\pi x/30$ and from the fusing

angles $U_{11}^1$ and $U_{11}^2$ above the positions of the two forward channel poles are known. Therefore, incorporating these and their crossed channel partners the S-matrix element $S_{11}$ must contain the blocks (10)(12)(18)(20). However, the bootstrap equation for the $\phi^3$ interaction $11 \rightarrow 1$ requires that $S_{11}(\theta - i\pi/3)S_{11}(\theta + i\pi/3) = S_{11}(\theta)$. For this to be satisfied, an extra factor $-(2)(28)$ must be included. These are the forward and crossed channel poles corresponding to another particle with mass $m_3 = 2m_1 \cos(\pi/30)$. This procedure can be repeated for the $11 \rightarrow 2$ and $11 \rightarrow 3$ fusings, introducing new particles (and more bootstrap constraints) each time a single pole, with positive residue, and its crossed channel partner are needed to satisfy the constraints. This system closes on 8 particle types, each with a different mass, $m_i$, which together form the Perron-Frobenius eigenvector of the Cartan matrix of the Lie algebra $E_8$.

## 2.5 Thermodynamic Bethe Ansatz

The S matrices described above are conjectured to be the IR limit of a perturbed CFT. However, weight can be added to these conjectures by verifying that the UV limit of the perturbations are indeed the proposed CFTs. One can do this by implementing a technique known as the Thermodynamic Bethe Ansatz (TBA) [30].

Begin by considering a relativistic quantum field theory defined on a torus with the two periods, $L$ and $R$, as shown in figure 2.12. The aim will be to take the limit $R \rightarrow \infty$ to recover an infinitely long cylinder of circumference $L$.

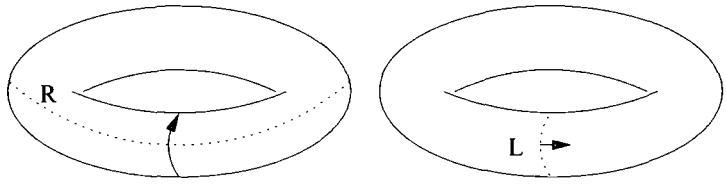


Figure 2.12: The two periods of a torus

There are two ways to set up the Hamiltonian description on a torus. On one hand states can be chosen to lie on the circle $L$, with time in the $R$ direction, as shown on the right of figure 2.12. These states are evolved by the Hamiltonian $H_L$ and are quantised with momenta $2\pi n/L$, $n \in \mathbb{Z}$. Taking the limit $R \rightarrow \infty$, the partition function, $Z(R, L) = Tr(e^{-RH_L})$, will be dominated by the ground state of

$H_L$ with energy $E_0(L)$:

$$Z(R, L) \sim e^{-RE_0(L)}. \tag{2.5.1}$$

Alternatively, one could take the states to lie along $R$, evolving in the time-like direction $L$ under the Hamiltonian $H_R$. The states are now quantised with momenta $2\pi n/R$ and the partition function is $Z(R, L) = Tr(e^{-LH_R})$. Recall from section 2.1 that the free energy of the system can be written in terms of the partition function as $F = -T \ln Z$, where the temperature $T$ now includes the Boltzmann constant. Here, the system is considered as a 1-dimensional system at a temperature $T = 1/L$. When the system size is large (so as $R \to \infty$), the free energy behaves as

$$F(L) = Rf(L) + O(R^{-1}) \tag{2.5.2}$$

where $f(L)$ is known as the bulk free energy per unit volume

$$f(L) = \lim_{R\to\infty} \frac{F(L)}{R} \tag{2.5.3}$$

(see, for example, [31] for more details). The partition function, in the limit $R \to \infty$ therefore behaves as

$$\ln Z(R, L) \sim -RLf(L)\,. \tag{2.5.4}$$

Equating these two descriptions gives the relation

$$E_0(L) = Lf(L). \tag{2.5.5}$$

The Hilbert space $\mathcal{H}_R$, is expected to be given by scattering states in the $R \to \infty$ limit, so one has some control over $\mathcal{H}_R$ which allows a quantisation condition to be written down and the limit of $Z$ to be found. The aim is then to evaluate the free energy using saddle point techniques, i.e. minimising the free energy subject to the constraint imposed by the quantisation condition. The ground state energy can then be read off from the result using the relation (2.5.5).

For simplicity, the TBA equations for a purely elastic scattering theory with $N$ identical particles, each with mass $M$, with two-particle scattering amplitude $S(\theta)$ will be derived. Consider a region of configuration space where the $N$ particles are all well separated, i.e. the distance between adjacent particles is much larger than the correlation length $1/M$. The off-mass-shell effects can then be neglected and the particles treated as if they are free, with on-shell energy and momenta $E_j =$

$M\cosh(\theta_j)$ and $p_j = M\sinh(\theta_j)$. This is valid provided $R >> 1/M$. In this region the N-particle state can be described by a Bethe wave function $\psi(x_1, \ldots, x_N) = A(Q)\exp(i\sum_j p_j x_j)$ where $A(Q)$ is a function dependent on the configuration of the particles whose exact form is not important here.

If two particles with initial positions $x_j << x_{j+1}$ approach one another, interact and move apart with their positions reversed to the point where $x_{j+1} << x_j$, the situation will again be such that the state can be described by a Bethe wave function as above. However, as a result of this interaction, the original wave function must be multiplied by the scattering amplitude $S(\theta_j - \theta_{j+1})$. The particle $x_j$ can be sent around the torus, in the direction $R$, with the wave function picking up an S-matrix contribution each time $x_j$ encounters another particle. Of course, when the particle returns to its original position, the wave function must equal the original. This periodicity imposes a quantisation condition on the momentum $p_j$, $j = 1, \ldots, N$:

$$e^{ip_j R}\prod_{i\neq j} S(\theta_j - \theta_i) = 1\,. \tag{2.5.6}$$

Taking the logarithm of this leads to a set of conditions on the rapidities $\theta_j$

$$MR\sinh(\theta_j) - i\sum_{i\neq j}\ln S(\theta_j - \theta_i) = 2\pi n_j \tag{2.5.7}$$

with $N$ integer numbers $n_j$.

This is quite a complicated system of transcendental equations but they become more tractable in the thermodynamic limit $R \to \infty$. The limit $N \to \infty$ must also be taken, where $N$ is the number of particles, so the density $N/R$ remains finite. In this limit the spectrum of rapidities condenses as the distance between adjacent rapidities $\theta_j - \theta_{j+1} \sim 1/MR$ so it becomes sensible to introduce a continuous density of particles, $\rho^r(\theta)$, which is defined as

$$\rho^r(\theta) = \frac{d}{\Delta\theta} \tag{2.5.8}$$

where $d$ is the number of particles with rapidity between $\theta$ and $\theta + \Delta\theta$. This is independent of the choice of interval $\Delta\theta$, provided $1/MR << \Delta\theta << 1$. The sum in (2.5.7) can now be replaced with an integral

$$MR\sinh\theta_j - i\int \ln S(\theta_j - \theta')\rho^r(\theta')\,d\theta' = 2\pi n_j\,. \tag{2.5.9}$$

This equation has solutions, $\theta$, for all integer $n$, not just the integers $n_j$ corresponding to an actual state. The rapidities $\theta$ corresponding to $n \neq n_j$ are known as holes, and the $\theta_j$ roots. The above equation can be differentiated to give an equation relating the root density $\rho^r(\theta)$ to the level density $\rho(\theta)$ (density of roots plus holes):

$$MR\cosh(\theta) + 2\pi \int \varphi(\theta - \theta')\rho^r(\theta')\, d\theta' = 2\pi\rho(\theta) \tag{2.5.10}$$

where $\varphi(\theta)$ is related to the $S$ matrix via $\varphi(\theta) = -\frac{i}{2\pi}\frac{d}{d\theta}\ln S(\theta)$.

If the theory consists of particles of 'fermionic' type then each state can only be occupied by one particle so the maximum number of rapidities in the interval $(\theta, \theta + \Delta\theta)$ is $D = \rho(\theta)\Delta\theta$. The actual number of roots in this interval is $d$, written in terms of the density $\rho^r(\theta)$ above. The densities $\rho$ and $\rho^r$ are insensitive to the exact configuration of roots so the number of different quantum states corresponding to each pair $\rho$ and $\rho^r$ is

$$\mathcal{N}(\rho, \rho^r) = \frac{D!}{d!(D-d)!}\,. \tag{2.5.11}$$

In the thermodynamic limit, the logarithm of this quantity gives the contribution of the rapidity interval $\Delta\theta$ to the entropy $\mathcal{S}$. By replacing the factorials above, using Stirling's formula $\ln\Gamma(z) \sim z\ln z - z + \ldots$, the entropy can be written as

$$\mathcal{S}(\rho, \rho^r) = \ln\mathcal{N}(\rho, \rho^r) = \int \rho\ln\rho - \rho^r\ln\rho^r - (\rho - \rho^r)\ln(\rho - \rho^r)\, d\theta\,. \tag{2.5.12}$$

Now the partition function, in the limit $R \to \infty$ becomes

$$\begin{aligned} Z(R, L) &= Tr_{\{\rho,\rho^r\}}\mathcal{N}(\rho, \rho^r)e^{-LH_R} \\ &= Tr_{\{\rho,\rho^r\}}e^{-LH_R + \mathcal{S}(\rho,\rho^r)} \end{aligned} \tag{2.5.13}$$

and total energy of the system, in terms of the density $\rho^r$ is

$$H_R(\rho^r) = \int M\cosh(\theta)\rho^r(\theta)\, d\theta\,. \tag{2.5.14}$$

Since $\ln Z(R, L) \sim -RLf(\rho, \rho^r)$ as $R \to \infty$, comparing this to (2.5.13), one can write the free energy as

$$\begin{aligned} -RLf(\rho, \rho^r) = \int [&-ML\cosh(\theta)\rho^r(\theta) + \rho(\theta)\ln\rho(\theta) - \rho^r(\theta)\ln\rho^r(\theta) \\ &-(\rho(\theta) - \rho^r(\theta))\ln(\rho(\theta) - \rho^r(\theta))]\, d\theta\,. \end{aligned} \tag{2.5.15}$$

The thermal equilibrium configuration can be obtained by minimising the free energy per unit length, $f$, with respect to $\rho$ and $\rho^r$, i.e. set $\delta(2.5.15)/\delta\rho^r(\theta) = 0$ where

$$\frac{\delta(2.5.15)}{\delta\rho^r(\theta)} = \frac{\partial(2.5.15)}{\partial\rho^r(\theta)} + \int \frac{\delta\rho(\theta')}{\delta\rho^r(\theta)} \frac{\partial(2.5.15)}{\partial\rho(\theta')}\, d\theta' . \tag{2.5.16}$$

The constraint (2.5.10) allows $\rho$ to be treated as a functional of $\rho^r$ and from this it is clear that

$$\frac{\delta\rho(\theta')}{\delta\rho^r(\theta)} = \varphi(\theta - \theta') \tag{2.5.17}$$

and it is also easy to show that

$$\frac{\delta}{\delta\rho^r(\theta')} \left(\rho^r(\theta) \ln \rho^r(\theta)\right) = \left(1 + \ln \rho^r(\theta)\right) \delta(\theta - \theta') \tag{2.5.18}$$

and

$$\begin{aligned} \frac{\delta}{\delta\rho^r(\theta')} \left(\left(\rho(\theta) - \rho^r(\theta)\right) \ln(\rho(\theta) - \rho^r(\theta))\right) = \\ - \left(1 + \ln(\rho(\theta) - \rho^r(\theta)\right) \delta(\theta - \theta') . \end{aligned} \tag{2.5.19}$$

The derivatives of (2.5.15) with respect to $\rho^r$ and $\rho$ depend on these densities only through the ratio $\rho^r/\rho$ and since $\rho(\theta) > \rho^r(\theta)$ it is useful to set

$$\frac{\rho^r(\theta)}{\rho(\theta) - \rho^r(\theta)} = e^{-\epsilon(\theta)} \tag{2.5.20}$$

where $\epsilon(\theta)$ is a real function known as the pseudoenergy. In terms of this, the derivatives of (2.5.15) are

$$\begin{aligned} \frac{\partial(2.5.15)}{\partial\rho^r(\theta)} &= -ML\cosh(\theta) - \ln\left(\frac{\rho^r(\theta)}{\rho(\theta) - \rho^r(\theta)}\right) \\ &= -ML\cosh(\theta) + \epsilon(\theta) \end{aligned} \tag{2.5.21}$$

and

$$\frac{\partial(2.5.15)}{\partial\rho(\theta)} = \ln\left(\frac{\rho(\theta)}{\rho(\theta) - \rho^r(\theta)}\right) = \ln\left(1 + e^{-\epsilon(\theta)}\right) . \tag{2.5.22}$$

So setting $\delta(2.5.15)/\delta\rho^r(\theta) = 0$ leads to a nonlinear integral equation known as the TBA equation:

$$\epsilon(\theta) = ML\cosh(\theta) - \int \varphi(\theta - \theta') \ln(1 + e^{-\epsilon(\theta)})\, d\theta'. \tag{2.5.23}$$

This TBA equation can now be used to simplify the expression of the free energy in (2.5.15). Denote the integrand in (2.5.15) by $I$ and writing this in terms of the pseudoenergy, $\epsilon(\theta)$, gives

$$I = -ML\cosh(\theta)\rho^r(\theta) + \rho(\theta)\ln(1 + e^{-\epsilon(\theta)}) + \rho^r(\theta)\epsilon(\theta) . \tag{2.5.24}$$

The constraint (2.5.10) can be used to replace $\rho(\theta)$ here, leaving

$$\begin{aligned} I = &- ML\cosh(\theta)\rho^r(\theta) + \frac{1}{2\pi}MR\cosh(\theta)\ln(1+e^{-\epsilon(\theta)}) \\ &+ \int \varphi(\theta-\theta')\rho^r(\theta')\,d\theta'\,\ln(1+e^{-\epsilon(\theta)}) + \rho^r(\theta)\epsilon(\theta)\,. \end{aligned} \tag{2.5.25}$$

This can be simplified using the TBA equation (2.5.23) to give

$$I = \frac{1}{2\pi}MR\cosh(\theta)\ln(1+e^{-\epsilon(\theta)})\,, \tag{2.5.26}$$

so the extremal free energy per unit length is then

$$f(L) = -\frac{1}{2\pi L}\int M\cosh(\theta)\ln(1+e^{-\epsilon(\theta)})\,d\theta\,. \tag{2.5.27}$$

Recall that the free energy is related to the ground state energy through $E_0(L) = Lf(L)$ and so

$$E_0(L) = -\frac{1}{2\pi}\int M\cosh(\theta)\ln(1+e^{-\epsilon(\theta)})\,d\theta\,. \tag{2.5.28}$$

The regularisation implicit in the TBA derivation sets the bulk free energy, $\mathcal{E}LM^2$, to zero so $E_0(L)$ given above is actually the Casimir energy. Comparing this to the Casimir energy of a CFT, $E_0 = -\pi c/6L$, one can define the effective central charge, or ground state scaling function, as

$$c_{\text{eff}}(l) = \frac{3l}{\pi^2}\int d\theta\,\cosh(\theta)\ln(1+e^{-\epsilon(\theta)})\,. \tag{2.5.29}$$

This is dependent on the dimensionless parameter $l = ML$. This will vanish as $l \to \infty$ which corresponds to the IR limit of the perturbed theory. The UV limit, when the CFT is recovered, corresponds to $l \to 0$. In this case the scaling function is related to the central charge of the CFT:

$$\lim_{l\to 0} c_{\text{eff}}(l) = c - \Delta_0\,. \tag{2.5.30}$$

Here $\Delta_0$ is the lowest scaling dimension of the CFT and since $\Delta_0 = 0$ for unitary theories, $c_{\text{eff}}(0) = c$ for those cases. This effective central charge provides a useful tool to check the validity of conjectured S-matrices for perturbed conformal field theories.

This description was extended to cover the diagonal purely elastic scattering theories associated to the ADE type Lie algebras in [32][33]. The number of particles in these theories corresponds to the rank $r$ of the algebra. The TBA system then consists of $r$ pseudoenergies, each associated with a particle of mass $m_a$, which satisfy

$$\epsilon_a = m_a L\cosh(\theta) - \sum_{b=1}^{r}\int d\theta'\,\phi_{ab}(\theta-\theta')\ln(1+e^{-\epsilon_b(\theta')}) \tag{2.5.31}$$

where $\phi_{ab}(\theta)$ is related to the scattering amplitude $S_{ab}(\theta)$

$$\phi_{ab}(\theta) = -\frac{i}{2\pi}\frac{d}{d\theta}S_{ab}(\theta)\,. \tag{2.5.32}$$

The Casimir energy can be written in terms of these pseudoenergies as

$$E(L) = -\frac{1}{2\pi}\sum_{a=1}^{r} m_a \int d\theta\, \cosh(\theta)\ln(1+e^{-\epsilon(\theta)})\,. \tag{2.5.33}$$

Zamolodchikov [34] found the following universal form for these TBA equations in terms of the incidence matrix $A_{ba}^{[\mathbf{G}]}$ of the associated Lie algebra:

$$\epsilon_a(\theta) = m_a L\cosh(\theta) - \frac{1}{\pi}\sum_{b=1}^{r}\int d\theta'\, A_{ba}^{[\mathbf{G}]}\varphi_h(\theta-\theta')\left(m_b L\cosh(\theta') - \ln(1+e^{\epsilon_b(\theta')})\right) \tag{2.5.34}$$

where the universal kernel, $\varphi_h$, now depends only on the Coxeter number, $h$, of the Lie algebra

$$\varphi_h(\theta) = \frac{h}{2\cosh(\frac{1}{2}h\theta)}. \tag{2.5.35}$$

He then remarked that these TBA equations encode one particular solution of a system of functional equations, known as the $Y$-system:

$$Y_a(\theta+i\pi/h)Y_a(\theta-i\pi/h) = \prod_{b=1}^{r}(1+Y_b(\theta))^{A_{ba}^{[\mathbf{G}]}} \tag{2.5.36}$$

where $Y_a(\theta) = \exp(\epsilon_a(\theta))$. By successive substitutions of (2.5.36) into itself, it can be shown (case by case) that these $Y$-functions are periodic

$$Y_a(\theta + i\pi(h+2)/h) = Y_a(\theta). \tag{2.5.37}$$

There are also various proofs for this conjecture [35, 36, 37, 38, 39, 40]. This observation has important consequences as it implies that the $Y$ functions admit the Laurent expansions

$$Y_a(\theta) = \sum_{k=-\infty}^{\infty} Y_a^{(k)} e^{\frac{2h\theta}{h+2}k} \tag{2.5.38}$$

and, as $L \to 0$, the functions $\ln(1+e^{-\epsilon_a(\theta)})$ acquire the form of a plateau of approximately constant height in the central region $-\ln(1/ML) << \theta << \ln(1/ML)$. It then follows that the function $L\big(E(L) - \mathcal{E}LM^2(\lambda)\big)/2\pi = -c_{\text{eff}}(l)/12$ can be expanded as a perturbative series in $L^{4h/(h+2)}$ [34].

These TBA equations correspond to perturbations resulting in massive quantum field theories. However, some perturbations of CFTs lead to massless theories in the

IR limit, which are necessarily RG fixed points. These RG flows therefore interpolate between two conformal field theories. The $\phi_{13}$ flows between the Virasoro minimal models are examples of this [29]. In these cases, the derivation of the TBA equations is not so straightforward so Al. Zamolodchikov [41][42][43] instead developed a strategy of making an educated guess of the TBA equations and then testing them by checking that they correctly reproduced UV data, such as the central charge of the UV CFT and the dimension of the perturbing operator. Perhaps more interestingly, Al. Zamolodchikov [44] also proposed a simple diagonal scattering theory, known as the 'staircase model', from which the TBA equations follow in the standard way, shown here. Numerical investigations of the solutions to these equations show the vacuum energy, which is proportional to the effective central charge, following a staircase type pattern which suggests there is an underlying theory whose RG flow passes by a sequence of $c < 1$, i.e. Virasoro minimal model, fixed points. This was extended to cover the $W_g$ minimal models in [45][46][47], however, as this thesis is concerned with perturbations resulting in massive scattering theories, no more will be said about these models here.

## 2.6 'ODE/IM' Correspondence

This section introduces a curious and useful link between functional relations of integrable models and spectral problems of ODEs, first found by Dorey and Tateo in [48]. These functional relations can be derived directly in terms of a CFT [49], but as only the final relations themselves will be of use later, a discussion of this derivation would deviate unnecessarily from the main point of the thesis. Instead, it will be shown how these relations arise quite naturally when statistical lattice models are solved using a particular method. The discussion presented here follows that found in the recent review [50].

### 2.6.1 Functional relations in Integrable Models

The specific lattice model used here is the six-vertex model. This is a simple generalisation of the Ising model, first solved by Lieb [51] and Sutherland [52]. Also see Baxter's book [53]. It can be defined on an $N \times M$ lattice with periodic boundary

conditions in both directions. On each link of the lattice a spin 1 or 2 is placed, depicted here by a right or left arrow, on the horizontal links, and an up or down arrow on the vertical links. This is often referred to as an 'ice-type' model as each vertex can be taken to represent an oxygen atom with each link being the bond between adjacent atoms. The Hydrogen ion, sitting on each bond, will lie closer to one of the ends, according to the direction of the arrow. The 'ice-rule' states that each oxygen atom should have two Hydrogen ions close to it and two far away, which translates to the condition that the flux of arrows through a vertex must be preserved. There are therefore six options for the spins around each vertex, hence the name 'six-vertex model'.

For real ice, each possibility is equally likely, but as a generalisation of this one can allow for different probabilities. The local Boltzmann weights, which assign a probability to each configuration, are defined here to be:

$$W\left[\begin{smallmatrix} & \uparrow & \\ \rightarrow & & \rightarrow \\ & \uparrow & \end{smallmatrix}\right] = W\left[\begin{smallmatrix} & \downarrow & \\ \leftarrow & & \leftarrow \\ & \downarrow & \end{smallmatrix}\right] = a \tag{2.6.1}$$

$$W\left[\begin{smallmatrix} & \downarrow & \\ \rightarrow & & \rightarrow \\ & \downarrow & \end{smallmatrix}\right] = W\left[\begin{smallmatrix} & \uparrow & \\ \leftarrow & & \leftarrow \\ & \uparrow & \end{smallmatrix}\right] = b \tag{2.6.2}$$

$$W\left[\begin{smallmatrix} & \uparrow & \\ \rightarrow & & \leftarrow \\ & \downarrow & \end{smallmatrix}\right] = W\left[\begin{smallmatrix} & \downarrow & \\ \leftarrow & & \rightarrow \\ & \downarrow & \end{smallmatrix}\right] = c \tag{2.6.3}$$

and the partition function is

$$Z = \sum_{\{\sigma\}} \prod_{\text{sites}} W\left[\begin{smallmatrix} \cdot & \cdot \\ \cdot & \cdot \end{smallmatrix}\right] \tag{2.6.4}$$

where $\{\sigma\} = \{\leftarrow, \rightarrow\}$. In the thermodynamic limit ($N, M \to \infty$), the overall normalisation of $a$, $b$ and $c$ factors out trivially from all quantities so it is convenient to reparametrise the two remaining degrees of freedom using the variables $\nu$ (the spectral parameter) and $\eta$ (the anisotropy)

$$a(\nu, \eta) = \sin(\eta + i\nu) \tag{2.6.5}$$

$$b(\nu, \eta) = \sin(\eta - i\nu) \tag{2.6.6}$$

$$c(\nu, \eta) = \sin(2\eta)\,. \tag{2.6.7}$$

It is usual to keep the anisotropy fixed in calculations, as different values of $\eta$ will turn out to correspond to different models. The spectral parameter, on the other hand, can be varied as it is not a physical parameter, a fact that will become apparent

later. Introducing the multi indices $\boldsymbol{\alpha} = (\alpha_1, \alpha_2, \ldots, \alpha_N)$ and $\boldsymbol{\alpha}' = (\alpha'_1, \alpha'_2, \ldots, \alpha'_N)$, the transfer matrix can be written as

$$T_{\boldsymbol{\alpha}}^{\boldsymbol{\alpha}'}(\nu) = \sum_{\beta_i} W\left[\begin{matrix}\beta_1 & \alpha'_1 \\ & \alpha_1\end{matrix}\beta_2\right](\nu) W\left[\begin{matrix}\beta_2 & \alpha'_2 \\ & \alpha_2\end{matrix}\beta_3\right](\nu) \ldots W\left[\begin{matrix}\beta_N & \alpha'_N \\ & \alpha_N\end{matrix}\beta_1\right](\nu)\,. \tag{2.6.8}$$

Since the boundary condition is also periodic in the vertical direction the partition function has the simple form

$$Z = Tr(T^M)\,. \tag{2.6.9}$$

Quantities of interest are given by the eigenvalues of the transfer matrix. For example, if $T$ has eigenvalues $t_0 > t_1 > \ldots$ then the free energy, in the limit $M \to 0$ is

$$F = -\frac{1}{M} \ln Z \to -\ln t_0\,. \tag{2.6.10}$$

One therefore needs to find the eigenvalues $t_0$, $t_1$, .... This can be done using the Bethe ansatz, which consists of two steps: first a guess is made for an eigenvector of $T$, depending on a finite number, $n$, of parameters $\nu_1, \nu_2, \ldots, \nu_n$, known as the 'roots'. This guess is then found to work, only if the set of roots, $\{\nu_i\}$, solve a set of coupled equations, known as the 'Bethe ansatz equations'. An elegant formulation of these equations is given by the algebraic Bethe ansatz, details of which can be found, for example, in appendix A of [50].

The standard form of the 'Bethe ansatz equations' (BAE) for the roots $\{\nu_1, \ldots, \nu_n\}$ are

$$(-1)^n \prod_{j=1}^{n} \frac{\sinh(2i\eta - \nu_k + \nu_j)}{\sinh(2i\eta - \nu_j + \nu_k)} = -\frac{a^N(\nu_k, \eta)}{b^N(\nu_k, \eta)}\,,\ k = 1, \ldots, n\,. \tag{2.6.11}$$

There is no unique solution to the BAE, but rather a discrete set of solutions, matching the fact that $T$ has many eigenvalues. For each solution $\{\nu_i\}$ the eigenvector $|\Psi\rangle$ of $T$ has eigenvalue

$$t(\nu) = a^N(\nu, \eta) \prod_{j=1}^{n} \frac{a(\nu_j - \nu - i\eta, \eta)}{b(\nu_j - \nu - i\eta, \eta)} + b^N(\nu + \eta) \prod_{j=1}^{n} \frac{a(\nu - \nu_j - i\eta, \eta)}{b(\nu - \nu_j - i\eta, \eta)}\,. \tag{2.6.12}$$

The algebraic Bethe ansatz also provides a simple proof that the transfer matrices, at different values of the spectral parameter $\nu$, commute:

$$[T(\nu), T(\nu')] = 0\,. \tag{2.6.13}$$

From this it is clear that the eigenvectors of $T$ cannot depend on $\nu$, therefore it is not a physical variable, as claimed earlier.

Periodic boundary conditions, as imposed here, are not the only boundary conditions for which this model is integrable. In fact, integrability is preserved when these periodic boundary conditions are modified by introducing a 'twist' (see for example, [54][55][56]). This amounts to adding a phase factor to the Boltzmann weights on one column of the lattice, say the $N^{th}$, so

$$W\left[\begin{matrix}\beta_N & \alpha'_N \\ & \alpha_N\end{matrix}\rightarrow\right](\nu) \;\rightarrow\; e^{-i\phi}W\left[\begin{matrix}\beta_N & \alpha'_N \\ & \alpha_N\end{matrix}\rightarrow\right](\nu) \tag{2.6.14}$$

$$W\left[\begin{matrix}\beta_N & \alpha'_N \\ & \alpha_N\end{matrix}\leftarrow\right](\nu) \;\rightarrow\; e^{i\phi}W\left[\begin{matrix}\beta_N & \alpha'_N \\ & \alpha_N\end{matrix}\leftarrow\right](\nu)\,. \tag{2.6.15}$$

The transfer matrix is then defined as in (2.6.8) and the algebraic Bethe ansatz goes through almost unchanged. The result is that the generalised transfer matrix $T(\nu,\phi)$ has eigenvalues

$$t(\nu,\phi) = e^{-i\phi}a^N(\nu,\eta)\prod_{j=1}^{n}\frac{a(\nu_j-\nu-i\eta,\eta)}{b(\nu_j-\nu-i\eta,\eta)} + e^{i\phi}b^N(\nu+\eta)\prod_{j=1}^{n}\frac{a(\nu-\nu_j-i\eta,\eta)}{b(\nu-\nu_j-i\eta,\eta)} \tag{2.6.16}$$

where the set of roots $\{\nu_1,\ldots,\nu_n\}$ satisfy the modified Bethe ansatz equations

$$(-1)^n\prod_{j=1}^{n}\frac{\sinh(2i\eta-\nu_k+\nu_j)}{\sinh(2i\eta-\nu_j+\nu_k)} = -e^{-2i\phi}\frac{a^N(\nu_k,\eta)}{b^N(\nu_k,\eta)}\,,\; k=1,\ldots,n\,. \tag{2.6.17}$$

An alternative approach to this is provided by Baxter [57]: since the transfer matrices $T(\nu)$ commute for different values of the spectral parameter $\nu$, the $T(\nu)$ can be simultaneously diagonalised and the eigenvectors $\Psi$ will not depend on $\nu$. One can therefore focus on the individual eigenvalues $t_0(\nu), t_1(\nu)\ldots$ as functions of $\nu$. Given the form of the Boltzmann weights in (2.6.5-2.6.7) and the claim that the eigenvectors are $\nu$-independent, these functions $t(\nu)$ are entire and $i\pi$-periodic. A matrix $Q(\nu)$ can now be defined, which commutes with itself and with $T$:

$$[Q(\nu),Q(\nu')] = [Q(\nu),T(\nu')] = 0 \tag{2.6.18}$$

and satisfies the $TQ$ relation

$$T(\nu)Q(\nu) = e^{-i\phi}a^N(\nu,\eta)Q(\nu+2i\eta) + e^{i\phi}b^N Q(\nu-2i\eta)\,. \tag{2.6.19}$$

The eigenvalues of $Q$ are also functions of $\nu$, denoted $q(\nu)$, which are also entire and, at least for the ground state, $i\pi$-periodic. They satisfy the eigenvalue relation, corresponding to (2.6.19)

$$t(\nu)q(\nu) = e^{-i\phi}a^N(\nu,\eta)q(\nu+2i\eta) + e^{i\phi}b^N(\nu,\eta)q(\nu-2i\eta)\,. \tag{2.6.20}$$

The BAE equations can then be extracted from (2.6.20) as follows: suppose that the zeros of $q(\nu)$ are at $\nu_1, \ldots, \nu_n$. Given the periodicity of $q(\nu)$, it can be written, up to an overall normalisation, as

$$q(\nu) = \prod_{l=1}^{n} \sinh(\nu - \nu_l)\,. \tag{2.6.21}$$

Now putting $\nu = \nu_i$ in (2.6.20) gives

$$0 = e^{-i\phi} a^N(\nu_i, \eta) q(\nu_i + 2i\eta) + e^{i\phi} b^N(\nu_i, \eta) q(\nu_i - 2i\eta) \tag{2.6.22}$$

and using the equation for $q(\nu)$, (2.6.21), this can be rearranged to

$$(-1)^n \prod_{l=1}^{n} \frac{\sinh(2i\eta - \nu_i + \nu_l)}{\sinh(2i\eta - \nu_l + \nu_i)} = -e^{-2i\phi} \frac{a^N(\nu_i, \eta)}{b^N(\nu_i, \eta)}\,, \; i = 1, \ldots, n\,. \tag{2.6.23}$$

This is the BAE from (2.6.17), and $t(\nu)$, given by (2.6.20), then matches the $t(\nu)$ found by the direct calculation. Baxter in fact established this $TQ$ relation (2.6.19) by an independent argument and then generalised it to the previously unsolved eight-vertex model [57][58]. See his book [53] for more details.

The continuum limit of the six vertex model is a unitary CFT with central charge $c = 1$. The $TQ$ relations, described above, therefore encode information about this CFT when this limit is taken. Alternatively, these functional relations can also be constructed directly in terms of a CFT, as proposed by Bazhanov, Lukyanov and Zamolodchikov in [49] and developed further in [59] and [60] . No more will be said about this approach here as it is not directly used in this thesis.

### 2.6.2 Ordinary differential equations

In order to make the link between the integrable model above and the theory of ordinary differential equations, the aim is to find a functional relation in the ODE theory which can be directly compared to the $TQ$ relation (2.6.19) above. This link was first found by Dorey and Tateo in [48] where the ODE

$$-\frac{d^2}{dx^2}\psi(x) - (ix)^{2M}\psi(x) = E\psi(x) \tag{2.6.24}$$

was considered, with $x$ a complex variable and $M > 1$. For a discussion of eigenvalue problems on a complex contour see, for example, [61][62][63]. The WKB approximation to the solutions $\psi$ gives the leading asymptotic

$$\psi(x) \sim P(x)^{-1/4} e^{\pm \int^x \sqrt{P(t)}dt} \tag{2.6.25}$$

as $|x| \to \infty$, with $P(x) = -(ix)^{2M} - E$. Since $M$ can take non-integer values, there needs to be a branch cut in the plane which is taken here along the positive imaginary axis. It is then natural to define general rays in the complex plane by $x = -i\rho e^{i\theta}$ with $\rho$ real. The WKB formula gives two leading order behaviours, as expected for a second order equation:

$$\psi_{\pm} \sim P^{-1/4} \exp\left( \pm \frac{1}{M+1} e^{i\theta(1+M)} \rho^{1+M} \right) . \tag{2.6.26}$$

Note that here $P(x)$ has been shifted by $E$, so that $P(x) = -(ix)^{2M}$, but this doesn't change the leading asymptotic for $M > 1$ so (2.6.26) is still valid. For most values of $\theta$, one of these solutions is exponentially growing, while the other is exponentially decaying. The two solutions swap roles when $Re(e^{i\theta(1+M)}) = 0$, and at this crossover point, neither solution dominates but instead both oscillate. This occurs when $\theta$ is

$$\theta = \pm \frac{\pi}{2M+2}, \pm \frac{3\pi}{2M+2}, \pm \frac{5\pi}{2M+2}, \dots \tag{2.6.27}$$

These values of $\theta$ will be called 'anti-Stokes lines' here, but note they are sometimes alternatively called 'Stokes lines'. The wedges between the lines are known as 'Stokes sectors' and one solution, the subdominant, will exponentially decay as $|x| \to \infty$ within each sector. This is a unique solution, up to a multiplicative constant, whereas the dominant solutions, those which exponentially grow as $|x| \to \infty$, are not. Taking the subdominant solutions in any two sectors will lead to an eigenvalue problem with a discrete spectra, but the choice of sectors is important as different pairs give different eigenvalue problems.

It is convenient to eliminate the factors of $i$ in the ODE above by the variable changes

$$x \to x/i\,, \quad E \to -E \tag{2.6.28}$$

so the ODE becomes

$$\left( -\frac{d^2}{dx^2} + x^{2M} - E \right) \psi(x) = 0\,. \tag{2.6.29}$$

This variable change also moves the branch cut to the negative real axis. With this shift, the anti-Stokes lines become

$$arg(x) = \pm \frac{\pi}{2M+2}, \pm \frac{3\pi}{2M+2}, \dots \tag{2.6.30}$$

with Stokes sectors defined as

$$S_k := \left| arg(x) - \frac{2\pi k}{2M+2} \right| < \frac{\pi}{2M+2}\,. \tag{2.6.31}$$

The ODE (2.6.29) has a so called 'basic' solution $y(x, E)$ which is an entire function on the cut plane. In the limit $|x| \to \infty$, with $|arg(x)| < \frac{3\pi}{2M+2}$, it has the asymptotic

$$y \sim \frac{1}{\sqrt{2i}} x^{-\frac{M}{2}} \exp\left[-\frac{1}{M+1} x^{M+1}\right] \tag{2.6.32}$$

which matches the WKB approximation in the Stokes sectors $S_{-1} \cup S_0 \cup S_1$. Note that this is subdominant in $S_0$ and dominant in $S_{-1}$ and $S_1$. Further solutions to the ODE can be generated as follows: consider the function $\widehat{y}(x) = y(ax, E)$ which solves the differential equation

$$\left(-\frac{d^2}{dx^2} + a^{2M+2} x^{2M} - a^2 E\right) \widehat{y}(x, E) = 0\,. \tag{2.6.33}$$

If $a^{2M+2} = 1$, $\widehat{y}(x, a^{-2}E)$ is a solution to the original ODE (2.6.29). By setting $\omega = e^{2\pi i/(2M+2)}$, one can define a whole set of solutions to (2.6.29)

$$y_k(x, E) := \omega^{k/2} y(\omega^{-k} x, \omega^{2k} E)\,. \tag{2.6.34}$$

By inspecting the asymptotics of $y_k$ it follows that $y_k$ is subdominant in $S_k$ and dominant in $S_{k\pm1}$. Furthermore, $y_k$ and $y_{k+1}$ are linearly independent and so form a basis of solutions so, for example, $y_{-1}$ can be expanded in the $\{y_0, y_1\}$ basis as

$$y_{-1}(x, E) = C(E) y_0(x, E) + \tilde{C}(E) y_1(x, E)\,. \tag{2.6.35}$$

This is an example of a Stokes relation and the coefficients, $C$ and $\tilde{C}$, are the 'Stokes multipliers'. These multipliers can be expressed in terms of Wronskians, where the Wronskian of two functions, $f(x)$ and $g(x)$ is

$$W[f, g] := fg' - f'g\,. \tag{2.6.36}$$

By considering the derivative of $W$, with respect to $x$, it is easy to show that the Wronskian of two solutions to a second order ODE, with no single derivative term, is independent of $x$ and is zero if and only if the solutions are linearly dependent. Since $y_0$ and $y_1$ are linearly independent, expressions can be found for $C(E)$ and $\tilde{C}(E)$ in terms of Wronskians. First, to simplify notation, let $W[y_j, y_k] \equiv W_{j,k}$ and notice, using (2.6.34), that

$$W_{j+1,k+1}(E) = W_{j,k}(\omega^2 E)\,. \tag{2.6.37}$$

By considering the asymptotic expressions for $y$, it also follows that

$$W_{0,1} = 1 \tag{2.6.38}$$

(for $M > 1$). Now, taking Wronskians of (2.6.35), first with $y_1$ and then with $y_0$ gives

$$C(E) = \frac{W_{-1,1}(E)}{W_{0,1}(E)} = W_{-1,1}(E) \tag{2.6.39}$$

$$\tilde{C}(E) = -\frac{W_{-1,0}(E)}{W_{0,1}(E)} = -\frac{W_{0,1}(\omega^2 E)}{W_{0,1}(E)} = -1\,. \tag{2.6.40}$$

With these simplifications, the Stokes relation (2.6.35) can be rewritten as

$$C(E)y_0(x,E) = y_{-1}(x,E) + y_1(x,E) \tag{2.6.41}$$

which, in terms of the original 'basic' solution $y(x,E)$, is

$$C(E)y(x,E) = \omega^{-1/2}y(\omega x, \omega^{-2}E) + \omega^{1/2}y(\omega^{-1}x, \omega^2 E)\,. \tag{2.6.42}$$

To compare this to the $TQ$ relation (2.6.19) found on the integrable model side, $x$ must be set to zero. Note, however, that if the derivative of (2.6.42) with respect to $x$ is taken first, this will swap the phase factors $\omega^{\pm 1/2}$. Defining

$$D_-(E) := y(0,E)\,, \quad D_+(E) := y'(0,E) \tag{2.6.43}$$

and setting $x = 0$ in the Stokes relation (2.6.42) implies

$$C(E)D_\mp(E) = \omega^{\mp 1/2}D_\mp(\omega^{-2}E) + \omega^{\pm 1/2}D_\mp(\omega^2 E) \tag{2.6.44}$$

which matches the $TQ$ relation (2.6.19), provided the twist parameter is set to $\phi = \frac{\pi}{2M+2}$ [48]. This link between the integrable model and an ODE also exists for other values of the twist parameter, but for this to work an angular momentum term $l(l+1)/x^2$ must be included in the ODE [64], which becomes

$$\left(-\frac{d^2}{dx^2} - (ix)^{2M} + \frac{l(l+1)}{x^2}\right)\Psi(x) = E\Psi(x)\,. \tag{2.6.45}$$

The same method, as used above, can be applied to this case [65]. The only subtlety arises in the final step when previously $x$ is set to zero. Here, because of the angular momentum term, this cannot be done directly but instead one must consider the asymptotics as $x \to 0$. The final Stokes relation, to be compared to the $TQ$ relation, is

$$C(E,l)D(E,l) = \omega^{-(l+1/2)}D(\omega^{-2}E,l) + \omega^{(l+1/2)}D(\omega^2 E,l) \tag{2.6.46}$$

where $D(E,l) := W[y,\psi](E,l)$, the Wronskian of the 'basic' solution, which is the same as in the simple case (2.6.32), and a solution defined via its asymptotics as $x \to 0$

$$\psi(x,E,l) \sim x^{l+1} + O(x^{l+3})\,. \tag{2.6.47}$$

This asymptotic fixes $\psi$ uniquely, provided $Re\, l > -3/2$. A second solution can be found by sending $l \to -1 - l$. The differential equation, but not the boundary condition, is invariant under this transformation so $\psi(x, E, -1 - l)$ is also a solution of (2.6.45). Near the origin, this behaves as $x^{-l}$, so for generic values of $l$, the pair of solutions $\psi(x, E, l)$ and $\psi(x, E, -1 - l)$ are linearly independent. Defining $D_-(E) := D(E, l)$ and $D_+(E) := D(E, -1 - l)$, then taking $l$ and $-1 - l$ in (2.6.46) gives

$$C(E, l)D_\mp(E) = \omega^{\mp(2l+1)/2} D_\mp(\omega^{-2}E) + \omega^{\pm(2l+1/2)/2} D_\mp(\omega^2 E)\,. \tag{2.6.48}$$

Comparing this to the $TQ$ relation (2.6.19), it is clear that the twist parameter is related to the angular momentum $l$ and the degree of the potential of ODE via

$$\phi = \frac{(2l+1)\pi}{2M+2} \tag{2.6.49}$$

and, in fact, the anisotropy parameter $\eta$ is also related to $M$:

$$\eta = \frac{\pi}{2}\frac{M}{M+1}\,. \tag{2.6.50}$$

This 'ODE/IM correspondence' has proved useful, mainly because the properties of ODEs and their solutions are somewhat better understood than those of the $T$ and $Q$ functions in integrable quantum field theories. Certain properties, conjectured to hold for these $T$ and $Q$ functions have been proven using the correspondence [64]. On the other hand, ideas from the theory of integrable models have been employed to gain insights into the spectral properties of certain ODEs. One example of this, which will be discussed further in Chapter 5, is the use of this correspondence to prove the reality of the spectrum, for certain $l$ and $M$, of the $\mathcal{PT}$-symmetric quantum mechanical problem, with Schrödinger equation (2.6.45) [66].

# Chapter 3

# Boundary Problems

So far, perturbed conformal field theories have been examined on both an infinite plane and a torus. An obvious question which now springs to mind is how does this story change when more general boundary conditions are imposed on the theory? This chapter aims to answer this by first looking at the effect of the boundary on a CFT, in particular, which boundary conditions preserve conformal invariance. The perturbation of this theory, by both bulk and boundary operators, is then discussed which leads on to the introduction of Reflection factors, or boundary S-matrices. Finally a method is proposed to link the reflection factors to specific conformal boundary conditions, using the TBA. This is analogous to the effective central charge $c_{\text{eff}}$ which provides a link between the S-matrix and the central charge of the bulk theory.

## 3.1 Boundary CFT

In a series of papers [67][68][69][13], Cardy explored the consequence of restricting a CFT to the upper half plane with the real axis as the boundary. The discussion presented here follows [68], along with Cardy's review [70]. All conformal transformations acting on the theory must preserve the boundary. This constrains the energy momentum tensor to satisfy $T(z) = \bar{T}(\bar{z})$ on the real axis. In Cartesian coordinates this becomes $T_{xy}|_{x=0} = 0$, so physically it corresponds to the requirement that no energy or momentum must flow across the boundary. The effect of this constraint is to eliminate half of the conformal generators as the holomorphic and antiholomorphic sectors are no longer independent.

Mapping the upper half plane into an infinite strip of width $R$ by $\omega = \frac{R}{\pi} \ln z$, there is no reason why the boundary conditions on either side of the strip must be the same, so they will be labelled as $\alpha$ and $\beta$, as shown in figure 3.1. Transforming this strip, with two boundary conditions, back to the upper-half plane produces a discontinuity in the boundary condition at $z = 0$. The effect of this is equivalent to inserting a boundary operator $\phi_{\alpha\beta}(0)$, known as a boundary condition changing operator, at the discontinuity.

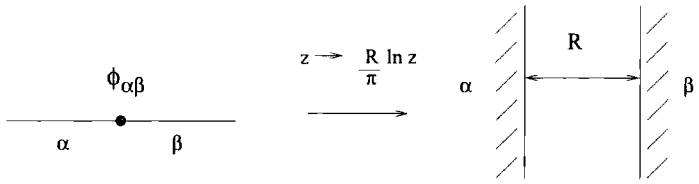


Figure 3.1: Mapping from the upper half plane into an infinite strip

Suppose this strip is now made periodic, becoming a cylinder of length $R$ and circumference $L$, with boundary conditions $\alpha$ and $\beta$ at each end. If time is taken in the $L$ direction, this corresponds to mapping the cylinder into a half-annulus in the upper-half plane by $z \to \exp(\pi z/R)$, shown in figure 3.2. The Hilbert space

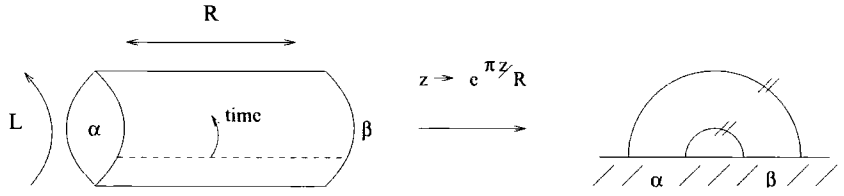


Figure 3.2: L-channel decomposition

decomposes into irreducible representations of one copy of the Virasoro algebra:

$$\mathcal{H}_{\alpha\beta} = \bigoplus_i n^i_{\alpha\beta} \mathcal{V}_i \tag{3.1.1}$$

where the non-negative integers, $n^i_{\alpha\beta}$, are the multiplicities. The boundary condition changing operator, mentioned above, is the highest weight state with weight $h_{\alpha\beta}$ equal to the lowest value of $h$ for which $n^h_{\alpha\beta} > 0$. Acting on this state with other local operators then gives the other representations with non-zero $n^h_{\alpha\beta}$. Following the method given in section 2.2.2, remembering that there is only one copy of the

Virasoro algebra here, it is easy to show that the Hamiltonian $H_{\alpha\beta}$ is given by

$$H_{\alpha\beta}^{\text{strip}} = \frac{\pi}{R}\left(L_0 - \frac{c}{24}\right). \tag{3.1.2}$$

It then follows that the cylinder partition function

$$Z^{cyl}(R, L) = Tr_{\mathcal{H}_{\alpha\beta}}(e^{-LH_{\alpha\beta}^{\text{strip}}(R)}) \tag{3.1.3}$$

can be decomposed into the Virasoro characters $\chi_i(q) = q^{-c/24}Tr_i q^{L_0}$ (first introduced in (2.2.46)) as

$$Z^{cyl}(R, L) = \sum_i n_{\alpha\beta}^i \chi_i(q) \tag{3.1.4}$$

where $q = \exp(-\pi L/R)$.

Taking time in the $R$ direction corresponds to mapping the cylinder to an annulus on the full complex plane by $z \longrightarrow \exp(-2\pi i z/L)$. This is shown in figure 3.3. The

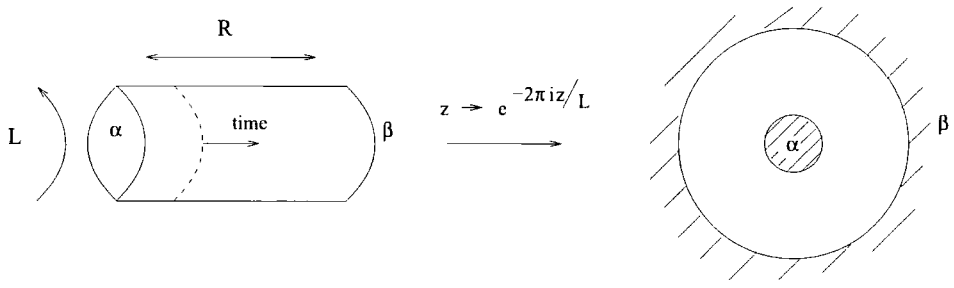


Figure 3.3: R-channel decomposition

Hilbert space is that of the bulk theory on the plane, which carries a representation of two copies of the Virasoro algebra. The cylinder Hamiltonian is therefore given by

$$H^{\text{circ}} = \frac{2\pi}{L}\left(L_0 + \bar{L}_0 - \frac{c}{12}\right). \tag{3.1.5}$$

For the partition function, it is useful here to refer back to the lattice description. In section 2.1.3, the partition function of a statistical model on an $n \times m$ lattice is written as

$$Z = \sum_{\mu_1,\ldots,\mu_m} \langle\mu_1|T|\mu_2\rangle\langle\mu_2|T|\mu_3\rangle \ldots \langle\mu_m|T|\mu_{m+1}\rangle \tag{3.1.6}$$

where $|\mu_i\rangle$ is a state describing the spin configuration on the $i^{\text{th}}$ row and the transfer matrix $T = \exp(-aH)$ evolves each state over the 'time' of a lattice spacing $a$. With this in mind, by writing the boundary conditions $\alpha$, $\beta$ in terms of boundary states

$|\alpha\rangle$ and $|\beta\rangle$ [68] and summing over only those states which satisfy the boundary conditions, the partition function becomes

$$Z^{cyl}_{\alpha\beta} = \langle\alpha|e^{-RH^{\text{circ}}(L)}|\beta\rangle. \tag{3.1.7}$$

The condition $T(z) = \bar{T}(\bar{z})$, under the mapping $z \to \omega \exp(-2\pi i z/L)$, becomes

$$\omega^2 T(\omega) = \bar{\omega}^2 \bar{T}(\bar{\omega}) \tag{3.1.8}$$

which corresponds to the following constraint on these boundary states:

$$(L_n - \bar{L}_{-n})|\alpha\rangle = 0. \tag{3.1.9}$$

For diagonal CFTs (i.e. CFTs whose torus partition function can be written as $Z = \sum_i n_i \chi_i(q)\chi_i(\bar{q})$) the solution to this constraint is unique and is given by the Ishibashi states:

$$\begin{aligned} |i\rangle\rangle &= \left(1 + \frac{L_{-1}\bar{L}_{-1}}{2h_i} + \dots\right)|i\rangle \quad , \quad |0\rangle\rangle = \left(1 + \frac{L_{-2}\bar{L}_{-2}}{c/2} + \dots\right)|0\rangle \\ \langle\langle i| &= \langle i|\left(1 + \frac{L_1\bar{L}_1}{2h_i} + \dots\right) \quad , \quad \langle\langle 0| = \langle 0|\left(1 + \frac{L_2\bar{L}_2}{c/2} + \dots\right) \end{aligned} \tag{3.1.10}$$

in terms of the highest weight state $|i\rangle$ with $h_i = \bar{h}_i$, and conformal vacuum $|0\rangle$ with $h = \bar{h} = 0$. There is one Ishibashi state for each bulk primary state and they can be normalised so that

$$\langle\langle i|e^{-RH^{\text{circ}}(L)}|j\rangle\rangle = \delta_{ij}\chi_i(\tilde{q}) \tag{3.1.11}$$

where $\tilde{q} = \exp(-4\pi R/L)$.

States corresponding to physical boundary conditions are not the Ishibashi states but are certain linear combinations of these, known as Cardy states:

$$|\alpha\rangle = \sum_j g^j_\alpha |j\rangle\rangle. \tag{3.1.12}$$

The coefficients $g^j_\alpha$ can be assumed to be real as it is always possible to normalise the fields in such a way that this is true. In this notation (3.1.7) becomes

$$Z_{\alpha\beta}(q) = \sum_j g^j_\alpha g^j_\beta \chi_j(\tilde{q}). \tag{3.1.13}$$

Equating the two partition functions (3.1) and (3.1.13), and using the modular transformation property of the characters

$$\chi_i(q) = \sum_j \mathcal{S}_{ij}\chi_j(\tilde{q}) \tag{3.1.14}$$

leads to the Cardy condition

$$\sum_i \mathcal{S}_{ij} n^i_{\alpha\beta} = g^j_\alpha g^j_\beta. \tag{3.1.15}$$

For diagonal CFTs (and non-diagonal minimal models) there is a complete solution to this condition. First a boundary state, $|\tilde{0}\rangle$ must be found such that $n^i_{\tilde{0}\tilde{0}} = \delta^i_{\tilde{0}}$, which from (3.1.15) must satisfy $(g^j_{\tilde{0}})^2 = \mathcal{S}_{0j}$. Since $\mathcal{S}_{0j} > 0$ this state can be defined as

$$|\tilde{0}\rangle = \sum_j (\mathcal{S}_{0j})^{1/2} |j\rangle\rangle \tag{3.1.16}$$

with further boundary states given by

$$|\tilde{l}\rangle = \sum_j \frac{\mathcal{S}_{lj}}{(\mathcal{S}_{0j})^{1/2}} |j\rangle\rangle. \tag{3.1.17}$$

Denoting the representation conjugate to $l$ by $\check{l}$, then for the boundary conditions $(\tilde{k}\check{\tilde{l}})$:

$$\sum_i \mathcal{S}_{ij} n^i_{\tilde{k}\check{\tilde{l}}} = g^j_{\tilde{k}} g^j_{\tilde{l}} = \frac{\mathcal{S}_{kj}\mathcal{S}_{lj}}{\mathcal{S}_{0j}}. \tag{3.1.18}$$

Comparing this to the Verlinde formula, which arises when a CFT is considered on a torus:

$$\sum_i \mathcal{S}_{ij} N^i_{kl} = \frac{\mathcal{S}_{kj}\mathcal{S}_{lj}}{\mathcal{S}_{0j}} \tag{3.1.19}$$

one can equate the multiplicities $n^i_{\tilde{k}\tilde{l}}$ to the fusion algebra coefficients $N^i_{kl}$. Therefore, for diagonal models, there is a bijection between the allowed primary fields in the bulk CFT and the allowed conformally invariant boundary conditions.

A quantity that is of particular interest in this thesis is Affleck and Ludwig's g-function, or 'ground state degeneracy'[3]. This appears when the cylinder partition function is considered in the limit that the length of the cylinder $R \to \infty$. The log of the partition function, in this limit will have the form

$$\ln Z_{\alpha\beta} \sim -R E_0^{\text{circ}}(L) + \text{constant} \tag{3.1.20}$$

where $E_0^{\text{circ}}(L) = F_L = -\pi c/6L$ and the constant is a boundary dependent term, defined as $\ln g_\alpha g_\beta$, with $g_\alpha$ the ground state degeneracy corresponding to the boundary state $|\alpha\rangle$.

Taking time along the cylinder, in the $R$ direction, the partition function has leading order behaviour

$$\begin{aligned} Z_{\alpha\beta} &= \langle\alpha|e^{-RH^{\rm circ}(L)}|\beta\rangle = \sum_n \langle\alpha|\psi_n\rangle e^{-RE_n^{\rm circ}(L)}\langle\psi_n|\beta\rangle \\ &\sim \langle\alpha|\Omega\rangle\langle\Omega|\beta\rangle e^{-RE_0^{\rm circ}(L)} \end{aligned} \tag{3.1.21}$$

where $|\Omega\rangle$ is the bulk ground state. Taking logs of this gives

$$\ln Z_{\alpha\beta} \sim -RE_0^{\rm circ}(L) + \ln g_\alpha g_\beta \tag{3.1.22}$$

with $g_\alpha = \langle\alpha|\Omega\rangle$. Now $\langle\alpha|\Omega\rangle = \sum_j g_\alpha^j \langle\langle j|\Omega\rangle$, but since all primary states are orthogonal, $\langle\langle j|\Omega\rangle = \langle\langle\Omega|\Omega\rangle$. Expanding the Ishibashi state as $\langle\langle\Omega|\Omega\rangle = \langle\Omega|\Omega\rangle + \langle\Omega|\frac{L_1\bar{L}_1}{2h_i}|\Omega\rangle + \ldots$ and using the fact that $\bar{L}_n|\Omega\rangle = 0$ for $n > 0$, the only non-zero term left in this expansion is the first. Therefore $\langle\alpha|\Omega\rangle = g_\alpha^\Omega$ and so it is clear from (3.1.12), (3.1.16) and (3.1.17) above that

$$g_0 = (\mathcal{S}_{0\Omega})^{1/2} \quad , \quad g_\alpha = \frac{\mathcal{S}_{\alpha\Omega}}{(\mathcal{S}_{0\Omega})^{1/2}}. \tag{3.1.23}$$

Affleck and Ludwig also proposed a $g$-theorem [3], later proven in [71], which is analogous to Zamolodchikov's $c$-theorem [29]. It states that the $g$-function decreases under renormalisation group flow from a less stable to a more stable critical point in the same bulk universality class. This means that if a CFT with boundary state $|\alpha\rangle$ is perturbed by a boundary perturbation only, while the bulk remains critical, then the resulting IR theory will be the same CFT with boundary $|\beta\rangle$ where $g_\beta < g_\alpha$. This no longer necessarily holds when a bulk perturbation is added.

## 3.2 Perturbed Boundary CFT

The perturbation of a CFT with a boundary was first considered by Ghoshal and Zamolodchikov in [72] and the discussion here will follow their work. First, consider a CFT in Euclidean space, with coordinates $(x, y)$ and impose a conformal boundary condition at $x = 0$. This theory can be perturbed by both a relevant bulk operator, $\varphi(x, y)$, and a relevant boundary operator, $\phi(y)$ with the resulting action taken to be

$$\mathcal{A} = \mathcal{A}_{BCFT} + \lambda \int_{-\infty}^{0} dx \int_{-\infty}^{\infty} dy\, \varphi(x, y) + \mu \int_{-\infty}^{\infty} dy\, \phi(y). \tag{3.2.1}$$

For a boundary CFT the condition $T_{xy}|_{x=0} = 0$ must be satisfied, but for the perturbed theory this constraint becomes

$$T_{xy}|_{x=0} = (-i)(T - \bar{T})|_{x=0} = \frac{d}{dy}\theta(y) \tag{3.2.2}$$

where $\theta(y)$ is some local boundary field. Of course, in general, even if the bulk perturbed theory is integrable the boundary conditions could spoil this integrability. However, if the boundary conditions satisfy

$$[T_{s+1} + \bar{\Theta}_{s-1} - \bar{T}_{s+1} - \Theta_{s-1}]|_{x=0} = \frac{d}{dy}\theta_s(y) \tag{3.2.3}$$

for some $s \in \{s\}$, $\theta_s$ again being some local boundary field and $T_{s+1}$ and $\Theta_{s-1}$ being the local bulk fields described in section 2.3, then an integral of motion for each $s$ can be found.

There are two ways to introduce the Hamiltonian picture in this theory. The first is to take $y$ to be the time direction so the boundary is a boundary in space and the Hilbert space $\mathcal{H}_B$ is associated to the half-line $x \in (-\infty, 0]$. Alternatively, $x$ can be taken to be the time direction, in which case the boundary is an initial condition which can be described by the boundary state $|B\rangle$ which will lie in the Hilbert space of the bulk theory. In this case the integrals of motion are the same as those for the bulk theory: $P_s = \int_{-\infty}^{\infty}(T_{s+1} + \Theta_{s-1})dy$ and $\bar{P}_s = \int_{-\infty}^{\infty}(\bar{T}_{s+1} + \bar{\Theta}_{s-1})dy$. Therefore, from (3.2.3), for the theory to be integrable the boundary states must satisfy

$$(P_s - \bar{P}_s)|B\rangle = 0\,. \tag{3.2.4}$$

There is no boundary analogue of Zamolodchikov's counting argument to determine the integrable perturbations; instead one must find some integrals of motion directly. For example, in [72], Ghoshal and Zamolodchikov conjectured that the Virasoro minimal models, perturbed by the bulk and boundary operators $\varphi_{(1,3)}$ and $\phi_{(1,3)}$ respectively, are integrable by first setting $\lambda = 0$, so perturbing at the boundary only, and finding solutions to (3.2.3) for $s = 1, 3, 5, \ldots$. They then argued that by dimensional analysis, parallel to that used by Zamolodchikov in [21] and described in section 2.3, these results remain valid for $\lambda \neq 0$. In general it is expected, although has never been proven, that adding a boundary perturbation to an integrable bulk PCFT will result in an integrable theory provided the boundary perturbing operator is the boundary operator corresponding to the bulk perturbing operator. Note that

as there is only one copy of the Virasoro algebra in the boundary theory, boundary operators have scaling dimension half that of the corresponding bulk operators. This expectation is certainly true in every case so far examined and if the boundary operator did not match the bulk operator in this way the situation would, in some sense, be akin to perturbing a bulk CFT by a combination of two relevant operators which is also not usually expected to lead to an integrable theory.

Perturbing by a bulk operator, with or without a boundary perturbation, will clearly alter the boundary conditions and in cases where this perturbation results in a massive theory with a particle description, it is necessary to understand how the particles interact with the boundary. The boundary analogue of the S-matrix elements, known as Reflection factors are therefore needed.

## 3.3 Reflection factors

In this section the S-matrix approach of section 2.4 is adapted to the semi-infinite plane. This problem was first treated in papers by Ghoshal and Zamolodchikov [72] and Fring and Koberle [73], but the discussion presented here follows that given in [72] and also [27].

Returning to (1+1) Minkowski space with time taken in the $y$ direction, the asymptotic states, in parallel to the bulk case, can be considered as particle creation operators $A_{a_i}(\theta_i)$ acting on the ground state $|0\rangle_B$:

$$|A_{a_1}(\theta_1)A_{a_2}(\theta_2)\dots A_{a_n}(\theta_n)\rangle = A_{a_1}(\theta_1)A_{a_2}(\theta_2)\dots A_{a_n}(\theta_n)|0\rangle_B. \tag{3.3.5}$$

For an in state, the rapidities $\theta_1,\dots,\theta_n$ are all positive, whereas for an out state they are all negative. The boundary can be thought of as an impenetrable particle, $B$ sitting at $x = 0$ so formally, the ground state can be written as

$$|0\rangle_B = B|0\rangle. \tag{3.3.6}$$

This description makes the analogy with the S-matrix theory in the bulk quite straightforward. The asymptotic in and out states become

$$A_{a_1}(\theta_1)A_{a_2}(\theta_2)\dots A_{a_n}(\theta_n)B \tag{3.3.7}$$

with the rapidities ordered as $\theta_1 > \theta_2 > \dots\theta_n > 0$ and $0 < \theta_1 < \theta_2 < \dots\theta_n$ respectively. As in the bulk case, the existence of the higher spin integrals of motion

constrain the in and out momenta to be equal and allow no particle production. The n particle S-matrix, which relates the in and out states via

$$\begin{aligned} &A_{a_1}(\theta_1)A_{a_2}(\theta_2)\dots A_{a_n}(\theta_n)|0\rangle_B \\ &= R^{b_1 b_2 \dots b_n}_{a_1 a_2 \dots a_n}(\theta_1,\theta_2,\dots,\theta_n)A_{b_1}(-\theta_1)A_{b_2}(-\theta_2)\dots A_{b_n}(-\theta_n)|0\rangle_B \end{aligned} \tag{3.3.8}$$

can be expressed in terms of the fundamental 2-particle S-matrix elements, $S^{b_1 b_2}_{a_1 a_2}$, and the one particle reflection factors $R^b_a$, where $m_a = m_b$. These reflection factors, defined by the relations

$$A_a(\theta)B = R^b_a(\theta)A_b(-\theta)B \tag{3.3.9}$$

are shown in figure 3.4.

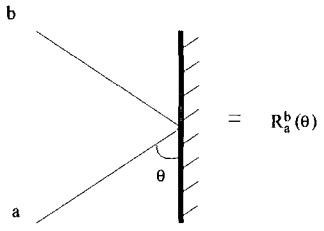


Figure 3.4: The reflection factor $R^b_a(\theta)$

The amplitudes $R^b_a$ must satisfy properties, analogous to those for the bulk theory described earlier. The first of these is the boundary Yang-Baxter equation, which results from the factorisation property, just as in the bulk case:

$$\begin{aligned} &R^{c_2}_{a_2}(\theta_2)S^{c_1 d_2}_{a_1 c_2}(\theta_1+\theta_2)R^{d_1}_{c_1}(\theta_1)S^{b_2 b_1}_{d_2 d_1}(\theta_1-\theta_2) = \\ &S^{c_1 c_2}_{a_1 a_2}(\theta_1-\theta_2)R^{d_1}_{c_1}(\theta_1)S^{d_2 b_1}_{c_2 d_1}(\theta_1+\theta_2)R^{b_2}_{d_2}(\theta_2)\,. \end{aligned} \tag{3.3.10}$$

This is shown in figure 3.5. The boundary unitarity condition is also a generalisation of the bulk case, coming from the requirement that the reflection factor is analytic and so (3.3.9) must make sense for negative rapidity. This leads to the constraint

$$R^c_a(\theta)R^b_c(-\theta) = \delta^b_a. \tag{3.3.11}$$

The analogue of the bulk crossing symmetry is less obvious and in fact corresponds to a boundary crossing-unitarity condition found by Ghoshal and Zamolodchikov in [72]. First, it is necessary to take time in the $x$ direction, i.e. consider the picture 3.4 from the side. The space of states, $\mathcal{H}$, is now that of the bulk theory with the

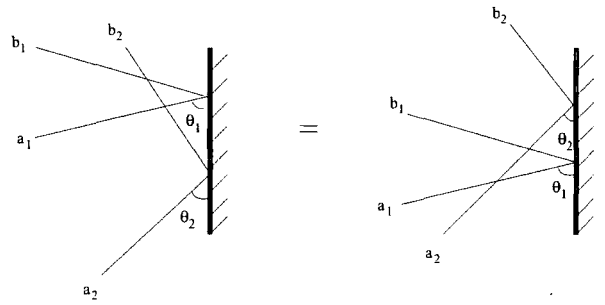


Figure 3.5: Boundary Yang-Baxter equation

boundary condition, at $x = 0$, being an initial condition described by a boundary state $|B\rangle$. Since $|B\rangle \in \mathcal{H}$ it must be a superposition of the asymptotic states

$$|A_{a_1}(\theta_1)\dots A_{a_n}(\theta_n)\rangle = A_{a_1}(\theta_1)\dots A_{a_n}(\theta_n)|0\rangle. \tag{3.3.12}$$

Now for a boundary state to be integrable it must satisfy

$$(Q_s - \bar{Q}_s)|B\rangle = 0 \tag{3.3.13}$$

and since $Q_s|A_a(\theta)\rangle = q_a^{(s)}e^{s\theta}|A_a(\theta)\rangle$, the eigenvalue of the operator $Q_s - \bar{Q}_s$ on (3.3.12) is

$$\sum_{i=1}^{n} 2q_{a_i}^{(s)} \sinh(s\theta_i). \tag{3.3.14}$$

Therefore, any particle $A_a$ can only enter the boundary state $|B\rangle$ in a pair $A_a(\theta)A_b(-\theta)$ of equal mass particles with opposite rapidities.

Ghoshal and Zamolodchikov [72] then argued that the relevant boundary state, written in terms of a 2-particle out state $A_a(-\theta)A_b(\theta)|0\rangle$ is

$$|B\rangle = \left(1 + \int_0^\infty K^{ab}(\theta)A_a(-\theta)A_b(\theta) + \dots\right)|0\rangle \tag{3.3.15}$$

where $K^{ab}$ is related to the reflection factor via

$$K^{ab}(\theta) = R_{\bar{a}}^{b}\left(\frac{i\pi}{2} - \theta\right). \tag{3.3.16}$$

This boundary state can also be expanded in terms of the in states $A_a(\theta)A_b(-\theta)|0\rangle$ as

$$|B\rangle = \left(1 + \int_0^\infty K^{ab}(-\theta)A_a(\theta)A_b(-\theta) + \dots\right)|0\rangle. \tag{3.3.17}$$

Since the in and out states are related by the S-matrix, this puts a constraint, known as the boundary crossing-unitarity condition, on $K^{ab}(\theta)$:

$$K^{ab}(\theta) = S^{ab}_{a'b'}(2\theta)K^{b'a'}(-\theta)\,. \tag{3.3.18}$$

This allows the boundary state (3.3.15) to be written as

$$|B\rangle = \left(1 + \frac{1}{2}\int_{-\infty}^{\infty} K^{ab}(\theta)A_a(-\theta)A_b(\theta) + \dots\right)|0\rangle. \tag{3.3.19}$$

The unitarity, Yang-Baxter and crossing constraints described so far allow the reflection factors to be fixed up to $R^b_a(\theta) \to R^b_a(\theta)\Phi_B(\theta)$, where $\Phi_B$ satisfies

$$\Phi_B(\theta) = \Phi_B(i\pi - \theta) \tag{3.3.20}$$

which is exactly the bulk CDD ambiguity.

Restricting to the case where the boundary scattering amplitudes are purely elastic, the unitarity condition (3.3.11) becomes

$$R_a(\theta)R_a(-\theta) = 1 \tag{3.3.21}$$

and crossing-unitarity (3.3.18), written in terms of the reflection factors, is

$$R_a(\theta)R_{\bar{a}}(\theta - i\pi) = S_{aa}(2\theta)\,. \tag{3.3.22}$$

There are also bootstrap constraints, as in the bulk S-matrix theory, which occur when bound states appear in the spectrum. With the introduction of the boundary there are now two types of bound states and therefore two bootstrap conditions to consider. The first of these is the analogue of the bulk bootstrap associated with the usual bulk bound states: if a particle $A_c$ is interpreted as the bound state of particles $A_a$ and $A_b$, i.e. if the bulk three-point coupling $C^{abc}$ is nonzero, then this system could interact with the boundary before or after the bound state is formed. However, these two situations are indistinguishable, due to the factorisation condition, which leads to the bootstrap constraint:

$$R_c(\theta) = R_a(\theta + i\bar{U}^b_{ac})R_b(\theta - i\bar{U}^a_{bc})S_{ab}(2\theta + i\bar{U}^b_{ac} - i\bar{U}^a_{bc}) \tag{3.3.23}$$

shown in figure 3.6. If particle $A_c$ is instead a bound state of $A_a$ with itself then $R_a$ is expected to have a bound state at $\theta = i\pi/2 - U^c_{aa}/2$ as shown in figure 3.7. The

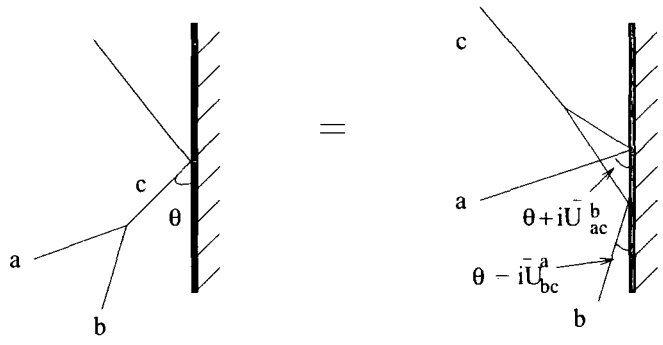


Figure 3.6: The boundary bootstrap constraint

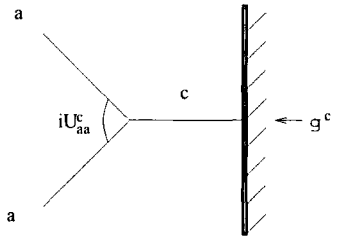


Figure 3.7: The boundary coupling of a bulk bound state

corresponding residue is

$$K^a(\theta) \approx \frac{i}{2}\frac{C^{aac}g^c}{\theta - iU^c_{aa}} \tag{3.3.24}$$

where $C^{aac}$ is the bulk three-point coupling and $g^c$ is the coupling of particle $A_c$ with the boundary.

It is also possible to find boundary bound states in the spectrum. These occur when an incoming particle binds to the boundary, thereby changing its state. The boundary fusing angle, $u^{\beta}_{\alpha a}$, is associated to a particle $A_a$, binding to the boundary and changing its state from $|\alpha\rangle$ to $|\beta\rangle$, as shown in figure 3.8. The reflection factor

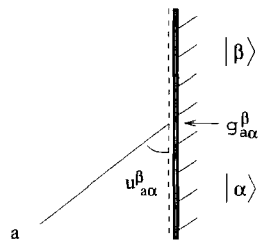


Figure 3.8: Boundary bound state

$R_a^\alpha$ will have an associated pole at $iu_{\alpha a}^\beta$ and around this pole it can be considered as

$$R_a^\alpha(\theta) \approx \frac{i}{2}\frac{g_{a\alpha}^\beta g_\beta^{a\alpha}}{\theta - iu_{\alpha a}^\beta} \tag{3.3.25}$$

in terms of the boundary couplings shown in figure 3.8. This also has an associated bootstrap condition, shown in figure 3.9, and given by

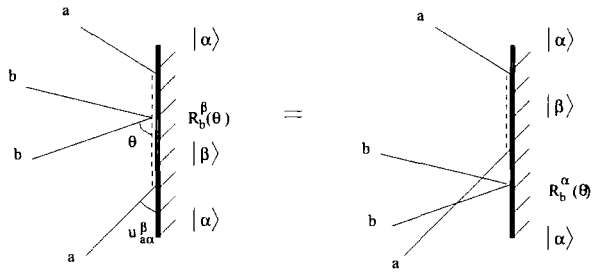


Figure 3.9: The boundary bound state bootstrap constraint

$$R_b^\beta(\theta) = S_{ab}(\theta - iu_{\alpha a}^\beta)R_b^\alpha(\theta)S_{ab}(\theta - iu_{\alpha a}^\beta)\,. \tag{3.3.26}$$

The difference in energy of these two boundary states can be written in terms of the mass of particle $a$ and the boundary fusing angle

$$e_\beta - e_\alpha = m_a \cos(u_{\alpha a}^\beta). \tag{3.3.27}$$

These bootstrap constraints can be used to construct reflection factors, in much the same way as the corresponding bulk constraints were used for the S-matrix. Assuming that all the boundary states can be formed from the vacuum state by binding a bulk particle to the boundary, once reflection factors for the vacuum boundary state are known for all bulk particles they can be examined for evidence pointing to further boundary states. Reflection factors can then be constructed for these boundary states using (3.3.26) which are then also searched. This is repeated until all poles are accounted for without the need to introduce any more boundary states.

Some care must be taken here, just as in the bulk case, since not all poles will correspond to boundary bound states. For example, reflection factors will, in general, contain simple poles which do not depend on any boundary parameter, although one would expect boundary bound states to depend on the properties of the boundary. These poles must therefore be simple reflections off the boundary given by the

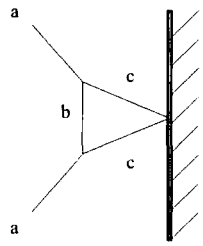


Figure 3.10: A boundary independent Coleman-Thun process

processes shown in diagram 3.7 and 3.10. The latter is a more complicated process which requires an appropriate bulk vertex. There are also two mechanisms by which boundary parameter dependent poles can exist, without the formation of new boundary bound states. The first of these is the boundary analogue of the 'u-channel' process in the bulk [74]: if a particle $a$, with rapidity $\theta$, binds to the boundary thereby exciting it to a state $|\beta\rangle$, then the reflection factor of the same particle on this new state, $R_a^\beta$, will have a pole at the same rapidity $\theta$. This occurs as the boundary initially emits particle $a$, which returns to its original state, the new state then being recreated by the incoming particle $a$, as shown in figure 3.11. The second mecha-

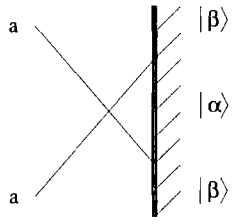


Figure 3.11: The 'u-channel' process

nism is via Coleman-Thun type processes [74], as shown in figure 3.12, which exist provided there are suitable bulk and boundary vertices to make them close. Naively they are second order, but they can be reduced to first order if there is a zero in the reflection factor, or in the case of the RHS of figure 3.12, in the S-matrix element at the appropriate rapidity. A point to note is that as the boundary parameter is varied, poles can change from describing a boundary bound state, to being due to a Coleman-Thun process. This will become clear later as a pole analysis of the 'mixed' boundary condition of the three-state Potts model is worked through.

The main problem here lies in constructing the reflection factors for the vacuum

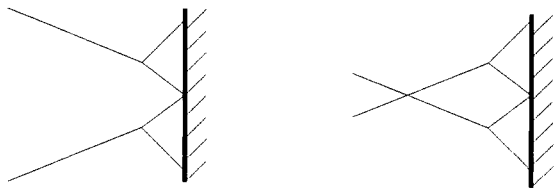

Figure 3.12: Boundary dependent Coleman-Thun processes

boundary state since, for a given bulk S-matrix, there are infinitely-many distinct sets of reflection factors consistent with these constraints, because any solution can be multiplied by a solution of the bulk bootstrap, unitarity and crossing equations to yield another solution [75]. To identify a set of reflection factors as physically relevant some more information is needed. A common basis for the conjecturing of bulk scattering amplitudes is a 'minimality hypothesis', that in the absence of other requirements one should look for solutions of the constraints with the smallest possible number of poles and zeros. This will be used later to construct a set of reflection factors for the $A$, $D$, $E$ related theories.

Of course, one still needs some way to test these reflection factors, to see if they are physical and to match them with conformal boundary conditions in the UV limit. In the bulk case, the S-matrices were matched to specific perturbed conformal field theories using the TBA $c_{\text{eff}}$, so what is needed is a boundary analogue of this. An obvious candidate for this is the $g$-function, defined by Affleck and Ludwig in [3]. An off-critical version of this must therefore be constructed.

## 3.4 Off-Critical g-function

In a massive model, the $g$-function can be defined in a similar way to the CFT version [76, 78, 4]. One starts with the partition function $Z_{\langle\alpha|\alpha\rangle}[L,R]$ for the theory on a finite cylinder of circumference $L$, length $R$ and boundary conditions of type $\alpha$ at both ends. In the $R$-channel description, time runs along the length of the cylinder, and the partition function is represented as a sum over an eigenbasis $\{|\psi_k\rangle\}$ of $H^{\text{circ}}(M,L)$, the Hamiltonian which propagates states along the cylinder:

$$Z_{\langle\alpha|\alpha\rangle}[L,R] = \langle\,\alpha|\,e^{-RH^{\text{circ}}(M,L)}\,|\alpha\,\rangle = \sum_{k=0}^{\infty}\,(\mathcal{G}^{(k)}_{|\alpha\rangle}(l))^2\,e^{-RE^{\text{circ}}_k(M,L)}\,. \tag{3.4.1}$$

Here $l = ML$, $M$ is the mass of the lightest particle in the theory, and

$$\mathcal{G}^{(k)}_{|\alpha\rangle}(l) = \frac{\langle\alpha|\psi_k\rangle}{\langle\psi_k|\psi_k\rangle^{1/2}} \,, \tag{3.4.2}$$

where $|\alpha\rangle$ is the (massive) boundary state [72] for the $\alpha$ boundary condition. At finite values of $l$ any possible infinite-volume vacuum degeneracy is lifted by tunnelling effects, making the ground state $|\psi_0\rangle$ unique. This gives $Z_{\langle\alpha|\alpha\rangle}$ the following leading and next-to-leading behaviour in the large-$R$ limit:

$$\ln Z_{\langle\alpha|\alpha\rangle}[L,R] \sim -RE_0^{\rm circ}(M,L) + 2\ln \mathcal{G}^{(0)}_{|\alpha\rangle}(l)\,. \tag{3.4.3}$$

It is the second, sub-leading term which characterises the massive $g$-function. Subtracting a linearly-growing piece $-f_{|\alpha\rangle}L$, the $g$-function for the boundary condition $\alpha$ at system size $l$ is defined to be

$$\ln g_{|\alpha\rangle}(l) = \ln \mathcal{G}^{(0)}_{|\alpha\rangle}(l) + f_{|\alpha\rangle}L \,. \tag{3.4.4}$$

The constant $f_{|\alpha\rangle}$ is equal to the constant (boundary) contribution to the ground-state energy $E_0^{\rm strip}(R)$ of the $L$-channel Hamiltonian $H^{\rm strip}(R) \equiv H^{\rm strip}_{\langle\alpha|\alpha\rangle}(R)$, which propagates states living on a segment of length $R$ and boundary conditions $\alpha$ at both ends.

An alternative expression for $g$ can be obtained by comparing (3.4.3) with the $L$-channel representation, a sum over the full set $\{E_k^{\rm strip}(R)\}$ of eigenvalues of $H^{\rm strip}(R)$:

$$Z_{\langle\alpha|\alpha\rangle}[L,R] = \sum_{k=0}^{\infty} e^{-LE_k^{\rm strip}(M,R)}\,. \tag{3.4.5}$$

As $R$ is sent to infinity, this gives the $g$-function:

$$\ln g_{|\alpha\rangle}(l) = \frac{1}{2}\lim_{R\to\infty}\left[\ln\left(\sum_{k=0}^{\infty} e^{-LE_k^{\rm strip}(M,R)}\right) + 2f_{|\alpha\rangle}L + RE_0^{\rm circ}(M,L)\right]. \tag{3.4.6}$$

In theories with only massive excitations in the bulk and no infinite-volume vacuum degeneracy, $\ln g_{|\alpha\rangle}(l)$ tends exponentially to zero at large $l$, while in the UV limit $l \to 0$ it reproduces the value of the $g$-function in the unperturbed boundary conformal field theory.

In the CFT case, at this point the modular invariance of the partition function was employed to solve for the $g$-function, however for massive theories this is not available and instead the energy, $E_k^{\rm strip}(M,R)$, must be estimated using the particle basis of states and thermodynamic Bethe Ansatz.

### 3.4.1 L-channel TBA

Consider the theory on a cylinder of length R and circumference L with boundary conditions $\alpha$ and $\beta$ at the ends. There are two TBA descriptions, the L-channel and the R-channel. The first construction of the off-critical g-function was made, in [76] (making use of results from [77]), using the L-channel TBA which will now be described. Taking time evolution along the circumference of length L the Hilbert space is constructed along the finite length R. In the limit $R \to \infty$, the Hilbert space in this description is given by scattering states and the construction of the TBA equation and minimisation of the free energy is analogous to the case with periodic boundary conditions described in section 2.5. The main difference here is that in the large $R$ limit, the partition function has a boundary contribution from the $g$-function, as shown in (3.4.3), so the TBA method results in an expression for this $g$-function. The details of this calculation are presented below.

Assume for convenience that the theory has N particles, all of the same type, and take them to be sufficiently well spaced to be considered asymptotic. Analogous to the TBA on the torus, discussed in section 2.5, when one particle moves towards another, interacts with it and moves past until it can again be taken to be asymptotic, the wavefunction picks up a factor of the S-matrix. If this particle moves to the right, bounces off the boundary, where the wavefunction picks up a factor of $R(\theta)$, and returns to its original position the resulting wavefunction should be equal to that obtained when the same particle performs the same operation to the left. This equality imposes the quantisation condition

$$e^{iMR\sinh(\theta_i)}\left(\prod_{j=1,j\neq i}^{N} S(\theta_i-\theta_j)\right)R_\beta(\theta_i) = e^{-iMR\sinh(\theta_i)}\left(\prod_{j=1,j\neq i}^{N} S(-\theta_i-\theta_j)\right)R_\alpha(-\theta_i). \tag{3.4.7}$$

By unitarity, $S^{-1}(\theta) = S(-\theta)$ and $R^{-1}(\theta) = R(-\theta)$ so this condition can be rewritten as

$$e^{2iMR\sinh(\theta_i)}\left(\prod_{j=1,,j\neq i}^{N} S(\theta_i-\theta_j)S(\theta_i+\theta_j)\right)R_\beta(\theta_i)R_\alpha(\theta_i) = 1 \tag{3.4.8}$$

with $\theta_i > 0$. Taking the logarithm of this

$$2iMR\sinh(\theta_i) + \sum_{j\neq i}(\ln S(\theta_i-\theta_j) + \ln S(\theta_i+\theta_j)) + \ln R_\beta(\theta_i) + \ln R_\alpha(\theta_i) = 2\pi i n. \tag{3.4.9}$$

In the thermodynamic limit, $R \to \infty$ and $N \to \infty$, a continuous particle density can be introduced

$$\rho^r(\theta) = \frac{d}{\Delta\theta} \tag{3.4.10}$$

where $d$ is the number of particles with rapidity between $\theta$ and $\theta + \Delta\theta$. This can be defined for negative rapidity by $\rho(-\theta) = \rho(\theta)$ and the quantisation condition, written in terms of this density, is

$$\begin{aligned} 2MR\cosh(\theta) + 2\pi \int \phi(\theta - \theta')\rho^r(\theta)d\theta' \\ + 2\pi\left(-2\phi(2\theta) + \frac{1}{2}\phi_\alpha(\theta) + \frac{1}{2}\phi_\beta(\theta) - \delta(\theta)\right) = 2\pi\rho(\theta) \end{aligned} \tag{3.4.11}$$

where $\rho(\theta) = \rho^r(\theta) + \rho^h(\theta)$ is the level density, $\phi(\theta) = -\frac{i}{2\pi}\frac{d}{d\theta}\ln S(\theta)$ and $\phi_\alpha(\theta) = -\frac{i}{\pi}\frac{d}{d\theta}\ln R_\alpha(\theta)$. Note that the terms $-4\pi\phi(2\theta) - 2\pi\delta(\theta)$ here result from the fact that the original sum in (3.4.9) is over $\theta_i$ where $\theta_i \neq 0$ and $\theta_i \neq \theta_j$.

The number of states, $\mathcal{N}[\rho^r(\theta)]$, with effective particle density $\rho^r(\theta)$ is given by the number of possible configurations of particles. If $D = \rho(\theta)\Delta\theta$ is the maximum number of rapidities in the interval $(\theta, \theta + \Delta\theta)$, this number is just

$$\mathcal{N}[\rho^r(\theta)] = \frac{D!}{d!(D-d)!}. \tag{3.4.12}$$

As in the torus TBA this can be written as

$$\mathcal{N}[\rho^r(\theta)] \sim \exp\left[\int \rho\ln\rho - \rho^r\ln\rho^r - (\rho - \rho^r)\ln(\rho - \rho^r)d\theta\right] \tag{3.4.13}$$

using Stirling's formula $\ln\Gamma(z) \sim z\ln z - z + \ldots$. The partition function is

$$Z = \sum_{\text{states}} e^{-LE} = \int \mathcal{D}[\rho^r(\theta)]\mathcal{N}[\rho^r(\theta)]e^{-LE[\rho^r(\theta)]} \tag{3.4.14}$$

where the energy of each configuration is

$$E = \int_0^\infty (M\cosh(\theta))\rho^r(\theta)d\theta. \tag{3.4.15}$$

In the $R \to \infty$ limit, the logarithm of the partition function is given by

$$\begin{aligned} \ln Z &\sim -RE_0^{circ}(L) + \ln(g_\alpha(L)g_\beta(L)) \\ &= \int_0^\infty \left[-LM\cosh(\theta)\rho^r(\theta) + \rho\ln\rho - \rho^r\ln\rho_(\rho - \rho^r)\ln(\rho - \rho^r)\right] d\theta \end{aligned} \tag{3.4.16}$$

and this can be minimised, subject to the constraint from (3.4.11), in the same way as the log of the torus partition function (2.5.15) was treated in section 2.5. First the TBA equation is found by setting $\delta(3.4.16)/\delta\rho^r(\theta) = 0$ where

$$\frac{\delta(3.4.16)}{\delta\rho^r(\theta)} = \frac{\partial(3.4.16)}{\partial\rho^r(\theta)} + \int \frac{\delta\rho(\theta')}{\delta\rho^r(\theta')}\frac{\partial(3.4.16)}{\partial\rho(\theta')}\,d\theta'. \tag{3.4.17}$$

Notice that the integrand of (3.4.16) is the same as that in (2.5.15), and the constraint (3.4.11) differs from (2.5.10) by terms independent of $\rho^r(\theta)$ therefore the TBA equation here is exactly that of the periodic boundary case

$$\epsilon(\theta) = ML\cosh(\theta) - \int \phi(\theta-\theta')\ln(1+e^{-\epsilon(\theta')})\,d\theta' \tag{3.4.18}$$

where the pseudoenergies are defined by $\rho^r(\theta)/(\rho(\theta)-\rho^r(\theta)) = e^{-\epsilon(\theta)}$, as before. The difference in this case comes when simplifying the integrand, $I$, of (3.4.16) using this TBA equation. Writing the integrand in terms of the pseudoenergies:

$$I = -ML\cosh(\theta)\rho^r(\theta) + \rho(\theta)\ln(1+e^{-\epsilon(\theta)}) + \rho^r(\theta)\epsilon(\theta) \tag{3.4.19}$$

and replacing $\rho(\theta)$ here with the constraint (3.4.11) gives

$$\begin{aligned} I = &- ML\cosh(\theta)\rho^r(\theta) + \frac{1}{\pi}MR\cosh(\theta)\ln(1+e^{-\epsilon(\theta)}) \\ &+ \int \phi(\theta-\theta')\rho^r(\theta')\,d\theta'\,\ln(1+e^{-\epsilon(\theta)}) \\ &+ \left(\frac{1}{2}\phi_\alpha(\theta) + \frac{1}{2}\phi_\beta(\theta) - 2\phi(2\theta) - \delta(\theta)\right)\ln(1+e^{-\epsilon(\theta)}) + \rho^r(\theta)\epsilon(\theta). \end{aligned} \tag{3.4.20}$$

Using the TBA equation then results in

$$\begin{aligned} &- RE_0^{circ}(L) + \ln(g_\alpha(L)g_\beta(L)) = \\ &\int_0^\infty \left(\frac{1}{\pi}MR\cosh(\theta) - 2\phi(2\theta) + \frac{1}{2}\phi_\alpha(\theta) + \frac{1}{2}\phi_\beta(\theta) - \delta(\theta)\right)\ln(1+e^{-\epsilon(\theta)})\,d\theta. \end{aligned} \tag{3.4.21}$$

Once the range of $\theta$ is extended by symmetry, the ground state energy, without the bulk contribution is given by

$$E_0^{circ}(L) = -\int M\cosh(\theta)\ln(1+e^{-\epsilon(\theta)})\frac{d\theta}{2\pi} \tag{3.4.22}$$

which is the usual result from the TBA on a torus, and the off-critical $g$-function is

$$\ln(g_\alpha(l)) = \frac{1}{4}\int (\phi_\alpha(\theta) - 2\phi(2\theta) - \delta(\theta))\ln(1+e^{-\epsilon(\theta)})\,d\theta. \tag{3.4.23}$$

This result can be extended to a theory with $N$ particle species where

$$\ln g_\alpha(l) = \frac{1}{4}\sum_{a=1}^{N}\int_{\mathbb{R}} d\theta\, \Theta_a(\theta)\ln(1+e^{-\epsilon_a(\theta)}), \tag{3.4.24}$$

$\Theta_a(\theta) = \left(\phi_\alpha^{(a)}(\theta) - 2\phi_{aa}(2\theta) - \delta(\theta)\right)$ and now $\phi_\alpha^{(a)} = -\frac{i}{\pi}\frac{d}{d\theta}\ln R_\alpha^{(a)}(\theta)$ and $\phi_{aa}(\theta) = -\frac{i}{2\pi}\frac{d}{\theta}\ln S_{aa}(\theta)$.

This was tested extensively for the Yang-Lee model (introduced below) in [79] using conformal perturbation theory (CPT) and the boundary truncated conformal space approach (BTCSA). It was shown that for non-zero $M$, the $l$-dependence of (3.4.24) is incorrect, both in the total change in $g_\alpha(l)$ between the UV and IR, and in the behaviour of the small-$l$ series expansion. However, the dependence of $g_\alpha(l)$ on boundary parameters at fixed $l$, and the ratios of the $g$ functions, $g_\alpha(l)/g_\beta(l)$ are in good agreement with the CPT and BTCSA results. The formula for $g_\alpha(l)$, given in (3.4.24), should therefore be modified by adding some boundary condition independent terms.

Possible sources of error in this construction of the $g$-function could be the saddle point evaluation of the partition function, or corrections from the next-to-leading term in Stirling's formula [79]. These problems will also exist in the calculation of the effective central charge, however as this is a leading order term, as opposed to the next-to-leading order $g$, the resulting errors are no larger than the numerical errors in the CPT and TCSA.

One might also think that problems with this equation ought to occur with the presence of boundary bound states in the spectrum. This was examined in [79], again for the Yang-Lee model. This is the nonunitary minimal model $\mathcal{M}_{2,5}$ with central charge $c = -22/5$. It has two primary fields $\mathbb{1}$ and $\varphi$ with conformal dimensions $h_{\mathbb{1}} = 0$ and $h_\varphi = -1/5$ respectively, and two conformal boundary conditions: $\mathbb{1}$ with no relevant boundary fields and $\Phi$ with one relevant boundary field $\phi$. The bulk spectrum contains a single particle, with two particle S-matrix [80]

$$S(\theta) = -(1)(2) \quad , \quad (x) = \frac{\sinh(\frac{\theta}{2} + \frac{i\pi x}{6})}{\sinh(\frac{\theta}{2} - \frac{i\pi x}{6})}. \tag{3.4.25}$$

The reflection factors corresponding to the boundary conditions $\Phi(\mu)$ (where $\mu$ is the boundary coupling) and $\mathbb{1}$ are [78]

$$R_{\Phi(\mu)}(\theta) = R_b(\theta) \quad , \quad R_{\mathbb{1}}(\theta) = R_0(\theta) \tag{3.4.26}$$

where

$$R_b(\theta) = \left(\frac{1}{2}\right)\left(\frac{3}{2}\right)\left(\frac{4}{2}\right)^{-1}\left[S\left(\theta + i\pi\frac{b+3}{6}\right)S\left(\theta - i\pi\frac{b+3}{6}\right)\right]^{-1} \tag{3.4.27}$$

and the relation between the boundary coupling $\mu$ and the parameter $b$ is [78][79]

$$\begin{aligned}\mu &= -|\mu_c|\sin\left(\frac{\pi(b+0.5)}{5}\right)M^{6/5} \qquad (3.4.28)\\ \mu_c &= -\pi^{3/5}2^{4/5}5^{1/4}\frac{\sin(2\pi/5)}{(\Gamma(3/4)\Gamma(4/5))^{1/2}}\left(\frac{\Gamma(2/3)}{\Gamma(1/6)}\right)^{6/5}.\end{aligned}$$

For this model, two concerns with the equation (3.4.24) were identified in [79]. The first is that the two distinct boundary conditions, $\Phi(\mu(b=0))$ and $\mathbb{1}$ are described by the same reflection factor and so have the same kernel function $\phi_0$, but they have different $g$-functions. The second problem is that the kernel $\phi_b$, describing the $\Phi(\mu(b))$ boundary condition has poles which are $b$-dependent and which cross the real axis for $b = \pm 1$. Taking (3.4.24), with the integration contour always along the real axis therefore leads to a $g$-function with discontinuities at $b = \pm 1$, whereas physical $g$-functions ought to be continuous in $b$. These problems are resolved if the integration contour, rather than being the real line in every case, is taken to be dependent on the boundary condition.

In [79], it is shown that the correct ratio of $g$-functions is found if the real line is taken as the contour for $\ln g_{\mathbb{1}}$. This is also the case for $\ln g_{\Phi(\mu(b))}$, when $-3 < b < -1$. To identify the relevant contour for the boundary condition $\Phi(\mu(b))$, for other values of $b$, the terms in the integrand of $\ln g_{\Phi(\mu(b))}$ with $b$-dependent poles must first be identified and treated separately:

$$\phi_b(\theta) = \phi_0(\theta) - \phi\left(\theta - i\pi\frac{b+3}{6}\right) - \phi\left(\theta + i\pi\frac{b+3}{6}\right) \tag{3.4.29}$$

so for $-3 < b < -1$

$$\ln g_{\Phi(\mu(b))} = \ln g_{\mathbb{1}} - \int_{-\infty}^{\infty}\left(\phi\left(\theta - i\pi\frac{b+3}{6}\right) + \phi\left(\theta + i\pi\frac{b+3}{6}\right)\right)\ln(1+e^{-\epsilon(\theta)})\frac{d\theta}{4\pi}. \tag{3.4.30}$$

The two terms in this integral give the same contribution when the contour is along the real axis, so for $-3 < b < -1$

$$\ln g_{\Phi(\mu(b))} - \ln g_{\mathbb{1}} = -\int_{-\infty}^{\infty}\phi\left(\theta - i\pi\frac{b+3}{6}\right)(1+e^{-\epsilon(\theta)})\frac{d\theta}{2\pi}. \tag{3.4.31}$$

Now $\phi(\theta - i\pi\frac{b+3}{6})$ has poles at

$$\theta = i\pi\frac{b-5}{6} + 2n\pi i \quad , \quad \theta = i\pi\frac{b-1}{6} + 2n\pi i$$
$$\theta = i\pi\frac{b+1}{6} + 2n\pi i \quad , \quad \theta = i\pi\frac{b+5}{6} + 2n\pi i \tag{3.4.32}$$

so when $b$ passes through $-1$, the contour must deform away from the real axis and encircle the pole at $i\pi(b+1)/6$. This pole is then called 'active'. The same then happens as $b$ passes through 1, when the pole at $i\pi(b-1)/6$ becomes 'active'. This is shown in figure 3.13, taken from [79].

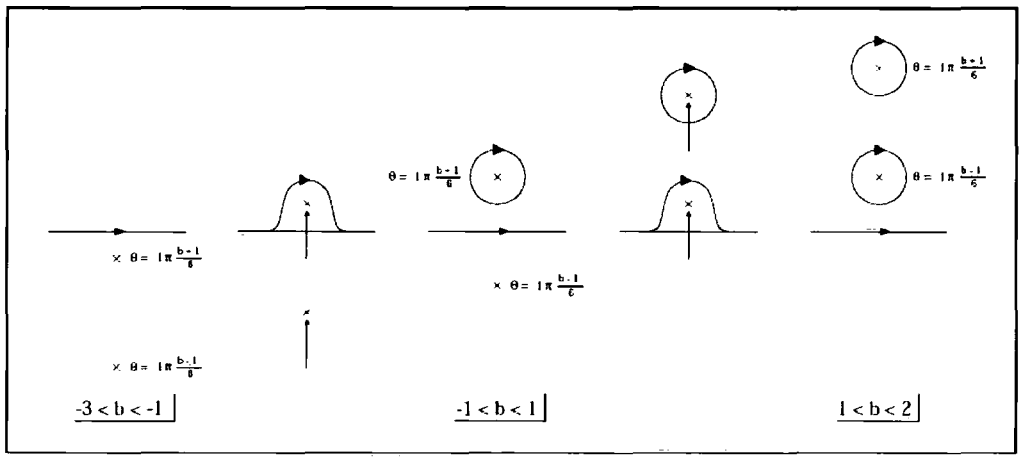


Figure 3.13: The contour for $\ln g_{\Phi(\mu(b))}$, from [79]

In [4], a new expression for the $g$ function was proposed and tested for the Lee-Yang case. The construction avoids the use of the saddle point approximation by employing an n-particle cluster expansion technique. Before this is discussed, it is necessary to introduce the $R$-channel TBA [76] as this will be used later on.

### 3.4.2 R-channel TBA

Taking time along the length, R, of the cylinder the partition function is

$$Z_{\alpha\beta} = \langle B_\alpha | e^{-RH} | B_\beta \rangle \tag{3.4.33}$$

where $H$ is the Hamiltonian of the bulk system. The boundary states can be written as [72]

$$|B\rangle = \exp\left(\int_0^\infty \frac{d\theta}{2\pi} K(\theta) A^\dagger(-\theta) A^\dagger(\theta)\right)|0\rangle \tag{3.4.34}$$

for infinite L. For simplicity, consider a model with 1 type of particle. The partition function for this model, in the R-channel, can be written as

$$Z_{ab} = \sum_{\alpha} \frac{\langle B_a|\alpha\rangle\langle\alpha|B_b\rangle}{\langle\alpha|\alpha\rangle} e^{-RE_\alpha} \tag{3.4.35}$$

with $E_\alpha = \sum_{i=1}^{N} 2M\cosh\theta_i$. Formally, this is a sum over all the states in the theory, but due to the form of the boundary state the only states $|\alpha\rangle$ which contribute to this sum must have the form

$$\begin{aligned} |\alpha_{2N}\rangle &= |\theta_N, -\theta_N, \ldots, \theta_1, -\theta_1\rangle \\ &= A^\dagger(\theta_N)A^\dagger(-\theta_N)\ldots A^\dagger(\theta_1)A^\dagger(-\theta_1)|0\rangle \end{aligned} \tag{3.4.36}$$

with $\theta_N > \theta_{N-1} > \ldots > \theta_1 > 0$. The inner product $\langle B_a|\alpha_{2N}\rangle$ is then given by

$$\begin{aligned} \langle B_a|\alpha_{2N}\rangle = \frac{1}{N!}\int_0^\infty \prod_{i=1}^{N} \frac{d\theta_i}{2\pi}\bar{K}_a(\theta_i) \\ \langle 0|A(-\theta_1)A(\theta_1)\ldots A(-\theta_N)A(\theta_N)A^\dagger(\theta_N)A^\dagger(-\theta_N)\ldots A^\dagger(\theta_1)A^\dagger(-\theta_1)|0\rangle. \end{aligned} \tag{3.4.37}$$

The operators $A$ and $A^\dagger$ can be rearranged using the Faddeev-Zamolodchikov algebra:

$$\begin{aligned} A^\dagger(\theta)A^\dagger(\theta') &= S(\theta-\theta')A^\dagger(\theta')A^\dagger(\theta) \\ A(\theta)A(\theta') &= S(\theta-\theta')A(\theta')A(\theta) \\ A(\theta)A^\dagger(\theta') &= S(\theta-\theta')A^\dagger(\theta')A^\dagger(\theta) + \delta(\theta-\theta') \end{aligned} \tag{3.4.38}$$

and using this (3.4.37) becomes

$$\langle B_a|\alpha_{2N}\rangle = (\delta(0))^N \prod_{i=1}^{N} \bar{K}_a(\theta_i) \tag{3.4.39}$$

where the $(\delta(0))^N$ term results from the terms $\prod_i \delta(\theta-\theta_i)$. Introducing pair creation operators defined as $B(\theta) = A(-\theta)A(\theta)$ and $B^\dagger(\theta) = A^\dagger(\theta)A^\dagger(-\theta)$ they can be easily shown to satisfy

$$\begin{aligned} B(\theta)B(\theta') &= B(\theta')B(\theta) \\ B^\dagger(\theta)B^\dagger(\theta') &= B^\dagger(\theta')B^\dagger(\theta) \\ B(\theta)B^\dagger(\theta') &= B^\dagger(\theta')B(\theta) + \delta^2(\theta-\theta') + \delta(\theta-\theta')S(\theta'-\theta)A^\dagger(-\theta')A(-\theta) \\ &\quad +\delta(\theta-\theta')A^\dagger(\theta')A(\theta). \end{aligned} \tag{3.4.40}$$

The norm $\langle\alpha_{2N}|\alpha_{2N}\rangle$ can be written in terms of these pair operators

$$\begin{aligned}\langle\alpha_{2N}|\alpha_{2N}\rangle &= \langle 0|A(-\theta_1)A(\theta_1)\dots A^\dagger(\theta_1)A^\dagger(-\theta_1)|0\rangle \\ &= \langle 0|B(\theta_1)B(\theta_2)\dots B^\dagger(\theta_2)B^\dagger(\theta_1)|0\rangle\end{aligned} \tag{3.4.41}$$

and using the algebra above this becomes

$$\langle\alpha_{2N}|\alpha_{2N}\rangle = (\delta(0))^{2N}. \tag{3.4.42}$$

Therefore the partition function is simply

$$Z_{ab} = \sum_\alpha \prod_{i=1}^{N} \bar{K}_a(\theta_i)K_b(\theta_i)e^{-R\sum_{i=1}^N 2M\cosh(\theta_i)}. \tag{3.4.43}$$

Following the method described earlier, the density of pairs of particles is introduced, $\rho^r(\theta) = d/\Delta\theta$, where $d$ is now the number of pairs of particles with rapidity in the interval $(\theta, \theta+\Delta\theta)$. In terms of this density, the energy becomes an integral:

$$E_\alpha = 2M\int d\theta\,\cosh(\theta)\rho^r(\theta) \tag{3.4.44}$$

and the partition function is

$$Z_{ab} = \int \mathcal{D}[\rho^r(\theta)]\exp\left(\int_0^\infty \left[\ln(\bar{K}_a(\theta)K_b(\theta)) - 2RM\cosh(\theta)\right]\rho^r(\theta)d\theta + \mathcal{S}(\rho^r)\right) \tag{3.4.45}$$

where $\mathcal{S}$ is the entropy of the particle configuration described by the distribution $\rho^r(\theta)$, as above.

The momenta are constrained by the quantisation condition on the states $|\alpha_{2N}\rangle$:

$$e^{iML\sinh(\theta_i)}S(2\theta_i)\prod_{j\neq i} S(\theta_i-\theta_j)S(\theta_i+\theta_j) = 1. \tag{3.4.46}$$

This is exactly the same as the quantisation condition found in the periodic case when each particle of rapidity $\theta$ is accompanied by another with rapidity $-\theta$. Taking logs of this, introducing the level density $\rho = \rho^r + \rho^h$, and differentiating gives

$$2\pi\rho = ML\cosh(\theta) - 2\pi\int_0^\infty \left(\phi(\theta-\theta') + \phi(\theta+\theta')\right)\rho^r(\theta')d\theta' \tag{3.4.47}$$

with $\phi(\theta) = -\frac{1}{2\pi i}\frac{d}{d\theta}\ln S(\theta)$. For large $L$, the logarithm of the partition function is

$$\begin{aligned}\ln Z_{ab} &\approx -LE_0^{\text{strip}}(R) \\ &= \int_0^\infty \left(\ln(\bar{K}_a(\theta)K_b(\theta)) - 2RM\cosh(\theta)\right)\rho^r(\theta) + \mathcal{S}(\rho^r).\end{aligned} \tag{3.4.48}$$

The TBA equation can be found, using the same method as described earlier: set $\delta(3.4.48)/\delta\rho^r(\theta) = 0$ where

$$\frac{\delta(3.4.48)}{\delta\rho^r(\theta)} = \frac{\partial(3.4.48)}{\partial\rho^r(\theta)} + \int \frac{\delta\rho(\theta')}{\delta\rho^r(\theta')}\frac{\partial(3.4.48)}{\partial\rho(\theta')}\,d\theta'. \tag{3.4.49}$$

Now from the constraint (3.4.47) it is clear that

$$\frac{\delta\rho(\theta')}{\delta\rho^r(\theta)} = \phi(\theta-\theta') + \phi(\theta+\theta') \tag{3.4.50}$$

and the derivative of (3.4.48) with respect to the level density is the same as for the previous cases

$$\frac{\partial(3.4.48)}{\partial\rho(\theta)} = \ln(1+e^{-\epsilon(\theta)}), \tag{3.4.51}$$

but the derivative with respect to the root density is different

$$\frac{\partial(3.4.48)}{\partial\rho^r(\theta)} = \ln(\bar{K}_a(\theta)K_b(\theta)) - 2RM\cosh(\theta) + \epsilon(\theta) \tag{3.4.52}$$

which leads to a TBA equation which is different to the $L$-channel and periodic boundary condition cases:

$$\begin{aligned}\epsilon(\theta) =& 2RM\cosh(\theta) - \ln(\bar{K}_a(\theta)K_b(\theta)) \\ &+ \int_0^\infty (\phi(\theta-\theta')\phi(\theta+\theta'))\ln(1+e^{-\epsilon(\theta')})\,d\theta'.\end{aligned} \tag{3.4.53}$$

Writing the integrand of (3.4.48), denoted $I$, in terms of the pseudoenergies gives

$$I = \left(\ln(\bar{K}_a(\theta)K_b(\theta)) - 2RM\cosh(\theta)\right)\rho^r(\theta) + \rho(\theta)\ln(1+e^{-\epsilon(\theta)}) + \rho^r(\theta)\epsilon(\theta) \tag{3.4.54}$$

and replacing $\rho$, using the constraint (3.4.47), leads to

$$\begin{aligned}I =& (\ln(\bar{K}_a K_b) - 2RM\cosh(\theta))\rho^r(\theta) + \frac{1}{2\pi}ML\cosh(\theta)\ln(1+e^{-\epsilon(\theta)}) \\ &+ \int_0^\infty (\phi(\theta-\theta') + \phi(\theta+\theta'))\,\rho^r(\theta')\ln(1+e^{-\epsilon(\theta)})\,d\theta' + \rho^r(\theta)\epsilon(\theta).\end{aligned} \tag{3.4.55}$$

Then, with the TBA equation (3.4.53), this simplifies to give

$$I = \frac{1}{2\pi}ML\cosh(\theta)\ln(1+e^{-\epsilon(\theta)}). \tag{3.4.56}$$

Since $\bar{K}(\theta) = K(-\theta)$, the term $\bar{K}_a(\theta)K_b(\theta)$ is even in $\theta$ so the domain of the definition of $\epsilon(\theta)$ can be extended to the whole real axis by $\epsilon(-\theta) = \epsilon(\theta)$. This can

also be extended to a theory with $N$ particle types, for which the ground state energy on an interval of length R is

$$E_0^{\text{strip}}(M,R) = -\sum_{a=1}^{N}\int_{\mathbb{R}}\frac{d\theta}{4\pi}M_a\cosh(\theta)L_a(\theta) + \mathcal{E}M_1^2R + f_\alpha + f_\beta \tag{3.4.57}$$

where $\mathcal{E}M_1^2R$ is the bulk contribution to the energy, $f_\alpha$, $f_\beta$ are R-independent contributions to the energy from the boundaries and $L_a(\theta) = \ln(1+e^{-\epsilon_a(\theta)})$. The TBA equation for this theory, written in terms of the reflection factors is

$$\begin{aligned}\epsilon_a(\theta) =& 2M_aR\cosh(\theta) - \ln\left(R_\alpha^{(a)}\left(i\frac{\pi}{2}-\theta\right)R_\beta^{(a)}\left(i\frac{\pi}{2}+\theta\right)\right)\\ &-\sum_{b=1}^{N}\int_{\mathbb{R}}d\theta'\phi_{ab}(\theta-\theta')L_b(\theta').\end{aligned} \tag{3.4.58}$$

In [78], generalisations of these equations are shown to govern the excited state energies $E_n^{\text{strip}}(M,R)$. The idea is to use analytic continuation to move between energy levels [81]. In [78], rather than derive the results using the method of [81], the formulae are conjectured and then checked using the boundary truncated conformal space approach (BTCSA). In the large $R$ limit these generalisations reduce to simple forms. If the $n^{\text{th}}$ excited state is made up of $m = \sum_{a=1}^{N} m^{(a)}$ particles, $m^{(a)}$ being the number of particles of type $a$, then

$$E_n^{\text{strip}}(M,R) - E_0^{\text{strip}}(M,R) = \sum_{a=1}^{N}\sum_{i=1}^{m^{(a)}} M_a\cosh(\theta_i^{(a)}) + O(e^{-RM}). \tag{3.4.59}$$

The rapidities, $\theta_i^{(a)}$, satisfy the Bethe ansatz equations

$$\begin{aligned}2\pi n_i^{(a)} &= 2M_aR\sinh(\theta_i^{(a)}) - i\ln(R_\alpha^{(a)}(\theta_i^{(a)})R_\beta^{(a)}(\theta_i^{(a)}))\\ &\quad -\sum_{b=1}^{N}\sum_{j\neq i} i\ln(-S_{ab}(\theta_i^{(a)}+\theta_j^{(b)}))\\ &\quad -\sum_{b=1}^{N}\sum_{j\neq i} i\ln(-S_{ab}(\theta_i^{(a)}-\theta_j^{(b)})).\end{aligned} \tag{3.4.60}$$

These equations are used in [4] to find an exact IR expansion of the $g$-function, by employing a cluster expansion. This will be briefly discussed below for a theory with only a single particle type.

### 3.4.3 Cluster Expansion

In the $R \to \infty$ limit, the $g$-function, given in (3.4.6), becomes

$$2\ln g_\alpha(l) = RE_0^{\text{circ}} + 2f_\alpha L - LE_0^{\text{strip}} + \ln\left(1 + \sum_{k=1}^{\infty} e^{-L(E_k^{\text{strip}} - E_0^{\text{strip}})}\right) + O(e^{-RM}) \tag{3.4.61}$$

and since, for $R \gg L \gg 0$, $E_0^{\text{strip}} = \mathcal{E}M^2R + 2f_\alpha + O(e^{-RM})$, the $g$-function, to leading order is

$$2\ln g_\alpha(l) \sim R(E_0^{\text{circ}} - \mathcal{E}M^2L) + \ln\left(1 + \sum_{k=1}^{\infty} e^{-L(E_k^{\text{strip}} - E_0^{\text{strip}})}\right). \tag{3.4.62}$$

The cluster expansion involves letting $L \to \infty$, along with $R \to \infty$, so that the right hand side of (3.4.62) can be expanded in terms of 1, 2,... particle contributions, each of which can be estimated using the Bethe ansatz approximated levels in (3.4.59) and (3.4.60). The hope is then to resum this expansion to give an exact expression for the $g$-function.

Taking the large-$R$ equation (3.4.62) and truncating at the one-particle level leaves

$$2\ln g_\alpha \sim R(E_0^{\text{circ}} - \mathcal{E}M^2L) + \ln\left(1 + \sum_{n_1>0} e^{-l\cosh(\theta_1(n_1))}\right) \tag{3.4.63}$$

and the one-particle Bethe ansatz is essentially that of a free particle

$$MR\sinh(\theta_1) - i\ln R_\alpha(\theta_1) = \pi n_1. \tag{3.4.64}$$

In the large-$R$ limit, there is a continuum of possible rapidities so the Bethe ansatz becomes

$$\frac{\Delta\theta_1}{\pi}\left(MR\cosh(\theta_1) - i\frac{d}{d\theta}\ln R_\alpha(\theta_1)\right) = 1. \tag{3.4.65}$$

The sum in (3.4.63) becomes an integral

$$\begin{aligned}\sum_{n_1>0} e^{-l\cosh(\theta_1)} &= \frac{1}{2}\left(\sum_{n_1=-\infty}^{\infty} e^{-l\cosh(\theta_1)} - e^{-l}\right) \\ &\to \frac{1}{2}\int_{\mathbb{R}} d\theta\,(J^{(1)}(\theta) - \delta(\theta))e^{-l\cosh(\theta)}\end{aligned} \tag{3.4.66}$$

with the Jacobian, $J^{(1)}(\theta)$, for the change of variables $n_1 \to \theta_1 \equiv \theta$, from (3.4.65), being

$$J^{(1)}(\theta) = \frac{MR}{\pi}\cosh(\theta) + \phi_\alpha(\theta) \tag{3.4.67}$$

where $\phi_\alpha = -\frac{i}{\pi}\frac{d}{d\theta}\ln R_\alpha$. The cosh term here cancels with the leading order part of $R(E_0^{\rm circ} - \mathcal{E}M^2L)$, so the one-particle contribution to $\ln g$ is

$$2\ln g = \frac{1}{2}\int_{\mathbb{R}} d\theta\,(\phi_\alpha - \delta(\theta))e^{-l\cosh(\theta)}. \tag{3.4.68}$$

This disagrees with the large-$l$ behaviour of (3.4.24), in particular, there is no $\phi(2\theta)$ term. However, the hope is that it gives an indication of how to modify the previous result (3.4.24). The assumption is that the final result will depend, like (3.4.24), on the single-particle energies only through the TBA pseudoenergies $\epsilon(\theta)$. The first observation to make, therefore, is that the large-$l$ asymptotic of (3.4.68) also emerges from

$$2[\ln g_\alpha]_D^{(1)} = \frac{1}{2}\int_{\mathbb{R}} d\theta\,(\phi_\alpha(\theta) - \delta(\theta))\ln(1+e^{-\epsilon(\theta)}) \tag{3.4.69}$$

which is the resummed, or 'dressed' version of (3.4.68). Numerically, in [4], it is shown that (3.4.69) is more accurate than (3.4.68) and this is because it actually contains, not just one-particle contributions, but $n > 1$ particle contributions also.

The next step is to consider the two-particle contributions. Some of these will be taken care of by the one-particle resummation, but there are some new terms:

$$\begin{aligned} 2\ln g_\alpha =& 2[\ln g_\alpha]_D^{(1)} + \frac{1}{2}\int_{\mathbb{R}^2} d\theta_1 d\theta_2\,\phi(\theta_1+\theta_2)\phi(\theta_1-\theta_2)e^{-l\cosh(\theta_1)-l\cosh(\theta_2)} \\ & - \frac{1}{2}\int_{\mathbb{R}} d\theta\,\phi(2\theta)e^{-2l\cosh(\theta)}. \end{aligned} \tag{3.4.70}$$

This can then be resummed as

$$\begin{aligned} 2[\ln g_\alpha]_D^{(2)} =& \frac{1}{2}\int_{\mathbb{R}^2} d\theta_1 d\theta_2\,\phi(\theta_1+\theta_2)\phi(\theta_1-\theta_2)e^{-\epsilon(\theta_1)-\epsilon(\theta_2)} \\ & - \frac{1}{2}\int_{\mathbb{R}} d\theta\,\phi(2\theta)e^{-2\epsilon(\theta)} \end{aligned} \tag{3.4.71}$$

and the final result is given by $2\ln g_\alpha = 2[\ln g_\alpha]_D^{(1)} + 2[\ln g_\alpha]_D^{(2)} + \ldots$.

The observation made in [4] is that if the first few terms are corrected with

$$e^{-l\cosh(\theta)} \to \frac{1}{1+e^{\epsilon(\theta)}} \tag{3.4.72}$$

then the only contribution from the next order is of the form

$$\begin{aligned} C_n = \frac{1}{n}\int_{\mathbb{R}^n} & d\theta_1\ldots d\theta_n\,\phi(\theta_1+\theta_1)\phi(\theta_2-\theta_3)\ldots\phi(\theta_n-\theta_1) \\ & \times e^{-l\cosh(\theta_1)}\ldots e^{-l\cosh(\theta_n)} \end{aligned} \tag{3.4.73}$$

along with an additional term containing a single integration over $\phi(2\theta)$. The final conjecture is then to replace $l\cosh(\theta)$ with $\epsilon(\theta)$ and resum as

$$\int_{\mathbb{R}} d\theta\,\phi(2\theta)\left(-\frac{1}{2}e^{-2l\cosh(\theta)}\right) \to -\int_{\mathbb{R}} d\theta\,\phi(2\theta)\left(\ln(1+e^{-\epsilon(\theta)}) - \frac{1}{1+e^{\epsilon(\theta)}}\right) \tag{3.4.74}$$

which leads to the final result

$$\begin{aligned} 2\ln g_\alpha(l) =& \frac{1}{2}\int_{\mathbb{R}} d\theta\,(\phi_\alpha(\theta) - \delta(\theta) - 2\phi(2\theta))\ln(1+e^{-\epsilon(\theta)}) \\ &+ \sum_{n=1}^{\infty}\frac{1}{n}\int_{\mathbb{R}^n}\frac{d\theta_1}{1+e^{\epsilon(\theta_1)}}\cdots\frac{d\theta_n}{1+e^{\epsilon(\theta_n)}} \\ &\times \phi(\theta_1+\theta_2)\phi(\theta_2-\theta_3)\ldots\phi(\theta_n-\theta_{n+1}) \end{aligned} \tag{3.4.75}$$

with $\theta_{n+1} = \theta_1$. This conjecture was tested numerically for the case of the Lee-Yang model in [4] and also extended to the purely elastic scattering theories with $N$ particle species, for which the exact $g$-function is proposed to be

$$\begin{aligned} 2\ln g_\alpha(l) =& \frac{1}{2}\sum_{a=1}^{N}\int_{\mathbb{R}} d\theta\,(\phi_\alpha^{(a)}(\theta) - \delta(\theta) - 2\phi_{aa}(2\theta))\ln(1+e^{-\epsilon_a(\theta)}) \\ &+ \sum_{n=1}^{\infty}\sum_{a_1\ldots a_n=1}^{N}\frac{1}{n}\int_{\mathbb{R}^n}\frac{d\theta_1}{1+e^{\epsilon_{a_1}(\theta_1)}}\cdots\frac{d\theta_n}{1+e^{\epsilon_{a_n}(\theta_n)}} \\ &\times \phi_{a_1a_2}(\theta_1+\theta_2)\phi_{a_2a_3}(\theta_2-\theta_3)\ldots\phi_{a_na_{n+1}}(\theta_n-\theta_{n+1}) \end{aligned} \tag{3.4.76}$$

where $\theta_{n+1} = \theta_1$ and $a_{n+1} = a_1$.

The derivation of this conjecture avoided some of the problems that could afflict a more direct calculation, for example, in working in the limit $l \to \infty$, the particles are always well separated so the accuracy of the Bethe ansatz is not in question. However, a direct approach would be desirable, especially for the generalisation to more complicated models. There has been an attempt at this by Woynarovich, [82], who proposed an expression for the $O(1)$ corrections to the free energy for a one-dimensional Bose gas with repulsive $\delta$-function interaction, obtained by calculating corrections to the standard saddle point result. Although his expression has some of the features of the result here there are important differences. In particular, for the field theory case, the result in [82] is divergent in the UV limit so it cannot be consistent with the $g$-function of a CFT. The direct construction of the $g$-function therefore remains an open problem.

In [4], only the conjecture (3.4.75) has been tested for the Lee-Yang model, so the aim of the next chapter is to test the generalisation of this, (3.4.76), for a variety of purely elastic scattering theories. This work has been published in [1].

# Chapter 4

# ADET cases

In this chapter the investigations of [4] are extended to a collection of theories for which boundary UV/IR relations have yet to be found, namely the minimal purely elastic scattering theories associated with the ADET series of diagrams [83, 32, 84, 85, 86, 87, 88]. The bulk S-matrices of these models have long been known, but less progress has been made in associating solutions of the boundary bootstrap equations with specific perturbed boundary conditions. A collection of minimal reflection factors for the ADET theories are presented, and then tested by checking the $g$-function flows that they imply. It is also shown how these reflection factors can be modified to incorporate a free parameter, which generalises a structure previously observed in the Lee-Yang model [78]. This enables the prediction of a number of new flows to be made between conformal boundary conditions.

## 4.1 The ADET family of purely elastic scattering theories

The purely elastic scattering theories that are treated in this chapter fall into two classes. The first class associates an S-matrix to each simply-laced Lie algebra $\mathfrak{g}$, of type A, D or E [83, 32, 84, 85]. These S-matrices are *minimal*, in that they have no zeros on the physical strip $0 \leq \Im m\,\theta \leq \pi$, and *one-particle unitary*, in that all on-shell three-point couplings, as inferred from the residues of forward-channel S-matrix poles, are real. They describe particle scattering in the perturbations of the coset conformal field theories $\widehat{\mathfrak{g}}_1 \times \widehat{\mathfrak{g}}_1/\widehat{\mathfrak{g}}_2$ by their $(1,1,\mathrm{ad})$ operators, where $\widehat{\mathfrak{g}}$ is the affine

algebra associated with $\mathfrak{g}$. More will be said about affine Lie algebras and coset models below. The unperturbed theories have central charge

$$c = \frac{2r_{\mathfrak{g}}}{(h+2)} \,, \tag{4.1.1}$$

where $r_{\mathfrak{g}}$ is the rank of $\mathfrak{g}$, and $h$ is its Coxeter number. These UV central charges can be recovered directly from the S-matrices, using the thermodynamic Bethe ansatz [30, 32] as described in section 2.5. Some of these theories are also perturbed Virasoro minimal models. These are listed in table 4.1 along with the corresponding critical statistical model and relevant perturbing operator.

| $\mathfrak{g}$ | Minimal Model | Statistical Model | Perturbing Operator $\phi_{r,s}$ | Conformal weight $h_{r,s}$ |
|---|---|---|---|---|
| $A_2$ | $\mathcal{M}_{5,6}$ | Three-state Potts | $\phi_{21}$ energy density | 2/5 |
| $E_6$ | $\mathcal{M}_{6,7}$ | Tricritical three-state Potts | $\phi_{12}$ thermal operator | 3/8 |
| $E_7$ | $\mathcal{M}_{4,5}$ | Tricritical Ising | $\phi_{12}$ energy operator | 1/10 |
| $E_8$ | $\mathcal{M}_{3,4}$ | Ising | $\phi_{13}$ magnetic field | 1/2 |

Table 4.1: Perturbed minimal models described by perturbations of the coset theories $\widehat{\mathfrak{g}}_1 \times \widehat{\mathfrak{g}}_1/\widehat{\mathfrak{g}}_2$

The ADE S-matrices describe the diagonal scattering of $r_{\mathfrak{g}}$ particle types, whose masses together form the Perron-Frobenius eigenvector of the Cartan matrix of $\mathfrak{g}$. This allows the particles to be attached to the nodes of the Dynkin diagram of $\mathfrak{g}$. Each S-matrix element can be conveniently written as a product of elementary blocks [83]

$$\{x\} = (x-1)(x+1) \,, \quad (x) = \frac{\sinh\left(\frac{\theta}{2} + \frac{i\pi x}{2h}\right)}{\sinh\left(\frac{\theta}{2} - \frac{i\pi x}{2h}\right)} \tag{4.1.2}$$

as

$$S_{ab} = \prod_{x \in A_{ab}} \{x\} \,, \tag{4.1.3}$$

for some index set $A_{ab}$. Note that

$$(0) = 1\,, \quad (h) = -1\,, \quad (-x) = (x)^{-1}\,, \quad (x \pm 2h) = (x)\,. \tag{4.1.4}$$

The notation (4.1.2) has been arranged so that the numbers $x$ are all integers. The sets $A_{ab}$ are tabulated in [83]; a universal formula expressing them in geometrical terms was found in [85], and is further discussed in [86, 87].

The S-matrices of the second class [89, 80, 90] are labelled by extending the set of ADE Dynkin diagrams to include the 'tadpole' $T_r$. They encode the diagonal scattering of $r$ particle types, and can be written in terms of the blocks (4.1.2) with $h = 2r+1$ [91]:

$$S_{ab} = \prod_{\substack{l=|a-b|+1 \\ \text{step } 2}}^{a+b-1} \{l\}\{h-l\}\,. \tag{4.1.5}$$

These S-matrix elements are again minimal, but they are not one-particle unitary, reflecting the fact that they describe perturbations of the non-unitary minimal models $\mathcal{M}_{2,2r+3}$, with central charge $c = -2r(6r+5)/(2r+3)$. The perturbing operator this time is $\phi_{13}$. The $T_r$ S-matrices are quantum group reductions of the sine-Gordon model at coupling $\beta^2 = 16\pi/(2r+3)$ [89], a fact that will be relevant later.

A self-contained classification of minimal purely elastic S-matrices is still lacking, but the results of [88] single out the ADET theories as the only examples having TBA systems for which all pseudoenergies remain finite in the ultraviolet limit.

The ADET diagrams are shown in figure 4.1, with nodes giving the conventions employed here for labelling the particles in each theory. For the $D_r$ theories, particles $r-1$ and $r$ are sometimes labelled $s$ and $s'$, or $s$ and $\bar{s}$, for $r$ even or odd respectively.

## 4.2 Affine Lie algebras and their role in Conformal Field Theories

Before the reflection factors for the *ADET* theories are presented it is useful to digress slightly and discuss CFTs with associated affine Lie algebras $\widehat{\mathfrak{g}}$. This serves, not only to understand the role of these infinite algebras, but also to introduce some formulae for the modular $\mathcal{S}$ matrices, which will be of use later in calculating the

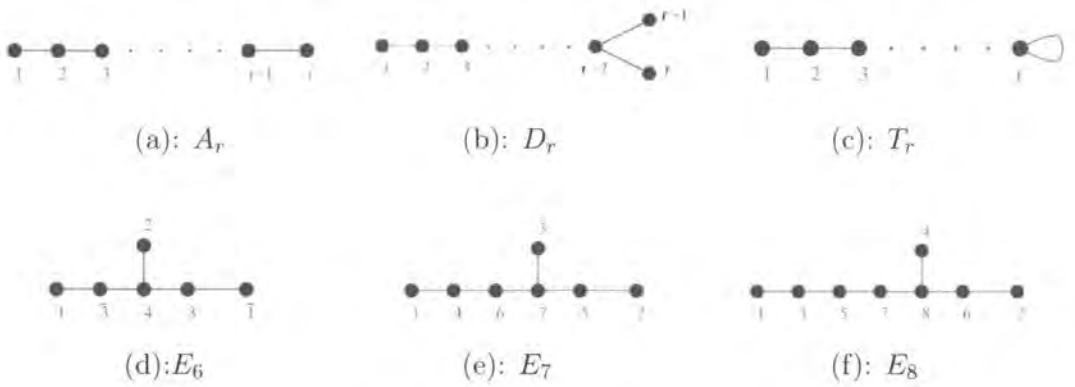

(a): $A_r$ (b): $D_r$ (c): $T_r$

(d):$E_6$ (e): $E_7$ (f): $E_8$

Figure 4.1: Dynkin diagrams for the $ADET$ Lie algebras

critical (CFT) $g$-functions for the $ADE$ related theories. The discussion presented here follows closely that found in chapters 14-18 of Di Francesco et al. [5] and in the review by Goddard and Olive [92]. See also the book by Kac [93] for more information.

### 4.2.1 Affine Lie algebras

Consider the generalisation of a Lie algebra $\mathfrak{g}$, with generators $J^a$, where elements of the algebra are also Laurent polynomials in some variable $t$. Denote the set of such polynomials by $\mathbb{C}[t, t^{-1}]$. This generalisation is called the loop algebra

$$\tilde{\mathfrak{g}} = \mathfrak{g} \otimes \mathbb{C}[t, t^{-1}] \tag{4.2.1}$$

generated by $J^a_n \equiv J^a \otimes t^n$; the generators satisfy the commutation relations

$$[J^a_n, J^b_m] = \sum_c i f^{ab}_c J^c_{n+m} \,. \tag{4.2.2}$$

A central extension of this algebra is obtained by adding a term of the form $\sum_i d^{ab}_{mni} \widehat{k}^i$ where $[J^a_n, \widehat{k}^i] = 0$. The constants $d^{ab}_{mni}$ are constrained by the Jacobi identity, and in a basis where the structure constants $f^{ab}_c$ are totally antisymmetric, all bar one of the central terms can be removed by a redefinition of the generators. The extended algebra is then

$$[J^a_n, J^b_m] = \sum_c i f^{ab}_c J^c_{n+m} + \widehat{k} n \delta_{ab} \delta_{n+m,0} \,. \tag{4.2.3}$$

A convenient basis for the finite-dimensional Lie algebra $\mathfrak{g}$ consists of a set of mutually commuting generators, $H^i_0$, $i = 1, \ldots, r_{\mathfrak{g}}$, of the Cartan subalgebra, along with particular combinations of the generators $J^a$, denoted $E^\alpha$, that satisfy

$$[H^i_0, E^\alpha] = \alpha^i E^\alpha \,. \tag{4.2.4}$$

The vector $\boldsymbol{\alpha} = (\alpha^i, \ldots, \alpha^{r_\mathfrak{g}})$ is called a root and $E^\alpha$ is the corresponding step operator. The root components are the non-zero eigenvalues of the $H_0^i$ in a particular representation, called the adjoint,where the Lie algebra itself serves as the vector space on which the generators act.

To construct a basis for the extended algebra, following the lines above, one must first construct the analogue of the Cartan subalgebra (CSA) of the finite Lie algebra. Starting with this CSA, $H_0^i$ of $\mathfrak{g}$, the central element $\widehat{k}$ can then be added giving an $(r+1)$-dimensional Abelian subalgebra. In the adjoint representation

$$ad(H_0^i)E_n^\alpha = [H_0^i, E_n^\alpha] = \alpha^i E_n^\alpha \tag{4.2.5}$$

$$ad(k)E_n^\alpha = [\widehat{k}, E_n^\alpha] = 0, \tag{4.2.6}$$

so each of the roots $(\alpha^1, \ldots, \alpha^{r_\mathfrak{g}}, 0) = (\boldsymbol{\alpha}, 0)$ is infinitely degenerate. To cure this problem, an extra element $L_0 = -t\frac{d}{dt}$ can be added to the algebra $\tilde{\mathfrak{g}}$ to distinguish between the $E_n^\alpha$ for different $n$. This satisfies the commutation relations $[L_0, J_n^a] = -nJ_n^a$, $[L_0, \widehat{k}] = 0$. The resulting algebra

$$\widehat{\mathfrak{g}} = \tilde{\mathfrak{g}} \oplus \mathbb{C}\widehat{k} \oplus \mathbb{C}L_0 \tag{4.2.7}$$

is an affine Lie algebra (also known as a Kac-Moody algebra). The usual basis is given by the generators of the CSA, $\widehat{H} = \{H_0^1, \ldots, H_0^{r_\mathfrak{g}}, \widehat{k}, L_0\}$, along with the step operators $E_n^\alpha$ and $H_n^i$ which correspond to the roots $\widehat{\boldsymbol{\alpha}}$ and $n\boldsymbol{\delta}$ respectively.

The next step is to find an analogue in $\widehat{\mathfrak{g}}$ of the invariant scalar product, or Killing form, on $\mathfrak{g}$. This must be symmetric and satisfy

$$\langle [Z, X], Y\rangle + \langle X, [Z, Y]\rangle = 0\,,\ X, Y, Z \in \widehat{\mathfrak{g}} \tag{4.2.8}$$

which constrains the inner products, up to an overall constant, to be

$$\begin{gathered}\langle J_n^a, J_m^b\rangle = \delta^{ab}\delta_{n+m,0}\,,\ \langle J_n^a, \widehat{k}\rangle = 0\,,\ \langle \widehat{k}, \widehat{k}\rangle = 0 \\ \langle J_n^a, L_0\rangle = 0\,, \langle L_0, \widehat{k}\rangle = -1.\end{gathered} \tag{4.2.9}$$

The only unspecified norm is $\langle L_0, L_0\rangle$ which is often chosen to be zero.

For an arbitrary representation, it is always possible to find a basis, $\{|\widehat{\lambda}\rangle\}$, of simultaneous eigenvectors of the CSA such that

$$\widehat{H}^i|\widehat{\lambda}\rangle = \widehat{\lambda}^i|\widehat{\lambda}\rangle\,. \tag{4.2.10}$$

The vector $\widehat{\boldsymbol{\lambda}}$ of simultaneous eigenvalues is known as an affine weight

$$\begin{aligned}\widehat{\boldsymbol{\lambda}} &= (\widehat{\lambda}(H_0^1), \ldots, \widehat{\lambda}(H_0^r); \widehat{\lambda}(k); \widehat{\lambda}(-L_0)) \\ &= (\boldsymbol{\lambda}; k_\lambda; n)\end{aligned} \tag{4.2.11}$$

where $\boldsymbol{\lambda}$ is a weight of $\mathfrak{g}$. The weights live in a space dual to the CSA and this can be encoded using the Killing form: for each element $\widehat{\lambda}(H)$ in the dual space, there must be an element $H_\lambda$ in the CSA, such that

$$\widehat{\lambda}(H) = \langle H_\lambda, H \rangle \,. \tag{4.2.12}$$

The scalar product of two weights is then induced by the Killing form

$$(\widehat{\boldsymbol{\lambda}}, \widehat{\boldsymbol{\mu}}) = (\boldsymbol{\lambda}, \boldsymbol{\mu}) + k_\lambda n_\mu + k_\mu n_\lambda. \tag{4.2.13}$$

As in the finite-dimensional case, weights in the adjoint representation are called roots. Since $\widehat{k}$ commutes with all the generators of $\widehat{\mathfrak{g}}$, its eigenvalue on the states of the adjoint representation is zero. The affine roots, associated with the generators $E_n^\alpha$ are therefore

$$\widehat{\boldsymbol{\alpha}} = (\boldsymbol{\alpha}; 0; n) \,,\; n \in \mathbb{Z} \,,\; \boldsymbol{\alpha} \in \Delta \tag{4.2.14}$$

where $\Delta$ denotes the set of all roots of $\mathfrak{g}$. This has the same scalar product as the finite case: $(\widehat{\boldsymbol{\alpha}}, \widehat{\boldsymbol{\beta}}) = (\boldsymbol{\alpha}, \boldsymbol{\beta})$. The roots associated to $H_n^i$ are

$$n\boldsymbol{\delta} = (0; 0; n) \,,\; n \in \mathbb{Z} \,,\; n \neq 0 \,. \tag{4.2.15}$$

These have length $(n\boldsymbol{\delta}, n\boldsymbol{\delta}) = 0$ and each one is orthogonal to all other roots so they are often called imaginary roots, whereas (4.2.14) are known as the real roots.

A basis of simple roots must now be identified, in which the expansion coefficients of any root are either all non-negative or all non-positive. This basis contains the $r$ finite simple roots $\boldsymbol{\alpha}_i$ of $\mathfrak{g}$ along with one extra simple root

$$\boldsymbol{\alpha}_0 = (-\boldsymbol{\psi}; 0; 1) \tag{4.2.16}$$

where $\boldsymbol{\psi}$ is the highest root of $\mathfrak{g}$, from which all roots of $\mathfrak{g}$ can be obtained by repeated subtraction of simple roots. A positive root is then given by

$$(\boldsymbol{\alpha}; 0; n) > 0 \,\text{if}\, n > 0, \text{ or if } n = 0 \text{ and } \boldsymbol{\alpha} \in \Delta_+ \,, \tag{4.2.17}$$

where $\Delta_+$ is the set of positive roots of $\mathfrak{g}$. The condition, $n > 0$ and $\boldsymbol{\alpha} \in \Delta$, for a positive root is not immediately obvious but by rearranging

$$\boldsymbol{\alpha} + n\boldsymbol{\delta} = n\boldsymbol{\alpha}_0 + (n-1)\boldsymbol{\psi} + (\boldsymbol{\psi} + \boldsymbol{\alpha}) \tag{4.2.18}$$

the expansion coefficients of the final two factors in terms of finite simple roots are non-negative. Given a set of affine simple roots and a scalar product, the extended Cartan matrix is defined in terms of the roots $\widehat{\boldsymbol{\alpha}}_i$ and coroots $\widehat{\boldsymbol{\alpha}}_j{}^\vee = 2\widehat{\boldsymbol{\alpha}}_j/|\widehat{\boldsymbol{\alpha}}_j|^2$

$$\begin{aligned} \widehat{C}_{ij} &= (\widehat{\boldsymbol{\alpha}}_i, \widehat{\boldsymbol{\alpha}}_j{}^\vee)\,,\ 0 \le i,j \le r_{\mathfrak{g}} \\ &= \frac{2(\widehat{\boldsymbol{\alpha}}_i, \widehat{\boldsymbol{\alpha}}_j)}{|\widehat{\boldsymbol{\alpha}}_j|^2}\,. \end{aligned} \tag{4.2.19}$$

From this definition it is clear that $\widehat{C}$ is formed from the Cartan matrix $C$ of $\mathfrak{g}$ by the addition of an extra row and column given by $(\boldsymbol{\alpha}_0, \boldsymbol{\alpha}_0{}^\vee) = |\boldsymbol{\psi}|^2 = 2$ and $(\boldsymbol{\alpha}_0, \widehat{\boldsymbol{\alpha}}_j{}^\vee) = -(\boldsymbol{\psi}, \boldsymbol{\alpha}_j{}^\vee)$. Note that the expansion coefficients of $\boldsymbol{\psi}$, when written in a basis of simple roots, or coroots of $\mathfrak{g}$, are known as marks $a_i$ and comarks $a_i^\vee$ respectively, so $-(\boldsymbol{\psi}, \boldsymbol{\alpha}_j{}^\vee) = -\sum_{i=1}^{r_{\mathfrak{g}}} a_i(\boldsymbol{\alpha}_i, \boldsymbol{\alpha}_j{}^\vee)$. All the information contained in the extended Cartan matrix can be encoded in the extended Dynkin diagram. This can be obtained from the Dynkin diagram of $\mathfrak{g}$ by adding an extra node corresponding to $\boldsymbol{\alpha}_0$ joined to the other nodes by $\widehat{C}_{0i}\widehat{C}_{i0}$ lines. The extended Dynkin diagrams for the ADE theories are shown in figure 4.2. The nodes are labelled by the ordering of the roots and the comark. Note that the zeroth comark (and mark) is defined to be 1 so the dual Coxeter number $\tilde{h} = \sum_{i=0}^{r_{\mathfrak{g}}} a_i^\vee$ is equal to the Coxeter number $h$ for these simply laced theories.

The affine Weyl group, $\widehat{W}$, like the finite-dimensional case, is generated by the reflections

$$\sigma_{\widehat{\boldsymbol{\alpha}}}(\widehat{\boldsymbol{\lambda}}) = \widehat{\boldsymbol{\lambda}} - (\widehat{\boldsymbol{\lambda}}, \widehat{\boldsymbol{\alpha}}^\vee)\widehat{\boldsymbol{\alpha}} \tag{4.2.20}$$

in the hyperplanes normal to the real roots $\widehat{\boldsymbol{\alpha}}$. This group permutes the real roots, as

$$\sigma_{\widehat{\boldsymbol{\alpha}}}(\widehat{\boldsymbol{\alpha}}') = (\sigma_{\boldsymbol{\alpha}}(\boldsymbol{\alpha}'); 0; n - (\boldsymbol{\lambda}, \boldsymbol{\alpha}^\vee)n') \tag{4.2.21}$$

where $\widehat{\boldsymbol{\alpha}} = (\boldsymbol{\alpha}; 0; n)$, $\widehat{\boldsymbol{\alpha}}' = (\boldsymbol{\alpha}'; 0; n')$ and $\sigma_{\boldsymbol{\alpha}}(\boldsymbol{\alpha}')$ is the Weyl reflection for the finite-dimensional case. The imaginary roots, on the other hand, are left invariant.

In physical applications, $L_0$ is often identified with energy so its spectrum must be bounded from below. Such a representation is known as a highest weight repre-

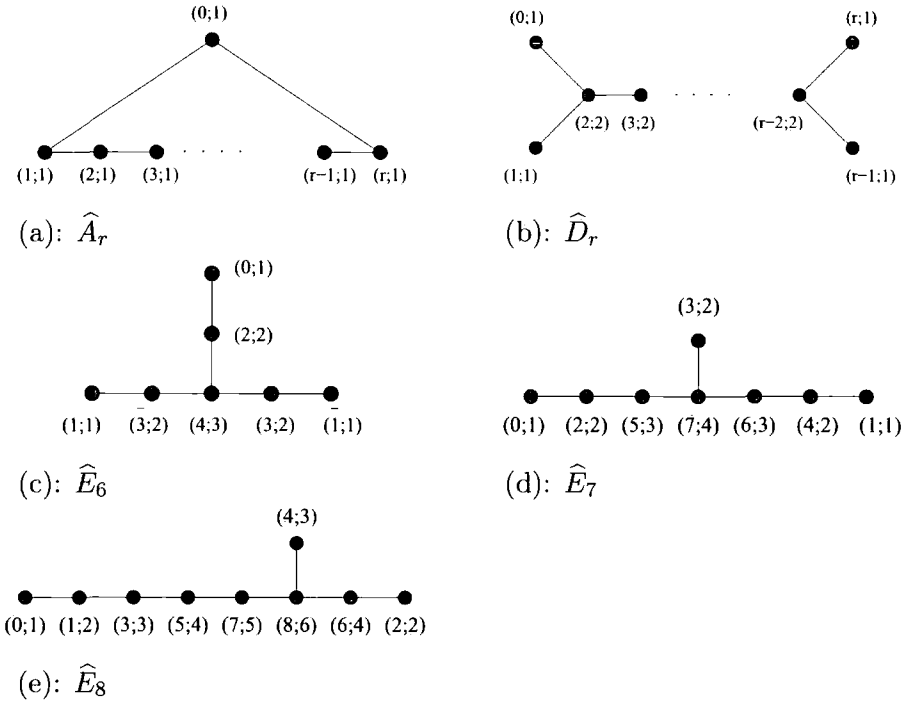


Figure 4.2: Extended Dynkin diagrams for the affine Lie algebras $\widehat{A}$, $\widehat{D}$ and $\widehat{E}$

sentation. Using the commutation relation $[L_0, J_n^a] = -nJ_n^a$, if $L_0|\widehat{\lambda}\rangle = \widehat{\boldsymbol{\lambda}}|\widehat{\lambda}\rangle$ then

$$L_0 J_n^a|\widehat{\lambda}\rangle = ([L_0, J_n^a] + J_n^a L_0)|\widehat{\lambda}\rangle = (\widehat{\boldsymbol{\lambda}} - n)J_n^a|\widehat{\lambda}\rangle \tag{4.2.22}$$

so the action of $J_n^a$ on an eigenvector of $L_0$ with eigenvalue $\widehat{\boldsymbol{\lambda}}$ gives an eigenvector of $L_0$ with eigenvalue $\widehat{\boldsymbol{\lambda}} - n$, if it is not annihilated. Since the spectrum of $L_0$ is required to be bounded from below there must be some lowest eigenvalue, $h_\lambda$, with corresponding eigenvector $|\widehat{\lambda}_h\rangle$ which satisfies

$$J_n^a|\widehat{\lambda}_h\rangle = 0 \quad , \quad n > 0\,. \tag{4.2.23}$$

In such a representation, all states can be built up from the 'vacuum states' which satisfy (4.2.23) by repeated application of the operators $J_{-n}^a$, $n > 0$. However, not all of these representations are unitary. It will be shown below, following [92], that the unitary representations can be characterised by the vacuum representation of the corresponding finite algebra $\mathfrak{g}$ or its highest weight $\boldsymbol{\mu}$, and the value of the central term $k$.

The highest weight state, $|\mu\rangle$, of the vacuum representation of $\mathfrak{g}$ satisfies

$$\begin{aligned} E_n^\alpha|\mu\rangle &= 0 \quad \text{if either } n > 0 \text{ or } n = 0 \text{ and } \boldsymbol{\alpha} \in \Delta_+ \\ H_n^i|\mu\rangle &= 0 \quad \text{if } n > 0\,. \end{aligned} \tag{4.2.24}$$

With respect to the CSA $\widehat{H} = (H, \widehat{k}, L_0)$, this state has weight $\widehat{\boldsymbol{\mu}} = (\boldsymbol{\mu}, k, \nu)$ and the weight $\widehat{\boldsymbol{\mu}}' = (\boldsymbol{\mu}', k, \nu')$ of any state in the representation has the property that $\widehat{\boldsymbol{\mu}} - \widehat{\boldsymbol{\mu}}'$ is a sum of positive roots. The representation is usually labelled by the highest weight $\widehat{\boldsymbol{\mu}}$ but $\nu$, the lowest eigenvalue of $L_0$, is often ignored as it is a matter of convention.

For each real root $\widehat{\boldsymbol{\alpha}} = (\boldsymbol{\alpha}; 0; n)$ of $\widehat{\mathfrak{g}}$ there is an $su(2)$ subalgebra generated by

$$E_n^{\alpha} \quad , \quad E_{-n}^{-\alpha} \quad , \quad \frac{2\widehat{\boldsymbol{\alpha}}.\widehat{H}}{|\widehat{\boldsymbol{\alpha}}|^2} = \frac{2(\boldsymbol{\alpha}.H + nk)}{\boldsymbol{\alpha}^2} . \tag{4.2.25}$$

The states in any unitary representation of $\widehat{\mathfrak{g}}$ must fall into multiplets of this $su(2)$ subalgebra which implies that its set of weights $\widehat{\boldsymbol{\mu}}'$ must be mapped into itself by the Weyl reflections (4.2.20). The weight $\widehat{\boldsymbol{\mu}}'$ must therefore satisfy the condition that $\widehat{\boldsymbol{\mu}} - \sigma(\widehat{\boldsymbol{\mu}}')$ is a sum of positive roots of $\widehat{\mathfrak{g}}$ for any $\sigma \in \widehat{W}$. Applying this to $\widehat{\boldsymbol{\mu}}' = \widehat{\boldsymbol{\mu}}$:

$$\widehat{\boldsymbol{\mu}} - \sigma_{\widehat{\boldsymbol{\alpha}}}(\widehat{\boldsymbol{\mu}}) = (\widehat{\boldsymbol{\mu}}, \widehat{\boldsymbol{\alpha}}^{\vee})\widehat{\boldsymbol{\alpha}} = [(\boldsymbol{\mu}, \boldsymbol{\alpha}^{\vee}) + kn](\boldsymbol{\alpha}; 0; n) \tag{4.2.26}$$

which, for a positive root $\widehat{\boldsymbol{\alpha}}$, gives

$$(\boldsymbol{\mu}, \widehat{\boldsymbol{\alpha}}^{\vee}) = \frac{2\boldsymbol{\mu}.\widehat{\boldsymbol{\alpha}}}{|\widehat{\boldsymbol{\alpha}}|^2} \in \mathbb{Z}_+ \cup 0 . \tag{4.2.27}$$

The weights can be expanded, like the roots, in a basis of simple roots, however for the representations of interest the coefficients of these expansions are not integers. A more convenient basis is provided by the fundamental weights, which are dual to the simple coroots. For the finite algebra, $\mathfrak{g}$, the fundamental weights $\boldsymbol{\lambda}_i$ are defined by $(\boldsymbol{\lambda}_i, \boldsymbol{\alpha}_j^{\vee}) = \delta_{ij}$ for $1 \leq i, j \leq r_{\mathfrak{g}}$. Any weight in a finite dimensional irreducible representation can be written in terms of these fundamental weights as $\boldsymbol{\lambda}' = \sum_{i=1}^{r_{\mathfrak{g}}} n_i \boldsymbol{\lambda}_i$ where the coefficients, $n_i \in \mathbb{Z}$ are known as Dynkin labels. The highest weight $\boldsymbol{\mu}$ of the representation is the one with all Dynkin labels $n_i \geq 0$. This is also called a dominant weight.

For the affine algebra $\widehat{\mathfrak{g}}$, the fundamental weights $\boldsymbol{\Lambda}_i$ are defined in much the same way

$$(\boldsymbol{\Lambda}_i, \widehat{\boldsymbol{\alpha}}_j^{\vee}) = \delta_{ij} \quad , \quad 0 \leq i, j \leq r_{\mathfrak{g}} . \tag{4.2.28}$$

The general solution to the condition (4.2.27), written in terms of these fundamental weights is

$$\widehat{\boldsymbol{\mu}} = \sum_{i=0}^{r_{\mathfrak{g}}} n_i \boldsymbol{\Lambda}_i \quad , \quad n_i \in \mathbb{Z}_+ \cup 0, \tag{4.2.29}$$

ignoring the component in the $L_0$ direction. Using (4.2.13) and the decomposition of the highest root of $\mathfrak{g}$ into a sum of coroots: $\boldsymbol{\psi} = \sum_{i=1}^{r} a_i \check{} \boldsymbol{\alpha}_i \check{}$, the affine fundamental weights can be shown to be given by

$$\boldsymbol{\Lambda}_i = (\boldsymbol{\lambda}_i; a_i \check{}; 0) \tag{4.2.30}$$

$$\boldsymbol{\Lambda}_0 = (\mathbf{0}; 1; 0) \tag{4.2.31}$$

in terms of the fundamental weights $\boldsymbol{\lambda}_i$ of $\mathfrak{g}$. They are assumed to be eigenstates of $L_0$ with zero eigenvalue. The Dynkin labels in (4.2.29), for $i = 1, \ldots r_{\mathfrak{g}}$ are therefore the same as those in the finite case and the $n_0$ label is then fixed by the $k$ eigenvalue, or rather the level $l$:

$$l = \frac{2k}{\boldsymbol{\psi}^2} = \sum_{i=0}^{r_{\mathfrak{g}}} n_i a_i \check{} = n_0 + \sum_{i=1}^{r_{\mathfrak{g}}} n_i a_i \check{}. \tag{4.2.32}$$

Note that for the simply laced theories here $l = k$. So for the physically interesting representations, often called integrable representations, the Dynkin labels are all non-negative $n_i \geq 0$, $i = 0, \ldots r_{\mathfrak{g}}$, and the representation can be specified by the level of the affine algebra $\widehat{\mathfrak{g}}$ along with the highest weight of the corresponding representation of the finite algebra $\mathfrak{g}$.

The Verma module of the highest weight state $|\widehat{\lambda}\rangle$ has the following singular vectors

$$E_0^{\alpha_i}|\widehat{\lambda}\rangle = E_1^{-\psi}|\widehat{\lambda}\rangle = 0 \tag{4.2.33}$$

$$(E_0^{-\alpha_i})^{\lambda_i+1}|\widehat{\lambda}\rangle = (E_{-1}^{\psi})^{k-(\lambda,\psi)+1}|\widehat{\lambda}\rangle = 0\,,\ i \neq 0\,. \tag{4.2.34}$$

But when these vectors are quotiented out from the Verma module, the resulting module is not finite dimensional, unlike the finite Lie algebra case. This is because the imaginary root can be subtracted from any weight without leaving the representation.

Define the grade to be the $L_0$ eigenvalue, shifted so that $L_0|\widehat{\lambda}\rangle = 0$ for the highest weight state $|\widehat{\lambda}\rangle$. At grade zero, all states are obtained from $|\widehat{\lambda}\rangle$ by applications of the finite Lie algebra generators, as these are the only generators of $\widehat{\mathfrak{g}}$ that don't change the $L_0$ eigenvalue. Therefore, the finite projection of the weights at grade zero are all the weights in the $\mathfrak{g}$ irreducible, finite dimensional representation of highest weight $\boldsymbol{\lambda}$. Weights at grade 1 can be obtained from those at grade zero that have positive zeroth Dynkin labels, by subtraction of $\boldsymbol{\alpha}_0$, followed by all possible subtractions of simple

roots, and so on. The important point to note here is that the finite projections of affine weights at a fixed grade are organised into a direct sum of irreducible finite dimensional representations of $\mathfrak{g}$, so once the $L_0$ eigenvalue is taken into account, the multiplicity of weights is finite.

The character of an integrable highest weight representation is defined as

$$ch_{\widehat{\boldsymbol{\lambda}}} = \sum_{\widehat{\boldsymbol{\lambda}}' \in \Omega_{\widehat{\lambda}}} mult_{\widehat{\boldsymbol{\lambda}}}(\widehat{\boldsymbol{\lambda}}') e^{\widehat{\boldsymbol{\lambda}}'} . \tag{4.2.35}$$

The sum here is over all weights $\widehat{\boldsymbol{\lambda}}'$ in the representation of highest weight state $|\widehat{\lambda}\rangle$, $mult_{\widehat{\boldsymbol{\lambda}}}(\widehat{\boldsymbol{\lambda}}')$ denotes the multiplicity of the weight $\widehat{\boldsymbol{\lambda}}'$ and $e^{\widehat{\boldsymbol{\lambda}}}$ is a formal exponential. This satisfies

$$e^{\widehat{\boldsymbol{\lambda}}'} e^{\widehat{\boldsymbol{\mu}}'} = e^{\widehat{\boldsymbol{\lambda}}' + \widehat{\boldsymbol{\mu}}'} \tag{4.2.36}$$

$$e^{\widehat{\boldsymbol{\lambda}}'}(\widehat{\boldsymbol{\xi}}) = e^{(\widehat{\boldsymbol{\lambda}}', \widehat{\boldsymbol{\xi}})} \tag{4.2.37}$$

where the $e$ on the RHS of (4.2.37) is a genuine exponential function, and $\widehat{\boldsymbol{\xi}}$ is an arbitrary weight.

The character (4.2.35) can be written in a form known as the Weyl-Kac character formula:

$$ch_{\widehat{\boldsymbol{\lambda}}} = e^{m_{\widehat{\lambda}}\delta} \frac{\sum_{w \in \widehat{W}} (-1)^w \Theta_{w(\widehat{\boldsymbol{\lambda}} + \widehat{\boldsymbol{\rho}})}}{\sum_{w \in \widehat{W}} (-1)^w \Theta_{w\widehat{\boldsymbol{\rho}}}} \tag{4.2.38}$$

where $(-1)^w$ is the signature of $w$, which is $+1$ or $-1$ if $w$ is composed of an even or an odd number of reflections by simple roots, the Weyl vector $\widehat{\boldsymbol{\rho}}$ is the weight where all Dynkin labels are unitary and $m_{\widehat{\boldsymbol{\lambda}}}$ is the modular anomaly

$$m_{\widehat{\boldsymbol{\lambda}}} = \frac{|\boldsymbol{\lambda} + \boldsymbol{\rho}|^2}{2(k + \tilde{h})} - \frac{|\boldsymbol{\rho}|^2}{2\tilde{h}} . \tag{4.2.39}$$

The generalised $\Theta$ functions, at a specific point $\widehat{\boldsymbol{\xi}} = -2\pi i(\varsigma; \tau; t)$ are given by

$$\Theta_{\widehat{\boldsymbol{\lambda}}}(\widehat{\boldsymbol{\xi}}) = e^{-2\pi i k t} \sum_{\boldsymbol{\alpha}^\vee \in Q^\vee} e^{-\pi i (2k(\boldsymbol{\alpha}^\vee, \varsigma) + 2(\boldsymbol{\lambda}, \varsigma) - \tau k |\boldsymbol{\alpha}^\vee + \boldsymbol{\lambda}/k|^2)} \tag{4.2.40}$$

where $Q^\vee$ is the coroot lattice of $\mathfrak{g}$. The normalised characters are $\chi_{\widehat{\boldsymbol{\lambda}}} = e^{-m_{\widehat{\lambda}}\delta} ch_{\widehat{\boldsymbol{\lambda}}}$ and at the point $\varsigma = t = 0$ they are known as specialised characters:

$$\chi_{\widehat{\boldsymbol{\lambda}}}(\tau) = q^{m_{\widehat{\lambda}}} \sum_{n \geq 0} d(n) q^n = q^{m_{\widehat{\lambda}}} Tr_{\widehat{\boldsymbol{\lambda}}} q^{L_0} \tag{4.2.41}$$

where $d(n)$ is the number of states at grade $n$ and $q = e^{2\pi i \tau}$.

Under modular transformations these specialised characters transform as

$$\chi_{\widehat{\boldsymbol{\lambda}}}(\tau+1) = \sum_{\widehat{\boldsymbol{\mu}}\in P_+^k} \mathcal{T}_{\widehat{\boldsymbol{\lambda}}\widehat{\boldsymbol{\mu}}}\chi_{\widehat{\boldsymbol{\mu}}}(\tau) \tag{4.2.42}$$

$$\chi_{\widehat{\boldsymbol{\lambda}}}(-1/\tau) = \sum_{\widehat{\boldsymbol{\mu}}\in P_+^k} \mathcal{S}_{\widehat{\boldsymbol{\lambda}}\widehat{\boldsymbol{\mu}}}\chi_{\widehat{\boldsymbol{\mu}}}(\tau)\,. \tag{4.2.43}$$

Note that the sum is over the weights in $P_+^k$, the set of integrable weights at level $k$, which indicates that characters in such representations transform into each other under the action of the modular group. The transformation $\tau \longrightarrow \tau+1$ induces a phase change only

$$\mathcal{T}_{\widehat{\boldsymbol{\lambda}}\widehat{\boldsymbol{\mu}}} = \delta_{\widehat{\boldsymbol{\lambda}}\widehat{\boldsymbol{\mu}}} e^{2\pi i m_{\widehat{\boldsymbol{\lambda}}}}\,, \tag{4.2.44}$$

whereas the modular $\mathcal{S}$ matrix is given by

$$\mathcal{S}_{\widehat{\lambda}\widehat{\mu}} = i^{|\Delta_+|}|P/Q^\vee|^{-\frac{1}{2}}(k+\tilde{h})^{-r_{\mathfrak{g}}/2}\sum_{w\in W}(-1)^w e^{-2\pi i(w(\boldsymbol{\lambda}+\boldsymbol{\rho}),\boldsymbol{\mu}+\boldsymbol{\rho})/(k+\tilde{h})} \tag{4.2.45}$$

where $|\Delta_+|$ is the number of positive roots in $\mathfrak{g}$, $P$ is the weight lattice and for $\mathfrak{g}$ simply laced $|P/Q^\vee| = |P/Q| = \det C_{ij}$ the determinant of the Cartan matrix. The matrices $\mathcal{S}$ and $\mathcal{T}$ are both unitary: $\mathcal{T}^{-1} = \mathcal{T}^\dagger$, $\mathcal{S}^{-1} = \mathcal{S}^\dagger$, and $\mathcal{S}$ simplifies to a product over the positive roots, $\Delta_+$, of $\mathfrak{g}$ when $\widehat{\boldsymbol{\mu}} = k\boldsymbol{\Lambda}_0$ (denoted $\mathbf{0}$ here):

$$\mathcal{S}_{\widehat{\boldsymbol{\lambda}}\mathbf{0}} = |P/Q^\vee|^{-1/2}(k+\tilde{h})^{-r_{\mathfrak{g}}/2}\prod_{\boldsymbol{\alpha}\in\Delta_+} 2\sin\left(\frac{\pi(\boldsymbol{\alpha},\boldsymbol{\lambda}+\boldsymbol{\rho})}{k+\tilde{h}}\right)\,. \tag{4.2.46}$$

Note that this is real and positive.

### 4.2.2 WZW models and Coset theories

The $\widehat{\mathfrak{g}}_k$ Wess-Zumino-Witten (WZW) models are conformal field theories for which the spectrum generating algebra is the affine Lie algebra $\widehat{\mathfrak{g}}$. Unusually for a CFT, they can be formulated directly in terms of an action, of the form

$$S^{WZW} = \frac{k}{16\pi}\int_{S^2} d^2x\, Tr(\partial^\mu g^{-1}\partial_\mu g) + k\Gamma \tag{4.2.47}$$

where $k$ is a positive integer and $\Gamma$ is the Wess-Zumino term $\Gamma = \frac{1}{24\pi}\int_{B^3} Tr(g^{-1}dg)^3$ which is an integral over a 3-dimensional space $B^3$ whose boundary is $S^2$. The conserved currents of this theory are asymmetric, a feature first noted by Witten in

[94]. They are given by $J = J^a t^a \sim \partial g g^{-1}$ and $\bar{J} = \bar{J}^a t^a \sim g^{-1}\bar{\partial} g$ and satisfy the OPE

$$J^a(z)J^b(w) \sim \frac{k\delta_{ab}}{(z-w)^2} + \sum_c i f_{abc} \frac{J^c(w)}{(z-w)} . \tag{4.2.48}$$

Expanding $J^a$ in terms of modes, using the Laurent expansion

$$J^a(z) = \sum_{n\in\mathbb{Z}} z^{-n-1} J^a_n \tag{4.2.49}$$

and using a similar method to the Virasoro case, as described in section 2.2, these modes can be shown to satisfy the commutation relations of the $\widehat{\mathfrak{g}}_k$ affine Lie algebra

$$[J^a_n, J^b_m] = \sum_c i f_{abc} J^c_{n+m} + k\delta_{ab}\delta_{n+m,0} . \tag{4.2.50}$$

Another copy of this relation holds for the $\bar{J}^a_n$ modes and $[J^a_n, \bar{J}^b_m] = 0$ so the two algebras are independent.

Conformal invariance of this theory can be shown by constructing the energy-momentum tensor with the appropriate algebraic properties using the Sugawara construction. This was the culmination of work done by several groups, but details and further references can be found, for example, in the reviews [5], [92]. Classically, the energy-momentrum tensor of this theory has the form $(1/2k)\sum_a J^a J^a$. For the quantum theory, the currents must be normal ordered to avoid a singularity so $T(z)$ can be taken to be

$$T(z) = \gamma \sum_a : J^a J^a : (z) . \tag{4.2.51}$$

The constant, $\gamma$, cannot be fixed from the classical theory as it is renormalised by quantum effects since the currents are not free fields. Instead it can be fixed by requiring that the OPE of $T$ with itself has the form

$$T(z)T(w) = \frac{c/2}{(z-w)^4} + \frac{2T(w)}{(z-w)^2} + \frac{\partial T(w)}{(z-w)} , \tag{4.2.52}$$

or by requiring $J^a$ to be a Virasoro primary field of dimension 1. The result is that

$$\gamma = \frac{1}{2(k+\tilde{h})} \tag{4.2.53}$$

where $k$ is the level and $\tilde{h}$ the dual Coxeter number. With this prefactor, the energy momentum tensor (4.2.51) satisfies the OPE (4.2.52) with central charge

$$c = \frac{k \dim \mathfrak{g}}{k+\tilde{h}} . \tag{4.2.54}$$

$T(z)$ can be written in terms of Virasoro modes

$$L_n = \frac{1}{2(k+\tilde{h})} \sum_a \sum_m : J_m^a J_{n-m}^a : \tag{4.2.55}$$

where the dots represent normal ordering of the modes: $J_m^a$ and $J_{n-m}^a$ commute if $n \neq 0$ so the ordering doesn't matter, but if $n = 0$ the term with the larger subindex must be placed to the right. The $L_n$ modes satisfy the Virasoro algebra and from the OPE of $T(z)$ with $J^a(z)$, which is the usual OPE of $T$ with a Virasoro primary field of dimension 1

$$T(z)J^a(w) = \frac{J^a(w)}{(z-w)^2} + \frac{\partial J^a(w)}{(z-w)} + \dots , \tag{4.2.56}$$

the commutation relation between the $L_n$ and $J_m^a$ modes can be found. The complete affine Lie and Virasoro algebra, written here for the holomorphic sector only, is then

$$\begin{aligned} [L_n, L_m] &= (n-m)L_{n+m} + \frac{c}{12} n(n^2-1)\delta_{n+m,0} \\ [L_n, J_m^a] &= -m J_{n+m}^a \\ [J_n^a, J_m^b] &= \sum_c i f_{abc} J_{n+m}^c + kn\delta_{ab}\delta_{n+m,0} \, . \end{aligned} \tag{4.2.57}$$

Equivalent relations hold for the antiholomorphic sector. Since $J_0^a$ commutes with the Virasoro generators, in particular with $L_0$, the finite Lie algebra $\mathfrak{g}$ is a symmetry algebra of the theory. This is not the case for the affine algebra $\widehat{\mathfrak{g}}$, which is the spectrum generating algebra.

A WZW primary field, $\phi_{\lambda,\mu}$, will transform covariantly with respect to the $\lambda$ representation of $\mathfrak{g}$ in the holomorphic sector, and the $\mu$ representation in the antiholomorphic sector. It satisfies the OPE

$$J^a(z)\phi_{\lambda\mu}(w,\bar{w}) \sim \frac{-t_\lambda^a \phi_{\lambda\mu}(w,\bar{w})}{z-w} \tag{4.2.58}$$

$$\bar{J}^a(\bar{z})\phi_{\lambda\mu}(w,\bar{w}) \sim \frac{\phi_{\lambda\mu}(w,\bar{w}) t_\mu^a}{\bar{z}-\bar{w}} \tag{4.2.59}$$

with $t_\lambda^a$ the matrix $t^a$ in the $\lambda$ representation. Focusing on the holomorphic sector only, a state $|\phi_\lambda\rangle$ can be associated to the field $\phi_\lambda$ by $\phi_\lambda(0)|0\rangle = |\phi_\lambda\rangle$. Expanding the currents in terms of modes $J^a(z) = \sum_n (z-w)^{-n-1} J_n^a(w)$, from the OPE above it is clear that the state $|\phi_\lambda\rangle$ must satisfy

$$J_0^a|\phi_\lambda\rangle = -t_\lambda^a|\phi_\lambda\rangle \tag{4.2.60}$$

$$J_n^a|\phi_\lambda\rangle = 0 \quad , \quad n > 0 \, . \tag{4.2.61}$$

These WZW primary fields are in fact also Virasoro primary. This can be seen by noticing that for $L_n$ with $n > 0$, the right most factor $J_m^a$ of (4.2.55) has $m > 0$ so

$$L_n|\phi_\lambda\rangle = 0 \quad \text{for } n > 0\,. \tag{4.2.62}$$

$L_0|\phi_\lambda\rangle$ also simplifies as only the zero modes $J_0^a$ contribute

$$L_0|\phi_\lambda\rangle = \frac{1}{2(k+\tilde{h})}\sum_a J_0^a J_0^a|\phi_\lambda\rangle\,. \tag{4.2.63}$$

This is proportional to the quadratic Casimir operator of $\mathfrak{g}$, $Q = \sum_a J^a J^a$. Evaluated on a highest-weight state $|\lambda\rangle$

$$Q|\lambda\rangle = (\boldsymbol{\lambda}, \boldsymbol{\lambda} + 2\boldsymbol{\rho})|\lambda\rangle \tag{4.2.64}$$

where $\boldsymbol{\rho}$ is the weight where all Dynkin labels are unity, known as the Weyl vector. $Q$ commutes with all generators of $\mathfrak{g}$ so its eigenvalue will be the same on all states of the representation. Therefore, one can associate a conformal weight $h_\lambda$ to $|\phi_\lambda\rangle$,

$$L_0|\phi_\lambda\rangle = h_\lambda|\phi_\lambda\rangle \tag{4.2.65}$$

where

$$h_\lambda = \frac{(\boldsymbol{\lambda}, \boldsymbol{\lambda} + 2\boldsymbol{\rho})}{2(k+\tilde{h})}\,. \tag{4.2.66}$$

From (4.2.62) and (4.2.65) $\phi_\lambda$ is clearly a Virasoro primary field, however the converse is not necessarily true; a Virasoro primary field can be a WZW descendant. All other states in the theory are of the form $J^a_{-n_1} J^b_{-n_2} \ldots |\phi_\lambda\rangle$ with $n_1, n_2$ positive integers. The primary fields correspond to the highest weights of integrable representations of the affine Lie algebra. Since there are a finite number of such weights for a fixed positive integer $k$ this means that there are a finite number of primary fields in the $\widehat{\mathfrak{g}}_k$ WZW model. Of course, these fields are primary with respect to the affine algebra, but there are an infinite number of Virasoro primary fields. Theories which are minimal with respect to either the Virasoro algebra or an extended symmetry algebra, are often called rational conformal fields theories, or RCFTs.

By analogy with the Virasoro case, the character of the integrable representation of $|\widehat{\lambda}\rangle$ is defined as

$$\chi_{\widehat{\lambda}}(\tau) = Tr_{\widehat{\lambda}} e^{2\pi i \tau (L_0 - c/24)} \tag{4.2.67}$$

with $L_0$ given by (4.2.55) and $c$ by (4.2.54). States at level $n$ in the module of $|\widehat{\lambda}\rangle$ have dimension $h_{\widehat{\lambda}} + n$, with $h_{\widehat{\lambda}}$ given in (4.2.66), so the character can be rewritten as

$$\chi_{\widehat{\lambda}}(\tau) = e^{2\pi i\tau(h_{\widehat{\lambda}} - c/24)} \sum_n d(n) e^{2\pi i n\tau} \tag{4.2.68}$$

where $d(n)$ is the number of states at level $n$. Using the formula

$$12|\boldsymbol{\rho}|^2 = \tilde{h} \dim \mathfrak{g}\,, \tag{4.2.69}$$

known as the 'Freudenthal-de Vries strange formula', it is easy to check that

$$h_{\widehat{\lambda}} - c/24 = m_{\widehat{\lambda}} \tag{4.2.70}$$

therefore (4.2.68) is just the specialised, and normalised, character of the irreducible highest weight representation of the affine Lie algebra $\widehat{\mathfrak{g}}_k$, from (4.2.41). This identification shows that the characters of the WZW primary fields transform into each other under the modular transformations with the modular $\mathcal{S}$ and $\mathcal{T}$ matrices given in (4.2.45) and (4.2.44) respectively. To obtain physical spectra, a modular invariant partition function must be constructed. This will not be discussed in detail here, but like in the Virasoro case, the diagonal theory, in which all primary fields transform with respect to the same representation in the holomorphic and antiholomorphic sectors, with each integrable representation appearing exactly once is modular invariant.

All of these results can be extended to models invariant under tensor products of Lie groups $G_1 \otimes G_2 \otimes \ldots$, for which the spectrum generating algebra is the direct sum of the corresponding affine algebras $(\widehat{\mathfrak{g}}_1)_{k_1} \oplus (\widehat{\mathfrak{g}}_2)_{k_2} \oplus \ldots$. The Sugawara construction can be used to find an energy-momentum tensor for each of these algebras and the total energy-momentum tensor is then the sum of these. The central charges of these components also sum to the total central charge $c$.

Of course, these models will all have $c > 1$, although all unitary RCFTs, including the Virasoro minimal models, can be built from WZW models with integer $k$. This is done using the coset construction, where a coset is a quotient of direct sums of WZW models.

To see how this works, consider $\widehat{\mathfrak{g}}$ and let $\widehat{\mathfrak{p}}$ be a subalgebra of $\widehat{\mathfrak{g}}$. The Sugawara construction can be applied to both $\mathfrak{g}$ and $\mathfrak{p}$ to obtain Virasoro generators $L^{\mathfrak{g}}$ and $L^{\mathfrak{p}}$ respectively. In general, they will have different prefactors and different $c$ numbers,

but they will satisfy the commutation relations

$$[L_m^{\mathfrak{g}}, J_n^a] = -nJ_{m+n}^a \quad , \quad a = 1, \ldots, \dim \mathfrak{g} \tag{4.2.71}$$

$$[L_m^{\mathfrak{p}}, J_n^a] = -nJ_{m+n}^a \quad , \quad a = 1, \ldots, \dim \mathfrak{p}\,. \tag{4.2.72}$$

Subtracting gives

$$[L_m^{\mathfrak{g}} - L_m^{\mathfrak{p}}, J_n^a] = 0 \quad , \quad a = 1, \ldots, \dim \mathfrak{p} \tag{4.2.73}$$

and a consequence of this is that

$$[L_m^{\mathfrak{g}} - L_m^{\mathfrak{p}}, L_n^{\mathfrak{p}}] = 0\,. \tag{4.2.74}$$

Defining $L_m^{(\mathfrak{g}/\mathfrak{p})} \equiv L_m^{\mathfrak{g}} - L_m^{\mathfrak{p}}$ leads to

$$[L_m^{(\mathfrak{g}/\mathfrak{p})}, L_n^{(\mathfrak{g}/\mathfrak{p})}] = [L_m^{\mathfrak{g}}, L_n^{\mathfrak{g}}] - [L_m^{\mathfrak{p}}, L_n^{\mathfrak{p}}] \tag{4.2.75}$$

so $L_m^{(\mathfrak{g}/\mathfrak{p})}$ satisfies the Virasoro algebra with central charge

$$c(\mathfrak{g}/\mathfrak{p}) = \frac{k_{\mathfrak{g}} \dim \mathfrak{g}}{k_{\mathfrak{g}} + \tilde{h}_{\mathfrak{g}}} - \frac{k_{\mathfrak{p}} \dim \mathfrak{p}}{k_{\mathfrak{p}} + \tilde{h}_{\mathfrak{p}}}\,. \tag{4.2.76}$$

The cosets of interest here are of the form $\widehat{\mathfrak{g}}_1 \times \widehat{\mathfrak{g}}_1/\widehat{\mathfrak{g}}_2$ where $\widehat{\mathfrak{g}}_k$ is the affine algebra associated to one of the simply-laced algebras $A$, $D$ or $E$. The central charge of these theories simplifies to

$$c = \dim \mathfrak{g} \left( \frac{2}{1+h} - \frac{2}{2+h} \right) = \frac{2r_{\mathfrak{g}}}{h+2}\,. \tag{4.2.77}$$

In general, to extract the $\widehat{\mathfrak{g}}/\widehat{\mathfrak{p}}$ coset conformal theory from the $\widehat{\mathfrak{g}}$ WZW model, the representations, $\widehat{\boldsymbol{\mu}}$, of $\widehat{\mathfrak{g}}$ must be decomposed into a direct sum of representations, $\widehat{\boldsymbol{\nu}}$, of $\widehat{\mathfrak{p}}$:

$$\widehat{\boldsymbol{\mu}} \mapsto \bigoplus_{\widehat{\boldsymbol{\nu}}} b_{\widehat{\boldsymbol{\mu}}\widehat{\boldsymbol{\nu}}} \widehat{\boldsymbol{\nu}}. \tag{4.2.78}$$

This decomposition corresponds to the character identity

$$\chi_{\widehat{\boldsymbol{\mu}}}(\tau) = \tilde{\chi}_{\widehat{\boldsymbol{\nu}}}(\tau) b_{\widehat{\boldsymbol{\mu}}\widehat{\boldsymbol{\nu}}}(\tau) \tag{4.2.79}$$

where $\chi_{\widehat{\boldsymbol{\mu}}}$ and $\tilde{\chi}_{\widehat{\boldsymbol{\nu}}}$ are the characters of the $\widehat{\mathfrak{g}}$ and $\widehat{\mathfrak{p}}$ representations $\widehat{\boldsymbol{\mu}}$ and $\widehat{\boldsymbol{\nu}}$ respectively and the branching function, $b_{\widehat{\boldsymbol{\mu}}\widehat{\boldsymbol{\nu}}}(\tau)$, is the character of the coset theory. Let $\Pi$ denote the projection matrix giving the explicit projection of every weight of $\mathfrak{g}$ onto a weight of $\mathfrak{p}$. Clearly for a coset character to be non zero

$$\Pi \boldsymbol{\mu} - \boldsymbol{\nu} \in \Pi Q \tag{4.2.80}$$

must be satisfied, where $Q$ is the root lattice of $\mathfrak{g}$. For the diagonal cosets of interest here, since $\mathrm{II}(Q \oplus Q) = Q$ this selection rule is particularly simple:

$$\boldsymbol{\mu} + \boldsymbol{\nu} - \boldsymbol{\rho} \in Q \tag{4.2.81}$$

where $\boldsymbol{\mu}, \boldsymbol{\nu}$ and $\boldsymbol{\rho}$ are weights of $\mathfrak{g}$.

The group of outer automorphisms of $\widehat{\mathfrak{g}}$, $O(\widehat{\mathfrak{g}})$, permutes the fundamental weights in such a way as to leave the extended Dynkin diagram invariant. Each fundamental weight is mapped to another with the same mark and comark so the level of the weight remains the same. The action of the group on an arbitrary weight, written in terms of the Dynkin labels, for the ADE theories is given in table 4.2, taken from [5]. The action of an element, $A \in O(\widehat{\mathfrak{g}})$, on a modular S-matrix element of $\widehat{\mathfrak{g}}$ at some

| $\mathfrak{g}$ | $O(\widehat{\mathfrak{g}})$ | Action of the $O(\widehat{\mathfrak{g}})$ generators |
|---|---|---|
| $A_r$ | $\mathbb{Z}_{r+1}$ | $a[n_0, n_1, \ldots, n_{r-1}, n_r] = [n_r, n_0, \ldots, n_{r-2}, n_{r-1}]$ |
| $D_{r=2l}$ | $\mathbb{Z}_2 \times \mathbb{Z}_2$ | $a[n_0, n_1, \ldots, n_{r-1}, n_r] = [n_1, n_0, n_2, \ldots, n_r, n_{r-1}]$ |
| | | $\tilde{a}[n_0, n_1, \ldots, n_{r-1}, n_r] = [n_r, n_{r-1}, n_{r-2}, \ldots, n_1, n_0]$ |
| $D_{r=2l+1}$ | $\mathbb{Z}_4$ | $\bar{a}[n_0, n_1, \ldots, n_{r-1}, n_r] = [n_{r-1}, n_r, n_{r-2}, \ldots, n_1, n_0]$ |
| $E_6$ | $\mathbb{Z}_3$ | $a[n_0, n_1, n_{\bar{1}}, n_2, n_3, n_{\bar{3}}, n_4] = [n_1, n_{\bar{1}}, n_0, n_{\bar{3}}, n_2, n_3, n_4]$ |
| $E_7$ | $\mathbb{Z}_2$ | $a[n_0, n_1, \ldots, n_7] = [n_1, n_0, n_4, n_3, n_2, n_6, n_5, n_7]$ |

Table 4.2: Outer automorphisms of ADE affine Lie algebras, from [5]

level $l$ is

$$S_{(A\boldsymbol{\mu})\boldsymbol{\mu}'} = S_{\boldsymbol{\mu}\boldsymbol{\mu}'} e^{2\pi i (A\boldsymbol{\Lambda}_0, \boldsymbol{\mu}'_0)}. \tag{4.2.82}$$

More information on this topic can be found, for example, in [5].

Coset fields for these diagonal theories are specified by triples $\{\widehat{\boldsymbol{\mu}}, \widehat{\boldsymbol{\nu}}; \widehat{\boldsymbol{\rho}}\}$ of $\widehat{\mathfrak{g}}$ weights at levels 1,1 and 2 and the modular S-matrix has the form

$$\mathcal{S}_{\{\widehat{\boldsymbol{\mu}},\widehat{\boldsymbol{\nu}};\widehat{\boldsymbol{\rho}}\}\{\widehat{\boldsymbol{\mu}}',\widehat{\boldsymbol{\nu}}';\widehat{\boldsymbol{\rho}}'\}} = \mathcal{S}^{(1)}_{\widehat{\boldsymbol{\mu}}\widehat{\boldsymbol{\mu}}'} \mathcal{S}^{(1)}_{\widehat{\boldsymbol{\nu}}\widehat{\boldsymbol{\nu}}'} \mathcal{S}^{(2)*}_{\widehat{\boldsymbol{\rho}}\widehat{\boldsymbol{\rho}}'}. \tag{4.2.83}$$

Under the action of $O(\widehat{\mathfrak{g}})$, given in (4.2.82), it transforms as

$$\begin{aligned} \mathcal{S}_{\{A\widehat{\boldsymbol{\mu}},A\widehat{\boldsymbol{\nu}};A\widehat{\boldsymbol{\rho}}\}\{\widehat{\boldsymbol{\mu}}',\widehat{\boldsymbol{\nu}}';\widehat{\boldsymbol{\rho}}'\}} &= e^{2\pi i (A\boldsymbol{\Lambda}_0, \boldsymbol{\mu}'+\boldsymbol{\nu}'-\boldsymbol{\rho}')} \mathcal{S}_{\{\widehat{\boldsymbol{\mu}},\widehat{\boldsymbol{\nu}};\widehat{\boldsymbol{\rho}}\}\{\widehat{\boldsymbol{\mu}}',\widehat{\boldsymbol{\nu}}';\widehat{\boldsymbol{\rho}}'\}} \\ &= \mathcal{S}_{\{\widehat{\boldsymbol{\mu}},\widehat{\boldsymbol{\nu}};\widehat{\boldsymbol{\rho}}\}\{\widehat{\boldsymbol{\mu}}',\widehat{\boldsymbol{\nu}}';\widehat{\boldsymbol{\rho}}'\}} \end{aligned} \tag{4.2.84}$$

since $\boldsymbol{\mu}' + \boldsymbol{\nu}' - \boldsymbol{\rho}' \in Q$ [95]. This suggests that $\mathcal{S}$ is a degenerate matrix, which cannot be the case since it represents a modular transformation. This degeneracy must therefore be removed by identifying the fields

$$\{A\widehat{\boldsymbol{\mu}}, A\widehat{\boldsymbol{\nu}}; A\widehat{\boldsymbol{\rho}}\} \equiv \{\widehat{\boldsymbol{\mu}}, \widehat{\boldsymbol{\nu}}; \widehat{\boldsymbol{\rho}}\} \quad \forall A \in O(\widehat{\mathfrak{g}}). \tag{4.2.85}$$

For these diagonal cosets, the orbit of every element $A$ of $O(\widehat{\mathfrak{g}})$ has the same order, $N$, which is simply the order of the global symmetry group of the model. With this field identification, every field in the theory will appear with multiplicity $N$. To remedy this, the partition function must be divided by this multiplicity, which has the effect of introducing $N$ into the coset modular $\mathcal{S}$-matrix [96]:

$$\mathcal{S}_{\{\widehat{\boldsymbol{\mu}},\widehat{\boldsymbol{\nu}};\widehat{\boldsymbol{\rho}}\}\{\widehat{\boldsymbol{\mu}}',\widehat{\boldsymbol{\nu}}';\widehat{\boldsymbol{\rho}}'\}} = N\mathcal{S}^{(1)}_{\widehat{\boldsymbol{\mu}}\widehat{\boldsymbol{\mu}}'}\mathcal{S}^{(1)}_{\widehat{\boldsymbol{\nu}}\widehat{\boldsymbol{\nu}}'}\mathcal{S}^{(2)}_{\widehat{\boldsymbol{\rho}}\widehat{\boldsymbol{\rho}}'}. \tag{4.2.86}$$

More information on field identifications can be found, for example, in [97].

## 4.3 Minimal reflection factors for purely elastic scattering theories

Returning now to the particle description of the purely elastic scattering theories, it is useful to note that a common basis for the conjecturing of bulk scattering amplitudes is a 'minimality hypothesis', that in the absence of other requirements one should look for solutions of the constraints with the smallest possible number of poles and zeros. In this section this principle is used to find sets of boundary amplitudes, one for each purely elastic S-matrix of type A, D or E. The amplitudes given below were at first conjectured [98] as a natural generalisation of the minimal versions of the $A_r$ affine Toda field theory amplitudes found in [99, 100]. The reasoning behind these conjectures will be explained shortly. More recently, Fateev [101] proposed a set of reflection factors for the affine Toda field theories. These were in integral form, and not all matrix elements were given. However, modulo some overall signs and small typos, the coupling-independent parts of Fateev's conjectures match those presented here. (This has also been found by Zambon [102], who obtained equivalent formulae to those recorded below taking Fateev's integral formulae as a starting point.)

Recall from section 3.3, the unitarity condition, for a purely elastic scattering

theory, is

$$R_a(\theta)R_a(-\theta) = 1 \tag{4.3.1}$$

and the crossing-unitarity condition is

$$R_a(\theta)R_{\bar{a}}(\theta - i\pi) = S_{aa}(2\theta)\,. \tag{4.3.2}$$

Whenever a bulk three-point coupling $C^{abc}$ is non-zero there is also a bootstrap constraint

$$R_c(\theta) = R_a(\theta + i\bar{U}^b_{ac})R_b(\theta - i\bar{U}^a_{bc})S_{ab}(2\theta + i\bar{U}^b_{ac} - i\bar{U}^a_{bc})\,. \tag{4.3.3}$$

Unitarity and crossing-unitarity together imply that the reflection factors must be $2\pi i$ periodic; unitarity then requires that they be products of the blocks $(x)$ introduced in section 4.1:

$$(x) = \frac{\sinh\left(\frac{\theta}{2} + \frac{i\pi x}{2h}\right)}{\sinh\left(\frac{\theta}{2} - \frac{i\pi x}{2h}\right)}\,, \tag{4.3.4}$$

which appear in the $ADE$ S-matrix elements as

$$S_{ab} = \prod_{x \in A_{ab}} \{x\}\,, \quad \{x\} = (x-1)\,(x+1)\,. \tag{4.3.5}$$

The crossing-unitarity constraint is then key for the analysis of minimality. Each pole or zero of $S_{aa}(2\theta)$ on the right hand side of (4.3.2) must be present in one or other of the factors on the left hand side of that equation. This sets a lower bound on the number of poles and zeros for the reflection factor $R_a(\theta)$.

To exploit this observation, it is convenient to work at the level of the larger blocks $\{x\} = (x-1)(x+1)$, the basic units for the bulk bootstrap equations [83, 85]. Define two complementary 'square roots' of these blocks as

$$\langle x\rangle = \left(\tfrac{x-1}{2}\right)\left(\tfrac{2h-x-1}{2}\right)^{-1} \quad , \quad \langle\widetilde{x}\rangle = \left(\tfrac{x+1}{2}\right)\left(\tfrac{2h-x+1}{2}\right)^{-1} \tag{4.3.6}$$

which have the basic properties

$$\langle x\rangle(\theta) = \langle\widetilde{x}\rangle(\theta + i\pi) \tag{4.3.7}$$

and

$$\langle x\rangle(\theta)\,\langle\widetilde{x}\rangle(\theta) = \{x\}\,(2\theta)\,. \tag{4.3.8}$$

The crossing-unitarity equation can then be solved, in a minimal fashion, by any product

$$R_a = \prod_{x \in A_{aa}} f_x \tag{4.3.9}$$

where each factor $f_x$ can be freely chosen to be $\langle x \rangle$ or $\langle \widetilde{x} \rangle$, modulo one subtlety: since $(0) = 1$, minimality requires that any factor $f_1$ be taken to be $\langle 1 \rangle$ rather than $\langle \widetilde{1} \rangle$. In fact there is always exactly one such factor for the diagonal S-matrix elements relevant here [86].* Pictorially these 'square root' blocks are shown in figure 4.3. Each

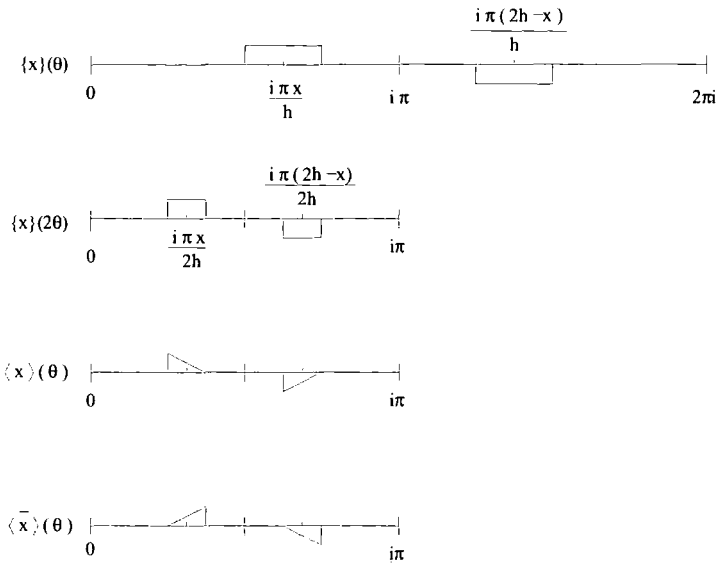


Figure 4.3: The 'square root' blocks

block $\{x\}(\theta)$ has a pole at $\theta = i\pi(x \pm 1)/h$, depicted in figure 4.3 by the edges of the block sitting above the horizontal ($\theta$) axis. Each of these poles has a corresponding zero (outside the physical strip); the positions of these zeros are given by the edges of the block sitting below the axis. Figure 4.3 also shows how the poles and zeros of each block of $S(2\theta)$, $\{x\}(2\theta)$, are split between the two square roots $\langle x \rangle$ and $\langle \widetilde{x} \rangle$.

There remains the constraint imposed by the bootstrap equations (4.3.3). To treat these it is necessary to know how the blocks $\langle x \rangle(\theta)$ and $\langle \widetilde{x} \rangle(\theta)$ transform under general shifts in $\theta$. As in [85, 86], these shifts are best discussed by defining

$$(x)_+(\theta) = \sinh\left(\frac{\theta}{2} + \frac{i\pi x}{2h}\right) \tag{4.3.10}$$

and then

$$\langle x \rangle_+ = \left(\tfrac{x-1}{2}\right)_+ \left(\tfrac{2h-x-1}{2}\right)_+^{-1} \quad , \quad \langle \widetilde{x} \rangle_+ = \left(\tfrac{x+1}{2}\right)_+ \left(\tfrac{2h-x+1}{2}\right)_+^{-1} \tag{4.3.11}$$

*One could also take $\langle x \rangle = \left(\frac{x-1}{2}\right)\left(\frac{x+1}{2}\right)$, $\langle \widetilde{x} \rangle = \left(\frac{2h-x-1}{2}\right)^{-1}\left(\frac{2h-x+1}{2}\right)^{-1}$ throughout, but this would break the pattern previously seen for the $A_r$ theories, and turns out not to fit with the $g$-function calculations later.

so that $(x) = (x)_+/(-x)_+$, $\langle x\rangle = \langle x\rangle_+/\langle\widetilde{-x}\rangle_+$ and $\langle\widetilde{x}\rangle = \langle\widetilde{x}\rangle_+/\langle -x\rangle_+$. Once a conjectured set of reflection factors (4.3.9) has been decomposed into these blocks, it is straightforward to implement the boundary bootstrap equations (4.3.3) using the properties

$$\langle x\rangle_+(\theta + i\pi y/h) = \langle x+y\rangle_+(\theta)\ , \quad \langle\widetilde{x}\rangle_+(\theta + i\pi y/h) = \langle\widetilde{x+y}\rangle_+(\theta)\,. \tag{4.3.12}$$

It is very easy, using the block diagrams shown in figure 4.3, to check the bootstrap equations. As an example this is done in figure 4.4 for the simple case of $A_2$. Here the Coxeter number $h = 3$, the fusing angles $U_{11}^2 = U_{22}^1 = \frac{2i\pi}{3}$, $S_{11}(\theta) = S_{22}(\theta) = \{1\}$ and $R_1(\theta) = R_2(\theta) = \langle 1\rangle$. Recall that each vertical edge of every block denotes the position of a pole (when the edge is above the axis) or a zero (when it is below the axis). Therefore, when multiplying two blocks at the same position, the result is to add the areas of the blocks (with a double height edge representing a double pole or zero), and if two blocks are sitting either side of the horizontal axis at the same position, their areas then cancel. This can be seen in figure 4.4.

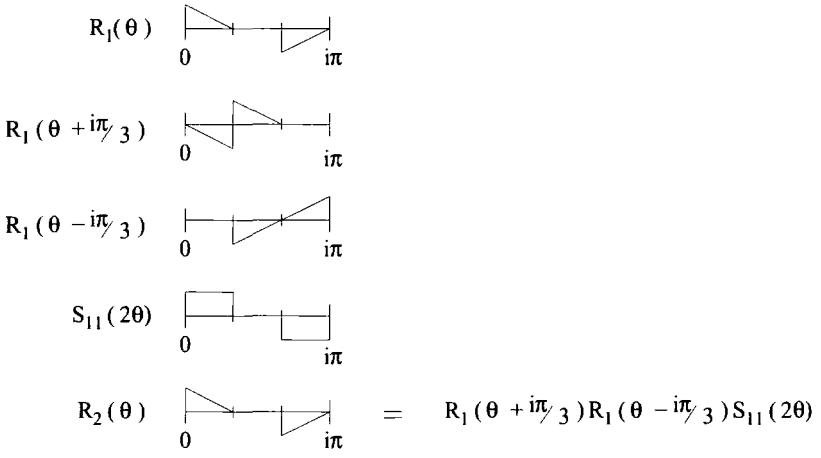


Figure 4.4: The bootstrap equation for $A_2$

For the ADE theories it turns out that the boundary bootstrap equations *can* all be satisfied by minimal conjectures of the form (4.3.9), and that the choice of blocks is then fixed uniquely. (From the point of view of the bootstrap equations alone, an overall swap between $\langle x\rangle$ and $\langle\widetilde{x}\rangle$ is possible, but the requirement that $f_1 = \langle 1\rangle$ fixes even this ambiguity.) The final answers are recorded below.

### $A_r$

The reflection factors for this case were given in [99]. In the current notation they are

$$R_a = \prod_{\substack{x=1 \\ x \text{ odd}}}^{2a-1} \langle x \rangle \,. \tag{4.3.13}$$

### $D_r$

The reflection factors, $R_a$, for $a = 1, \ldots, r-2$ are

$$\begin{aligned} R_a &= \prod_{\substack{x=1 \\ x \text{ odd}}}^{2a-1} \langle x \rangle \prod_{\substack{x=1 \\ \text{step } 4}}^{2a-1} \langle h-x \rangle \prod_{\substack{x=1 \\ \text{step } 4}}^{2a-5} \langle \widetilde{h-x-2} \rangle \,, \text{ for } a \text{ odd} \\ R_a &= \prod_{\substack{x=1 \\ x \text{ odd}}}^{2a-1} \langle x \rangle \prod_{\substack{x=1 \\ \text{step } 4}}^{2a-3} \langle \widetilde{h-x} \rangle \langle h-x-2 \rangle \,, \text{ for } a \text{ even} \,, \end{aligned} \tag{4.3.14}$$

while for $a = r-1$ and $r$

$$\begin{aligned} R_{r-1} &= R_r = \prod_{\substack{x=1 \\ \text{step } 4}}^{2r-5} \langle x \rangle \,, \text{ for } r \text{ odd} \\ R_{r-1} &= R_r = \prod_{\substack{x=1 \\ \text{step } 4}}^{2r-3} \langle x \rangle \,, \text{ for } r \text{ even} \,, \end{aligned} \tag{4.3.15}$$

### $E_6$

$$\begin{aligned} R_1 &= R_{\bar{1}} = \langle 1 \rangle \langle 7 \rangle \\ R_2 &= \langle 1 \rangle \langle 5 \rangle \langle 7 \rangle \langle \widetilde{11} \rangle \\ R_3 &= R_{\bar{3}} = \langle 1 \rangle \langle 3 \rangle \langle 5 \rangle \langle 7 \rangle \langle \widetilde{7} \rangle \langle 9 \rangle \\ R_4 &= \langle 1 \rangle \langle 3 \rangle^2 \langle 5 \rangle^2 \langle \widetilde{5} \rangle \langle 7 \rangle^2 \langle \widetilde{7} \rangle \langle 9 \rangle \langle \widetilde{9} \rangle \langle 11 \rangle \end{aligned} \tag{4.3.16}$$

$E_7$

$$
\begin{aligned}
R_1 &= \langle 1\rangle\langle 9\rangle\langle 17\rangle \\
R_2 &= \langle 1\rangle\langle 7\rangle\langle 11\rangle\langle \widetilde{17}\rangle \\
R_3 &= \langle 1\rangle\langle 5\rangle\langle 7\rangle\langle 9\rangle\langle \widetilde{11}\rangle\langle 13\rangle\langle 17\rangle \\
R_4 &= \langle 1\rangle\langle 3\rangle\langle 7\rangle\langle 9\rangle\langle \widetilde{9}\rangle\langle 11\rangle\langle 15\rangle\langle \widetilde{17}\rangle \\
R_5 &= \langle 1\rangle\langle 3\rangle\langle 5\rangle\langle 7\rangle\langle \widetilde{7}\rangle\langle 9\rangle^2\langle 11\rangle\langle \widetilde{11}\rangle\langle 13\rangle\langle \widetilde{15}\rangle\langle 17\rangle \\
R_6 &= \langle 1\rangle\langle 3\rangle\langle 5\rangle^2\langle 7\rangle\langle \widetilde{7}\rangle\langle 9\rangle^2\langle \widetilde{9}\rangle\langle 11\rangle\langle \widetilde{11}\rangle\langle 13\rangle^2\langle \widetilde{15}\rangle\langle 17\rangle \\
R_7 &= \langle 1\rangle\langle 3\rangle^2\langle 5\rangle^2\langle \widetilde{5}\rangle\langle 7\rangle^3\langle \widetilde{7}\rangle\langle 9\rangle^2\langle \widetilde{9}\rangle^2\langle 11\rangle^3\langle \widetilde{11}\rangle\langle 13\rangle\langle \widetilde{13}\rangle^2\langle 15\rangle^2\langle \widetilde{17}\rangle
\end{aligned}
\tag{4.3.17}
$$

$E_8$

$$
\begin{aligned}
R_1 &= \langle 1\rangle\langle 11\rangle\langle 19\rangle\langle \widetilde{29}\rangle \\
R_2 &= \langle 1\rangle\langle 7\rangle\langle 11\rangle\langle 13\rangle\langle \widetilde{17}\rangle\langle 19\rangle\langle 23\rangle\langle \widetilde{29}\rangle \\
R_3 &= \langle 1\rangle\langle 3\rangle\langle 9\rangle\langle 11\rangle\langle \widetilde{11}\rangle\langle 13\rangle\langle 17\rangle\langle 19\rangle\langle \widetilde{19}\rangle\langle 21\rangle\langle \widetilde{27}\rangle\langle 29\rangle \\
R_4 &= \langle 1\rangle\langle 5\rangle\langle 7\rangle\langle 9\rangle\langle 11\rangle\langle \widetilde{11}\rangle\langle 13\rangle\langle 15\rangle\langle \widetilde{15}\rangle\langle 17\rangle\langle 19\rangle\langle \widetilde{19}\rangle\langle 21\rangle\langle \widetilde{23}\rangle\langle 25\rangle\langle 29\rangle \\
R_5 &= \langle 1\rangle\langle 3\rangle\langle 5\rangle\langle 7\rangle\langle 9\rangle\langle \widetilde{9}\rangle\langle 11\rangle^2\langle \widetilde{11}\rangle\langle 13\rangle\langle \widetilde{13}\rangle\langle 15\rangle^2\langle 17\rangle\langle \widetilde{17}\rangle\langle 19\rangle^2\langle \widetilde{19}\rangle\langle 21\rangle\langle \widetilde{21}\rangle \\
&\quad \langle 23\rangle\langle \widetilde{25}\rangle\langle 27\rangle\langle \widetilde{29}\rangle \\
R_6 &= \langle 1\rangle\langle 3\rangle\langle 5\rangle\langle 7\rangle\langle \widetilde{7}\rangle\langle 9\rangle^2\langle 11\rangle^2\langle \widetilde{11}\rangle\langle 13\rangle^2\langle \widetilde{13}\rangle\langle 15\rangle\langle \widetilde{15}\rangle\langle 17\rangle^2\langle \widetilde{17}\rangle\langle 19\rangle\langle \widetilde{19}\rangle^2 \\
&\quad \langle 21\rangle^2\langle 23\rangle\langle \widetilde{23}\rangle\langle 25\rangle\langle \widetilde{27}\rangle\langle 29\rangle \\
R_7 &= \langle 1\rangle\langle 3\rangle\langle 5\rangle^2\langle 7\rangle^2\langle \widetilde{7}\rangle\langle 9\rangle^2\langle \widetilde{9}\rangle\langle 11\rangle^2\langle \widetilde{11}\rangle^2\langle 13\rangle^3\langle \widetilde{13}\rangle\langle 15\rangle^2\langle \widetilde{15}\rangle^2\langle 17\rangle^3\langle \widetilde{17}\rangle\langle 19\rangle^2 \\
&\quad \langle \widetilde{19}\rangle^2\langle 21\rangle^2\langle \widetilde{21}\rangle\langle 23\rangle\langle \widetilde{23}\rangle^2\langle 25\rangle^2\langle \widetilde{27}\rangle\langle 29\rangle \\
R_8 &= \langle 1\rangle\langle 3\rangle^2\langle 5\rangle^2\langle \widetilde{5}\rangle\langle 7\rangle^3\langle \widetilde{7}\rangle\langle 9\rangle^3\langle \widetilde{9}\rangle^2\langle 11\rangle^4\langle \widetilde{11}\rangle^2\langle 13\rangle^3\langle \widetilde{13}\rangle^3\langle 15\rangle^4\langle \widetilde{15}\rangle^2\langle 17\rangle^3\langle \widetilde{17}\rangle^3 \\
&\quad \langle 19\rangle^4\langle \widetilde{19}\rangle^2\langle 21\rangle^2\langle \widetilde{21}\rangle^3\langle 23\rangle^3\langle \widetilde{23}\rangle\langle 25\rangle\langle \widetilde{25}\rangle^2\langle 27\rangle^2\langle \widetilde{29}\rangle
\end{aligned}
\tag{4.3.18}
$$

For the $T$ series the story is different: it is *not* possible to satisfy the boundary bootstrap equations with a conjecture of the form (4.3.9). This means that the minimal reflection factors for these models are forced by the bootstrap to have extra poles and zeros beyond those required by crossing-unitarity alone. The general proposal

will be given in eq. (4.5.4) below, but the situation can be understood using the boundary $T_1$, or Lee-Yang, model: the minimal reflection factor found in [78] for the single particle in this model bouncing off the $|\mathbb{1}\rangle$ boundary is

$$R^{|\mathbb{1}\rangle} = (\tfrac{1}{2})(\tfrac{3}{2})(\tfrac{4}{2})^{-1} \ . \tag{4.3.19}$$

The simpler function $(\frac{1}{2})(\frac{4}{2})^{-1}$ would have been enough to satisfy crossing-unitarity, but then the boundary bootstrap would not have held, and so (4.3.19) really is a minimal solution. This observation fits nicely with the $g$-function calculations to be reported later: had the minimal reflection factors for the $T_r$ theories fallen into the pattern seen for other models, there would have been a mismatch between the predicted UV values of the $g$-functions and the known values from conformal field theory.

## 4.4 One-parameter families of reflection factors

The minimal reflection factors introduced in the last section have no free parameters. However, combined perturbations of a boundary conformal field theory by relevant bulk and boundary operators involve a dimensionless quantity – the ratio of the induced bulk and boundary scales – on which the reflection factors would be expected to depend. To describe such situations, the minimality hypothesis must be dropped and the conjectures extended.

A first observation, rephrasing that of [75], is that given *any* two solutions $R_a(\theta)$ and $R'_a(\theta)$ of the reflection unitarity, crossing-unitarity and bootstrap relations (4.3.1), (4.3.2) and (4.3.3), their ratios $Z_a(\theta) \equiv R_a(\theta)/R'_a(\theta)$ automatically solve one-index versions of the bulk unitarity, crossing and bootstrap equations (2.4.18), (2.4.19) and (2.4.24):

$$Z_a(\theta)Z_a(-\theta) = 1 \ , \quad Z_a(\theta) = Z_{\bar{a}}(i\pi - \theta) \ , \tag{4.4.1}$$

$$Z_{\bar{c}}(\theta) = Z_a(\theta - i\bar{U}^b_{ac})Z_b(\theta + i\bar{U}^a_{bc}) \ . \tag{4.4.2}$$

The minimal reflection factors $R_a(\theta)$ can therefore be used as multiplicative 'seeds' for more general conjectures $R'_a(\theta) = R_a(\theta)/Z_a(\theta)$, with the parameter-dependent parts $Z_a(\theta)^{-1}$ constrained via (4.4.1) and (4.4.2). An immediate solution is $Z_a^{|d\rangle}(\theta) = S_{da}(\theta)$ for any (fixed) particle type $d$ in the theory, where the ket symbol is used here to

indicate that the label $|d\rangle$ might ultimately refer to one of the possible boundary states of the theory. However, this does not yet introduce a parameter. Noting that a symmetrical shift in $\theta$ preserves all the relevant equations, one possibility is to take

$$Z_a^{|d,C\rangle}(\theta) = S_{da}(\theta + C)S_{da}(\theta - C)\,, \tag{4.4.3}$$

with $C$ at this stage arbitrary. This is indeed the solution adopted by the boundary scaling Lee-Yang example studied in [78]. This model is the $r = 1$ member of the $T_r$ series described earlier, and corresponds to the perturbation of the non-unitary minimal model $\mathcal{M}_{25}$ by its only relevant bulk operator, $\varphi$, of conformal dimensions $\Delta_\varphi = \overline{\Delta}_\varphi = -\frac{1}{5}$. The minimal model has two conformally-invariant boundary conditions which were labelled $|\mathbb{1}\rangle$ and $|\Phi\rangle$ in [78]. The $|\mathbb{1}\rangle$ boundary has no relevant boundary fields, and has a minimal reflection factor, given by (4.3.19) above. On the other hand, the $|\Phi\rangle$ boundary has one relevant boundary field, denoted by $\phi$, and gives rise to a one-parameter family of reflection factors

$$R^{|b\rangle}(\theta) = R^{|\mathbb{1}\rangle}(\theta)/Z^{|b\rangle}(\theta)\,. \tag{4.4.4}$$

The factor $Z^{|b\rangle}(\theta)$ has exactly the form mentioned above:

$$Z^{|b\rangle}(\theta) = S(\theta + i\tfrac{\pi}{6}(b+3))S(\theta - i\tfrac{\pi}{6}(b+3)) \tag{4.4.5}$$

where $S(\theta)$ is the bulk S-matrix, and the parameter $b$ can be related to the dimensionless ratio $\mu^2/\lambda$ of the bulk and boundary couplings $\lambda$ and $\mu$ [78, 79]. (Since there is only one particle type in the Lee-Yang model, the indices $a$, $d$ and so on are omitted. The notation here has also been changed slightly from that of [78] to avoid confusing the parameter $b$ with a particle label.) †

As an initial attempt to extend (4.4.4) to the remaining ADET theories one could therefore try

$$R_a^{|d,C\rangle}(\theta) = R_a(\theta)/Z_a^{|d,C\rangle}(\theta)\,, \tag{4.4.6}$$

with $Z_a^{|d,C\rangle}(\theta)$ as in (4.4.3). This manoeuvre certainly generates mathematically-consistent sets of reflection amplitudes, but in the more general cases it is not the most economical choice. Consider instead the functions obtained by replacing the

† There are also boundary-changing operators, but these were not considered in [78, 79].

blocks $\{x\}$ in (4.1.3) by the simpler blocks $(x)$ [45]:

$$S^F_{ab} = \prod_{x \in A_{ab}} (x) \ . \tag{4.4.7}$$

For the Lee-Yang model, $S^F(\theta)$ coincides with $S(\theta)$, but for other theories it has fewer poles and zeros. The bootstrap constraints are only satisfied up to signs, but if $S^F$ is used to define a function $Z_a^{|d,C\rangle}$ as

$$Z_a^{|d,C\rangle}(\theta) = S^F_{da}(\theta + i\tfrac{\pi}{h}C) S^F_{da}(\theta - i\tfrac{\pi}{h}C) \tag{4.4.8}$$

then these signs cancel, and so (4.4.8) provides a more "minimal" generalisation of the family of Lee-Yang reflection factors which nevertheless preserves all of its desirable properties. Setting $d$ equal to the lightest particle in the theory generally gives the family with the smallest number of additional poles and zeros, but, as will be seen later, all cases have a role to play.

The normalisation of the shift was changed in passing from (4.4.3) to (4.4.8); this is convenient because, as a consequence of the property

$$(x - C)(\theta) \times (x + C)(\theta) = (x)(\theta + i\tfrac{\pi}{h}C) \times (x)(\theta - i\tfrac{\pi}{h}C) \, , \tag{4.4.9}$$

$Z_a^{|d,C\rangle}$ simplifies to

$$Z_a^{|d,C\rangle} = \prod_{x \in A_{ad}} (x - C)\,(x + C) \ . \tag{4.4.10}$$

The factors $(Z_a^{|d,C\rangle})^{-1}$ therefore coincide with the coupling-constant dependent parts of the affine Toda field theory S-matrices of [83, 32], with $C$ related to the parameter $B$ of [83] by $C = 1 - B$.

## 4.5 Boundary $T_r$ theories as reductions of boundary sine-Gordon

The reflection factors presented so far are only conjectures, and no evidence has been given linking them to any physically-realised boundary conditions. The best signal in this respect will come from the exact $g$-function calculations to be reported in later sections. However, for the $T_r$ theories, alternative support for the general scheme comes from an interesting relation with the reflection factors of the sine-Gordon model.

In the bulk, the $T_r$ theories can be found as particularly-simple quantum group reductions of the sine-Gordon model at certain values of the coupling, in which the soliton and antisoliton states are deleted leaving only the breathers [89]. Quantum group reduction in the presence of boundaries has yet to be fully understood, but the simplifications of the $T_r$ cases allow extra progress to be made. This generalises the analysis of [78] for $T_1$, the Lee-Yang model, but has some new features.

The boundary S-matrix for the sine-Gordon solitons was found by Ghoshal and Zamolodchikov in [72], and extended to the breathers by Ghoshal in [103]. To match the notation used above for the ADE theories, the sine-Gordon bulk coupling constant $\beta$ is traded for

$$h = \frac{16\pi}{\beta^2} - 2\,. \tag{4.5.1}$$

Ghoshal and Zamolodchikov expressed their matrix solution to the boundary Yang-Baxter equation for the sine-Gordon model[‡] in terms of two parameters $\xi$ and $k$. However for the scalar part (which is the whole reflection factor for the breathers) they found it more convenient to use $\eta$ and $\vartheta$, related to $\xi$ and $k$ by

$$\cos\eta\,\cosh\vartheta = -\frac{1}{k}\cos\xi\ , \quad \cos^2\eta + \cosh^2\vartheta = 1 + \frac{1}{k^2}\ . \tag{4.5.2}$$

Ghoshal-Zamolodchikov's reflection factor for the $a^{\text{th}}$ breather on the $|\eta,\vartheta\rangle$ boundary can then be written as

$$R_a^{|\eta,\vartheta\rangle}(\theta) = R_0^{(a)}(\theta)R_1^{(a)}(\theta) \tag{4.5.3}$$

where

$$R_0^{(a)} = \frac{\left(\frac{h}{2}\right)(a+h)}{\left(a+\frac{3h}{2}\right)}\prod_{l=1}^{a-1}\frac{(l)\,(l+h)}{\left(l+\frac{3h}{2}\right)^2} \tag{4.5.4}$$

is the boundary-parameter-independent part, and

$$R_1^{(a)}(\theta) = S^{(a)}(\eta,\theta)S^{(a)}(i\vartheta,\theta) \tag{4.5.5}$$

with

$$S^{(a)}(\nu,\theta) = \prod_{\substack{l=1-a\\ \text{step } 2}}^{a-1}\frac{\left(\frac{2\nu}{\pi} - \frac{h}{2} + l\right)}{\left(\frac{2\nu}{\pi} + \frac{h}{2} + l\right)} \tag{4.5.6}$$

contains the dependence on $\eta$ and $\vartheta$. In these formulae the blocks $(x)$ are the same as those defined in (4.1.2) for the minimal ADE theories, with $h$ now given by (4.5.1).

[‡]also found by de Vega and Gonzalez Ruiz [104]

Now for the quantum group reduction. In the bulk, suppose that $\beta^2$ is such that

$$h = 2r + 1\,, \qquad r \in \mathbb{N}\,. \tag{4.5.7}$$

At these values of the coupling, Smirnov has shown [89] that a consistent scattering theory can be obtained by removing all the solitonic states, leaving $r$ breathers with masses $M_a = \frac{\sin(\pi a/h)}{\sin(\pi/h)} M_1$. The scattering of these breathers is then given by the $T_r$ S-matrix (4.1.5). In order to explain all poles without recourse to the solitons, extra three-point couplings must be introduced, some of which are necessarily imaginary, consistent with the $T_r$ models being perturbations of nonunitary conformal field theories. In the presence of a boundary, these extra couplings give rise to extra boundary bootstrap equations, which further constrain the boundary reflection factors and impose a relation between the parameters $\eta$ and $\vartheta$. This can be seen by a direct analysis of the boundary bootstrap equations but it is more interesting to take another route, as follows.

First recall the observation of [78], that the reflection factors for the boundary Lee-Yang model match solutions of the boundary Yang-Baxter equation for the sine-Gordon model at

$$\xi \to i\infty\,. \tag{4.5.8}$$

The Lee-Yang case corresponds to $r = 1$, $h = 3$, but here it is supposed that the same constraint should hold more generally (see also [76]). The condition must be translated into the $(\eta, \vartheta)$ parametrisation. One degree of freedom can be retained by allowing $k$ to tend to infinity as the limit (4.5.8) is taken. The relations (4.5.2) then become

$$\cos\eta \cosh\vartheta = A\,, \quad \cos^2\eta + \cosh^2\vartheta = 1\,. \tag{4.5.9}$$

The constant $A$ can be tuned to any value by taking $\xi$ and $k$ to infinity suitably, and so the first equation in (4.5.9) is not a constraint; solving the second for $i\vartheta$,

$$i\vartheta = \eta + \frac{\pi}{2} + (r-d)\pi\,, \quad d \in \mathbb{Z}\,. \tag{4.5.10}$$

(The shift by $r$ is included for later convenience.) This appears to give a countable infinity of one-parameter families of reflection factors, but this is not so: the blocks $(x)$ in (4.5.5) and (4.5.6) depend on the boundary parameters only through the combination

$$\frac{2i\vartheta}{\pi} = \frac{2\eta}{\pi} + 2(r-d) + 1\,. \tag{4.5.11}$$

Since $(x+2h) = (x)$, the reflection factors for $d$ are therefore the same as those for $d+h$. In addition, the freedom to redefine the parameter $\eta$ gives an extra invariance of the one-parameter families under $d \to 2r-d$. The full set of options is therefore realised by

$$d = 0, 1, \ldots r\,. \tag{4.5.12}$$

Note also that $R_1^{(a)}(\theta)$, the coupling-dependent part of the reflection factor, is trivial if $d = 0$. Thus the limit (4.5.8) corresponds to $r$ one-parameter families of breather reflection factors, and one 'isolated' case. This matches the counting of conformal boundary conditions (the set of bulk Virasoro primary fields [67]) for the $\mathcal{M}_{2,2r+3}$ minimal models, and the fact that of these boundary conditions, all but one have the relevant $\phi_{13}$ boundary operator in their spectra.

To see how this fits in with the ideas presented earlier, $\eta$ is swapped for $C$, defined by

$$\frac{2\eta}{\pi} = d - \frac{h}{2} + C\,. \tag{4.5.13}$$

Then, starting from (4.5.5) and relabelling,

$$\begin{aligned} R_1^{(a)} &= \prod_{\substack{l=1-a \\ \text{step } 2}}^{a-1} \frac{(-h+d+l+C)}{(d+l+C)} \frac{(-d+l+C)}{(h-d+l+C)} \\ &= \prod_{\substack{l=1-a \\ \text{step } 2}}^{a-1} (-d-l-C)(-d-l+C)(-h+d+l+C)(-h+d+l-C) \\ &= \prod_{\substack{l=1-a+d \\ \text{step } 2}}^{a+d-1} (-l-C)(-l+C)(-h+l+C)(-h+l-C)\,. \end{aligned} \tag{4.5.14}$$

Since the first $a-d$ terms in the last product cancel if $a > d$, it is easily seen that $R_1^{(a)}$ coincides with $(Z_a^{|d,C\rangle})^{-1}$, as expressed by (4.4.10), for the $T_r$ S-matrix (4.1.5).

## 4.6 Some aspects of the off-critical $g$-functions

The main tool of use here in linking reflection factors to specific boundary conditions will be the formula for an exact off-critical $g$-function introduced in [4]. This was described in section 3.4 but further properties, and some modifications which will be relevant later, are discussed here.

### 4.6.1 The exact $g$-function for diagonal scattering theories

In section 3.4, considerations of the infrared (large-$l$) asymptotics and a conjectured resummation led to the proposal of a general formula for the exact $g$-function of a purely elastic scattering theory. However in section 4.6.2 below, it is argued that the result given in (3.4.76) needs to be modified by the introduction of a simple symmetry factor whenever there is coexistence of vacua at infinite volume. This happens in the low-temperature phases of the $E_6$, $E_7$, A and D models. The more-general result is

$$\ln g_{|\alpha\rangle}(l) = \ln C_{|\alpha\rangle} + \frac{1}{4}\sum_{a=1}^{r_{\mathfrak{g}}} \int_{\mathbb{R}} d\theta \left(\phi_a^{|\alpha\rangle}(\theta) - \delta(\theta) - 2\phi_{aa}(2\theta)\right) \ln\left(1 + e^{-\epsilon_a(\theta)}\right) + \Sigma(l) \tag{4.6.1}$$

where $C_{|\alpha\rangle}$ is the symmetry factor to be discussed shortly, and the functions $\phi_a^{|\alpha\rangle}(\theta)$ and $\phi_{ab}(\theta)$ are related to the bulk and boundary scattering amplitudes $S_{ab}(\theta)$ and $R_a^{|\alpha\rangle}(\theta)$, as before, by

$$\phi_a^{|\alpha\rangle}(\theta) = -\frac{i}{\pi}\frac{d}{d\theta} \ln R_a^{|\alpha\rangle}(\theta)\,, \tag{4.6.2}$$

$$\phi_{ab}(\theta) = -\frac{i}{2\pi}\frac{d}{d\theta} \ln S_{ab}(\theta)\,. \tag{4.6.3}$$

The boundary-condition-independent piece $\Sigma(l)$ is exactly that given in (3.4.76):

$$\Sigma(l) = \frac{1}{2}\sum_{n=1}^{\infty} \sum_{a_1 \ldots a_n = 1}^{r_{\mathfrak{g}}} \frac{1}{n} \int_{\mathbb{R}^n} \frac{d\theta_1}{1 + e^{\epsilon_{a_1}(\theta_1)}} \cdots \frac{d\theta_n}{1 + e^{\epsilon_{a_n}(\theta_n)}} \times \left(\phi_{a_1 a_2}(\theta_1 + \theta_2)\phi_{a_2 a_3}(\theta_2 - \theta_3) \ldots \phi_{a_n a_{n+1}}(\theta_n - \theta_{n+1})\right) \tag{4.6.4}$$

with $\theta_{n+1} = \theta_1$, $a_{n+1} = a_1$. Recall that the functions $\epsilon_a(\theta)$, called pseudoenergies, solve the bulk TBA equations

$$\epsilon_a(\theta) = M_a L \cosh\theta - \sum_{b=1}^{r_{\mathfrak{g}}} \int_{\mathbb{R}} d\theta'\, \phi_{ab}(\theta - \theta')\, L_b(\theta')\,, \qquad a = 1, \ldots, r_{\mathfrak{g}}\,, \tag{4.6.5}$$

where $L_a(\theta) = \ln(1 + e^{-\epsilon_a(\theta)})$, and the ground-state energy of the theory on a circle of circumference $L$ is given in terms of these pseudoenergies by

$$E_0^{\mathrm{circ}}(M, L) = -\sum_{a=1}^{r_{\mathfrak{g}}} \int_{\mathbb{R}} \frac{d\theta}{2\pi} M_a \cosh\theta\, L_a(\theta) + \mathcal{E} L M^2 \tag{4.6.6}$$

where $\mathcal{E} L M^2$ is the bulk contribution to the energy.

As mentioned in section 3.4, the formula (4.6.1) has been checked in detail, but only for the $r_{\mathfrak{g}} = 1$, $C_{|\mathbb{1}\rangle} = 1$ case corresponding to the Lee-Yang model [4]. The results below will confirm that it holds in more general cases, provided $C_{|\alpha\rangle}$ is appropriately chosen.

### 4.6.2 Models with internal symmetries

The scaling Lee-Yang model, on which the analysis of [4] was mostly concentrated, is a massive integrable quantum field theory with fully diagonal scattering and a single vacuum. However many models lack one or both these properties. In this section this analysis will be extended to models possessing, in infinite volume, $N$ equivalent vacua but still described by purely elastic scattering theories[§]. For the ADE-related theories the $N$ equivalent vacua are related by a global symmetry $\mathcal{Z}$. When these systems are in their low-temperature phases, the original formula for $g(l)$, as given in (3.4.76), should be corrected slightly, by including a 'symmetry factor' $C_{|\alpha\rangle}$.

Low-temperature phases are common features of two dimensional magnetic spin systems below their critical temperatures. A discrete symmetry $\mathcal{Z}$ of the Hamiltonian $H$ is spontaneously broken, and a unique ground state is singled out from a multiplet of equivalent degenerate vacua. This contrasts with the high-temperature phase, where the ground state is $\mathcal{Z}$-invariant.

The prototype of two-dimensional spin systems is the Ising model, so this case will be treated first. The Ising Hamiltonian for zero external magnetic field is invariant under a global spin reversal transformation ($\mathcal{Z} = \mathbb{Z}_2$), and at low temperatures $T < T_c$ this symmetry is spontaneously broken and there is a doublet $\{|+\rangle, |-\rangle\}$ of vacuum states transforming into each other under a global spin-flip:

$$|\pm\rangle \to |\mp\rangle\,. \tag{4.6.7}$$

The $\mathbb{Z}_2$ symmetry of $H$ is preserved under renormalisation and it also characterises the continuum field theory version of the model: in the low-temperature phase the bulk field theory has two degenerate vacua $\{|+\rangle, |-\rangle\}$ with excitations, the massive

[§]Integrable models with non-equivalent vacua are typically associated to non-diagonal scattering like, for example, the $\phi_{13}$ perturbations of the minimal $\mathcal{M}_{p,q}$ models [105].

kinks $K_{[+-]}(\theta)$, $K_{[-+]}(\theta)$, corresponding to field configurations interpolating between these vacua.

In infinite volume the ground state is either $|+\rangle$ or $|-\rangle$, and the transition from $|+\rangle$ to $|-\rangle$ (or vice-versa) can only happen in an infinite interval of time. On the other hand in a finite volume $V$, tunnelling is allowed: a kink with finite speed can span the whole volume segment in a finite time interval. The interest here is in the scaling limit of the Ising model on a finite cylinder and the open-segment direction of length $R$ is taken as the space coordinate. Time is then periodic with period $L$. If the boundary conditions are taken to be fixed, of type $+$, at both ends of the segment, then the only multi-particle states which can propagate have an even number of kinks, of the form

$$K_{[+-]}(\theta_1)K_{[-+]}(\theta_2)\dots K_{[-+]}(\theta_n)\ ,\quad (\text{n even})\,. \tag{4.6.8}$$

For $R$ large, the rapidities $\{\theta_j\}$ are quantised according to the Bethe ansatz equations

$$r\sinh\theta_j - i\ln R^{|+\rangle}(\theta_j) = \pi j\,,\quad (r = MR,\ j = 1,2,\dots)\,, \tag{4.6.9}$$

where $R^{|+\rangle}(\theta)$ is the amplitude describing the scattering of particles off a wall with fixed boundary conditions of type $+$.

At low temperatures $Z_{\langle+|+\rangle}[L,R]$ therefore receives contributions only from states with an even number of particles. It is conveniently written in the form (see for example [106]):

$$Z_{\langle+|+\rangle}[L,R] = \frac{1}{2}Z^{(0)}_{\langle+|+\rangle}[L,R] + \frac{1}{2}Z^{(1)}_{\langle+|+\rangle}[L,R] \tag{4.6.10}$$

where

$$Z^{(b)}_{\langle+|+\rangle}[L,R] = e^{-LE_0^{\rm strip}(M,R)}\prod_{j>0}\left(1+(-1)^b e^{-l\cosh\theta_j}\right),\quad (l = ML)\,, \tag{4.6.11}$$

$E_0^{\rm strip}(M,R)$ is the ground-state energy, and the set $\{\theta_j\}$ is quantised by (4.6.9). This can be seen by expanding the product in (4.6.11) and noticing that the contributions from states with an even number of particles and those from states with an odd number of particles each appear with the coefficients $(-1)^{2nb}$ and $(-1)^{(2n+1)b}$, $n\in\mathbb{Z}$ respectively. The contribution from states with an odd number of particles therefore cancels from the combination given in (4.6.10), leaving only that from states with an even number of particles. In order to extract the subleading contributions to $Z_{\langle+|+\rangle}$, as in [4] set

$$Z_{\langle+|+\rangle}[L,R] = \tfrac{1}{2}e^{\ln Z^{(0)}_{\langle+|+\rangle}[L,R]} + \tfrac{1}{2}e^{\ln Z^{(1)}_{\langle+|+\rangle}[L,R]}\ , \tag{4.6.12}$$

and in the limit $R \to \infty$ use Newton's approximation to transform sums into integrals. The result is

$$\begin{aligned} \ln Z^{(b)}_{\langle +|+\rangle}[L,R] &\sim \frac{1}{2}\int_{\mathbb{R}} d\theta \left(\frac{r}{\pi}\cosh(\theta) + \phi^{|+\rangle}(\theta) - \delta(\theta)\right) \ln(1+(-1)^b e^{-l\cosh\theta}) \\ &= 2\ln g^{(b)}_{|+\rangle}(l) - RE_0^{\text{circle},b}(M,L)\ ,\ (b=0,1)\,. \end{aligned} \tag{4.6.13}$$

From (4.6.13) it follows that at finite values of $l$ as $R \to \infty$

$$\ln Z^{(0)}_{\langle +|+\rangle}[L,R] - \ln Z^{(1)}_{\langle +|+\rangle}[L,R] \to +\infty \tag{4.6.14}$$

and therefore

$$\begin{aligned} Z_{\langle +|+\rangle}[L,R] &\sim \left(g_{|+\rangle}(l)\right)^2 e^{-RE_0^{\text{circle}}(M,L)} \sim \frac{1}{2} Z^{(0)}_{\langle +|+\rangle}[L,R] \\ &= \tfrac{1}{2}\left(g^{(0)}_{|+\rangle}(l)\right)^2 e^{-RE_0^{\text{circle}}(M,L)}\ , \end{aligned} \tag{4.6.15}$$

where $E_0^{\text{circle}}(M,L) \equiv E_0^{\text{circle},0}(M,L)$ is the ground state energy for the system with periodic boundary conditions.

Notice that $Z^{(0)}_{\langle +|+\rangle}[L,R]$ takes contributions from states with both even and odd number of particles. In fact, following section 3.4, $g^{(0)}_{|+\rangle} = g^{eq.(3.4.76)}_{\textbf{fixed}}$ and

$$g_{|+\rangle}(l) = g_{|-\rangle}(l) = \frac{1}{\sqrt{2}} g^{eq.(3.4.76)}_{\textbf{fixed}}\ . \tag{4.6.16}$$

In conclusion, the appearance of the extra symmetry factor $C_{|+\rangle} = \frac{1}{\sqrt{2}}$ is related to the kink selection rule restricting the possible multi-particle states. In the Ising model this was seen in the exact formula for the low-temperature partition function $Z_{\langle +|+\rangle}[L,R]$, by it being written as an averaged sum of $Z^{(0)}_{\langle +|+\rangle}[L,R]$ and $Z^{(1)}_{\langle +|+\rangle}[L,R]$.

In more general theories with discrete symmetries, similar considerations apply. Consider a set of $i = 1,2,\ldots N$ 'fixed' boundary conditions, matching the $i = 1,2,\ldots N$ vacua. A derivation of $Z_{\langle i|i\rangle}$ as in section 3.4, including *all* multi-particle states satisfying the Bethe momentum quantisation conditions, will give an incorrect answer, since some states will be forbidden by the kink structure. Instead, one can construct a new boundary state

$$|U\rangle = \sum_{j=1}^{N} |j\rangle\,, \tag{4.6.17}$$

and consider the partition function $Z_{\langle U|i\rangle}$. Since boundary scattering does not mix vacua it is clear that the only effect of replacing $|i\rangle$ by $|U\rangle$ is to eliminate the kink

condition on allowed multiparticle states. Thus the counting of states on an interval with $U$ at one end and $i$ at the other is exactly the same as it would be in a high-temperature phase with the reflection factor at both ends being $R_{|i\rangle}(\theta)$, and the derivation in section 3.4 goes through to find at large $R$

$$\ln Z_{\langle U|i\rangle}[L,R] \sim -RE_0^{\rm circ}(M,L) + 2\ln \mathcal{G}^{(0)}(l)\,. \tag{4.6.18}$$

Recall, from section 3.4, that $\mathcal{G}^{(0)}(l)$ is the massive $g$-function, defined by

$$\mathcal{G}^{(0)}_{|\alpha\rangle}(l) = \frac{\langle\,\alpha|\psi_0\,\rangle}{\langle\,\psi_0|\psi_0\,\rangle^{1/2}}\,, \tag{4.6.19}$$

which is related to the $g$-function for the boundary condition $\alpha$ by a linearly-growing piece $-f_{|\alpha\rangle}L$:

$$\ln g_{|\alpha\rangle}(l) = \ln \mathcal{G}^{(0)}_{|\alpha\rangle}(l) + f_{|\alpha\rangle}L\,. \tag{4.6.20}$$

$\mathcal{G}^{(0)}$ is therefore – up to a linear term – given by (4.6.1) with $\phi_a^{|\alpha\rangle}(\theta) = \phi_a^{|i\rangle}(\theta)$ and $C_{|\alpha\rangle} = 1$. On the other hand, since all vacua are related by the discrete symmetry $\mathcal{Z}$ and the finite-volume vacuum state $|\psi_0\rangle$ must be symmetrical under this symmetry, $\langle\,\psi_0|i\,\rangle = \langle\,\psi_0|j\,\rangle\ \forall\, i,j$, and so

$$\left(\mathcal{G}^{(0)}(l)\right)^2 = \frac{\langle\,U|\psi_0\,\rangle\langle\,\psi_0|i\,\rangle}{\langle\,\psi_0|\psi_0\,\rangle} = N\frac{\langle\,\psi_0|i\,\rangle^2}{\langle\,\psi_0|\psi_0\,\rangle} = N\left(\mathcal{G}^{(0)}_{|i\rangle}(l)\right)^2. \tag{4.6.21}$$

Hence

$$g_{|i\rangle}(l) = \tfrac{1}{\sqrt{N}}g(l) \tag{4.6.22}$$

and $g_{|i\rangle}(l)$ is given by the formula (4.6.1) with $C_{|i\rangle} = \frac{1}{\sqrt{N}}$.

An immediate consequence is that in the infrared, $g_{|i\rangle}(l)$ does not tend to one. Instead,

$$\lim_{l\to\infty} g_{|i\rangle}(l) = C_{|i\rangle} = \frac{1}{\sqrt{N}}\,. \tag{4.6.23}$$

This perhaps-surprising claim can be justified independently. Recall from section 3.3 that in infinite volume, boundary states can be described using a basis of scattering states [72]:

$$|B\rangle = \left(1 + \frac{1}{2}\int_{-\infty}^{\infty} K^{ab}(\theta)A_a(-\theta)A_b(\theta) + \ldots\right)|0\rangle \tag{4.6.24}$$

where $|0\rangle$ is the bulk vacuum for an infinite line. In finite but large volumes, the same expression provides a good approximation to the boundary state, the only modification normally being that the momenta of the multiparticle states must be quantised by the relevant Bethe ansatz equations. However a subtlety arises when there is a

degeneracy among the bulk vacua, in situations where the boundary condition distinguishes between these vacua. Take the case of a fixed boundary condition which picks out one of the degenerate vacua, say $i$: then the state $|0\rangle$ on the RHS of (4.6.24) is $|i\rangle$. However when calculating the finite-volume $g$-function, one must consider $\langle \psi_0|B \rangle$, where $\langle\psi_0|$ is the finite-volume vacuum. (Note that the bulk energy is normalised to zero when considering (4.6.24), so this inner product gives $g$ directly, rather than $\mathcal{G}$.) In large but finite volumes, the tunnelling amplitude between the infinite-volume bulk vacua is non-zero and so the appropriately-normalised finite volume ground state is the symmetric combination

$$\langle\psi_0| = \frac{1}{\sqrt{N}} \sum_{j=1}^{N} \langle j| \,. \tag{4.6.25}$$

The limiting value of $g$ in the infrared is therefore not 1, but $1/\sqrt{N}$, as found in the exact calculation earlier.

Table 4.3 lists the central charge, the Coxeter number, the symmetry group $\mathcal{Z}$, and the number of degenerate vacua for the ADET models. For the $A_r$, $D_r$, $E_6$ and $E_7$ theories at low temperatures there is a coexistence of $N$ vacuum states $|i\rangle$, $i = 1, 2, \ldots, N$, with $N = r+1$, 4, 3 and 2 respectively. The corresponding symmetry factor $C_{|i\rangle}$, for fixed-type boundary conditions which pick out a single bulk vacuum, is always $1/\sqrt{N}$.

### 4.6.3 Further properties of the exact $g$-function

An important property of the sets of TBA equations under consideration here concerns the so-called Y-functions [34],

$$Y_a(\theta) = e^{\epsilon_a(\theta)}. \tag{4.6.26}$$

Recall from section 2.5 that these functions satisfy a set of functional relations called a Y-system:

$$Y_a(\theta + \tfrac{i\pi}{h}) Y_a(\theta - \tfrac{i\pi}{h}) = \prod_{b=1}^{r_{\mathfrak{g}}} (1 + Y_b(\theta))^{A_{ba}^{[\mathbf{G}]}} \,, \tag{4.6.27}$$

where $A_{ba}^{[\mathbf{G}]}$ is the incidence matrix of the Dynkin diagram labelling the TBA system. Defining an associated set of T-functions through the relations

$$Y_a(\theta) = \prod_{c=1}^{r_{\mathfrak{g}}} (T_c(\theta))^{A_{ca}^{[\mathbf{G}]}} \quad , \quad 1 + Y_a(\theta) = T_a(\theta + i\tfrac{\pi}{h}) T_a(\theta - i\tfrac{\pi}{h}) \tag{4.6.28}$$

| Model | $c_{\text{eff}}(0)$ | Coxeter number $h$ | Global symmetry $\mathcal{Z}$ | $N$ |
|---|---|---|---|---|
| $A_r$ | $\frac{2r}{r+3}$ | $r+1$ | $\mathbb{Z}_{r+1}$ | $r+1$ |
| $D_r$ ($r$ even) | 1 | $2r-2$ | $\mathbb{Z}_2 \times \mathbb{Z}_2$ | 4 |
| $D_r$ ($r$ odd) | 1 | $2r-2$ | $\mathbb{Z}_4$ | 4 |
| $E_6$ | $\frac{6}{7}$ | 12 | $\mathbb{Z}_3$ | 3 |
| $E_7$ | $\frac{7}{10}$ | 18 | $\mathbb{Z}_2$ | 2 |
| $E_8$ | $\frac{1}{2}$ | 30 | $\mathbb{Z}_1$ | 1 |
| $T_r$ | $\frac{2r}{2r+3}$ | $2r+1$ | $\mathbb{Z}_1$ | 1 |

Table 4.3: Data for the ADET purely elastic scattering theories. The symmetry factor $C_{|i\rangle}$ for fixed-type boundary conditions is $1/\sqrt{N}$ in each case, where $N$ is the number of degenerate vacua in the low-temperature phase.

then

$$T_a(\theta + i\tfrac{\pi}{h})T_a(\theta - i\tfrac{\pi}{h}) \prod_{c=1}^{r_{\mathfrak{g}}} (T_c(\theta))^{-A_{ca}^{[\mathbf{G}]}} = 1 + Y_a^{-1}(\theta) \ . \tag{4.6.29}$$

In addition, the T-functions satisfy

$$T_a(\theta + \tfrac{i\pi}{h})T_a(\theta - \tfrac{i\pi}{h}) = 1 + \prod_{b=1}^{r_{\mathfrak{g}}} (T_b(\theta))^{A_{ba}^{[\mathbf{G}]}} \ . \tag{4.6.30}$$

Fourier transforming the logarithm of equation (4.6.29), solving taking the large $\theta$ asymptotic into account, and transforming back recovers the (standard) formula

$$\ln T_a(\theta) = \frac{LM_a}{2\cos(\frac{\pi}{h})} \cosh\theta - \sum_{b=1}^{r_{\mathfrak{g}}} \int_{\mathbb{R}} d\theta' \, \chi_{ab}(\theta - \theta') \, L_b(\theta') \, , \qquad a = 1, \dots r_{\mathfrak{g}} \, , \tag{4.6.31}$$

where [34, 88]

$$\chi_{ab}(\theta) = -\int_{\mathbb{R}} \frac{dk}{2\pi} \, e^{ik\theta} \left(2\cosh(k\pi/h)\mathbb{1} - A^{[\mathbf{G}]}\right)^{-1}_{ab} = -\frac{i}{2\pi}\frac{d}{d\theta} S^F_{ab}(\theta) \, . \tag{4.6.32}$$

The result (4.6.31) allows a connection to be made between the exact $g$-functions for the parameter-dependent reflection factors in section 4.4 and the T functions. Taking the reflection factors defined by (4.4.8) and (4.4.6)

$$R_a^{|b,C\rangle} = R^{(a)}(\theta)/(S^F_{ab}(\theta - i\tfrac{\pi}{h}C)S^F_{ab}(\theta + i\tfrac{\pi}{h}C)) \tag{4.6.33}$$

and using (4.6.1),

$$\ln g_{|b,C\rangle}(l) = \ln g(l) - \frac{1}{2}\sum_{a=1}^{r_{\mathfrak{g}}} \int_{\mathbb{R}} d\theta' \chi_{ab}(\theta' - i\tfrac{\pi}{h}C) L_b(\theta') - \frac{1}{2}\sum_{a=1}^{r_{\mathfrak{g}}} \int_{\mathbb{R}} d\theta' \chi_{ab}(\theta' + i\tfrac{\pi}{h}C) L_b(\theta') \,. \tag{4.6.34}$$

Comparing this result with (4.6.31) and using the property $T_b(\theta) = T_b(-\theta)$,

$$\ln g_{|b,C\rangle}(l) = \ln g(l) + \ln T_b\left(i\frac{\pi}{h}C\right) - \frac{LM_b}{2\cos\frac{\pi}{h}} \cos\left(\frac{\pi}{h}C\right) \tag{4.6.35}$$

or, subtracting the linear contribution:

$$\mathcal{G}^{(0)}_{|b,C\rangle}(l) = \mathcal{G}^{(0)}(l) T_b\left(i\frac{\pi}{h}C\right) \,. \tag{4.6.36}$$

Exact relations between $g$- and T- functions in various situations where the bulk remains critical were observed in [107, 49, 108]. These were extended off-criticality to a relation between the $\mathcal{G}$- and $T$- function of the Lee-Yang model in [79]. The generalisation of [79] proposed here relies on the specific forms of the one-parameter families of reflection factors in section 4.4, and so provides some further motivation for their introduction.

It is sometimes helpful to have an alternative representation for the infinite sum $\Sigma(l)$ in (4.6.1), the piece of the $g$-function which does not depend on the specific boundary condition. It can be checked that, for values of $l$ such that the sum converges,

$$\Sigma(l) = \sum_{n=1}^{\infty} \frac{1}{n} \mathrm{Tr} K^n - \sum_{n=1}^{\infty} \frac{1}{2n} \mathrm{Tr} H^n \tag{4.6.37}$$

where

$$K_{ab}(\theta,\theta') = \frac{1}{2}\frac{1}{\sqrt{1+e^{\epsilon_a(\theta)}}}\Big(\phi_{ab}(\theta+\theta') + \phi_{ab}(\theta-\theta')\Big)\frac{1}{\sqrt{1+e^{\epsilon_b(\theta')}}} \tag{4.6.38}$$

and

$$H_{ab}(\theta,\theta') = \frac{1}{\sqrt{1+e^{\epsilon_a(\theta)}}}\phi_{ab}(\theta-\theta')\frac{1}{\sqrt{1+e^{\epsilon_b(\theta')}}} \,. \tag{4.6.39}$$

The identity

$$\ln \mathrm{Det}(I-M) = \mathrm{Tr}\ln(I-M) = -\sum_{n=1}^{\infty}\frac{1}{n}\mathrm{Tr} M^n \tag{4.6.40}$$

then allows $\Sigma(l)$ to be rewritten as

$$\Sigma(l) = \frac{1}{2}\ln \mathrm{Det}\Big(\frac{I-H}{(I-K)^2}\Big) \,. \tag{4.6.41}$$

This formula makes sense even when the original sum diverges, a fact that will be used in the next section.

## 4.7 UV values of the $g$-function

Taking into account the effect of vacuum degeneracies described above, a first test of the reflection factors found earlier is to calculate the $l \to 0$ limit of (4.6.1). The value of $g_{|\alpha\rangle}(0)$ should match the value of a conformal field theory $g$-function, either of a Cardy state or of a superposition of such states.

As $l \to 0$, the pseudoenergies $\epsilon_a(\theta)$ tend to constants, which are denoted here by $\epsilon_a$. Their values were tabulated by Klassen and Melzer in [32], who also observed an elegant formula for the integrals of the logarithmic derivatives of the bulk S-matrix elements, later proven in [86]:

$$\int_{\mathbb{R}} d\theta\, \phi_{ab}(\theta) = -\mathcal{N}_{ab}\,, \tag{4.7.1}$$

where $\mathcal{N}_{ab}$ is related to the Cartan matrix $\mathcal{C}$ of the associated Lie algebra by $\mathcal{N} = 2\mathcal{C}^{-1} - 1$.[¶] The integrals of the logarithmic derivatives of the reflection factors are also needed. Writing

$$R_a = \prod_{x \in A}(x) \tag{4.7.2}$$

for some set $A$, the required integrals are

$$\int_{\mathbb{R}} d\theta\, \phi_a^{|\alpha\rangle}(\theta) = -2\sum_{x \in A}\left(1 - \frac{x}{h}\right)\,\mathrm{sign}[x/h] \tag{4.7.3}$$

with $\mathrm{sign}[0] = 0$. For the minimal ADE reflection factors found in section 4.3 these evaluate to

$$\int_{\mathbb{R}} d\theta\, \phi_a^{|\alpha\rangle}(\theta) = 1 - \mathcal{N}_{aa}\,, \tag{4.7.4}$$

while for the $T_r$ reflection factors (4.5.4),

$$\int_{\mathbb{R}} d\theta\, \phi_a^{|\alpha\rangle}(\theta) = -2\mathcal{N}_{aa}\,. \tag{4.7.5}$$

To calculate the UV limit of $\Sigma(l)$, define a matrix $\mathcal{M}$ whose elements are

$$\mathcal{M}_{ab} = -\frac{\mathcal{N}_{ab}}{1 + e^{\epsilon_a}}\,, \tag{4.7.6}$$

[¶]The Cartan matrix for $T_r$ is taken to be $\begin{pmatrix} 2 & -1 & & & \\ -1 & 2 & -1 & & \\ & & \ddots & & \\ & & & 2 & -1 \\ & & & -1 & 1 \end{pmatrix}$

in terms of which

$$\Sigma(0) = \frac{1}{4}\sum_{n=1}^{\infty}\frac{1}{n}(e_1^n + \ldots + e_r^n) = -\frac{1}{4}\ln\left((1-e_1)\ldots(1-e_r)\right) \tag{4.7.7}$$

where $e_1, \ldots, e_r$ are the eigenvalues of $\mathcal{M}$. When one of these eigenvalues is larger than 1, the infinite sum does not converge (this is the case for $A_r$, $r \geq 5$, $D_r$, $r \geq 4$ and $E_r$) but the RHS of (4.7.7) gives the correct analytic continuation, since it follows from (4.6.41).

### 4.7.1 $T_r$

Begin with the $T_r$ theories, whose UV limits are the non-unitary minimal models $\mathcal{M}_{2,2r+3}$. There are $r+1$ 'pure' conformal boundary conditions, and the corresponding values of the conformal $g$-functions can be found using the formula

$$g_{(1,1+d)} = \frac{\mathcal{S}_{(1,1+r);(1,1+d)}}{|\mathcal{S}_{(1,1+r),(1,1)}|^{1/2}} \quad , \quad d = 0, \ldots, r \tag{4.7.8}$$

where $(1, 1+r)$ is the ground state of the bulk theory, with lowest conformal weight, $(1,1)$ is the 'conformal vacuum' – with conformal weight 0 – and $\mathcal{S}$ is the modular S-matrix. Recall from section 2.2.2 that the components of $\mathcal{S}$ for a general minimal model $\mathcal{M}_{p'p}$ are

$$\mathcal{S}_{(n,m);(\rho,\sigma)} = 2\sqrt{\frac{2}{pp'}}(-1)^{1+m\rho+n\sigma}\sin\left(\pi\frac{p}{p'}n\rho\right)\sin\left(\pi\frac{p'}{p}m\sigma\right) \ , \tag{4.7.9}$$

where $1 \leq n, \rho \leq p'-1$, $1 \leq m, \sigma \leq p-1$ and, to avoid double-counting, $m < \frac{p}{p'}n$ and $\rho < \frac{p}{p'}\sigma$. For the $T_r$ theories, $p' = 2$ and $p = 2r+3$, and so $n$ and $\rho$ are both equal to 1 while $m$ and $\sigma$ range from 1 to $r+1$, as in (4.7.8).

The values predicted by (4.7.8) should be compared with the values of $g_{|\alpha\rangle}(0)$ calculated from (4.6.1). For the boundary-parameter-independent part of the reflection factor from (4.5.4), which is the $d = 0$ case of the 'quantum group reduced' options (4.5.12), the second term of (4.6.1) evaluates to

$$\begin{aligned}
&\frac{1}{4}\sum_{a=1}^{r}\int_{\mathbb{R}} d\theta\left(\phi_a^{|\alpha\rangle}(\theta) - \delta(\theta) - 2\phi_{aa}(2\theta)\right)\ln\left(1+e^{-\epsilon_a}\right) \\
&\qquad = -\frac{1}{2}\sum_{a=1}^{r} a\ln\left(1+\frac{\sin^2\left(\frac{\pi}{2r+3}\right)}{\sin\left(\frac{a\pi}{2r+3}\right)\sin\left(\frac{(a+2)\pi}{2r+3}\right)}\right) \\
&\qquad = \ln\left(\frac{\sin\left(\frac{\pi}{2r+3}\right)\sin^r\left(\frac{(r+2)\pi}{2r+3}\right)}{\sin^{r+1}\left(\frac{(r+1)\pi}{2r+3}\right)}\right) ,
\end{aligned} \tag{4.7.10}$$

while $\Sigma(0)$, calculated using (4.7.7), is

$$-\frac{1}{4}\ln\left((1-e_1)\dots(1-e_r)\right) = \frac{1}{2}\ln\left(\frac{2}{\sqrt{2r+3}}\sin\left(\frac{(r+1)\pi}{2r+3}\right)\right) . \tag{4.7.11}$$

Adding these terms together and using some simple trigonometric identities reveals a dramatic simplification:

$$g(l)|_{l=0} = \left(\frac{2}{\sqrt{2r+3}}\sin\left(\frac{\pi}{2r+3}\right)\right)^{\frac{1}{2}} = g_{(1,1)} \tag{4.7.12}$$

for all $r$. This suggests that the minimal $T_r$ reflection factors (4.5.5) describe bulk perturbations of the boundary conformal field theory with $(1,1)$ boundary conditions. Notice that among all of the possible conformal boundary conditions in the unperturbed theory, this is the only one with no relevant boundary operators, matching the fact that the minimal reflection factors (4.5.5) have no free parameters.

### 4.7.2 $A_r$, $D_r$ and $E_r$

The ADE cases exhibit an interestingly uniform structure: substituting (4.7.1) and (4.7.4) into (4.6.1) shows that the UV limit of the second, reflection-factor-dependent, term of (4.6.1) is always zero when the minimal reflection factors from section 4.3 are used. This result can be confirmed by examining the contributions of the blocks $(x)$ of $S(2\theta)$, and $\langle x\rangle$ (or $\langle\widetilde{x}\rangle$) of $R^{|\alpha\rangle}(\theta)$, as follows. Since the bulk S-matrix can be written as

$$S_{ab}(\theta) = \prod_{x\in A_{ab}} \{x\}(\theta) \tag{4.7.13}$$

where $\{x\} = (x+1)(x-1)$, $S_{ab}(2\theta)$ can be written similarly:

$$S_{ab}(2\theta) = \prod_{x\in A_{ab}} [x](\theta) \tag{4.7.14}$$

where

$$[x] = \left(\frac{x+1}{2}\right)\left(\frac{x-1}{2}\right)\left(\frac{2h-x+1}{2}\right)^{-1}\left(\frac{2h-x-1}{2}\right)^{-1} . \tag{4.7.15}$$

Summing the contributions of each block $[x]$, it is easily seen that

$$2\int_{\mathbb{R}} d\theta\, \phi_{aa}(2\theta) = \sum_{x\in A_{aa}}\left(\frac{2x}{h} + \delta_{x,1} - 2\right) . \tag{4.7.16}$$

The minimal reflection factors discussed in section 4.3 can be written in a similar way:

$$R_a = \prod_{x \in A_{aa}} f_x \tag{4.7.17}$$

where each $f_x$ is either $\langle x \rangle$ or $\langle \widetilde{x} \rangle$. The contribution to $\int d\theta\, \phi_a^{|\alpha\rangle}(\theta)$ from each $\langle x \rangle$ is $-2 + 2x/h + 2\delta_{x,1}$ and from each $\langle \widetilde{x} \rangle$ is $-2 + 2x/h$. Noting that every minimal reflection factor contains the block $\langle 1 \rangle$ exactly once, this integral can be written as

$$\int_{\mathbb{R}} d\theta\, \phi_a^{|\alpha\rangle}(\theta) = \sum_{x \in A_{aa}} \left( \frac{2x}{h} + 2\delta_{x,1} - 2 \right), \tag{4.7.18}$$

and so

$$\int_{\mathbb{R}} d\theta \left( \phi_a^{|\alpha\rangle}(\theta) - \delta(\theta) - 2\phi_{aa}(2\theta) \right) = 0 \tag{4.7.19}$$

for every A, D and E theory, as claimed. Working backwards, this gives a general proof of the formula (4.7.4), given (4.7.1).

With the reflection-factor-dependent term giving zero, the sum of $\Sigma(0)$ and the symmetry factor should correspond to a conformal $g$-function value. To find these values in a uniform way, the diagonal coset description $\widehat{\mathfrak{g}}_1 \times \widehat{\mathfrak{g}}_1 / \widehat{\mathfrak{g}}_2$ will be employed, where $\widehat{\mathfrak{g}}_l$ is the affine Lie algebra at level $l$ associated to one of the A, D or E Lie algebras [109]. Recall that coset fields are specified by triples $\{\widehat{\boldsymbol{\mu}}, \widehat{\boldsymbol{\nu}}; \widehat{\boldsymbol{\rho}}\}$ of $\widehat{\mathfrak{g}}$ weights at levels 1, 1 and 2, and the $g$-function for the corresponding conformal boundary condition can be written in terms of the modular S-matrix of the coset model $\mathcal{S}_{\{\mathbf{0},\mathbf{0};\mathbf{0}\}\{\widehat{\boldsymbol{\mu}},\widehat{\boldsymbol{\nu}};\widehat{\boldsymbol{\rho}}\}}$ as

$$g_{\{\widehat{\boldsymbol{\mu}},\widehat{\boldsymbol{\nu}};\widehat{\boldsymbol{\rho}}\}} = \frac{\mathcal{S}_{\{\mathbf{0},\mathbf{0};\mathbf{0}\}\{\widehat{\boldsymbol{\mu}},\widehat{\boldsymbol{\nu}};\widehat{\boldsymbol{\rho}}\}}}{\sqrt{\mathcal{S}_{\{\mathbf{0},\mathbf{0};\mathbf{0}\}\{\mathbf{0},\mathbf{0};\mathbf{0}\}}}}. \tag{4.7.20}$$

Once the level $l$ has been specified, the representation of $\widehat{\mathfrak{g}}_l$ is completely determined by the Dynkin labels of the corresponding representation of $\mathfrak{g}$. For example, the label $\mathbf{0}$ is given to the vacuum representation, where $n_i = 0$, $i = 1, \ldots, r_{\mathfrak{g}}$ for both $\widehat{\mathfrak{g}}_1$ and $\widehat{\mathfrak{g}}_2$.

For the level 1 representations of simply laced affine Lie algebras, the characters have a particularly simple form [110, 111]:

$$\chi_{\widehat{\boldsymbol{\mu}}}(q) = \frac{1}{\eta^{r_{\mathfrak{g}}}(q)} \theta_{\widehat{\boldsymbol{\mu}}}(q) \tag{4.7.21}$$

where $q = \exp(2\pi i\tau)$ and the generalised $\theta$ and Dedekind $\eta$ functions are

$$\theta_{\widehat{\boldsymbol{\mu}}}(q) = \sum_{\boldsymbol{\mu}\in Q} q^{\frac{1}{2}(\boldsymbol{\mu},\boldsymbol{\mu})} \tag{4.7.22}$$

$$\eta(q) = q^{\frac{1}{24}} \prod_{n=1}^{\infty}(1-q^n). \tag{4.7.23}$$

Under the modular transformation $\tau \to -\frac{1}{\tau}$ the theta function transforms as

$$\theta_{\widehat{\boldsymbol{\mu}}} \to (-i\tau)^{r_{\mathfrak{g}}/2} \frac{1}{\sqrt{|P/Q|}} \sum_{\boldsymbol{\nu}\in P/Q} e^{-2\pi i(\boldsymbol{\nu},\,\boldsymbol{\mu})}\theta_{\widehat{\boldsymbol{\nu}}} \tag{4.7.24}$$

where $P$ and $Q$ are the weight lattice and root lattice respectively [111, 93], and the $\eta$ function becomes

$$\eta(-\frac{1}{\tau}) = (-i\tau)^{\frac{1}{2}}\eta(\tau). \tag{4.7.25}$$

The modular $\mathcal{S}$-matrix for level 1 is therefore

$$\mathcal{S}^{(1)}_{\widehat{\boldsymbol{\mu}}\widehat{\boldsymbol{\nu}}} = \frac{1}{\sqrt{|P/Q|}} e^{-2\pi i(\boldsymbol{\nu},\boldsymbol{\mu})}. \tag{4.7.26}$$

For the coset description of the $g$-function, (4.7.20), one needs to compute $\mathcal{S}^{(1)}_{\mathbf{0}\widehat{\boldsymbol{\mu}}}$ which is simply

$$\mathcal{S}^{(1)}_{\mathbf{0}\widehat{\boldsymbol{\mu}}} = \frac{1}{\sqrt{|P/Q|}}. \tag{4.7.27}$$

It is important to note that $P/Q$ is isomorphic to the centre of the group under consideration [112, 97]. The group of field identifications of the coset is also isomorphic to the centre of this group so consequently (4.7.27) becomes

$$\mathcal{S}^{(1)}_{\mathbf{0}\widehat{\boldsymbol{\mu}}} = \frac{1}{\sqrt{N}} \quad , \quad \text{for all } \widehat{\boldsymbol{\mu}}. \tag{4.7.28}$$

The $g$-function can now be written in terms of the level 2 modular $\mathcal{S}$ matrices only:

$$g_{\{\widehat{\boldsymbol{\mu}},\widehat{\boldsymbol{\nu}},\widehat{\boldsymbol{\rho}}\}} = g_{\widehat{\boldsymbol{\rho}}} = \frac{\mathcal{S}^{(2)}_{\mathbf{0}\widehat{\boldsymbol{\rho}}}}{\sqrt{\mathcal{S}^{(2)}_{\mathbf{00}}}}. \tag{4.7.29}$$

As is clear from (4.7.29), identifying the conformal $g$-function value will only pin down the level 2 representation. For $E_8$, since there is only one possible level 1 representation (with Dynkin labels $n_i = 0$, $i = 1, \ldots, 8$), by specifying the level 2 representation the coset field is fixed. However, for other cases, although the coset selection and identification rules (4.2.81),(4.2.85) do constrain the possible coset representations there is still some ambiguity left, in general. For example, for the $A_r$

cases the selection and identification rules are quite simple and the possible cosets, given a fixed level 2 weight, are shown in table 4.4. The notation is as follows: $\widehat{\boldsymbol{\mu}}_j$, $\widehat{\boldsymbol{\nu}}_j$ are level 1 weights and $\widehat{\boldsymbol{\rho}}_j$ is the level 2 weight with Dynkin labels $n_i = 1$ for $i = j$ and $n_i = 0$, $i = 1, \ldots, r$ otherwise. The labels $\widehat{\boldsymbol{\mu}}_0$, $\widehat{\boldsymbol{\nu}}_0$ and $\widehat{\boldsymbol{\rho}}_0$ now represent $\mathbf{0}$ with Dynkin labels $n_i = 0$, $i = 1, \ldots, r$.

| Fixed level 2 weight $\widehat{\boldsymbol{\rho}}$ | Level 1 weight $\widehat{\boldsymbol{\mu}}$ | Level 1 weight $\widehat{\boldsymbol{\nu}}$ | Number of coset fields $\{\widehat{\boldsymbol{\mu}}, \widehat{\boldsymbol{\nu}}; \widehat{\boldsymbol{\rho}}\}$ |
|---|---|---|---|
| $\mathbf{0}$ | $\mathbf{0}$<br>$\widehat{\boldsymbol{\mu}}_i$ | $\mathbf{0}$<br>$\widehat{\boldsymbol{\nu}}_{r+1-i}$, $i = 1, \ldots r$ | $r+1$ |
| $\widehat{\boldsymbol{\rho}}_j$<br>$j = 1, \ldots [(r+1)/2]$ | $\widehat{\boldsymbol{\mu}}_i$<br>$\widehat{\boldsymbol{\mu}}_{j+k}$ | $\widehat{\boldsymbol{\nu}}_{j-i}$, $i = 0, \ldots j$<br>$\widehat{\boldsymbol{\nu}}_{r+1-k}$, $k = 1, \ldots r-j$ | $r+1$ |

Table 4.4: $A_r$ coset fields, indicating the number of distinct fields for each level 2 weight; in the first column, $[x]$ denotes the integer part of $x$

The coset fields for the $A_2$ (three-state Potts model) and $E_7$ (tricritical Ising model) cases, along with the corresponding boundary condition labels from [113] and [114] respectively, are given in tables 4.5 and 4.6 as concrete examples.

It is useful to note that for the $A_r$, $D_r$, $E_6$ and $E_7$ models, $\mathcal{S}_{\mathbf{00}} = \mathcal{S}_{\mathbf{0}\widehat{\boldsymbol{\rho}}}$ only when $\widehat{\boldsymbol{\rho}} = A\mathbf{0}$ for some $A \in O(\widehat{\mathfrak{g}})$ [115] and for each such $\boldsymbol{\rho}$ there is a unique coset field, so the number of fields with $g$-function equal to $g_{\{\widehat{\boldsymbol{\mu}},\widehat{\boldsymbol{\nu}},\mathbf{0}\}}$ is equal to the size of the orbit of $\mathbf{0}$. On the other hand, $E_8$ has no diagram symmetry, but it is also exceptional in that $\mathcal{S}_{\mathbf{00}} = \mathcal{S}_{\mathbf{0}\widehat{\boldsymbol{\rho}}_2}$ where $\widehat{\boldsymbol{\rho}}_2$ has Dynkin labels $n_2 = 1$, all other $n_i = 0$. Physically, this is to be expected as the two fields correspond to the two fixed boundary conditions $(-)$ and $(+)$, which clearly must have equal $g$-function values. (This exceptional equality is discussed from a more mathematical perspective in, for example, [115].)

From (4.2.82) it is clear that $\mathcal{S}_{\mathbf{0}(A\widehat{\boldsymbol{\rho}})} = \mathcal{S}_{\mathbf{0}\widehat{\boldsymbol{\rho}}}$ is also true for $\widehat{\boldsymbol{\rho}} \neq \mathbf{0}$. For the $A$ and $E$ models at level 2, these are found to be the only cases where $\mathcal{S}_{\mathbf{0}\widehat{\boldsymbol{\rho}}_i} = \mathcal{S}_{\mathbf{0}\widehat{\boldsymbol{\rho}}_j}$; for the $D_r$ models there is more degeneracy.

The modular $\mathcal{S}$ matrices, $\mathcal{S}_{\mathbf{0}\widehat{\boldsymbol{\rho}}}$ can be calculated with (4.2.46), alternatively, algorithms for computing these matrices are given by Gannon in [116]; Schellekens

| $A_2$ | | |
|---|---|---|
| Coset field | Boundary label from [113] | Level 2 weight label from table 4.7 |
| $\{[1,0,0],[1,0,0];[2,0,0]\}$<br>$\{[0,0,1],[0,1,0];[2,0,0]\}$<br>$\{[0,1,0],[0,0,1];[2,0,0]\}$ | $A$<br>$B$<br>$C$ | $\mathbf{0}$ |
| $\{[1,0,0],[0,1,0];[1,1,0]\}$<br>$\{[0,0,1],[0,0,1];[1,1,0]\}$<br>$\{[0,1,0],[1,0,0];[1,1,0]\}$ | $AB$<br>$BC$<br>$AC$ | $\widehat{\boldsymbol{\rho}}_1$ |

Table 4.5: $A_2$ coset fields with the corresponding boundary labels and level 2 weight labels from table 4.7. The weights are given in terms of Dynkin labels $[n_0, n_1, n_2, \ldots]$

has also produced a useful program for their calculation [117]. The level 2 modular S-matrix elements for A, D and E theories needed to calculate the UV values of the $g$-functions using (4.7.29) are given in table 4.7. The representations are labelled by the Dynkin labels, $n_i$, $i = 0, \ldots, r$. The number of coset fields corresponding to each label is equal to the order of the orbit of that level 2 weight, under the outer automorphism group $O(\widehat{\mathfrak{g}})$. Note for $D_r$, $r$ even, the weights $\widehat{\boldsymbol{\rho}}_{r-1}$ and $\widehat{\boldsymbol{\rho}}_r$ are in different orbits, each with order 2, whereas for $r$ odd they are in the same orbit with order 4, so in both cases there are 4 coset fields with the same $g$-function value.

For each coset, the possible CFT values of the $g$-function can now be calculated using (4.7.29) and the modular S-matrix elements given in table 4.7. Working case-by-case, these numbers can be checked against the sums $\ln C_{|\alpha\rangle} + \Sigma(0)$, the UV limits of the off-critical $g$-functions $g(l)$ for the minimal reflection factors described in section 4.3. In every case, they are found to be

$$\ln g(l)|_{l=0} = \ln C_{|\alpha\rangle} + \Sigma(0) = \ln g_{\mathbf{0}} \tag{4.7.30}$$

provided that the symmetry factors $C_{|\alpha\rangle}$ are assigned as in table 4.3. The explicit $g$-function values are given in table 4.8.

For some minimal models, $g_{\mathbf{0}}$ can be compared to the values of the $g$-function

| $E_7$ | | |
|---|---|---|
| Coset field | Boundary label from [114] | Level 2 weight label from table 4.7 |
| $\{[1,0,\ldots,0],[1,0,\ldots,0],[2,0,\ldots,0]\}$<br>$\{[0,1,0,\ldots],[0,1,0,\ldots];[2,0,\ldots,0]\}$ | $(-)$<br>$(+)$ | $\mathbf{0}$ |
| $\{[1,0,\ldots,0],[0,1,0,\ldots];[1,1,0,\ldots,0]\}$ | $(d)$ | $\widehat{\rho}_1$ |
| $\{[1,0,\ldots,0],[1,0,\ldots,0];[0,0,1,0,\ldots]\}$<br>$\{[0,1,0,\ldots],[0,1,0,\ldots];[0,0,1,0,\ldots]\}$ | $(-0)$<br>$(0+)$ | $\widehat{\rho}_2$ |
| $\{[1,0,\ldots,0],[0,1,0,\ldots];[0,0,0,1,0,\ldots]\}$ | $(0)$ | $\widehat{\rho}_3$ |

Table 4.6: $E_7$ coset fields with the corresponding boundary labels and level 2 weight labels from table 4.7. The weights are given in terms of Dynkin labels $[n_0, n_1, n_2, \ldots]$

corresponding to known cases, thereby matching the reflection factors to physical boundary conditions. For the three-state Potts model ($A_2$), the tricritical Ising model ($E_7$) and the Ising model ($E_8$) the corresponding boundary condition is the 'fixed' condition in each case [113, 114, 3]. Note the number of coset fields with $g$-function equal to $g_{\mathbf{0}}$ corresponds to the number of degenerate vacua, and hence to the number of possible 'fixed' boundary conditions for all $A$, $D$ and $E$ models.

## 4.8 Checks in conformal perturbation theory

The off-critical $g$-functions only match boundary conformal field theory values in the far ultraviolet. Moving away from this point one expects a variety of corrections, some of which were analysed using conformal perturbation theory in [79]. The expansion provided by the exact $g$-function result is instead about the infrared, but convergence is sufficiently fast that the first few terms of the UV expansion can be extracted numerically, allowing a comparison with conformal perturbation theory to be made. In [4] this was done for the boundary Lee-Yang model; in this section the more general proposals for the case of the three-state Potts model are tested. In [79], the

| | S-matrix element | Labels |
|---|---|---|
| $A_r$ | $\mathcal{S}^{(2)}_{\mathbf{00}} = \frac{2^{\frac{h+3}{2}}}{(h+2)\sqrt{h}} \sin\left(\frac{\pi}{h+2}\right) \prod_{k=1}^{\left[\frac{h+1}{2}\right]} \sin\left(\frac{k\pi}{h+2}\right)$ | $\mathbf{0}$ : $n_0 = 2$, $n_i = 0$ for $i = 1, \ldots, r$ |
| | $\mathcal{S}^{(2)}_{\mathbf{0}\widehat{\boldsymbol{\rho}}_j} = \frac{2^{\frac{h+3}{2}}}{(h+2)\sqrt{h}} \sin\left(\frac{(j+1)\pi}{h+2}\right) \prod_{k=1}^{\left[\frac{h+1}{2}\right]} \sin\left(\frac{k\pi}{h+2}\right)$ | $\widehat{\boldsymbol{\rho}}_j$ : $n_0 = 1$, $n_i = \begin{cases} 0 & i \neq j \\ 1 & i = j \end{cases}$ for $j = 1, \ldots, [h/2]$, where $[x]$ is the integer part of $x$ and $h$ is the Coxeter number. |
| $D_r$ | $\mathcal{S}^{(2)}_{\mathbf{00}} = \frac{1}{4}\sqrt{\frac{2}{r}}$ | $\mathbf{0}$ : $n_0 = 2$, $n_i = 0$ for $i = 1, \ldots, r$ |
| | $\mathcal{S}^{(2)}_{\mathbf{0}\widehat{\boldsymbol{\rho}}_1} = \mathcal{S}^{(2)}_{\mathbf{0}\widehat{\boldsymbol{\rho}}_j} = 2\mathcal{S}^{(2)}_{\mathbf{00}}$ | $\widehat{\boldsymbol{\rho}}_1$ : $n_0 = n_1 = 1$, all other $n_i = 0$ |
| | | $\widehat{\boldsymbol{\rho}}_j$ : $n_0 = 0$, $n_i = \begin{cases} 0 & i \neq j \\ 1 & i = j \end{cases}$ for $j = 2, \ldots, r/2$ |
| | $\mathcal{S}^{(2)}_{\mathbf{0}\widehat{\boldsymbol{\rho}}_{r-1}} = \mathcal{S}^{(2)}_{\mathbf{0}\widehat{\boldsymbol{\rho}}_r} = \frac{1}{2\sqrt{2}}$ | $\widehat{\boldsymbol{\rho}}_{r-1}$ : $n_0 = n_{r-1} = 1$, all other $n_i = 0$ |
| | | $\widehat{\boldsymbol{\rho}}_r$ : $n_0 = n_r = 1$, all other $n_i = 0$ |
| $E_6$ | $\mathcal{S}^{(2)}_{\mathbf{00}} = \frac{2}{\sqrt{21}} \sin\left(\frac{2\pi}{h+2}\right)$ | $\mathbf{0}$ : $n_0 = 2$, $n_i = 0$ for $i = 1, \bar{1}, 2, 3, \bar{3}, 4$ |
| | $\mathcal{S}^{(2)}_{\mathbf{0}\widehat{\boldsymbol{\rho}}_j} = \frac{2}{\sqrt{21}} \sin\left(\frac{2(4-j)\pi}{h+2}\right)$ for $j = 1, 2$ | $\widehat{\boldsymbol{\rho}}_1$ : $n_0 = 1$, $n_1 = 1$ all other $n_i = 0$ |
| | | $\widehat{\boldsymbol{\rho}}_2$ : $n_0 = 0$, $n_2 = 1$ all other $n_i = 0$ |
| $E_7$ | $\mathcal{S}^{(2)}_{\mathbf{00}} = \frac{2}{\sqrt{h+2}} \sin\left(\frac{4\pi}{h+2}\right)$ | $\mathbf{0}$ : $n_0 = 2$, $n_i = 0$ for $i = 1, \ldots, 7$ |
| | $\mathcal{S}^{(2)}_{\mathbf{0}\widehat{\boldsymbol{\rho}}_1} = 2\sqrt{\frac{2}{h+2}} \sin\left(\frac{8\pi}{h+2}\right)$ | $\widehat{\boldsymbol{\rho}}_1$ : $n_0 = 1$, $n_1 = 1$ all other $n_i = 0$ |
| | $\mathcal{S}^{(2)}_{\mathbf{0}\widehat{\boldsymbol{\rho}}_2} = \frac{2}{\sqrt{h+2}} \sin\left(\frac{8\pi}{h+2}\right)$ | $\widehat{\boldsymbol{\rho}}_2$ : $n_0 = 0$, $n_2 = 1$ all other $n_i = 0$ |
| | $\mathcal{S}^{(2)}_{\mathbf{0}\widehat{\boldsymbol{\rho}}_3} = 2\sqrt{\frac{2}{h+2}} \sin\left(\frac{4\pi}{h+2}\right)$ | $\widehat{\boldsymbol{\rho}}_3$ : $n_0 = 0$, $n_3 = 1$ all other $n_i = 0$ |
| $E_8$ | $\mathcal{S}^{(2)}_{\mathbf{00}} = \mathcal{S}^{(2)}_{\mathbf{0}\widehat{\boldsymbol{\rho}}_2} = \frac{1}{2}$ | $\mathbf{0}$ : $n_0 = 2$, $n_i = 0$, for all $i = 1, \ldots, 8$ |
| | | $\widehat{\boldsymbol{\rho}}_2$ : $n_0 = 0$, $n_2 = 1$, all other $n_i = 0$ |
| | $\mathcal{S}^{(2)}_{\mathbf{0}\widehat{\boldsymbol{\rho}}_1} = \frac{1}{\sqrt{2}}$ | $\widehat{\boldsymbol{\rho}}_1$ : $n_0 = 0$, $n_1 = 1$ all other $n_i = 0$ |

Table 4.7: Level 2 modular S-matrix elements for A, D and E models

| | $C_{\|\alpha\rangle}$ | $g_0$ | Number of fields |
|---|---|---|---|
| $A_r$ | $\frac{1}{\sqrt{r+1}}$ | $\left(\frac{2^{\frac{h+3}{2}}}{(h+2)\sqrt{h}}\sin\left(\frac{\pi}{h+2}\right)\prod_{k=1}^{\left[\frac{h+1}{2}\right]}\sin\left(\frac{k\pi}{h+2}\right)\right)^{1/2}$ | $r+1$ |
| $D_r$ | $\frac{1}{2}$ | $\frac{1}{2}\left(\frac{2}{r}\right)^{1/4}$ | 4 |
| $E_6$ | $\frac{1}{\sqrt{3}}$ | $\left(\frac{2}{\sqrt{21}}\sin\left(\frac{2\pi}{h+2}\right)\right)^{1/2}$ | 3 |
| $E_7$ | $\frac{1}{\sqrt{2}}$ | $\left(\frac{2}{\sqrt{h+2}}\sin\left(\frac{4\pi}{h+2}\right)\right)^{1/2}$ | 2 |
| $E_8$ | 1 | $\frac{1}{\sqrt{2}}$ | 2 |

Table 4.8: UV $g$-function values calculated from the minimal reflection factors for the A, D and E models

treatment of conformal perturbation theory concentrated on the non-unitary Lee-Yang case whereas here a general discussion of the leading bulk-induced correction to the $g$-function in the (simpler to treat) unitary cases will be presented.

Consider a unitary conformal field theory on a circle of circumference $L$, perturbed by a bulk spinless primary field $\varphi$ with scaling dimension $x_\varphi = \Delta_\varphi + \overline{\Delta}_\varphi$. The perturbed Hamiltonian is then

$$H = H_0 + \lambda H_1 \tag{4.8.1}$$

where

$$H_0 = \frac{2\pi}{L}\left(L_0 + \overline{L}_0 - \frac{c}{12}\right) \tag{4.8.2}$$

and

$$H_1 = \left(\frac{L}{2\pi}\right)^{1-x_\varphi}\oint \varphi(e^{i\theta})\,d\theta\,. \tag{4.8.3}$$

For $\lambda$ real in the ADE models a $\lambda$–$M$ relation of the form

$$M(\lambda) = \kappa|\lambda|^{1/(2-x_\varphi)} \quad ; \qquad |\lambda(M)| = \left(\frac{M}{\kappa}\right)^{2-x_\varphi} \tag{4.8.4}$$

is also expected, with $\kappa$ a model-dependent constant.

Leaving the boundary unperturbed, there is a conformal boundary condition $\alpha$, with boundary state $|\alpha\rangle$. Set $g_{|\alpha\rangle} \equiv g^0_{|\alpha\rangle} = \langle\alpha|0\rangle$ and $g^\varphi_{|\alpha\rangle} = \langle\alpha|\varphi\rangle$, where $|0\rangle$ and $|\varphi\rangle$ are the states corresponding to the fields 1 and $\varphi$. Since the theory is unitary, $|0\rangle$ is also the unperturbed ground state; and since $\varphi$ is primary, $\langle 0|\varphi|0\rangle = 0$.

The aim is to calculate $\ln\mathcal{G}_{|\alpha\rangle}(\lambda, L) = \ln\langle\alpha|\Omega\rangle$ where $|\alpha\rangle$ is the unperturbed CFT boundary state, and $|\Omega\rangle$ is the PCFT vacuum. This will be a power series in the

dimensionless quantity $\lambda L^{2-x_\varphi}$; here, the coefficient of the linear term, $d_1^{|\alpha\rangle}$, will be found. The calculation follows [79], but is a little different (and in fact simpler) because the theory is unitary, so that the ground state is the conformal vacuum $|0\rangle$.

First-order perturbation theory implies

$$|\Omega\rangle = |0\rangle + \lambda {\sum_a}' \Omega_a |\psi_a\rangle + \dots \tag{4.8.5}$$

where the sum is over all states excluding $|0\rangle$, $\langle\psi_a|0\rangle = 0$ and

$$\Omega_a = \frac{\langle\psi_a|H_1|0\rangle}{\langle 0|H_0|0\rangle - \langle\psi_a|H_0|\psi_a\rangle} \,. \tag{4.8.6}$$

Since the theory is unitary, $\langle 0|H_0|0\rangle - \langle\psi_a|H_0|\psi_a\rangle = -\langle\psi_a|\frac{2\pi}{L}(L_0 + \overline{L}_0)|\psi_a\rangle$. Using rotational invariance as well,

$$\lambda {\sum_a}' \Omega_a |\psi_a\rangle = -\frac{\lambda L^{2-x_\varphi}}{(2\pi)^{1-x_\varphi}} {\sum_a}' \frac{|\psi_a\rangle\langle\psi_a|\varphi(1)|0\rangle}{\langle\psi_a|L_0+\overline{L}_0|\psi_a\rangle} \,. \tag{4.8.7}$$

Hence

$$|\Omega\rangle = |0\rangle - \frac{\lambda L^{2-x_\varphi}}{(2\pi)^{1-x_\varphi}} (1-P)\frac{1}{L_0+\overline{L}_0}(1-P)\varphi(1)|0\rangle + \dots \tag{4.8.8}$$

where $P = |0\rangle\langle 0|$ is the projector onto the ground state. Using the formula $\frac{1}{L_0+\overline{L}_0} = \int_0^1 q^{L_0+\overline{L}_0-1}\, dq$,

$$\langle\alpha|\Omega\rangle = \langle\alpha|0\rangle - \frac{\lambda L^{2-x_\varphi}}{(2\pi)^{1-x_\varphi}}\langle\alpha|\,(1-P)\int_0^1 \frac{dq}{q}\, q^{L_0+\overline{L}_0}(1-P)\varphi(1)|0\rangle + \dots \tag{4.8.9}$$

Since $\langle 0|\varphi|0\rangle = 0$ and $q^{L_0+\overline{L}_0}\varphi(1)|0\rangle = q^{L_0+\overline{L}_0}\varphi(1)q^{-L_0-\overline{L}_0}|0\rangle = q^{x_\varphi}|0\rangle$ this last expression simplifies to

$$\langle\alpha|\Omega\rangle = \langle\alpha|0\rangle - \frac{\lambda L^{2-x_\varphi}}{(2\pi)^{1-x_\varphi}}\int_0^1 dq\, q^{x_\varphi-1}\langle\alpha|\varphi(q)|0\rangle + \dots \tag{4.8.10}$$

Now $\langle\alpha|\varphi(q)|0\rangle$ is a disc amplitude, and by Möbius invariance it is given by

$$\langle\alpha|\varphi(q)|0\rangle = g^{\varphi}_{|\alpha\rangle}\,(1-q^2)^{-x_\varphi} \,. \tag{4.8.11}$$

(This is a significant simplification over the nonunitary case discussed in [79], where the corresponding amplitude had to be expressed in terms of hypergeometric functions.)

Taking logarithms,

$$\begin{aligned} \ln \mathcal{G}_{|\alpha\rangle}(\lambda, L) &= \ln g_{|\alpha\rangle} - \frac{\lambda L^{2-x_\varphi}}{(2\pi)^{1-x_\varphi}}\frac{g^{\varphi}_{|\alpha\rangle}}{g_{|\alpha\rangle}}\int_0^1 dq\, q^{x_\varphi-1}(1-q^2)^{-x_\varphi} + \dots \\ &= \ln g_{|\alpha\rangle} + d_1^{|\alpha\rangle} L^{2-x_\varphi} + \dots \end{aligned} \tag{4.8.12}$$

and doing the integral,

$$d_1^{|\alpha\rangle} = -\frac{1}{2(2\pi)^{1-x_\varphi}} \frac{g^{\varphi}_{|\alpha\rangle}}{g_{|\alpha\rangle}} \, \mathrm{B}(1-x_\varphi, x_\varphi/2) \tag{4.8.13}$$

where $\mathrm{B}(x,y) = \Gamma(x)\Gamma(y)/\Gamma(x+y)$ is the Euler beta function.

This is a general result. As a non-trivial check, specialise to the 3-state Potts model, described by the $A_2$ scattering theory. There are three possible values A, B and C of the microscopic spin variable, related by an $S_3$ symmetry. At criticality the model corresponds to a $c = 4/5$ conformal field theory. The primary fields are the identity $I$, a doublet of fields $\{\psi, \psi^\dagger\}$ of dimensions $\Delta_\psi = \overline{\Delta}_\psi = 2/3$, the energy operator $\varepsilon$ of dimensions $\Delta_\varepsilon = \overline{\Delta}_\varepsilon = 2/5$ and a second doublet of fields $\{\sigma, \sigma^\dagger\}$ with dimensions $\Delta_\sigma = \overline{\Delta}_\sigma = 1/15$. The bulk perturbing operator $\varphi$ which leads to the $A_2$ scattering theory is $\varepsilon$, and so $x_\varphi = \Delta_\varepsilon + \overline{\Delta}_\varepsilon = 4/5$. Boundary conditions and states for the unperturbed model are discussed in [68, 113]. One of the three 'fixed' boundary states, say $|A\rangle$, can be written in terms of $W_3$-Ishibashi states as [68]

$$|A\rangle = |\tilde{I}\rangle \equiv K \left[ |\, I \,\rangle\!\rangle + X |\, \varepsilon \,\rangle\!\rangle + |\, \psi \,\rangle\!\rangle + |\, \psi^\dagger \,\rangle\!\rangle + X |\, \sigma \,\rangle\!\rangle + X |\, \sigma^\dagger \,\rangle\!\rangle \right] \tag{4.8.14}$$

where $K^4 = (5-\sqrt{5})/30$ and $X^2 = (1+\sqrt{5})/2$. Hence

$$\ln g_{|A\rangle} = \ln K = -0.5961357674\ldots, \quad g^{\varphi}_{|A\rangle}/g_{|A\rangle} = X = 1.2720196495\ldots \tag{4.8.15}$$

Putting everything into (4.8.13), the CPT prediction for the coefficient of the first perturbative correction to the $g$-function for fixed boundary conditions in the three-state Potts model is

$$d_1^{|A\rangle} = -3.011357884\ldots \tag{4.8.16}$$

The 3-state Potts model also admits 'mixed' boundary conditions AB, BC and CA [118]. For later use note, from [68], that the corresponding boundary state is

$$|AB\rangle = K \left[ X^2 |\, I \,\rangle\!\rangle - X^{-1} |\, \varepsilon \,\rangle\!\rangle + X^2 |\, \psi \,\rangle\!\rangle + X^2 |\, \psi^\dagger \,\rangle\!\rangle - X^{-1} |\, \sigma \,\rangle\!\rangle - X^{-1} |\, \sigma^\dagger \,\rangle\!\rangle \right] \tag{4.8.17}$$

so that, for the AB boundary, one instead finds

$$d_1^{|AB\rangle} = -\frac{1}{X^4} d_1^{|A\rangle} . \tag{4.8.18}$$

The results (4.8.15) and (4.8.16) can be compared to the numerical evaluation of the exact $g$-function result, written in terms of $\lambda L^{6/5}$ using Fateev's formula [119]

$$\kappa = \frac{3\Gamma(4/3)}{\Gamma^2(2/3)} (2\pi)^{5/6} (\gamma(2/5)\gamma(4/5))^{5/12} = 4.504307863\ldots \tag{4.8.19}$$

where $\gamma(x) = \Gamma(x)/\Gamma(1-x)$. Setting $x = \lambda L^{6/5} = -(l/\kappa)^{6/5}$ (remembering that $(T - T_c) \propto \lambda < 0$) a fit to the numerical data yields

$$\begin{aligned} \ln g(l) &= -0.596135768 - 0.49999991\, l - 3.0113570\, x \\ &\quad - 0.909937\, x^2 + 0.3982\, x^3 + 1.0\, x^4 + \ldots \end{aligned} \tag{4.8.20}$$

which agrees well with (4.8.15) and (4.8.16). The match of the constant term in (4.8.20) with $\ln g_{|A\rangle}$ from (4.8.15) is guaranteed by the exact formula, and so serves as a check on the accuracy of our numerics. A calculation of the coefficient of the irregular (in $x$) term, proportional to $l$, as in [79], predicts the value 0.5, again in good agreement with the numerical results here.

## 4.9 One-parameter families and RG flows

Just as the minimal reflection factors were tested in section 4.7, the same can now be done with the one-parameter families of reflection factors. These reflection factors, $R_a^{|d,C\rangle}$, depend on the parameter $C$ and are given in (4.4.6) and (4.4.10).

### 4.9.1 The ultraviolet limit

If the parameter dependent reflection factors are used as input to calculate the $g$-function, (4.6.1), and the limit $l \to 0$ is taken then

$$g^{|d\rangle} \equiv g_{|d,C\rangle}(l)|_{l=0} = g_0\, T_d\ , \tag{4.9.1}$$

where $T_d = T_d(\theta)|_{l=0}$ is a $\theta$-independent constant. From (4.6.28) and (4.6.26)

$$T_d = \sqrt{1 + e^{\epsilon_d}} \tag{4.9.2}$$

where the $\epsilon_d$ values can be found in [32]. For every ADET theory, (4.9.1) leads to a possible CFT $g$-function value.

For $M > 0$ there will be many massive bulk flows as the parameter $C$ is varied. However, it should be possible to tune $C$, as the limit $l \to 0$ is taken, so as to give a massless boundary flow between the conformal $g$-function $g^{|d\rangle}$, corresponding to the UV limit of the reflection factor $R_a^{|d,C\rangle}$, and $g$, corresponding to the UV limit of the minimal reflection factor. These flows are depicted in figure 4.5. Note that the UV

$g$-function corresponding to the minimal reflection factors ($g_0$ for the ADE cases and $g_{(1,1)}$ for $T_r$) is the smallest conformal value in all cases so, by Affleck and Ludwig's $g$-theorem [3][71], this is a stable fixed point of the boundary RG flow.

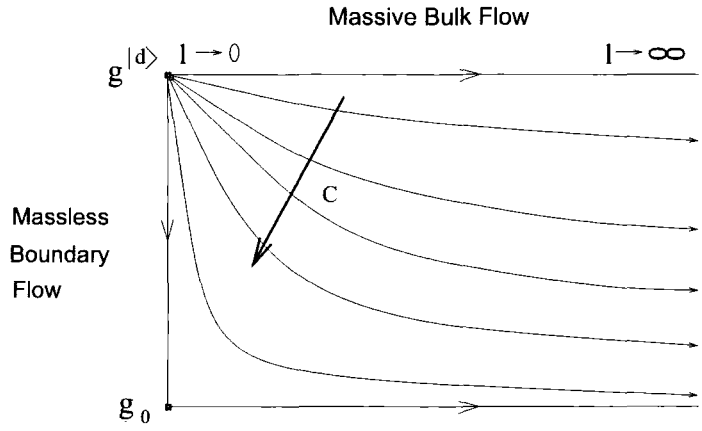


Figure 4.5: The expected RG flow pattern

For the $T_r$ case

$$g^{|d\rangle} = g_{(1,d+1)} \quad \text{for} \quad d = 1, \ldots, r. \tag{4.9.3}$$

This is consistent with a simple pattern of flows

$$(1, d{+}1) \to (1, 1) \quad \text{for} \quad d = 1, \ldots, r. \tag{4.9.4}$$

The conformal values corresponding to the UV limits of $g^{|d\rangle}$ for the A, D and E cases are given in tables 4.9 and 4.10. Again the boundary flows

$$g^{|d\rangle} \to g_0 \tag{4.9.5}$$

are expected in each case. Notice that in many cases the UV $g$-function values are sums of 'simple' CFT values, corresponding to flows from superpositions of Cardy boundary conditions, driven by boundary-changing operators.

The conjectured flow for the three-state Potts model ($A_2$), $g_{\widehat{\rho}_1} \to g_0$, corresponds to the 'mixed–to–fixed' flow ($AB \to A$) found by Affleck, Oshikawa and Saleur [113], and by Fredenhagen [120].

Similarly, the flow $g_{\widehat{\rho}_1} \to g_0$ in the tricritical Ising model ($E_7$) corresponds to the 'degenerate–to–fixed' ($(d) \to (-)$ or $(d) \to (+)$) flows of [121, 120]. Notice that $g_0 + g_{\widehat{\rho}_2} \to g_0$ in $E_7$ matches the CFT $g$ values for the flow $(-) \oplus (0+) \to (-)$ conjectured in [120]. However this latter flow is driven by the boundary field with

| $A_r$ | $D_r$ |
|---|---|
| $g^{\|1\rangle} = g^{\|r\rangle} = g_{\widehat{\rho}_1}$<br>$g^{\|2\rangle} = g^{\|r-1\rangle} = g_{\widehat{\rho}_2}$<br>$\vdots$<br>$g^{\|r/2\rangle} = g^{\|r/2+1\rangle} = g_{\widehat{\rho}_{r/2}}$ for $r$ even<br>$g^{\|h/2\rangle} = g_{\widehat{\rho}_{h/2}}$ for $r$ odd | $g^{\|i\rangle} = (i+1)g_0$ for $i = 1, \ldots, r-2$<br>$g^{\|r-1\rangle} = g^{\|r\rangle} = g_{\widehat{\rho}_{r-1}} = g_{\widehat{\rho}_r}$ |

Table 4.9: UV $g$-function values for A and D models

| | $E_6$ | | $E_7$ | $E_8$ |
|---|---|---|---|---|
| $g^{\|1\rangle}$ | $g^{\|\overline{1}\rangle}$ | $g_{\widehat{\rho}_1}$ | $g_{\widehat{\rho}_1}$ | $g_0 + g_{\widehat{\rho}_1}$ |
| $g^{\|2\rangle}$ | | $g_0 + g_{\widehat{\rho}_2}$ | $g_0 + g_{\widehat{\rho}_2}$ | $2g_0 + g_{\widehat{\rho}_1}$ |
| $g^{\|3\rangle}$ | $g^{\|\overline{3}\rangle}$ | $g_{\widehat{\rho}_1} + g_{\widehat{\rho}_2}$ | $g_{\widehat{\rho}_1} + g_{\widehat{\rho}_3}$ | $2g_0 + 2g_{\widehat{\rho}_1}$ |
| $g^{\|4\rangle}$ | | $g_0 + g_{\widehat{\rho}_1} + 2g_{\widehat{\rho}_2}$ | $g_0 + 2g_{\widehat{\rho}_2}$ | $3g_0 + 2g_{\widehat{\rho}_1}$ |
| $g^{\|5\rangle}$ | | | $g_0 + 3g_{\widehat{\rho}_2}$ | $5g_0 + 3g_{\widehat{\rho}_1}$ |
| $g^{\|6\rangle}$ | | | $2g_{\widehat{\rho}_1} + 2g_{\widehat{\rho}_3}$ | $5g_0 + 4g_{\widehat{\rho}_1}$ |
| $g^{\|7\rangle}$ | | | $3g_0 + 6g_{\widehat{\rho}_2}$ | $9g_0 + 6g_{\widehat{\rho}_1}$ |
| $g^{\|8\rangle}$ | | | | $16g_0 + 12g_{\widehat{\rho}_1}$ |

Table 4.10: UV $g$-function values for $E_6$, $E_7$ and $E_8$ models

scaling dimension 3/5, which is inappropriate for the $E_7$ coset description. A more careful analysis shows that the flow described here, which is driven by a boundary field with scaling dimension 1/10, must start from either $(+)\oplus(0+)$ or $(-)\oplus(-0)$, and flow to $(+)$ or $(-)$. This serves as a useful reminder that the $g$-function values alone do not pin down a boundary condition, and that this ambiguity can be physically significant in situations involving superpositions of boundaries.

### 4.9.2 On the relationship between the UV and IR parameters

The one-parameter families of boundary scattering theories introduced above should describe simultaneous perturbations of boundary conformal field theories by relevant bulk and boundary operators. The action is

$$\mathcal{A}_{|\alpha\rangle} = \mathcal{A}^{\mathbf{BCFT}}_{|\alpha\rangle} + \mathcal{A}^{\mathbf{BULK}} + \mathcal{A}^{\mathbf{BND}}_{|\alpha\rangle} \tag{4.9.6}$$

where $\mathcal{A}^{\mathbf{BCFT}}_{|\alpha\rangle}$ is the unperturbed boundary CFT action. Suppose that the boundary condition is imposed at $x = 0$; in general it might correspond to a superposition of $N_{|\alpha\rangle}$ Cardy states. Denoting these by $|c\rangle$, $c = 1, 2, \ldots, N_{|\alpha\rangle}$, the boundary is in the state

$$|\alpha\rangle = \sum_{c=1}^{N_{|\alpha\rangle}} n_{|c\rangle} |c\rangle \,, \tag{4.9.7}$$

with $n_{|c\rangle} \in \mathbb{N}$. The bulk perturbing term is

$$\mathcal{A}^{\mathbf{BULK}} = \lambda \int_{-\infty}^{0} dx \int_{-\infty}^{\infty} dy \; \varphi(x, y) \tag{4.9.8}$$

while the boundary perturbing part is

$$\mathcal{A}^{\mathbf{BND}}_{|\alpha\rangle} = \sum_{c,d=1}^{N_{|\alpha\rangle}} \mu_{\langle c|d\rangle} \int_{-\infty}^{\infty} dy \; \phi_{\langle c|d\rangle}(y) \,. \tag{4.9.9}$$

The operators $\phi_{\langle c|c\rangle}$ live on a single Cardy boundary, while the $\phi_{\langle c|d\rangle}$ with $c \neq d$ are boundary changing operators. Since $\phi_{\langle c|d\rangle} = \phi^{\dagger}_{\langle d|c\rangle}$, in a unitary theory one also expects (see for example [122])

$$\mu_{\langle c|d\rangle} = \mu^{*}_{\langle d|c\rangle} \,. \tag{4.9.10}$$

Using periodicity arguments to analyse the behaviour of the ground-state energy on a strip with perturbed boundaries as in [34] and [78] (see also (4.9.15) and (4.9.16)

below), one can argue that the scaling dimensions of the fields $\phi_{\langle c|d\rangle}$ must, in these integrable cases, be half that of the bulk perturbing operator $\varphi$ :

$$x_\phi = \frac{x_\varphi}{2} = \frac{2}{h+2} \tag{4.9.11}$$

for the ADE systems and

$$x_\phi = \frac{x_\varphi}{2} = \frac{2-h}{h+2} \tag{4.9.12}$$

for the $T_r$ models. The results recorded in (4.9.3) and tables 4.9 and 4.10 provide information about the conformal boundary conditions associated with the one-parameter families of reflection factors. For $T_r$ and $A_r$ the boundary is always found to be in a pure Cardy state, while for $D_r$, $E_6$ and $E_7$ this is true only in one case per model, and in the $E_8$-related theories the UV boundary always corresponds to a non-trivial superposition of the states $|\pm\rangle$ and $|\mathbf{free}\rangle$. This observation fits nicely with the conformal field theory results for the Ising model [68]: from (4.9.11) it is clear that for the $E_8$ coset description the integrable boundary perturbation must have dimension $x_\phi = 1/16$, and indeed the only boundary operators with this dimension in the Ising model are $\phi_{\langle\pm|\mathbf{free}\rangle}$ and $\phi_{\langle\mathbf{free}|\pm\rangle}$.

For simplicity, only the cases involving a single Cardy boundary will be discussed here, where

$$\mathcal{A}^{\mathbf{BND}}_{|\alpha\rangle} = \mu \int_{-\infty}^{\infty} dy\ \phi(y)\ . \tag{4.9.13}$$

As in the Ising and Lee-Yang examples of [72, 78], a simple formula is expected to link the couplings $\lambda$ and $\mu$ of bulk and boundary fields to the parameter $C$ in the reflection factors. However, without a precise identification of the operator $\phi$ it is hard to see how such a relation can be determined. Even so, a general argument combined with a numerically-supported conjecture allows the relation formula to be fixed up to a single overall dimensionless constant. This goes as follows. In section 4.6.3 it was shown that in all cases

$$\mathcal{G}^{(0)}_{|d,C\rangle}(l) = \mathcal{G}^{(0)}(l)\, T_d(i\tfrac{\pi}{h}C) \tag{4.9.14}$$

where $T_d$ is the TBA-related T-function, and $\mathcal{G}^{(0)}(l)$ is the CPT $\mathcal{G}$-function corresponding to the minimal reflection factor, for which there is no boundary perturbation. In addition, $T_d(\theta) \equiv T_d(\theta, l)$ is even in $\theta$, $T_d(\theta) = T_d(-\theta)$, and periodic, $T_d(\theta + i\pi\frac{h+2}{h}) = T_d(\theta)$, and so it can be Fourier expanded as

$$T_d(i\tfrac{\pi}{h}C) = c_0(l) + \sum_{k=1}^{\infty} c_k(l) \cos\left(\frac{2\pi k}{h+2}C\right)\ . \tag{4.9.15}$$

The observation of [91], that $T_a(\theta, l)$ admits an expansion with finite domain of convergence in the pair of variables $a_\pm = (le^{\pm\theta})^{\frac{2h}{h+2}}$, can now be used to see that

$$c_0(l) = c_0 + O\left(l^{\frac{4h}{h+2}}\right) \ , \ c_1(l) = c_1 l^{\frac{2h}{h+2}} + O\left(l^{\frac{4h}{h+2}}\right) \ . \tag{4.9.16}$$

The minimal $\mathcal{G}$-function also has an expansion

$$\ln \mathcal{G}^{(0)}(l) = \ln \mathcal{G}^{(0)} + \sum_{k=1}^{\infty} g_k l^{k(2-2x_\phi)} \tag{4.9.17}$$

while the conformal perturbation theory expansion of $\mathcal{G}^{(0)}_{|d,C\rangle}$ has the form (see [79])

$$\ln \mathcal{G}^{(0)}_{|d,C\rangle}(\lambda, \mu, L) = \sum_{m,n=1}^{\infty} c_{mn} (\mu L^{1-x_\phi})^m (\lambda L^{2-2x_\phi})^n . \tag{4.9.18}$$

Comparing (4.9.14) – (4.9.17) with (4.9.18) one can conclude that, so long as $c_{10} \neq 0$, the relationship between $C$ and $\mu$ must have the form

$$\mu = \widehat{\mu}_0 \cos\left(\frac{2\pi}{h+2} C\right) M^{\frac{2h}{h+2}} = \widehat{\mu}_0 \cos\left(\frac{2\pi}{h+2} C\right) M^{1-x_\phi} \tag{4.9.19}$$

where $\widehat{\mu}_0$ is an unknown dimensionless constant. However the result (4.9.19) can only be correct if $1 - x_\phi = 2h/(h+2)$. This is true only in the non-unitary $T_r$ models, and indeed it reproduces the Lee-Yang result of [4] when specialised to $T_1$. For the ADE theories, $1 - x_\phi = h/(h+2)$ so $c_{10}$, the first $\mu$-dependent correction to $\mathcal{G}$, must be zero. (This is not surprising since in a unitary CFT this correction is proportional to $\langle \phi \rangle^{\mathbf{disk}}_{|\alpha\rangle} = 0$.) The first contribution is then at order $O(\mu^2) = O(M^{2-2x_\phi})$, and at this order there is an overlap between the expansions of $T_d(\theta, l)$ and $\mathcal{G}^{(0)}(l)$. This leads to the less-restricted result

$$\mu^2 = \widehat{k}_0 \left(\widehat{z} + \cos\left(\frac{2\pi}{h+2} C\right)\right) M^{\frac{2h}{h+2}} = \widehat{k}_0 \left(\widehat{z} - \cos\left(\frac{2\pi}{h+2} C\right)\right) M^{2-2x_\phi} \tag{4.9.20}$$

where now both $\widehat{k}_0$ and $\widehat{z}$ are unknown constants. Consider now the Ising model, for which the $\mu - C$ formula is known [72]. Written in terms of $C$ it becomes

$$\left(h^{\text{ref[72]}}\right)^2 = \mu^2 = 2M\left(1 + \cos(\tfrac{\pi}{2} C)\right) \Rightarrow \mu = 2\sqrt{M}\cos(\tfrac{\pi}{4} C) \, . \tag{4.9.21}$$

Thus the boundary magnetic field is an even function of $C$. It is then tempting to conjecture that $\widehat{z} = 1$ for all the $g_{|1,C\rangle}$ cases in the $A_r$ models, and, to preserve the

perfect square property, that $\widehat{z}$ is either 1 or $-1$ in all other ADE single boundary condition situations:

$$\widehat{z} = 1 \;:\; \mu = \widehat{\mu}_0 \cos\left(\frac{\pi C}{h+2}\right) M^{1-x_\phi} \leftrightarrow \frac{\mu}{\sqrt{\lambda}} = \widehat{\mu}_0 \kappa^{1-x_\phi} \cos\left(\frac{\pi C}{h+2}\right); \quad (4.9.22)$$

$$\widehat{z} = -1 \;:\; \mu = \widehat{\mu}_0 \sin\left(\frac{\pi C}{h+2}\right) M^{1-x_\phi} \leftrightarrow \frac{\mu}{\sqrt{\lambda}} = \widehat{\mu}_0 \kappa^{1-x_\phi} \sin\left(\frac{\pi C}{h+2}\right). \quad (4.9.23)$$

Return now to the physical picture of flows parametrised by $C$ depicted in figure 4.5. At $\lambda = 0$ the bulk mass is zero, and the only scale in the problem is that induced by the boundary coupling $\mu$. The massless boundary flow down the left-hand edge of the diagram therefore corresponds to varying $|\mu|$ from 0 to $\infty$. If $\lambda$ is instead kept finite and nonzero while $|\mu|$ is sent to infinity, the flow will collapse onto the lower edge of the diagram, flowing from $g_{\mathbf{0}}$ in the UV. For the $g$-function calculations to reproduce this behaviour, the reflection factor should therefore reduce to its minimal version as $|\mu| \to \infty$. For (4.9.22), $|\mu| \to \infty$ corresponds to $C \to i\infty$, which does indeed reduce the reflection factor as required. On the other hand, taking $|\mu| \to \infty$ in (4.9.23), requires $C \to \pi(h+2)/2 + i\infty$. While the reduction is again achieved in the limit, real analyticity of the reflection factors is lost at intermediate values of $\mu$. For this reason option (4.9.22) might be favoured, but more detailed work will be needed to make this a definitive conclusion.

In fact, the proposal (4.9.22) can be checked at $\mu = 0$ in the 3-state Potts model ($h = 3$), as follows. Consider the results (4.8.16) and (4.8.18) and set

$$\delta_1 = -\kappa^{-6/5}\left(d_1^{|AB\rangle} - d_1^{|A\rangle}\right) = \kappa^{-6/5}\left(1 + \frac{1}{X^4}\right) d_1^{|A\rangle} = -0.683763720\ldots \quad (4.9.24)$$

According to the conclusions of section 4.9.1 and (4.9.22),

$$\mathcal{G}^{(0)}_{|AB\rangle}(l) = \mathcal{G}^{(0)}_{|A\rangle}(l) T_1(\tfrac{\pi}{3}C)|_{C=5/2} \;, \quad (4.9.25)$$

and $\delta_1$ should match the coefficients $t_1$ of $l^{6/5}$ in the expansion of the function $T_1(\theta, l)|_{\theta=0}$ about $l = 0$. Noticing that $T_1(\theta, l) = T_2(\theta, l) = T_{\mathbf{LY}}(\theta, l)$, table 6 of [79] can be used: $\ln T_{\mathbf{LY}}(i\pi(b+3)/6) = \epsilon(i\pi(b+3)/6)$, $C = 5/2$ corresponds to $b = 2$, $hM^{-6/5} = h_c = -0.6852899839$, and so one finds

$$t_1 \sim 0.9977728224\, h_c = -0.683763721\ldots \quad (4.9.26)$$

which within numerical accuracy is equal to $\delta_1$.

## 4.10 Boundary bound states of the three-state Potts model

Another way to check the proposals made here is to look at the boundary pole structure of the reflection factors. In this section the boundary parameter dependent reflection factor for the three-state Potts model will be examined, which extends the work done for the Yang-Lee model in [74]. Each pole in the physical strip must correspond to a boundary bound state, unless a 'u-channel' or boundary Coleman-Thun type diagram can be drawn, as described in section 3.3. The boundary bound state bootstrap condition will be used to construct reflection factors for the excited state boundaries and the aim is to close the bootrap on a finite number of excited boundaries, and so conjecture the boundary spectrum.

Recall that the 3-state Potts model has one of 3 possible spins, $A$, $B$ or $C$ at each lattice site. It is described by the $A_2$ scattering theory where the two particles correspond to a kink/anti-kink pair which interpolate between the spins $A \to B \to C$ and $A \to C \to B$ respectively. Particle 2 can be interpreted as a bound state of particle 1 with itself, and vice-versa, so the bulk fusing angles are $U_{11}^2 = U_{22}^1 = 2\pi/3$ and the $S$-matrix elements are $S_{11} = S_{22} = (2)$, $S_{12} = -(1)$. The parameter dependent reflection factors, described in section 4.4 are

$$R_1^{|0\rangle} = (-2)(-1+C)(-1-C) \tag{4.10.1}$$

$$R_2^{|0\rangle} = (-2)(-2+C)(-2-C) \tag{4.10.2}$$

where $|0\rangle$ denotes the boundary ground state here. In the limit $C \to i\infty$, the parameter dependent blocks disappear from these reflection factors leaving $R_1 = R_2 = (-2)$. There are no poles in the physical strip of these reflection factors, and so no boundary bound states as expected since this corresponds to a 'fixed' boundary condition. When the parameter $C = 5/2$, the boundary condition is the 'mixed' condition, say $AB$, so both spin $A$ or $B$ is allowed at the boundary, but not spin $C$. The parameter can therefore be thought of as indicating the preference of the boundary to be either spin $A$ or $B$ as it moves away from $C = 5/2$.

The positions of the poles, and zeros, of (4.10.1) and (4.10.2) are shown in figure 4.6 as $C$ is varied. The pole positions are shown as solid lines, the zeros as dashed lines and the axes are dotted lines. Note that the physical strip for reflection

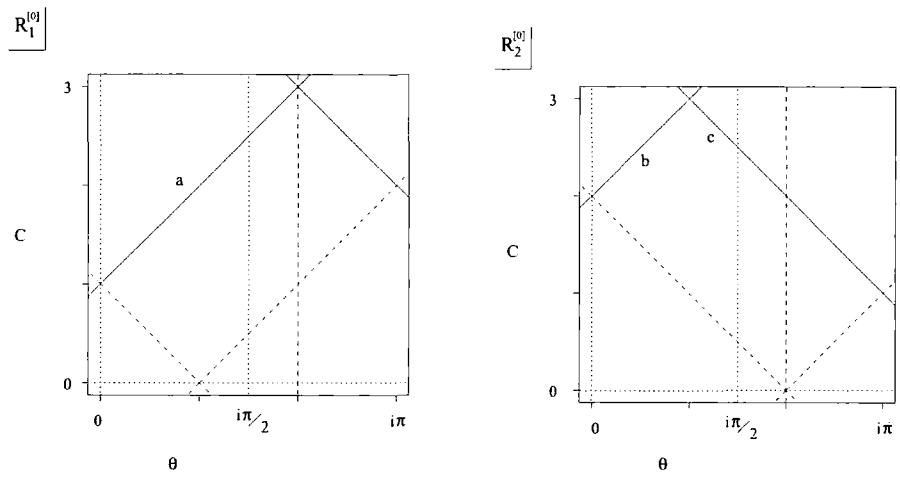


(a): $R_1^{|0\rangle}$ (b): $R_2^{|0\rangle}$

Figure 4.6: The poles and zeros of $R_1^{|0\rangle}$ and $R_2^{|0\rangle}$. The poles are solid lines, the zeros are dashed lines and the axes are dotted lines.

factors is $0 \leq \theta \leq i\pi/2$ (half that of the bulk $S$-matrices) so a line at $\theta = i\pi/2$ is also included for guidance. The reflection factors (4.10.1) and (4.10.2) are symmetric about $C = 0$ and $C = 3$ so the search for poles can be restricted to the physical strip with $0 \leq C \leq 3$. For $R_1^{|0\rangle}$ the only interesting pole occurs at $\theta = i\pi(C-1)/3$ denoted $a$ in figure 4.6(a). This must correspond to a bound state, with fusing angle $(C-1)\pi/3$, exciting the boundary to state $|1\rangle$. The difference in energies between these two states is

$$e_1 - e_0 = m\cos\left(\frac{(C-1)\pi}{3}\right) \tag{4.10.3}$$

which vanishes when $C = 5/2$, indicating that the levels $|0\rangle$ and $|1\rangle$ are degenerate at this point and for $C > 5/2$, their roles swap, with $|1\rangle$ now acting as the ground state and $|0\rangle$ an excited state. This is precisely as expected when the kink picture is considered: associating $|0\rangle$ with, say, $A$ and particle 1 with the kink, then $|1\rangle$ will be $B$. These two states become degenerate at $C = 5/2$, when the boundary condition is $AB$. Now as $C$ increases above 5/2, the ground state becomes $|1\rangle$, and since acting on $B$ with the antikink (particle 2) will give $A$ one would expect $R_2^{|1\rangle}(C > 5/2) = R_1^{|0\rangle}(C < 5/2)$ and $R_1^{|1\rangle}(C > 5/2) = R_2^{|0\rangle}(C < 5/2)$. $R_{1,2}^{|1\rangle}$ can be found using the boundary bound state bootsrap condition given in (3.3.26):

$$\begin{aligned} R_1^{|1\rangle} &= R_1^{|0\rangle} S_{11}(\theta + C - 1) S_{11}(\theta - C + 1) \\ &= (-2)(-1+C)(3-C) \end{aligned} \tag{4.10.4}$$

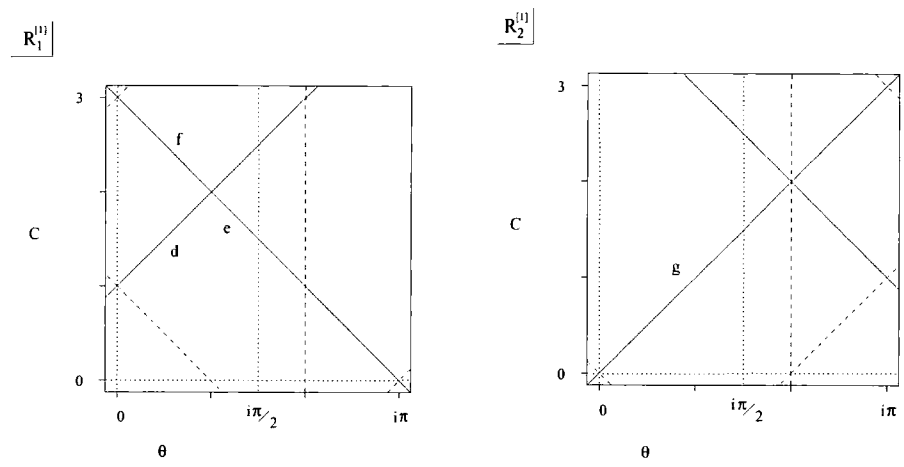


(a): $R_1^{|1\rangle}$ (b): $R_2^{|1\rangle}$

Figure 4.7: The poles and zeros of $R_1^{|1\rangle}$ and $R_2^{|1\rangle}$. The poles are solid lines, the zeros are dashed lines and the axes are dotted lines.

$$\begin{aligned} R_2^{|1\rangle} &= R_2^{|0\rangle} S_{21}(\theta + C - 1) S_{21}(\theta - C + 1) \\ &= (-2)(-2 - C)(C)\,. \end{aligned} \tag{4.10.5}$$

Using the property $(x \pm 2h) = (x)$, where $h = 3$ here, it is easy to show that

$$R_1^{|0\rangle}(C = \tfrac{5}{2} - \epsilon) = (-2)(\tfrac{3}{2} - \epsilon)(\tfrac{5}{2} + \epsilon) = R_2^{|1\rangle}(C = \tfrac{5}{2} + \epsilon) \tag{4.10.6}$$

$$R_2^{|0\rangle}(C = \tfrac{5}{2} - \epsilon) = (-2)(\tfrac{1}{2} - \epsilon)(\tfrac{3}{2} + \epsilon) = R_1^{|1\rangle}(C = \tfrac{5}{2} + \epsilon) \tag{4.10.7}$$

so in fact, one only needs to consider poles in the physical strip for $0 \leq C \leq 5/2$ to get the full picture.

In $R_2^{|0\rangle}$, there is one such pole at $i(C-2)\pi/3$, labelled $b$ in figure 4.6. This corresponds to a bound state, creating the boundary state $|2\rangle$, with energy

$$e_2 = e_0 + m\cos\left(\frac{(C-2)\pi}{3}\right). \tag{4.10.8}$$

The rapidities of the poles in $R_1^{|1\rangle}$ and $R_2^{|1\rangle}$ are shown in figure 4.7. The pole, labelled $d$ in figure 4.7(a) is just the 'u-channel' version of pole $a$, shown in figure 4.8(a), whereas pole $e$ corresponds to the Colemann-Thun process shown in figure 4.8(b). Naively, this ought to represent a double pole, but note that there is a zero in $R_2^{|0\rangle}$ at $i\pi(2-C)/3$, which reduces the order appropriately. Diagram 4.8(b) is only valid for $C < 2$, at which point a bound state must form, with fusing angle $(3-C)\pi/3$, creating a state $|3\rangle$, labelled in 4.7 by $f$. The pole at $i\pi C/3$ in $R_2^{|1\rangle}$ ($g$ in figure 4.7(b))

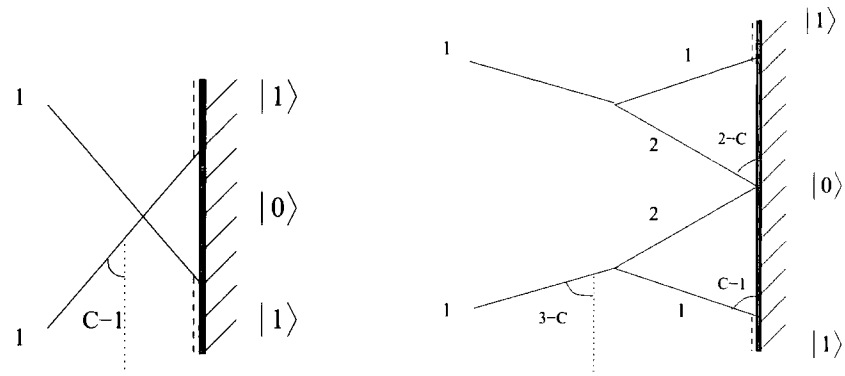


(a): pole $d$ (b): pole $e$

Figure 4.8: Coleman-Thun diagrams for poles $d$ and $e$ in $R_1^{|1\rangle}$

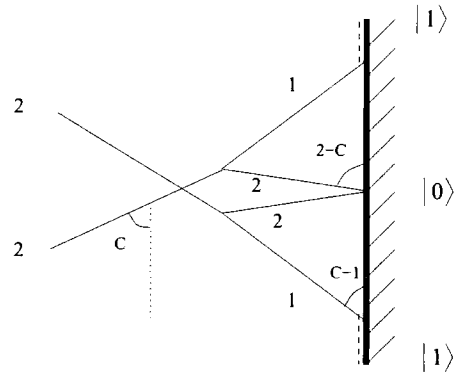


Figure 4.9: Coleman-Thun process diagram for pole $g$ in $R_2^{|1\rangle}$

has another Coleman-Thun description, shown in figure 4.9, which again due to the zero at $i\pi(2-C)/3$ in $R_2^{|0\rangle}$ describes a simple, rather than a double pole.

As shown in (4.10.8), the energy of $|2\rangle$ is

$$e_2 = e_0 + m\cos\left(\frac{(C-2)\pi}{3}\right) \tag{4.10.9}$$

where $e_0$ is the energy of $|0\rangle$ and $m$ is the mass of the kink/anti-kink. For state $|3\rangle$ the energy is

$$\begin{aligned} e_3 &= e_0 + m\cos\left(\frac{(C-1)\pi}{3}\right) + m\cos\left(\frac{(3-C)\pi}{3}\right) \\ &= e_0 + m\cos\left(\frac{(C-2)\pi}{3}\right) = e_2\,. \end{aligned} \tag{4.10.10}$$

As the states $|2\rangle$ and $|3\rangle$ have the same energy, the minimal assumption is that they are the same state. This is supported by the fact that the reflection factors $R_i^{|2\rangle}$ and

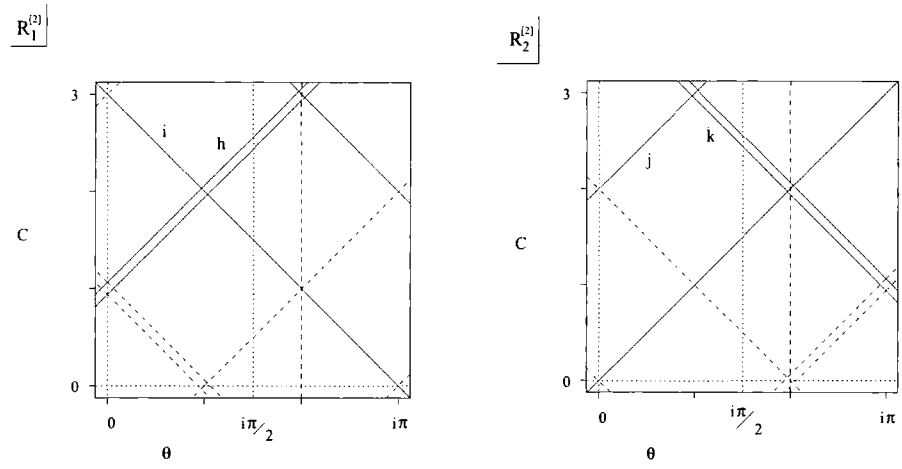


(a): $R_1^{|2\rangle}$ (b): $R_2^{|2\rangle}$

Figure 4.10: The poles and zeros of $R_1^{|2\rangle}$ and $R_2^{|2\rangle}$. Double poles (and zeros) are shown by double lines.

$R_i^{|3\rangle}$, $i = 1, 2$ are also equal:

$$\begin{aligned} R_1^{|2\rangle} &= R_1^{|0\rangle} S_{21}(\theta + C - 2) S_{21}(\theta - C + 2) \\ &= (-2)(-1 + C)^2(-1 - C)(3 - C) = R_1^{|3\rangle} \end{aligned} \tag{4.10.11}$$

$$\begin{aligned} R_2^{|2\rangle} &= R_2^{|0\rangle} S_{22}(\theta + C - 2) S_{22}(\theta - C + 2) \\ &= (-2)(-2 + C)(-2 - C)^2(C) = R_2^{|3\rangle} \end{aligned} \tag{4.10.12}$$

and

$$\begin{aligned} R_1^{|2\rangle}(C = \tfrac{5}{2} - \epsilon) &= R_1^{|3\rangle}(C = \tfrac{5}{2} - \epsilon) \\ &= (\tfrac{3}{2} - \epsilon)^2(\tfrac{5}{2} + \epsilon)(\tfrac{1}{2} + \epsilon) \\ &= R_2^{|2\rangle}(C = \tfrac{5}{2} + \epsilon) = R_2^{|3\rangle}(C = \tfrac{5}{2} + \epsilon)\,. \end{aligned} \tag{4.10.13}$$

The poles in $R_i^{|2\rangle}$ ($R_i^{|3\rangle}$) are shown in figure 4.10 (double poles are shown by double lines). The double pole at $i\pi(C-1)/3$ in $R_1^{|2\rangle}$ ($h$ in figure 4.10(a)), can be described in two ways: in terms of state $|2\rangle$ by figure 4.11(a), or state $|3\rangle$ by figure 4.11(b). In these cases there is no zero at $i\pi(3-C)/3$ in either $R_1^{|0\rangle}$ or $R_2^{|0\rangle}$, or at $i\pi(C-2)/3$ in $R_2^{|1\rangle}$ so these really are second order diagrams. The pole at $i\pi(3-C)/3$ ($i$ in figure 4.10(a)) cannot be easily described in terms of state $|2\rangle$, but has a simple description in terms of $|3\rangle$ as the 'u-channel' version of pole $f$, shown in figure 4.12.

The single pole at $i\pi(C-2)/3$ in $R_2^{|2\rangle}$ ($j$ in figure 4.10(b)) is the 'u-channel' version of pole $b$, as shown in figure 4.13(a), whereas the double pole at $i\pi(4-C)/3$ ($k$ in

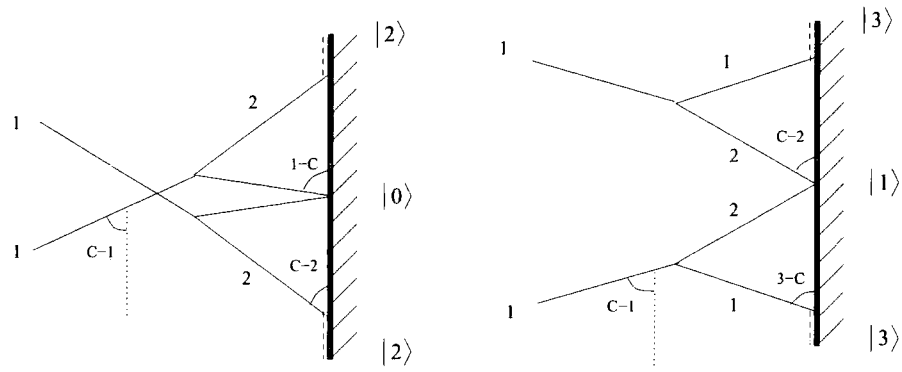


(a): pole $h$, in terms of $|2\rangle$ (b): pole $h$, in terms of $|3\rangle$

Figure 4.11: Coleman-Thun diagrams for the double pole $h$ in $R_1^{|2\rangle=|3\rangle}$

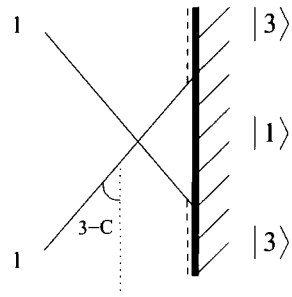


Figure 4.12: Coleman-Thun diagram for pole $i$ in $R_1^{|2\rangle}$

figure 4.10) is explained by figure 4.13(b). Once again there is no zero in $R_1^{|0\rangle}$ at $i\pi(3-C)/3$, so this is indeed second order.

The boundary bound state bootstrap therefore closes on three states $|0\rangle$, $|1\rangle$ and $|2\rangle$. The energies of $|1\rangle$ and $|2\rangle$, in terms of $e_0$, the energy of $|0\rangle$, are

$$e_1 = e_0 + m\cos\left(\frac{(C-1)\pi}{3}\right) \tag{4.10.14}$$

$$e_2 = e_0 + m\cos\left(\frac{(C-2)\pi}{3}\right). \tag{4.10.15}$$

They are shown in figure 4.14, as a function of the boundary parameter $C$, indicating at what values they appear in the spectrum. In figure 4.14(a), the energy of the ground state $e_0$ is set to zero, and $e_1$ and $e_2$ are given in units of the kink/antikink mass $m$. In order to show the symmetry between $e_0$ and $e_1$ more clearly, in figure 4.14(b), $e_0$ is taken to be $e_0 = \frac{m}{2}(1-\cos(\frac{(C-1)\pi}{3}))$ and again units of the kink/antikink mass $m$ are used. The one particle threshold ($e_0+m$, for $C<5/2$ and $e_1+m$ for $C>5/2$), above which the spectrum is continuous, is also shown in bold in figure 4.14(b). It

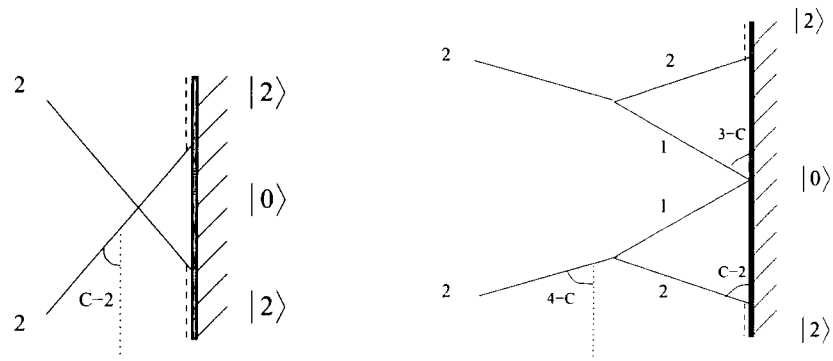


(a): pole $j$ (b): pole $k$

Figure 4.13: Coleman-Thun diagrams for poles $j$ and $k$ in $R_2^{|2\rangle}$

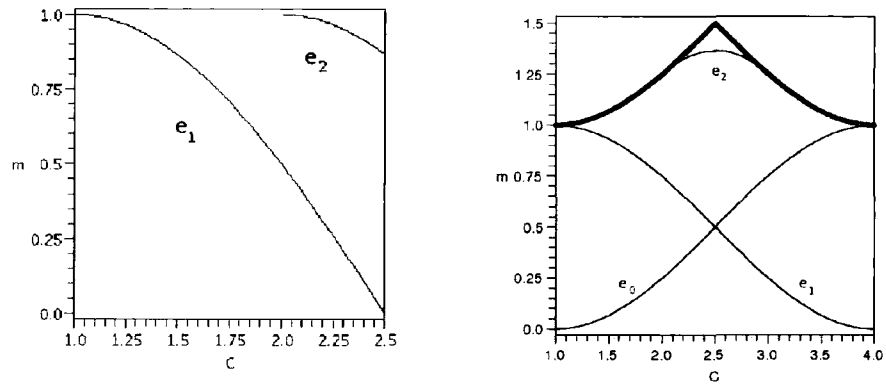


(a): $e_0 = 0$ (b): $e_0 = \frac{m}{2}(1 - \cos(\frac{(C-1)\pi}{3}))$

Figure 4.14: The boundary spectrum of the three-state Potts model, in units of the kink/antikink mass $m$. The bold curve is the one particle threshold.

should be possible to verify the spectrum shown in figure 4.14(b) using the boundary truncated conformal space approach [78].

# Chapter 5

# $\mathcal{PT}$ symmetry breaking and exceptional points

This chapter is concerned with the study of a family of $\mathcal{PT}$-symmetric Hamiltonians, and in particular, in the Jordon block structures which emerge as the $\mathcal{PT}$ symmetry is spontaneously broken. At first sight, this has little in common with the previous work in this thesis, however the ODE/IM correspondence, described in section 2.6.2, does have an important role to play. Before this is discussed there will be a brief introduction to $\mathcal{PT}$-symmetric quantum mechanics, which follows the recent review [50].

## 5.1 $\mathcal{PT}$-symmetric Quantum Mechanics

The study of $\mathcal{PT}$-symmetric quantum mechanical theories began in private communication between Bessis and Zinn-Justin, who considered the spectrum of the Hamiltonian $H = p^2 + ix^3$, with the corresponding Schrödinger equation

$$\left(-\frac{d^2}{dx^2} + ix^3\right)\psi(x) = E\psi(x)\,, \quad \psi(x) \in L^2(\mathbb{R})\,. \tag{5.1.1}$$

Although this Hamiltonian is not Hermitian, and so the usual arguments to show the reality of the eigenvalues do not apply, numerical studies of this problem led Bessis and Zinn-Justin to conjecture that the spectrum of $H$ is in fact both real and positive. Bender and Boettcher [63] suggested that the reality of the spectrum of this non-Hermitian Hamiltonian is due to it having $\mathcal{PT}$-symmetry, where the parity $\mathcal{P}$ acts by sending $x \to -x$ and $p \to -p$, whereas the time reversal, $\mathcal{T}$, sends $p \to -p$ and

$i \rightarrow -i$. When the Hamiltonian, $H$, is $\mathcal{PT}$-symmetric the following commutation relation holds: $[H, \mathcal{PT}] = 0$. If $H$ and $\mathcal{PT}$ are also simultaneously diagonalisable (which is not necessarily the case as $\mathcal{PT}$ is a non-linear operator) it can be shown that the spectrum of $H$ is real, as follows [123]: working in the basis in which both $H$ and $\mathcal{PT}$ are simultaneously diagonal, so $H|\phi\rangle = E|\phi\rangle$ and $\mathcal{PT}|\phi\rangle = a|\phi\rangle$, where $a$ is a constant, then using $(\mathcal{PT})^2 = 1$, $|\phi\rangle = \mathcal{PTPT}|\phi\rangle = a^*a|\phi\rangle$ so $a$ is in fact a pure phase. It can therefore be absorbed into $|\phi\rangle$ with the transformation $|\phi\rangle \rightarrow a^{1/2}|\phi\rangle$ so that $\mathcal{PT}|\phi\rangle = |\phi\rangle$ and $H\mathcal{PT}|\phi\rangle = E|\phi\rangle$. Since $H$ and $\mathcal{PT}$ commute, this is also equal to $\mathcal{PT}H|\phi\rangle = E^*|\phi\rangle$ and so $E$ must be real.

Consider now the situation where $H$ and $\mathcal{PT}$ are not simultaneously diagonalisable, so $\mathcal{PT}|\phi\rangle = |\psi\rangle$ where $|\psi\rangle \neq a|\phi\rangle$. Using the commutation relation of $H$ and $\mathcal{PT}$, $H\mathcal{PT}|\phi\rangle = \mathcal{PT}H|\phi\rangle$, it is clear that $H|\psi\rangle = E^*|\psi\rangle$ so $|\psi\rangle$ is an eigenvector of $H$ with eigenvalue $E^*$. In these cases the $\mathcal{PT}$-symmetry of $H$ is said to be spontaneously broken; the energy eigenvalues are no longer real, but appear in complex-conjugate pairs. The $\mathcal{PT}$ operator acts to interchange the eigenvectors with complex-conjugate eigenvalues [123].

Bender and Boettcher looked at a generalisation of the Bessis-Zinn-Justin problem, the Hamiltonian $H_M = p^2 - (ix)^{2M}$ ($M$ real and $> 0$), and proposed that the spectrum of this is real and positive for $M \geq 1$ [63]. As $M$ decreases below 1, they found that infinitely-many real eigenvalues pair off and become complex, and as $M$ reaches 0.5, the last real eigenvalue diverges to infinity. They interpreted this 'phase transition' at $M = 1$ as the spontaneous breaking of the $\mathcal{PT}$ symmetry of $H_M$. A further generalisation was made by Dorey and Tateo in [65], where an angular momentum term was added to the Hamiltonian:

$$H_{M,l} = p^2 - (ix)^{2M} + \frac{l(l+1)}{x^2}, \quad (M, \, l \text{ real and } M > 0). \tag{5.1.2}$$

The conjecture made in [65], was that the spectrum of $H_{M,l}$ is real and positive for $M \geq 1$ and $|2l + 1| < M + 1$. For both of these generalisations, $x$ is no longer restricted to the real line, so it is important to consider what boundary conditions to impose, as taking the quantisation contour to tend to infinity in different pairs of Stokes sectors will lead to different eigenvalue problems, as mentioned in Section 2.6.2. Note that when $M = 1$ the Hamiltonian $H_1 = p^2 + x^2$ is that of the simple harmonic oscillator, for which the quantisation contour is the real axis. When the

angular momentum term is introduced, this contour must be continued around the singularity at the origin. In general, $M$ can take non-integer values and so to ensure that the $-(ix)^{2M}$ term is single valued, a branch cut must be made. This is taken along the positive imaginary axis here, and so the continuation of the contour around the origin should be taken through the lower half plane. As $M$ increases above 1, the resulting eigenvalue problem will be the correct continuation of the the simple harmonic oscillator, provided the quantisation contour tends to infinity in those Stokes sectors which contain the real axis for $M = 1$, namely $S_1$ and $S_{-1}$, where

$$S_k := \left| arg(x) - \frac{2\pi k}{2M+2} \right| < \frac{\pi}{2M+2} . \tag{5.1.3}$$

The Stokes sectors $S_1$ and $S_{-1}$ rotate towards the negative imaginary axis as $M$ increases, but for $M < 2$, the real axis remains within these sectors and so can be taken as the quantisation contour (with suitable continuation around the singularity at the origin). When $M = 2$, the anti-Stokes lines which form the upper boundary of the sectors $S_1$ and $S_{-1}$ lie along the real axis, so for $M \geq 2$ the contour must be deformed from the real axis, down into the lower half plane [63], as shown in figure 5.1.

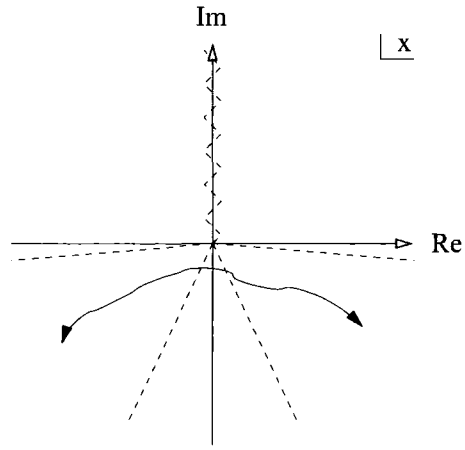


Figure 5.1: A wavefunction contour for $M \geq 2$

The spectrum of the following family of $\mathcal{PT}$-symmetric eigenvalue problems, first studied in detail in [66, 124], are of particular interest in this thesis:

$$\left[ -\frac{d^2}{dx^2} - (ix)^{2M} - \alpha(ix)^{M-1} + \frac{l(l+1)}{x^2} \right] \psi(x) = E\,\psi(x) , \quad \psi(x) \in L^2(\mathcal{C}) . \tag{5.1.4}$$

For $M = 1$, this also reduces to the simple harmonic oscillator (with energy $E + \alpha$), and the addition of the inhomogeneous term $(ix)^{M-1}$ has no effect on the Stokes sectors so the contour $\mathcal{C}$ is the same as that described above and shown in figure 5.1. This problem is invariant under the replacement $l \to -1-l$, and it will be convenient in the following to trade $l$ for $\lambda := l + \frac{1}{2}$, so that the symmetry is between $\lambda$ and $-\lambda$.

The first interesting feature of (5.1.4), shared with many $\mathcal{PT}$-symmetric problems, is the reality of the spectrum for many values of the parameters $\alpha$ and $l$. More precisely, for $M > 1$ and $M$, $\alpha$ and $\lambda = l + \frac{1}{2}$ real, the spectrum of (5.1.4) is

- *real* if $\alpha < M + 1 + 2|\lambda|$ ; (5.1.5)
- *positive* if $\alpha < M + 1 - 2|\lambda|$ . (5.1.6)

This was proved in [66] via the ODE/IM correspondence. This proof will be discussed shortly, but first it is worth seeing how the functional equations for this ODE differ from the simpler case described in section 2.6.2 [66] (see also [50]).

## 5.2 Functional relations

As a small simplification, the factors of $i$ can be eliminated from (5.1.4) by replacing $x$ with $z := x/i$ and setting $\Phi(z) := \psi(x/i)$, so that the eigenproblem (5.1.4) becomes

$$\left(-\frac{d^2}{dz^2} + z^{2M} + \alpha z^{M-1} + \frac{\lambda^2 - \frac{1}{4}}{z^2}\right)\Phi_k(z) = \mathcal{E}_k \Phi_k(z)\,, \quad \Phi_k(z) \in L^2(i\mathcal{C}) \tag{5.2.1}$$

where $\mathcal{E}_k = -E_k$. Note that the quantisation contour has also been rotated by 90°; the new contour is shown in figure 5.2.

In parallel to the discussion presented in Section 2.6.2, the Stokes relations can be found by first defining the 'basic' solution, subdominant in the $S_0$ sector, which in this case is

$$y(z, \mathcal{E}, \alpha, \lambda) \sim \frac{z^{-M/2-\alpha/2}}{\sqrt{2i}} e^{-\frac{z^{M+1}}{M+1}}\,. \tag{5.2.2}$$

From this 'basic' solution the following set of solutions can be generated:

$$y_k(z, \mathcal{E}, \alpha, \lambda) = \omega^{k/2+k\alpha/2} y(\omega^{-k} z, \omega^{2k}\mathcal{E}, \omega^{(M+1)k}\alpha, \lambda)\,, \quad \omega = e^{\frac{\pi i}{M+1}} \tag{5.2.3}$$

for integer $k$, with each pair of solutions $\{y_k, y_{k+1}\}$ forming a basis. Following the same argument given in section 2.6.2, a Stokes relation can be found, of the form

$$C(\mathcal{E}, \alpha, \lambda) y_0(z, \mathcal{E}, \alpha, \lambda) = y_{-1}(z, \mathcal{E}, \alpha, \lambda) + y_1(z, \mathcal{E}, \alpha, \lambda) \tag{5.2.4}$$

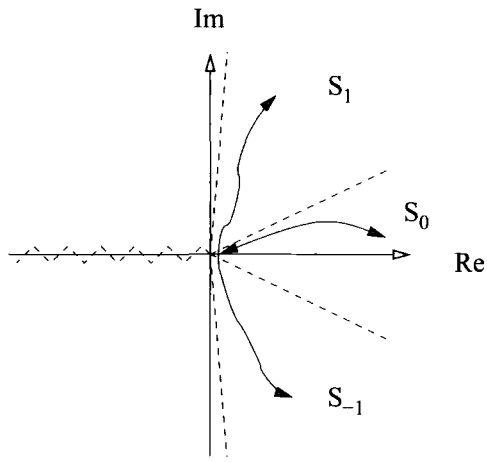


Figure 5.2: Quantisation contours for the lateral and radial problems

with the Stokes multiplier

$$C(\mathcal{E},\alpha,\lambda) = W_{-1,1}\,. \tag{5.2.5}$$

Recall that $W_{j,k}$ is shorthand for the Wronskian of the functions $y_j$ and $y_k$:

$$W_{j,k} \equiv W[y_j, y_k] = y_j y_k' - y_j' y_k\,. \tag{5.2.6}$$

Since $\omega^{M+1} = -1$, the only values of $\alpha$ to appear in the functions $y_k(z,\mathcal{E},\alpha,\lambda)$ are $\alpha$ and $-\alpha$ and so it is convenient to define

$$C^{(\pm)}(\mathcal{E}) := C(\mathcal{E},\pm\alpha,\lambda)\,, \quad y^{(\pm)}(z,\mathcal{E}) := y(z,\mathcal{E},\pm\alpha,\lambda)\,. \tag{5.2.7}$$

Putting $\pm\alpha$ into (5.2.4) then leads to the pair of coupled equations

$$\begin{aligned} C^{(+)}(\mathcal{E})y^{(+)}(z,\mathcal{E}) &= \omega^{-(1+\alpha)/2}y^{(-)}(\omega z,\omega^{2M}\mathcal{E}) \\ &\quad +\omega^{(1+\alpha)/2}y^{(-)}(\omega^{-1}z,\omega^{-2M}\mathcal{E}) \end{aligned} \tag{5.2.8}$$

$$\begin{aligned} C^{(-)}(E)y^{(-)}(z,\mathcal{E}) &= \omega^{-(1-\alpha)/2}y^{(+)}(\omega z,\omega^{2M}\mathcal{E}) \\ &\quad +\omega^{(1-\alpha)/2}y^{(+)}(\omega^{-1}z,\omega^{-2M}\mathcal{E})\,. \end{aligned} \tag{5.2.9}$$

Now, consider the solutions to the radial problem, $\psi_\pm(z,\mathcal{E},\alpha,\lambda)$, which are defined at the origin by

$$\psi(z,\alpha,\lambda) = \psi_+(z,\alpha,\lambda) \sim z^{\lambda+\frac{1}{2}} \tag{5.2.10}$$

with $\psi_-(z,\alpha,\lambda) = \psi(z,\alpha,-\lambda)$. The $z$ dependence of the Stokes relations can be removed by projecting onto these solutions. Let $D(\mathcal{E},\alpha,\lambda) = W[y,\psi_+](\mathcal{E},\alpha,\lambda)$ and

write $D^{(\pm)}(\mathcal{E}) = D(\mathcal{E}, \pm\alpha, \lambda)$. The Stokes relations then become

$$C^{(+)}(\mathcal{E})D^{(+)}(\mathcal{E}) = \omega^{-(2\lambda+\alpha)/2}D^{(-)}(\omega^{2M}\mathcal{E}) + \omega^{(2\lambda+\alpha/2)}D^{(-)}(\omega^{-2M}\mathcal{E}) \tag{5.2.11}$$

$$C^{(-)}(\mathcal{E})D^{(-)}(\mathcal{E}) = \omega^{-(2\lambda-\alpha)/2}D^{(+)}(\omega^{2M}\mathcal{E}) + \omega^{(2\lambda-\alpha/2)}D^{(+)}(\omega^{-2M}\mathcal{E}). \tag{5.2.12}$$

It is worth noting a few features of the multipliers $C$ and $D$ here. $C^{(\pm)}$ is defined as the Wronskian of the subdominant solutions in the $S_1$ and $S_{-1}$ sectors. This Wronskian is zero if and only if the two solutions are linearly dependent, so in fact the solution is subdominant in both sectors. Such a solution is an eigenfunction of this lateral problem and so $C^{(\pm)}$ is a spectral determinant of this: the zeros of $C^{\pm}(\mathcal{E})$ are the eigenvalues of the eigenproblem (5.2.1) with $\Phi_k(z) \in L^2(iC)$. $D^{(\pm)}(\mathcal{E})$ is also a spectral determinant, but for the radial problem, with boundary conditions set as $x \to 0$ and $x \to +\infty$. This is easily seen as $D$ is the Wronskian of two solutions, one subdominant in the $S_0$ sector, and one which decays as $z \to 0$. The zeros of $D(\mathcal{E})$ are therefore the eigenvalues of the radial problem. Note that the quantisation contour for this problem is along the real axis, as shown in figure 5.2, so this problem is Hermitian.

Now, for $M > 1$, WKB estimates show that the function $D^{(\pm)}(\mathcal{E})$ has order less than 1 [65], so Hadamard's factorisation theorem can be applied in its simplest form. This states that, if $D(0, \lambda) \neq 0$ then $D(\mathcal{E}, \lambda)$ can be written as an infinite product over its zeros. This constraint holds as it can be shown that [66]

$$D^{(\pm)}(\mathcal{E})|_{\mathcal{E}=0} = \frac{1}{\sqrt{2i}}\left(\frac{M+1}{2}\right)^{\frac{2\lambda\mp\alpha}{2M+2}-\frac{1}{2}} \frac{\Gamma\left(\frac{2\lambda}{M+1}\right)}{\Gamma\left(\frac{2\lambda\pm\alpha}{2M+2}+\frac{1}{2}\right)} \tag{5.2.13}$$

and so

$$D^{(\pm)}(\mathcal{E}, \lambda) = D^{(\pm)}(0, \lambda)\prod_{n=0}^{\infty}\left(1 - \frac{\mathcal{E}}{\mathcal{E}_n}\right). \tag{5.2.14}$$

Using (5.2.13) in (5.2.12), along with the identity

$$\Gamma\left(\frac{1}{2}+\theta\right)\Gamma\left(\frac{1}{2}-\theta\right) = \frac{\pi}{\cos(\theta\pi)} \tag{5.2.15}$$

and remembering that $D^{(-)}(\mathcal{E}) = D(\mathcal{E}, -\alpha, \lambda)$ and $\omega = e^{\frac{\pi i}{M+1}}$ gives

$$\begin{aligned} C(\mathcal{E}, \alpha, \lambda)|_{\mathcal{E}=0} &= C^{(+)}(\mathcal{E})|_{\mathcal{E}=0} \\ &= \left(\frac{M+1}{2}\right)^{\frac{\alpha}{M+1}} \frac{2\pi}{\Gamma\left(\frac{1}{2}+\frac{2\lambda-\alpha}{2M+2}\right)\Gamma\left(\frac{1}{2}-\frac{2\lambda+\alpha}{2M+2}\right)}. \end{aligned} \tag{5.2.16}$$

## 5.3 Reality proof

The functional relations given above can now be used to reproduce the proof of (5.1.5) and (5.1.6) [66] (see also [50]), using techniques inspired by the Bethe ansatz.

First, define the zeros of the spectral determinant $C^{(+)}(\mathcal{E}) = C(\mathcal{E}, \alpha, \lambda)$ to be the set $\{-E_k\}$, and the zeros of $D^{(\pm)}(\mathcal{E})$ to be the set $\{\mathcal{E}_k^{(\pm)}\}$. Putting $\mathcal{E} = -E_k$ in (5.2.12) will fix the left of (5.2.12) to zero and so this equation can be rearranged to

$$\frac{D^{(-)}(\omega^2 E_k)}{D^{(-)}(\omega^{-2} E_k)} = -\omega^{-2\lambda-\alpha}, \tag{5.3.1}$$

and using the factorised form of $D^{(-)}$ for $M > 1$, (5.2.14) puts constraints on the $E_k$:

$$\prod_{n=1}^{\infty} \left( \frac{\mathcal{E}_n^{(-)} + \omega^2 E_k}{\mathcal{E}_n^{(-)} + \omega^{-2} E_k} \right) = -\omega^{-2\lambda-\alpha}, \quad k = 1, 2, \ldots \tag{5.3.2}$$

Each $\mathcal{E}_n^{(-)}$ is an eigenvalue of an Hermitian operator $H_{M,-\alpha,\lambda}$ and is therefore real. Performing a Langer transformation [125] on $H_{M,\alpha,\lambda}$, by setting $z = e^x$, $y(z) = e^{x/2}\phi(x)$, shows that $\mathcal{E}_n^{(-)}$ solves the following eigenproblem

$$\left( -\frac{d^2}{dx^2} + e^{(2M+2)x} - \alpha e^{(M+1)x} + \lambda^2 - \mathcal{E}^{(-)} e^{2x} \right) \phi(x) = 0 . \tag{5.3.3}$$

If $\alpha < 0$, this is an everywhere positive potential and so $\mathcal{E}^{(-)}$ is positive. Without loss of generality, it can be assumed that $\lambda \geq 0$, since the original problem is invariant under $\lambda \to -\lambda$ and so $\mathcal{E}^{(-)}$ will be positive for $\alpha < \lambda$.

In fact, by considering the value of $D^{(-)}(\mathcal{E})|_{\mathcal{E}=0}$, given in (5.2.13), it is clear that this first vanishes when $\alpha = M + 2\lambda + 1$, and so all $\mathcal{E}_n^{(-)}$ must be positive up to this point. Taking the modulus squared of (5.3.2) and writing the eigenvalues of (5.2.1) as $E_k = |E_k| e^{i\delta_k}$ gives

$$\prod_{n=1}^{\infty} \left( \frac{|\mathcal{E}_n^{(-)}|^2 + |E_k|^2 + 2\mathcal{E}_n^{(-)} |E_k| \cos(\frac{2\pi}{M+1} + \delta_k)}{|\mathcal{E}_n^{(-)}|^2 + |E_k|^2 + 2\mathcal{E}_n^{(-)} |E_k| \cos(\frac{2\pi}{M+1} - \delta_k)} \right) = 1 . \tag{5.3.4}$$

For $\alpha < M + 2\lambda + 1$, all $\mathcal{E}_n^{(-)}$ are positive and so each term in the product is greater than, less than, or equal to one dependent only on the values of the cosine in the numerator and denominator, which are independent of the index $n$. The product will therefore only be equal to one if each individual term is equal to one, which for $E_k \neq 0$ requires $\cos(\frac{2\pi}{M+1} + \delta_k) = \cos(\frac{2\pi}{M+1} - \delta_k)$, or equivalently

$$\sin\left( \frac{2\pi}{M+1} \right) \sin(\delta_k) = 0 . \tag{5.3.5}$$

As $M > 1$, this implies that

$$\delta_k = m\pi \, , \; m \in \mathbb{Z} \, . \tag{5.3.6}$$

Relaxing the condition on $\lambda$ now, this shows that the eigenvalues of (5.1.4) for $M > 1$ and $\alpha < M + |2\lambda|$ are real. Note that most of the $E_k$ become complex as $M$ falls below 1 [63], at least for $\alpha = 0$. This coincides with the point at which the order of $D^{(-)}(\mathcal{E})$ is greater than 1, and so the factorised form of $D^{(-)}(\mathcal{E})$ given by Hadamard's factorisation theorem no longer has such a simple form and this proof breaks down.

To prove the positivity at general values of $M > 1$, one must first consider the case of $M = 1$. This is the simple harmonic oscillator with angular momentum term (where $\alpha$ is absorbed as a shift in $\mathcal{E}$), which is exactly solvable for all $\lambda$ and $\alpha$ in terms of confluent hypergeometric functions

$$y(z, \mathcal{E}, \alpha, \lambda) = \frac{1}{\sqrt{2i}} z^{\lambda+\frac{1}{2}} e^{-z^2/2} U(\tfrac{1}{2}(\lambda+1) - \tfrac{\mathcal{E}-\alpha}{4}, \lambda+1, z^2) \, . \tag{5.3.7}$$

Now, using the analytic continuation formula, from [126]

$$U(a, b, ze^{2\pi i n}) = (1 - e^{-2\pi i b n}) \frac{\Gamma(1-b)}{\Gamma(1+a-b)} M(a, b, z) + e^{-2\pi i b n} U(a, b, z) \tag{5.3.8}$$

the Wronskian

$$W[U(a, b, z), M(a, b, z)] = \frac{\Gamma(b)}{\Gamma(a)} z^{-b} e^z \tag{5.3.9}$$

and, for $b > 1$, the $|z| \to 0$ asymptotic

$$U(a, b, z) \sim \frac{\Gamma(b-1)}{\Gamma(a)} z^{1-b} + \ldots \tag{5.3.10}$$

it can be shown [65][66] that

$$C(\mathcal{E}, \alpha, \lambda)|_{M=1} = \frac{2\pi}{\Gamma(\frac{1}{2} + \frac{2\lambda+\mathcal{E}-\alpha}{4}) \Gamma(\frac{1}{2} - \frac{2\lambda-\mathcal{E}+\alpha}{4})} \, . \tag{5.3.11}$$

The eigenvalues of (5.1.4), for $M = 1$, are therefore $E_k = 4k + 2 - \alpha \pm 2\lambda$, $k = 1, 2, \ldots$. They are all real for all real values of $\alpha$ and $\lambda$, and are all positive for $\alpha < 2 - |2\lambda|$.

For $M > 1$, provided $\alpha$ remains less than $M + 1 + |2\lambda|$, all eigenvalues $E_k$ will be confined to the real axis and so the point at which the first eigenvalue becomes negative will be signalled by the presence of a zero in $C(-E, \alpha, \lambda)$ at $E = 0$. Recall, from (5.2.16), that

$$C(\mathcal{E}, \alpha, \lambda)|_{\mathcal{E}=0} = \left(\frac{M+1}{2}\right)^{\frac{\alpha}{M+1}} \frac{2\pi}{\Gamma\left(\frac{1}{2} + \frac{2\lambda-\alpha}{2M+2}\right) \Gamma\left(\frac{1}{2} - \frac{2\lambda+\alpha}{2M+2}\right)} \tag{5.3.12}$$

and so the first zero when $\mathcal{E} = -E = 0$ appears when $\alpha = M + 1 - |2\lambda|$; the spectrum is therefore entirely positive for all $\alpha < M + 1 - |2\lambda|$ and $M > 1$.

Figure 5.3 shows the regions of parameter space for which the reality and positivity of the spectrum has been proved. So far, the reality of the spectrum of (5.1.4) has been proven for $(\alpha, 2\lambda) \in B \cup C \cup D$, and positivity for $(\alpha, 2\lambda) \in D$. This proof does not show that the reality of the spectrum breaks down for all, or indeed any, of the points in $A$, although this breakdown has been observed numerically for several points. In [124], Dorey, Dunning and Tateo explored the boundary of $A$, where they described a mechanism by which the breakdown of reality occurs. They also showed numerically that the phase diagram for $M = 3$ has a much more interesting structure than is shown in figure 5.3. A discussion of their work is presented below.

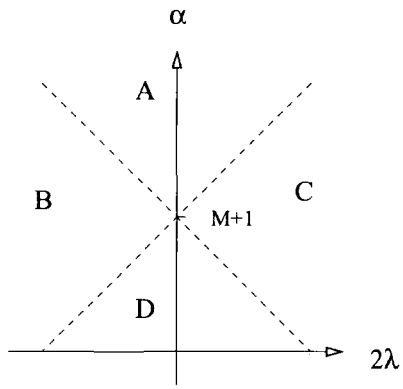


Figure 5.3: The approximate 'phase diagram' at fixed $M$. The spectrum is entirely real in regions $B$, $C$ and $D$, and positive in region $D$.

## 5.4 Investigating the frontiers of the region of reality

It is convenient here to adopt a new set of coordinates in the $(2\lambda, \alpha)$ plane defined by

$$\alpha_{\pm} = \frac{1}{2M+2}[\alpha - M - 1 \pm 2\lambda]\,. \tag{5.4.1}$$

The frontiers of the region (5.1.5) of guaranteed reality are the lines, at $\pm 45°$ in the $(2\lambda, \alpha)$ plane, given by $\alpha_{\pm} = 0$. In this section, arguments from supersymmetric quantum mechanics will be used to show that his model has a protected $E = 0$ energy

level along these lines, and that level crossing with this protected $E = 0$ level can be seen as the mechanism by which the first levels pair-off and become complex as the region (5.1.5) is left [124]. This argument will also be extended to the lines $\alpha_\pm = m$, $m \in \mathbb{N}$, for the $M = 3$ case, using the quasi-exact solvability of the model at these points.

On the line $\alpha_+ = 0$, $\alpha = M + 1 - 2\lambda$ and the ODE (5.1.4) becomes

$$\left(-\frac{d^2}{dz^2} + z^{2M} + \alpha z^{M-1} + \frac{\lambda^2 - \frac{1}{4}}{z^2}\right)\Phi(z) = -E\Phi(z)\,. \tag{5.4.2}$$

This factorises as

$$Q_+Q_-\Phi = -E\Phi \tag{5.4.3}$$

with

$$Q_\pm = \pm\frac{d}{dz} + z^M - \frac{2\lambda - 1}{2z}\,, \tag{5.4.4}$$

and such a factorisation usually points to a relationship with supersymmetry. It is easily seen that (5.4.3) has an $E = 0$ eigenfunction in $L^2(i\mathcal{C})$:

$$\psi(z) = z^{\frac{1}{2}-\lambda}e^{\frac{z^{M+1}}{M+1}}\,, \quad Q_-\psi(z) = 0\,, \tag{5.4.5}$$

which can be interpreted as having unbroken supersymmetry. All other eigenfunctions are paired with those of the SUSY partner Hamiltonian $\widehat{H} = Q_-Q_+$, which can be found by replacing $(\alpha_+, \alpha_-) = (0, -\frac{2\lambda}{M+1})$ with $(\widehat{\alpha}_+, \widehat{\alpha}_-) = (-1, -1 - \frac{2\lambda-2}{M+1}) = (-1, \alpha_- - \frac{M-1}{M+1})$. This problem is symmetric in $\lambda$ so sending $\lambda \to -\lambda$ gives the $E = 0$ eigenfunction on the line $\alpha_- = 0$. The boundaries between the regions in figure 5.3 coincide with the presence of the (supersymmetric) zero-energy state in the spectrum. Ordinarily, this would be expected to be the ground state of the theory, which is the case on the boundary of $D$. On the boundary of $A$, however, this is only true for $\alpha < M + 3$, due to level crossing which is not ruled out here by the usual theory of SUSY quantum mechanics as this problem is not Hermitian.

To see this level crossing, consider $C(\mathcal{E}, \alpha, l)|_{\mathcal{E}=0}$, as given in (5.3.12), which in the $\alpha_\pm$ coordinates is

$$C(-E, \alpha_+, \alpha_-)|_{E=0} = \left(\frac{M+1}{2}\right)^{1+\alpha_++\alpha_-} \frac{2\pi}{\Gamma(-\alpha_+)\Gamma(-\alpha_-)}\,. \tag{5.4.6}$$

This is zero when either $\alpha_+$ or $\alpha_-$ vanishes, as expected by the presence of the state $\psi$ in the spectrum. Level-crossing occurs when a further level passes through zero.

To find the points where this occurs, consider the SUSY partner potential, which is isospectral to $H$ except for the elimination of $\psi$. Replacing $\alpha_\pm$ in (5.4.6) with $\widehat{\alpha}_\pm$

$$\begin{aligned} C(-E,\widehat{\alpha}_+,\widehat{\alpha}_-)|_{E=0,\widehat{\alpha}_+=1} &= \left(\frac{M+1}{2}\right)^{\widehat{\alpha}_-} \frac{2\pi}{\Gamma(-\widehat{\alpha}_-)} \\ &= \left(\frac{M+1}{2}\right)^{\widehat{\alpha}_-} \frac{2\pi}{\Gamma(\frac{M-1}{M+1}-\alpha_-)}. \end{aligned} \tag{5.4.7}$$

Level-crossings with the state $\psi$ are indicated by simple zeros of (5.4.7), at $(\alpha_+,\alpha_-) = \left(0, n+\frac{M-1}{M+1}\right)$, $n = 0,1,\ldots$. Swapping $\alpha_+$ and $\alpha_-$ (using the $\lambda \to -\lambda$ symmetry) throughout gives level-crossings on the line $\alpha_- = 0$. Note that these level-crossings are exact as $\psi$ is protected by supersymmetry, and cannot mix with any other state. As soon as this supersymmetric line is left level mixing can occur. In $\mathcal{PT}$-symmetric systems, eigenvalues are all either real, or occur in complex-conjugate pairs. Complex eigenvalues can therefore only be formed via the intermediate coinciding of two (or more) previously-real eigenvalues. The supersymmetry on the lines $\alpha_+ = 0$ and $\alpha_- = 0$ provides a mechanism for this pairing-off to occur, and for the formation of the associated exceptional points [124]. Exceptional points occur in the spectrum of an eigenvalue problem whenever the coalescence of two or more eigenvalues is accompanied by a coalescence of the corresponding eigenvectors; at such points there is a branching of the spectral Riemann surface [127, 128, 129, 130]. For one-dimensional problems of the sort under discussion here, genuine degeneracies of levels are impossible – since the Wronskian of any two solutions which both decay in some asymptotic direction must vanish – and so levels in this problem can only coincide at exceptional points. Quadratic exceptional points must therefore exist at

$$(\alpha_+,\alpha_-) = \left(0, n+\frac{M-1}{M+1}\right) \quad \text{and} \quad (\alpha_+,\alpha_-) = \left(n+\frac{M-1}{M+1}, 0\right) \tag{5.4.8}$$

for $n \in \mathbb{N}$.

There is also a protected zero-energy level along the lines $\alpha_\pm = m \in \mathbb{N}$. Exceptionally, for $M = 3$ a similar line of argument can be applied here, using a higher-order supersymmetry to eliminate this zero energy level along with $2m$ others [66][124], which allows the positions of further quadratic exceptional points to be identified. As will become clear shortly, this is related to the fact that, for $M = 3$, the model is quasi-exactly solvable along these lines.

Specialising now to $M = 3$, the eigenproblem (5.2.1) becomes

$$\left(-\frac{d^2}{dz^2} + z^6 + \alpha z^2 + \frac{\lambda^2 - \frac{1}{4}}{z^2}\right)\Phi_k(z) = -E_k\Phi_k(z)\,, \quad \Phi_k(x) \in L^2(i\mathcal{C})\,. \tag{5.4.9}$$

If boundary conditions are imposed at $z = 0$ and $z = +\infty$, the problem (5.4.9) is quasi-exactly solvable whenever $\alpha$ and $\lambda$ are related by $\alpha = -(4J + 2\lambda)$ for some integer $J$, and $J$ energy levels can be computed exactly [131]. Bender and Dunne [132] found an elegant method to find the corresponding wavefunctions, square integrable along the positive real axis. The solutions to (5.4.9) must have this property along the contour $i\mathcal{C}$, but with minor modifications the approach of [132] can still be used. First, look for solutions of the form

$$\psi_\pm(z) = e^{\frac{z^4}{4}} z^{\pm\lambda+\frac{1}{2}} \sum_{n=0}^{\infty} a_n P_n(E) z^{2n} \tag{5.4.10}$$

where

$$a_n = \left(-\frac{1}{4}\right)^n \frac{1}{n!\,\Gamma(n + \pm\lambda + 1)}\,. \tag{5.4.11}$$

The functions $\psi_\pm(z)$ can be shown to solve (5.4.9) if the coefficients $P_n$ satisfy the recursion relation

$$P_n = -EP_{n-1} + 16(\alpha/4 \mp \lambda/2 - n + 1)(n - 1)(n - 1 \pm \lambda)P_{n-2}\,,\ n \geq 1 \tag{5.4.12}$$

with the condition that $P_m = 0$, $m < 0$. The normalisation is set by the initial condition $P_0 = 1$. If $\alpha/4 \mp \lambda/2 \equiv J$ is a positive integer, then the second term on the RHS of (5.4.12) vanishes for $n = J + 1$, and so $P_{J+1}(E)$ is proportional to $P_J(E)$, as are all subsequent coefficients $P_{m>J+1}(E)$. At a zero of $P_J(E)$ the series therefore terminates and the $J$ QES energy levels are found as those $E$ that satisfy $P_J(E) = 0$. Due to the choice of exponential prefactor in (5.4.10) (inverse to that in [132]), the corresponding $\psi_\pm(z)$ will automatically satisfy the revised boundary conditions. Note, since the boundary conditions are not being imposed at the origin, both signs of $\lambda$ lead to acceptable solutions.

For simplicity, choose $+\lambda$ in (5.4.10) so $\alpha = 4J + 2\lambda$ ($-\lambda$ can be recovered using the $\lambda \to -\lambda$ symmetry) and write $P_n$, for $n \geq J + 1$ as

$$P_{n+J} = P_J Q_n\,. \tag{5.4.13}$$

The $Q_n$ then satisfy the recursion relation

$$Q_n = -EQ_{n-1} + 16(1 - n)(n + J - 1)(n + J - 1 + \lambda)Q_{n-2} \tag{5.4.14}$$

with initial condition $Q_0 = 1$. This matches the $P_n$ relation if $J \to \widehat{J} = -J$, or alternatively, $\alpha_J \to \widehat{\alpha}_J = -\alpha_J/2 + 3\lambda$ and $\lambda \to \widehat{\lambda}_J = \alpha_J/4 + \lambda/2$. Then

$$Q_n(E, \alpha_J, \lambda) = P_n(E, \widehat{\alpha}_J, \widehat{\lambda}_J)\,. \tag{5.4.15}$$

This has an interesting consequence for the series expansion of (5.4.10), which can be seen by rewriting it as

$$\begin{aligned}\psi(z, E, \alpha_J, \lambda) &= e^{\frac{z^4}{4}} z^{\lambda+\frac{1}{2}} \left[\ldots + \sum_{n=J}^{\infty} \left(-\frac{1}{4}\right)^n \frac{P_n(E, \alpha_J, \lambda)}{n!\,\Gamma(n+\lambda+1)} z^{2n}\right] \\ &= e^{\frac{z^4}{4}} z^{\lambda+\frac{1}{2}} \left[\ldots + \sum_{n=0}^{\infty} \left(-\frac{1}{4}\right)^{n+J} \frac{P_J(E, \alpha_J, \lambda) Q_n(E, \alpha_J, \lambda)}{(n+J)!\,\Gamma(n+J+\lambda+1)} z^{2(n+J)}\right]\end{aligned} \tag{5.4.16}$$

where the dots represent lower order terms. Compare this with the expansion of $\psi(z, E, \widehat{\alpha}_J, \widehat{\lambda}_J)$:

$$\psi(z, E, \widehat{\alpha}_J, \widehat{\lambda}_J) = e^{\frac{z^4}{4}} z^{\widehat{\lambda}+\frac{1}{2}} \sum_{n=0}^{\infty} \left(-\frac{1}{4}\right)^n \frac{P_n(z, E, \widehat{\alpha}_J, \widehat{\lambda}_J)}{n!\,\Gamma(n+\widehat{\lambda}+1)} z^{2n} \tag{5.4.17}$$

which, using (5.4.15) and $\widehat{\lambda}_J = J + \lambda$ becomes

$$\psi(z, E, \widehat{\alpha}_J, \widehat{\lambda}_J) = e^{\frac{z^4}{4}} z^{\lambda+J+\frac{1}{2}} \sum_{n=0}^{\infty} \left(-\frac{1}{4}\right)^n \frac{Q_n(E, \alpha_J, \lambda)}{n!\,\Gamma(n+J+\lambda+1)} z^{2n}\,. \tag{5.4.18}$$

It now follows that $\psi(z, E, \alpha_J, \lambda)$ is mapped onto a function proportional to $\psi(z, E, \widehat{\alpha}_J, \widehat{\lambda}_J)$ by the differential operator

$$\begin{aligned}Q_J(\lambda) &= e^{\frac{z^4}{4}} z^{\lambda+J+\frac{1}{2}} \left(\frac{1}{z}\frac{d}{dz}\right)^J e^{-\frac{z^4}{4}} z^{-\lambda-\frac{1}{2}} \\ &= z^J \left(\frac{1}{z}\frac{d}{dz} - z^2 - \frac{2\lambda+1}{2z^2}\right)^J\,.\end{aligned} \tag{5.4.19}$$

It can therefore be shown that $Q_J(\lambda)$ maps the eigenfunctions of $H(\alpha_J, \lambda)$ to those of $H(\widehat{\alpha}_J, \widehat{\lambda}_J)$, or to zero [66]. The eigenfunctions which are mapped to zero are those for which $P_J(E, \alpha_J, \lambda)$ vanishes, which are precisely the QES levels. The operator $Q_J$ is therefore a generalisation of the supersymmetry operator $Q_+$ for $J > 1$.

The argument for the level-crossing along the $\alpha_\pm = 0$ lines can now be extended further for the $M = 3$ case [124]. In terms of the $\alpha_\pm$ notation, the QES levels occur at $(\alpha_+, \alpha_-) = (\alpha_+, \frac{1}{2}(J-1))$, for $J$ a positive integer, which in the dual problem (with the

QES states removed from the spectrum) becomes $(\widehat{\alpha}_+, \widehat{\alpha}_-) = (\alpha_+ - J/2, -\frac{1}{2}(J+1))$. Substituting this into $C|_{E=0}$ (5.4.6):

$$C(-E, \widehat{\alpha}_+, \widehat{\alpha}_-)|_{E=0,\widehat{\alpha}_-=-\frac{1}{2}(J+1)} = \left(\frac{M+1}{2}\right)^{\widehat{\alpha}_+ - \frac{1}{2}(J-1)} \frac{2\pi}{\Gamma(-\widehat{\alpha}_+)\Gamma(\frac{1}{2}(J+1))}$$
$$= \left(\frac{M+1}{2}\right)^{-\frac{1}{2}(J-1)+\widehat{\alpha}_+} \frac{2\pi}{\Gamma(-\alpha_+ + \frac{J}{2})\Gamma(\frac{1}{2}(J+1))} \tag{5.4.20}$$

which is zero when $\alpha_+ = J/2 + n$. Recall from above that the protected zero-energy levels lie on the lines $\alpha_\pm = m \in \mathbb{N}$ so if $\alpha_+ = m$, $J$ must be even and the quadratic exceptional points occur for

$$(\alpha_+, \alpha_-) = (m, n + \frac{1}{2}), \quad n, m \in \mathbb{N}. \tag{5.4.21}$$

Replacing $\lambda$ with $-\lambda$ in the above simply swaps $\alpha_\pm$, so there are also quadratic exceptional points at

$$(\alpha_+, \alpha_-) = (n + \frac{1}{2}, m), \quad n, m \in \mathbb{N}. \tag{5.4.22}$$

It is also worth noting that the levels which become complex at these exceptional points are always in the QES part of the spectrum. This is easy to show once it is noted that the 'dual' problems, with $(\widehat{\alpha}_+, \widehat{\alpha}_-) = (\alpha_+ - J/2, \frac{1}{2}(J+1))$, always lie in regions of the parameter space covered by the reality proof given above [124]. Since the spectrum of this dual problem is identical to that of the original, minus the QES levels, it is clear that the non-QES levels must always remain real. It also follows that the QES eigenvalues are symmetric about zero, i.e. both $E$ and $-E$ are contained in the QES sector of the spectrum.

Numerical investigations at $M = 3$, reported in [124], showed that the way in which the spectrum of (5.1.4) becomes complex has considerably more structure than (5.1.5) might suggest. The curved, cusped line of figure 5.4 is a line of exceptional points which indicates where the first pair of complex eigenvalues is formed as the region of reality is left; it only touches the dotted lines $\alpha_\pm = 0$ at the isolated points given in (5.4.8), but it will be shown that the smooth segments are quadratic exceptional points, where two levels coalesce, while the cusps themselves are cubic points.

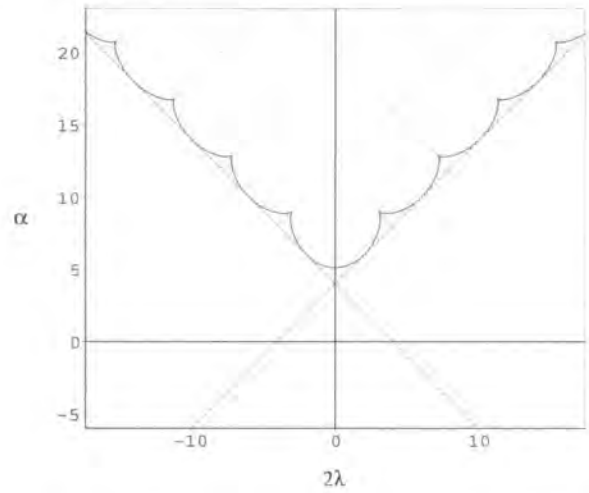


Figure 5.4: The domain of unreality in the $(2\lambda, \alpha)$ plane for $M = 3$, with portions of lines with protected zero-energy levels also shown. The horizontal axis is $2\lambda = 2l + 1$.

The additional dotted lines in figure 5.4 are the lines $\alpha_{\pm} \in \mathbb{N}$. As mentioned earlier, the model has a protected zero-energy level, and for $M = 3$, is also quasi-exactly solvable along these lines. It is worth noting that the cusps in figure 5.4 appear to lie exactly on these lines, to within numerical accuracy.

If one asks when a second pair of complex eigenvalues is formed, and so on, figure 5.5 is obtained, again for $M = 3$. This plot is adapted from [50]; the same pattern was independently found by Sorrell [133] via a complex WKB treatment of the problem. Note the pattern of cusps is repeated, with the cusps again lying on lines of protected zero-energy levels, and the curve touching the lines $\alpha_{\pm} = m \in \mathbb{N}$ at the points given in (5.4.21) and (5.4.22).

The analysis of [124] left a number of questions open. While the merging and subsequent complexification of levels is suggestive of exceptional points and a Jordan block structure for the Hamiltonian, this has not been demonstrated explicitly. The apparent siting of the cusps on lines with simultaneous quasi-exact solvability and protected zero-energy levels has not been proved; in particular, it is not clear whether this feature should be associated with the zero-energy level (in which case it should persist for $M \neq 3$) or with the quasi-exact solvability (in which case it might be lost for $M \neq 3$). Finally, and connected with this last question, the general pattern away from $M = 3$ has not been explored.

These issues are addressed in the rest of this chapter. For $M = 3$ the positions

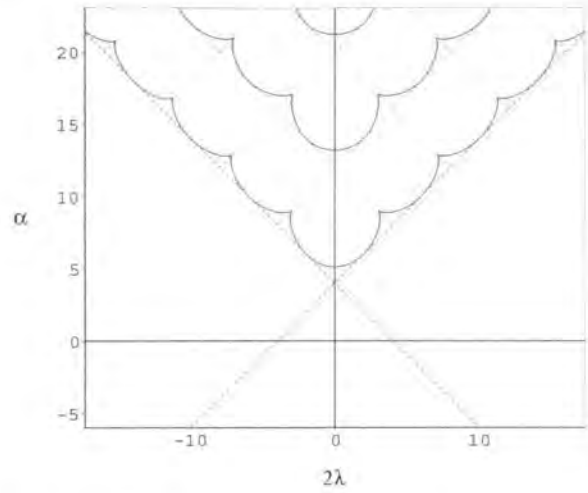


Figure 5.5: The $(2\lambda, \alpha)$ plane for $M = 3$, showing lines across which further pairs of complex eigenvalues are formed.

of the cusps are investigated, and it will be proved that they do indeed lie on QES lines. The exceptional points in the spectrum will be examined and the Jordan form at such points found. Finally, the situation for $M \neq 3$ will be explored numerically, and the picture that emerges will be verified with a perturbative study near $M = 1$. This work can be found in [2]

## 5.5 The M = 3 problem revisited – cusps and QES lines

The first question to be addressed is what are the exact locations of the cusps? As shown above, the levels which become complex at exceptional points are always in the QES part of the spectrum, so the cubic exceptional points arise when three zero-energy levels appear in the QES sector of the spectrum. Since these eigenvalues are symmetric about $E = 0$, this occurs for odd $J$, and it is precisely this symmetry that constrains the cusp to lie exactly on QES lines. Figure 5.6 shows a surface plot of the energy levels for $(2\lambda, \alpha)$ in the vicinity of the cusp at $(2\lambda, \alpha) = (-3, 9)$ (or $(\alpha_+, \alpha_-) = (\frac{1}{4}, 1)$). This shows the merging of two energy levels (at the bottom right and top left of the plot) and then the cusp being formed in the centre of the plot where three energy levels merge at a single point. The superimposed line indicates

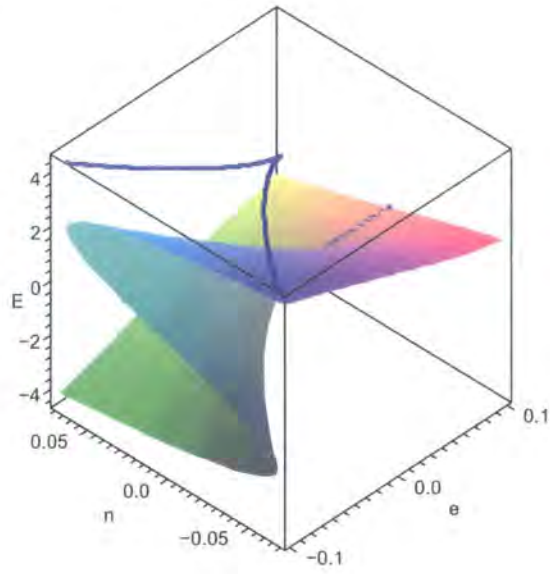


Figure 5.6: Surface plot of energy levels in the vicinity of the first cusp at $(2\lambda, a) = (-3, 9)$, or $(\alpha_+, \alpha_-) = (\frac{1}{4}, 1)$. The axes are $\epsilon = \alpha_+ - \frac{1}{4}$, $\eta = 1 - \alpha_-$ and $E$. The superimposed line indicates the merging of levels.

the merging of levels and the $E = 0$ line is also included.

The exact locations of the cusps can be found by examining the Bender-Dunne polynomials $P_J(E)$. For odd values of $J$, these polynomials split into a polynomial in $E^2$ multiplied by an overall factor of $E$, the first two being

$$P_3(E) = -E(E^2 + 96 \pm 64\lambda) \tag{5.5.1}$$

$$P_5(E) = -E(E^4 + 320(\pm\lambda + 5/2)E^2 + 2048(8\lambda^2 + 40\lambda + 41)) \,. \tag{5.5.2}$$

It follows that there will be three zero-energy levels whenever

$$\left.\frac{P_J(E)}{E}\right|_{E=0} = 0 \,. \tag{5.5.3}$$

Swapping to the notation $\alpha_\pm$, the cusp positions for positive values of $\lambda$ (which corresponds to taking $-\lambda$ in (5.4.10)) lie on the lines $\alpha_+ = (J-1)/2 = \mathbb{N}^+$, each line having precisely $\alpha_+$ cusps. Using the Bender-Dunne relation (5.4.12), the constraint (5.5.3) is equivalent to $Q_{\alpha_+}(\alpha_-) = 0$ where $Q_n$ satisfies the first order recurrence relation

$$\begin{aligned} Q_n(\alpha_-) = \prod_{j=1}^{n} &(2j-1)(2j-2\alpha_+-2)(2j+2(\alpha_- - \alpha_+)-1) \\ &+4n(2n-2\alpha_+-1)(n+\alpha_- - \alpha_+))Q_{n-1}(\alpha_-) \end{aligned} \tag{5.5.4}$$

| $\alpha_+$ | $\alpha_-$ |
|---|---|
| 1 | $\frac{1}{4}$ |
| 2 | $\frac{3}{4} \pm \frac{3\sqrt{2}}{8}$ |
| 3 | $\frac{5}{4}, \frac{5}{4} \pm \frac{\sqrt{70}}{8}$ |
| 4 | $\frac{7}{4} \pm \frac{\sqrt{86+5\sqrt{190}}}{8}, \frac{7}{4} \pm \frac{\sqrt{86-5\sqrt{190}}}{8}$ |
| 5 | $\frac{9}{4}, \frac{9}{4} \pm \frac{\sqrt{170+7\sqrt{214}}}{8}, \frac{9}{4} \pm \frac{\sqrt{170-7\sqrt{214}}}{8}$ |

Table 5.1: Location of some of the cusps in the $(\alpha_+, \alpha_-)$-plane for $M = 3$.

with $Q_0(\alpha_-) = 1$. Solving the recursion relation (5.5.4) gives

$$Q_{\alpha_+}(\alpha_-) = {}_3F_2([\tfrac{1}{2}, -\alpha_+, \tfrac{1}{2} + \alpha_- - \alpha_+], [\tfrac{1}{2} - \alpha_+, 1 + \alpha_- - \alpha_+], 1) \prod_{j=1}^{\alpha_+} (j + \alpha_- - \alpha_+) \,, \tag{5.5.5}$$

which is a polynomial in $\alpha_-$ of degree $\alpha_+$. Mapping back to the variables

$$(\lambda, \alpha) = (\pm 2(\alpha_+ - \alpha_-), 4(1 + \alpha_+ + \alpha_-)) \,, \tag{5.5.6}$$

the zeros of $Q_{\mathbb{N}^+}(\alpha_-) = 0$ match all the cusp positions shown in figure 5.5, to within the numerical accuracy. Table 5.1 shows the location of the first few cusps. Having located the exceptional points, the next step if to show their Jordon block explicitly.

## 5.6 The Jordan block at an exceptional point

At an exceptional point, the Hamiltonian can be arranged so that it contains an $n \times n$ Jordan block, where $n$ is the number of merging levels: two for the quadratic exceptional points, and three for the cubic ones. In general it is hard to see this explicitly, since the eigenfunctions of (5.4.9) cannot be found exactly. However for $M = 3$, the fact that the model is quasi-exactly solvable (QES) on the lines $\alpha_\pm \in \mathbb{N}$ can be exploited. Furthermore, as explained above, any levels which coalesce and become complex on these lines must lie in the QES sector of the model. Near to the exceptional points on the QES lines it is therefore a good approximation to truncate the Hilbert space to that part of the QES sector which contains the coalescing levels. This will be used to see the Jordan blocks for the first quadratic and cubic exceptional points.

To do this, begin with the Hamiltonian, $H_0$, at the exceptional point, and restrict to the space of states which merge at this point. Then perturb about this point,

along the QES line by writing the full Hamiltonian, $H_p$ as $H_p = H_0 + V$. The aim is to expand $H_p$, using the wavefunctions of $H_0$ as a basis, i.e. one needs to calculate

$$H_{mn} = \langle\tilde{\phi}_m|H_p|\phi_n\rangle = \langle\tilde{\phi}_m|H_0|\phi_n\rangle + \langle\tilde{\phi}_m|V|\phi_n\rangle \tag{5.6.1}$$

where $\{\phi_m, \phi_n\}$ is the basis for the Jordan block form of $H_0$, and $\{\tilde{\phi}_m, \tilde{\phi}_n\}$ is the appropriate dual basis. The expectation is that the eigenvalues of $H_{mn}$, to leading order, will correspond to the eigenvalues of the the merging QES states. Before $H_{mn}$ can be calculated, the appropriate basis for $H_0$ must be found. A general method for finding such a basis, in cases where a suitable one-parameter family of eigenfunctions is known exactly as the exceptional point is approached is, outlined below

### 5.6.1 Basis for an $n \times n$ Jordan block

To illustrate a method that can be used to construct the basis of an $n \times n$ Jordan block, which arises when $n$ eigenstates merge, the following toy model will be employed. Take an $n \times n$ matrix $L$, depending on one parameter $\epsilon$:

$$L(\epsilon) = \begin{pmatrix} 0 & 1 & 0 & \dots \\ \vdots & \ddots & \ddots & 0 \\ 0 & \dots & 0 & 1 \\ \epsilon & 0 & \dots & 0 \end{pmatrix}. \tag{5.6.2}$$

This has $n$ independent eigenvectors

$$\psi_j = \begin{pmatrix} 1 \\ e^{(2\pi ij/n)}\epsilon^{1/n} \\ e^{(4\pi ij/n)}\epsilon^{2/n} \\ \vdots \\ e^{2\pi(n-1)ij/n}\epsilon^{(n-1)/n} \end{pmatrix}, \; j = 1 \dots n. \tag{5.6.3}$$

When $\epsilon = 0$, $L(\epsilon)$ has a Jordan block form, but at this point all $n$ eigenvectors $\psi_j$ become equal and so no longer form a basis. A new basis must therefore be constructed, consisting of the vectors $\psi^{(k)}$, $k = 0 \dots n-1$ which satisfy

$$L(\epsilon)\psi^{(0)}\big|_{\epsilon=0} = 0 \tag{5.6.4}$$

$$L(\epsilon)\psi^{(k)}\big|_{\epsilon=0} = \psi^{(k-1)}\big|_{\epsilon=0}, \; k = 1 \dots n-1. \tag{5.6.5}$$

For simplicity, begin with the eigenvector $\psi_n$ where

$$L(\epsilon)\psi_n(\epsilon) = \epsilon^{1/n}\psi_n(\epsilon). \tag{5.6.6}$$

Clearly $\psi^{(0)} = \psi_n(\epsilon)$ satisfies the first condition (5.6.4) above. Choosing $\psi^{(0)}$ to be another $\psi_j$ here should work equally well but would need a different normalisation for $\psi^{(k)}$ below.

Before the other basis vectors are constructed, it is convenient to introduce some notation. Let

$$D \equiv n\epsilon^{\frac{n-1}{n}}\frac{d}{d\epsilon} \tag{5.6.7}$$

and

$$\tilde{L} \equiv \frac{dL}{d\epsilon}. \tag{5.6.8}$$

Note that $L$ is linear in $\epsilon$ so $\frac{d\tilde{L}}{d\epsilon} = 0$. $D$ and $L$ satisfy the following commutation relations

$$[D, \epsilon^{k/n}] = k\epsilon^{(k-1)/n} \tag{5.6.9}$$

$$[D, L] = n\epsilon^{(n-1)/n}\tilde{L} \tag{5.6.10}$$

$$[D, \tilde{L}] = 0. \tag{5.6.11}$$

Finally, define

$$\psi^{(k+1)} \equiv \frac{1}{k+1}D\psi^{(k)}. \tag{5.6.12}$$

By induction, it is easy to show that acting with $D$ on (5.6.6) $k$ times for $1 \leq k \leq n-1$ gives

$$\sum_{j=0}^{k-1}\prod_{i=0}^{j}\frac{(n-i)}{(j+1)!}\epsilon^{\frac{n-j-1}{n}}\tilde{L}\psi^{(k-j-1)} + L\psi^{(k)} = \psi^{(k-1)} + \epsilon^{\frac{1}{n}}\psi^{(k)}. \tag{5.6.13}$$

When $\epsilon = 0$ this satisfies (5.6.5), so an appropriate basis is

$$\psi^{(0)} = \psi_n \tag{5.6.14}$$

and

$$\psi^{(k)} = \frac{1}{k}D\psi^{(k-1)} \tag{5.6.15}$$

for $k = 1\ldots, n-1$. Recall that $\psi_n$ was chosen for simplicity here, but other $\psi_j$ should work equally well with some changes to normalisations.

### 5.6.2 A quadratic exceptional point

The method outlined above will now be used to show the existence of a Jordan block in the Hamiltonian for the first quadratic exceptional point.

Recall that the quadratic exceptional points occur at even values of $J$ so let $J = 2$, and take $+\lambda$ in (5.4.10) so $J \equiv \alpha/4 - \lambda/2$. Then $\alpha = 2\lambda + 8$ and the eigenvalue problem is now

$$\left(-\frac{d^2}{dz^2} + z^6 + (2\lambda + 8)z^2 + \frac{\lambda^2 - \frac{1}{4}}{z^2} + E\right)\psi = 0. \tag{5.6.16}$$

In the $\alpha_\pm$ notation from (5.4.1), this corresponds to $\alpha_+ = \frac{1}{2}(\lambda + 1)$ and $\alpha_- = 1/2$. Let $\lambda = 2\epsilon - 1$, then the exceptional point occurs when $\epsilon = 0$. This is the point at which two levels merge and the Hamiltonian can be written in a Jordan block form.

At this point the recursion relation for $P_n$, (5.4.12), becomes

$$P_n = -EP_{n-1} + 16(3 - n)(n - 1)(n + 2\epsilon - 2)P_{n-2} \tag{5.6.17}$$

which terminates when $n = 3$. The energy eigenvalues of the two QES levels are given by the roots of $P_2$: $E_\pm = \pm i\sqrt{32\epsilon} = \pm 4\sqrt{-2\epsilon}$. The corresponding eigenstates, from (5.4.10), are

$$\Psi_\pm = ae^{\frac{z^4}{4}} z^{2\epsilon - \frac{1}{2}} \sqrt{2\epsilon}\left(1 \mp \frac{iz^2}{\sqrt{2\epsilon}}\right) \tag{5.6.18}$$

where $\Psi_\pm = \psi_+^{eq.(5.4.10)}|_{E_\pm}$ and $a$ is some normalisation constant to be determined later. The Jordan form of the Hamiltonian can be seen by working with the basis [129]

$$\begin{aligned} \phi^{(0)} &= \Psi_+|_{\epsilon=0} = -aie^{z^4/4} z^{3/2} \\ \phi^{(1)} &= 2b\sqrt{\epsilon}\frac{d\Psi_+}{d\epsilon}\bigg|_{\epsilon=0} = ab\sqrt{\frac{2}{z}} e^{z^4/4} \end{aligned} \tag{5.6.19}$$

with $b$ another normalisation constant. The unperturbed Hamiltonian is

$$H_0 = -\frac{d^2}{dz^2} + \frac{3}{4z^2} + 6z^2 + z^6 \tag{5.6.20}$$

and in order to satisfy the requirements $H_0\phi^{(0)} = 0$ and $H_0\phi^{(1)} = \phi^{(0)}$, $b$ is fixed to be $b = -\frac{i}{4\sqrt{2}}$. Note, however, that this basis is not unique as the basis $\{\alpha\phi^{(0)}, \alpha\phi^{(1)} + \beta\phi^{(0)}\}$ also satisfies the Jordan block constraints for any constants $\alpha$ and $\beta$. The general Jordan basis, in this case, is therefore given by

$$\phi_0 = -i\alpha e^{z^4/4} z^{3/2} \tag{5.6.21}$$

$$\phi_1 = e^{z^4/4}\left(-\frac{i\alpha}{4\sqrt{z}} + \beta z^{3/2}\right). \tag{5.6.22}$$

The integrals $\int_\gamma \phi_m\phi_n\,dz$, $\{m,n\}\in\{0,1\}$, must now be calculated in order to fix these constants and to identify the relevant dual basis $\{\tilde\phi_m,\tilde\phi_n\}$, which must satisfy $\int_\gamma \phi_0\tilde\phi_0\,dz = \int_\gamma \phi_1\tilde\phi_1\,dz = 1$ and $\int_\gamma \phi_0\tilde\phi_1\,dz = \int_\gamma \phi_1\tilde\phi_0\,dz = 0$. The contour, here and in subsequent calculations, is taken to be $\gamma = -\gamma_{-1}+\gamma_0+\gamma_1$, where $\gamma_\pm(t) = t\exp(\pm i\pi/4)$, $\varepsilon\le t\le\infty$, $\gamma_0 = \varepsilon e^{it}$, $-\pi/4\le t\le\pi/4$ and $\varepsilon$ is a small positive number which avoids any singularities at $z=0$. The integrals are given by

$$\int_\gamma \phi_0\phi_0\,dz = -\alpha^2\int_\gamma e^{z^4/2}z^3\,dz = 0 \tag{5.6.23}$$

$$\int_\gamma \phi_0\phi_1\,dz = \int_\gamma e^{z^4/2}\left(-\frac{\alpha^2 z}{4}-i\alpha\beta z^3\right)dz = -\frac{i\alpha^2}{8}\sqrt{2\pi} \tag{5.6.24}$$

$$\int_\gamma \phi_1\phi_1\,dz = \int_\gamma e^{z^4/2}\left(-\frac{\alpha^2}{16z}-\frac{i\alpha\beta z}{2}+\beta^2 z^3\right) = \frac{\alpha}{4}\left(\beta\sqrt{2\pi}-\frac{i\alpha\pi}{8}\right) \tag{5.6.25}$$

Fixing $\int_\gamma \phi_1\phi_1\,dz = 0$ sets $\beta$ to

$$\beta = \frac{i\alpha}{8}\sqrt{\frac{\pi}{2}} \tag{5.6.26}$$

and the requirement that $\int_\gamma \phi_0\phi_1\,dz = 1$ sets $\alpha$ to

$$\alpha = (1+i)\left(\frac{8}{\pi}\right)^{1/4}. \tag{5.6.27}$$

The basis is now fixed and the dual basis can be taken to be $\tilde\phi_0 = \phi_1$ and $\tilde\phi_1 = \phi_0$.

The full Hamiltonian is $H_p = H_0 + V$ where $V = \frac{4\epsilon(\epsilon-1)}{z^2} + 4\epsilon z^2$, so $H_{mn}$ must now be calculated, where

$$\begin{aligned} H_{mn} &= \langle\tilde\phi_m|H_p|\phi_n\rangle \\ &= \langle\tilde\phi_m|H_0|\phi_n\rangle + 4\epsilon(\epsilon-1)\langle\tilde\phi_m|z^{-2}|\phi_n\rangle + 4\epsilon\langle\tilde\phi_m|z^2|\phi_n\rangle \end{aligned} \tag{5.6.28}$$

with $\{\phi_m,\phi_n\} = \{\phi_0,\phi_1\}$ from above. The aim here is to find the eigenvalues of $H_p$, to leading order only. If $\langle\tilde\phi_1|V|\phi_0\rangle \sim a_{10}\epsilon$, for some coefficient $a_{10}$ then to leading order $E_{p;\pm}\approx\pm\sqrt{a_{10}\epsilon}$, so no other matrix elements need to be considered. This is the case here as $\langle\tilde\phi_1|V|\phi_0\rangle$, for $V = \frac{4\epsilon(\epsilon-1)}{z^2} + 4\epsilon z^2$ is given by

$$\langle\tilde\phi_1|V|\phi_0\rangle = 16\epsilon(\epsilon-2)\approx -32\epsilon\,. \tag{5.6.29}$$

Therefore, to leading order

$$E_{p;\pm}\approx\pm 4\sqrt{-2\epsilon} \tag{5.6.30}$$

which are equal to the QES eigenvalues $E_\pm$, as expected.

### 5.6.3 A cubic exceptional point

The first cubic exceptional point occurs when $J = 3$ and $\alpha = 2\lambda + 12$. In the $\alpha_\pm$ notation, this corresponds to $(\alpha_+, \alpha_-) = (1 + \lambda/2, 1)$, but in table 5.1 the position of the first cusp is given as $(\alpha_+, \alpha_-) = (1/4, 1)$ (note $\alpha_+$ and $\alpha_-$ have been exchanged here using the $\lambda \to -\lambda$ symmetry). If $\lambda = 2\epsilon - 3/2$, this point then corresponds to $\epsilon = 0$. The eigenvalue problem, in terms of $\epsilon$ is

$$\left(-\frac{d^2}{dz^2} + \frac{(4\epsilon - 2)(4\epsilon - 4)}{4z^2} + (4\epsilon + 9)z^2 + z^6 + E\right)\psi = 0 \tag{5.6.31}$$

and the recursion relation for $P_n$ is

$$P_n = -EP_{n-1} + 16(4 - n)(n - 1)(n + 2\epsilon - 5/2)P_{n-2}. \tag{5.6.32}$$

The roots of $P_3$ give the energy eigenvalues of the three QES levels: $E_0 = 0$, $E_\pm = \pm 8\sqrt{-2\epsilon}$. The corresponding eigenstates are

$$\begin{aligned} \Psi_0 &= e^{z^4/4} z^{2\epsilon-1} a \left(1 + \frac{2z^4}{4\epsilon + 1}\right) \\ \Psi_\pm &= e^{z^4/4} z^{2\epsilon-1} a \left(1 \mp \frac{4\sqrt{-2\epsilon}z^2}{4\epsilon - 1} - \frac{2z^4}{4\epsilon - 1}\right) \end{aligned} \tag{5.6.33}$$

where $a$ is some normalisation to be fixed later. Note that when $\epsilon = 0$ the 3 QES eigenstates above merge and so there is only one known eigenstate at this point, namely

$$\Psi_0|_{\epsilon=0} = a\, e^{z^4/4} \left(\frac{1}{z} + 2z^3\right). \tag{5.6.34}$$

Moving away from the cusp, along the QES line, the perturbed Hamiltonian would correspond to a toy model matrix of the form

$$L(\epsilon) = \begin{pmatrix} 0 & 1 & 0 \\ \epsilon/2 & 0 & 1 \\ 0 & \epsilon/2 & 0 \end{pmatrix}. \tag{5.6.35}$$

This is not the form discussed earlier in section 5.6.1 and in fact, to use the method described there to find the Jordan basis one would need to know the eigenfunctions of the Hamiltonian along the line perpendicular to this QES line. Unfortunately, as these functions are not known analytically the basis functions will have to be found by solving the constraints directly. The relevant basis $\phi_0$, $\phi_1$ and $\phi_2$ must satisfy

$$\begin{aligned} H_0\phi_0 &= 0 \\ H_0\phi_1 &= \phi_0 \\ H_0\phi_2 &= \phi_1 \end{aligned} \tag{5.6.36}$$

where $H_0$ is the Hamiltonian at the cusp

$$H_0 = -\frac{d^2}{dz^2} + z^6 + 9z^2 + \frac{2}{z^2}. \tag{5.6.37}$$

Note that $H_0\,\Psi_0|_{\epsilon=0} = 0$ so one can take $\phi_0 = \Psi_0|_{\epsilon=0}$. Then solving (5.6.36) for $\phi_1$ and $\phi_2$, using maple, gives

$$\begin{aligned} \phi_1 &= e^{z^4/4}\left(\frac{az}{2} + b\left(\frac{1}{z} + 2z^3\right)\right) \\ \phi_2 &= e^{z^4/4}\left(\frac{a}{16z} + \frac{bz}{2} + c\left(\frac{1}{z} + 2z^3\right)\right) \end{aligned} \tag{5.6.38}$$

with $a$, $b$ and $c$ constants. These are not the most general solutions to (5.6.36) as a term proportional to $e^{-z^4/4}$ can be added to both but as this term does not satisfy the boundary conditions it is not included here.

Now that a basis has been constructed, the corresponding dual basis, $\tilde{\phi}_0$, $\tilde{\phi}_1$ and $\tilde{\phi}_2$, must be found which satisfies

$$\begin{aligned} \int_\gamma \phi_i\tilde{\phi}_i\,dz &= 1\,, \text{ for } i = 0,1,2 \\ \int_\gamma \phi_i\tilde{\phi}_j\,dz &= 0\,, \text{ for } i \neq j. \end{aligned} \tag{5.6.39}$$

From [129] this dual basis is expected to be $\tilde{\phi}_0 = \phi_2$, $\tilde{\phi}_1 = \phi_1$ and $\tilde{\phi}_2 = \phi_0$ and this is supported by the fact that $\int_\gamma \phi_0\phi_0\,dz = \int_\gamma \phi_0\phi_1\,dz = 0$ and $\int_\gamma \phi_1\phi_1\,dz \propto a^2$. Fixing $\int_\gamma \phi_2\phi_2\,dz = 0$ and $\int_\gamma \phi_1\phi_2\,dz = 0$ constrains the coefficients $b$ and $c$ to be

$$\begin{aligned} b &= -\frac{a\pi}{16\Gamma(3/4)^2} \\ c &= \frac{a(3\pi^2 - 8\Gamma(3/4)^4)}{512\Gamma(3/4)^4}. \end{aligned} \tag{5.6.40}$$

Then requiring $\int_\gamma \phi_1\phi_1\,dz = \int_\gamma \phi_0\phi_2\,dz = 1$ fixes $a^2$:

$$a^2 = -\frac{2^{11/4}i}{\Gamma(3/4)}. \tag{5.6.41}$$

Choosing the root with positive real part for $a$, the basis is fixed to be

$$\begin{aligned} \phi_0 &= \frac{(1-i)2^{7/8}}{\sqrt{\Gamma\left(\frac{3}{4}\right)}}e^{z^4/4}\left(\frac{1}{z} + 2z^3\right) \\ \phi_1 &= \frac{(i-1)2^{7/8}}{16\Gamma\left(\frac{3}{4}\right)^{5/2}}e^{z^4/4}\left(\frac{\pi}{z} - 8z\Gamma\left(\frac{3}{4}\right)^2 + 2\pi z^3\right) \\ \phi_2 &= \frac{(1-i)2^{7/8}}{512\Gamma\left(\frac{3}{4}\right)^{9/2}}e^{z^4/4}\left(\frac{24\Gamma\left(\frac{3}{4}\right)^4 + 3\pi^2}{z} - 16\pi\Gamma\left(\frac{3}{4}\right)^2 z + 6\pi^2 z^3 - 16\Gamma\left(\frac{3}{4}\right)^4 z^3\right) \end{aligned} \tag{5.6.42}$$

with the dual basis $\tilde{\phi}_0 = \phi_2$, $\tilde{\phi}_1 = \phi_1$ and $\tilde{\phi}_2 = \phi_0$.

As in the quadratic case, not all matrix elements need to be calculated in order to find the eigenvalues to leading order. If $\langle\tilde{\phi}_2|V|\phi_0\rangle \sim a_{20}\epsilon$ then the eigenvalues are given by this alone:

$$E_{p;j} \approx (a_{20}\epsilon)^{1/3} e^{\frac{2\pi i j}{3}} + O(\epsilon^{2/3}) \text{ for } j = 0, 1, 2. \tag{5.6.43}$$

If, however, $\langle\tilde{\phi}_2|V|\phi_0\rangle \sim \epsilon^2$ but $\langle\tilde{\phi}_1|V|\phi_0\rangle = \langle\tilde{\phi}_2|V|\phi_1\rangle \sim a_{10}\epsilon$ then to leading order

$$E_{p;0} \approx 0 + O(\epsilon) \tag{5.6.44}$$

$$E_{p;\pm} \approx \pm\sqrt{2a_{10}\epsilon} + O(\epsilon). \tag{5.6.45}$$

One should begin, therefore, by calculating $\langle\tilde{\phi}_2|V|\phi_0\rangle$ which, for $V = \frac{4\epsilon^2-6\epsilon}{z^2} + 4\epsilon z^2$, is given by

$$\langle\tilde{\phi}_2|V|\phi_0\rangle = \frac{128\pi\epsilon^2}{3\Gamma\left(\frac{3}{4}\right)^2}. \tag{5.6.46}$$

Since this is of order $\epsilon^2$, $\langle\tilde{\phi}_1|V|\phi_0\rangle = \langle\tilde{\phi}_2|V|\phi_1\rangle$ is also needed:

$$\begin{aligned}\langle\tilde{\phi}_1|V|\phi_0\rangle &= \langle\tilde{\phi}_2|V|\phi_1\rangle \\ &= -\frac{8\epsilon}{3\Gamma\left(\frac{3}{4}\right)^4}\left(24\Gamma\left(\frac{3}{4}\right)^4 - 12\Gamma\left(\frac{3}{4}\right)^4\epsilon + \pi^2\epsilon\right) \\ &\approx -64\epsilon.\end{aligned} \tag{5.6.47}$$

The eigenvalues can now be written down as

$$\begin{aligned}E_{p;0} &\approx O(\epsilon) \\ E_{p;\pm} &\approx \pm 8i\sqrt{2\epsilon} + O(\epsilon)\end{aligned} \tag{5.6.48}$$

which for small $\epsilon$ correspond to the QES eigenvalues given above.

To investigate the shape of this cusp it is also necessary to perturb away from the exceptional point in the direction perpendicular to the QES line, i.e. along $\eta$ where $\alpha = -4\eta + 9$ and $\lambda = 2\eta - 3/2$, or $\alpha_+ = 1/4$ and $\alpha_- = -\eta + 1$. The Hamiltonian is now

$$H_{p'} = -\frac{d^2}{dz^2} + z^6 + (-4\eta + 9)z^2 + \frac{(2\eta - 2)(2\eta - 1)}{z^2} \tag{5.6.49}$$

which will be considered as a perturbation of $H_0$, $H_{p'} = H_0 + V'$, with $V' = -4\eta z^2 + \frac{4\eta^2-6\eta}{z^2}$. The matrix element $\langle\tilde{\phi}_2|V'|\phi_0\rangle$ is found to be:

$$\langle\tilde{\phi}_2|V'|\phi_0\rangle = \frac{128\eta\pi(\eta - 3)}{3\Gamma\left(\frac{3}{4}\right)^2} \approx -\frac{128\pi\eta}{\Gamma\left(\frac{3}{4}\right)^2} \tag{5.6.50}$$

and since this is of order $\eta$ there is no need to calculate any more terms to find the eigenvalues, which are given by

$$E_{p';j} \approx 4\left(-\frac{2\pi}{\Gamma(3/4)^2}\right)^{1/3} e^{\frac{2\pi ij}{3}}\eta^{1/3} + O(\eta^{2/3}), \text{ for } j = 0, 1, 2. \tag{5.6.51}$$

A matrix which has eigenvalues (5.6.48) and (5.6.51) in the limits $\eta \to 0$ and $\epsilon \to 0$ respectively, to leading order is

$$\begin{pmatrix} 0 & 1 & 0 \\ -64\epsilon & 0 & 1 \\ -\frac{128\pi\eta}{\Gamma(3/4)^2} & -64\epsilon & 0 \end{pmatrix}. \tag{5.6.52}$$

This has the characteristic polynomial $X^3 + 128\epsilon X + \frac{128\pi\eta}{\Gamma(3/4)^2} = 0$. Now the curve of exceptional points occurs when $dX/d\epsilon \to \infty$ (or equivalently $dX/d\eta \to \infty$). Since

$$\frac{dX}{d\epsilon} = \frac{-128X}{3X^2 + 128\epsilon} \tag{5.6.53}$$

the requirement $dX/d\epsilon \to \infty$ fixes

$$X = \pm\sqrt{-\frac{128\epsilon}{3}}. \tag{5.6.54}$$

Substituting this into the characteristic polynomial above and restricting to $\epsilon \leq 0$ gives the following relation between $\eta$ and $\epsilon$:

$$\eta = \pm\frac{2}{3}\sqrt{\frac{128}{3}}\frac{\Gamma(3/4)^2}{\pi}|\epsilon|^{3/2}. \tag{5.6.55}$$

For $\epsilon > 0$ the relation (5.6.54) is not real indicating that there are no exceptional points in this region, which matches with the numerical results. In terms of the $\alpha_\pm$ notation, $\alpha_+ = \epsilon + 1/4$ and $\alpha_- = -\eta + 1$ so this relation becomes:

$$\alpha_- = 1 \pm \frac{2}{3}\sqrt{\frac{128}{3}}\frac{\Gamma(3/4)^2}{\pi}(1/4 - \alpha_+)^{3/2} \tag{5.6.56}$$

which is valid for $\alpha_-$ close to 1 and $0 << \alpha_+ \leq 1/4$.

A comparison between the prediction (5.6.56) and numerical data is shown in figure 5.7. A surface plot of the energy levels in the vicinity of this cusp, given by solutions to the characteristic polynomial above, is shown in figure 5.6, along with the shape of the cusp given by (5.6.56).

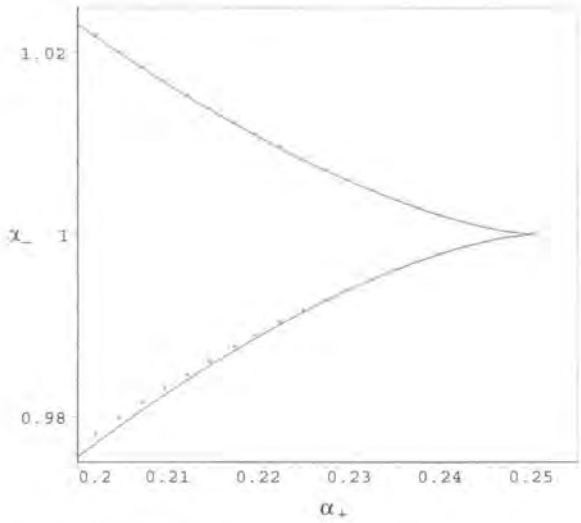


Figure 5.7: The shape of the cusp for $M = 3$. The crosses are the prediction (5.6.56) and the solid line is the numerical result.

## 5.7 Numerical results for $1 < M < 3$

Having established the existence of quadratic and cubic exceptional points at $M = 3$, the situation at other values of $M$ will now be explored. There is a theorem, due to Whitney [134], which states that fold and cusp singularities (corresponding to the curves of exceptional points seen at $M = 3$) are the only singularities that are stable under perturbation, so this pattern of cusped lines must persist, at least while $M$ is close to 3. Recall also that protected zero-energy levels lie on the lines $\alpha_\pm = n$ for all values of $M$. However, away from $M = 3$ quasi-exact solvability is lost, and so one of the properties which confined the cusps at $M = 3$ to the protected lines $\alpha_\pm = n$, namely the symmetry of the set of merging levels under $E \to -E$, may no longer hold.

Figures 5.8, 5.9 and 5.10 show the cusped lines for $M = 2$, 1.5 and 1.3. The plots were obtained by a direct numerical solution of the ODE.

As predicted, the overall pattern remains the same, but the cusps move away from the protected zero-energy lines. The points where the outermost cusped line touches the supersymmetric zero-energy lines $\alpha_\pm = 0$ are known exactly, from (5.4.8). As $M$ decreases from 3, they move down from the midpoints between $\alpha_\mp = n$ and $\alpha_\mp = n+1$ along the lines $\alpha_\pm = 0$. At the same time, the numerical data appears to show the

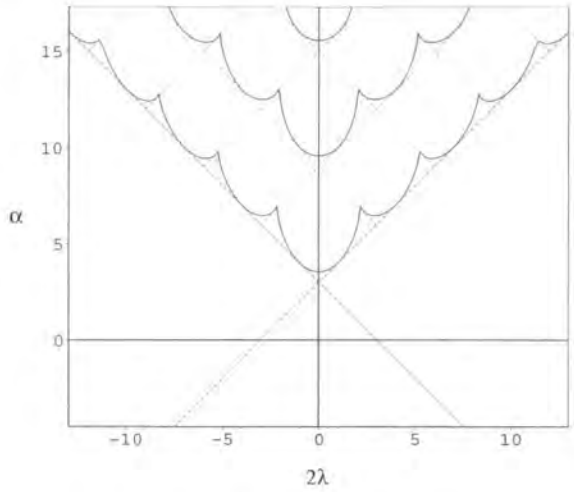


Figure 5.8: Cusps for $M = 2$.

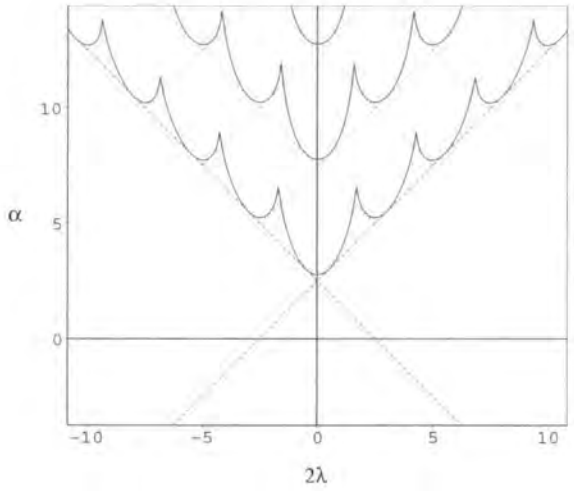


Figure 5.9: Cusps for $M = 1.5$.

cusps moving upwards, at least on the rescaled coordinates of the plots, which keep the lines of protected zero-energy levels at constant locations. To investigate this further, the next section explores the pattern of lines for $M = 1^+$, exploiting the fact that for $M = 1$ the problem can be solved exactly.

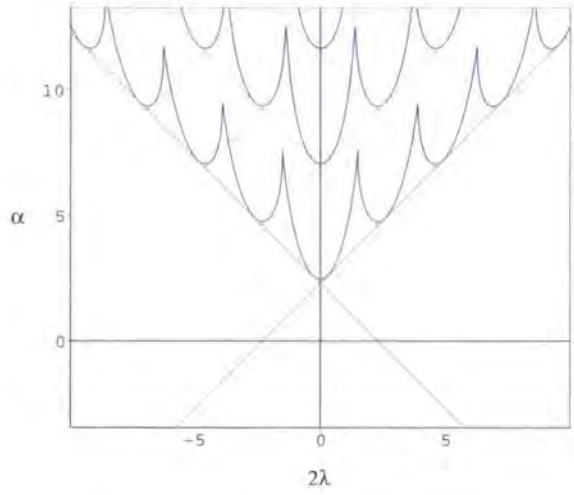


Figure 5.10: Cusps for $M = 1.3$.

## 5.8 Perturbation theory about $M = 1$

### 5.8.1 Exceptional points via near-degenerate perturbation theory

Return now to the original formulation of the eigenvalue problem, namely

$$H_M \psi(x) = E\,\psi(x)\,, \quad \psi(x) \in L^2(\mathcal{C}) \tag{5.8.1}$$

where

$$H_M = -\frac{d^2}{dx^2} - (ix)^{2M} - \alpha(ix)^{M-1} + \frac{\lambda^2 - \frac{1}{4}}{x^2}\,. \tag{5.8.2}$$

For $M$ near 1, the contour $\mathcal{C}$ can run along the real axis for $|x| \to \infty$, dipping just below it at the origin. This problem can be solved exactly for $M = 1$ - it is the $\mathcal{PT}$-symmetric simple harmonic oscillator [135, 65] and the spectrum is entirely real. (Note, for $\lambda^2 - \frac{1}{4} \neq 0$ the reality of the spectrum is not completely trivial, owing to the departure of the quantisation contour from the real axis near the origin.) As $M$ increases above 1, pairs of eigenvalues can become complex; as discussed earlier, this must be preceded by the coincidence of two real eigenvalues and so the first complex eigenvalues will be found at points in the $(2\lambda, \alpha)$ plane at which the spectrum had degeneracies for $M = 1$. The aim here is to investigate exactly how this occurs.

In [123], Bender *et al.* studied the special case of $\alpha = \lambda^2 - \frac{1}{4} = 0$, using the exactly-known $M = 1$ eigenfunctions $|n\rangle$, $n = 0, 1, 2 \ldots$. The full Hilbert space

was truncated to the subspace spanned by $|2n-1\rangle$ and $|2n\rangle$, and $H_M$ expanded within that subspace about $H_{M=1}$. Diagonalising the resulting $2 \times 2$ matrix allowed an approximation to the eigenvalues of $H_M$ to be found for $M$ near to 1. However, as shown in [136], this approximation predicts level-merging for both signs of the perturbation rather than the one sign actually observed, and when applied to the pair of levels $|2n\rangle$ and $|2n+1\rangle$, it predicts that they too will merge, contrary to the actual behaviour of the model. These problems can be traced to the fact that the energy levels at $M = 1$ and $\alpha = \lambda^2 - \frac{1}{4} = 0$ are equally spaced, making the truncation to the subspace spanned by $|2n-1\rangle$ and $|2n\rangle$ unjustified.

For the more general Hamiltonian (5.8.2) the presence of $\lambda$ prevents this problem, as $\lambda$ can be tuned so as to make a couple of levels very close to each other relative to all of the rest. Truncation to these two levels will then yield a good approximation to their behaviour for $M$ close to 1. To see how a reliable prediction of exceptional points can emerge from this approach, it is worth examining a simple $2 \times 2$ example which illustrates the main features.

Consider the 'unperturbed' Hamiltonian

$$H_1(\eta) = \begin{pmatrix} 2\eta & 0 \\ 0 & -2\eta \end{pmatrix} \tag{5.8.3}$$

with exactly-known eigenvalues $\pm 2\eta$, and add to it the perturbation

$$V_\epsilon(\eta) = \begin{pmatrix} -\epsilon/\eta & -i\epsilon/\eta \\ -i\epsilon/\eta & \epsilon/\eta \end{pmatrix} \tag{5.8.4}$$

Here $\epsilon$ is the perturbing parameter (corresponding to $M - 1$ in the full problem) and the factors of $1/\eta$ capture the fact that nearby levels in the unperturbed problem interact more strongly as they approach each other. Then $H_{1+\epsilon} := H_1 + V_\epsilon$ has eigenvalues

$$E_\pm = \pm 2\sqrt{\eta^2 - \epsilon} \tag{5.8.5}$$

and there is an exceptional point for just one sign of the perturbing parameter, at $\epsilon = \eta^2$. The singular nature of the $\eta \to 0$ limit in this presentation of the Hamiltonian makes it hard to see the emergence of the Jordan block. For this, as in [130], define a pair of matrices

$$P = \frac{1}{\sqrt{2}} \begin{pmatrix} 1 & i \\ i & 1 \end{pmatrix}, \quad R = \begin{pmatrix} q & 0 \\ 0 & 1/q \end{pmatrix} \tag{5.8.6}$$

where $q^2 = 2i\epsilon/\eta$. Then $H_{1+\epsilon}$ is similar to

$$\widehat{H}_{1+\epsilon} = R^{-1}P^{-1}H_{1+\epsilon}PR = \begin{pmatrix} 0 & 1+\eta^2/\epsilon \\ 4\epsilon & 0 \end{pmatrix} \tag{5.8.7}$$

which, at $\eta = 0$, has the expected perturbed Jordan block form.

Returning to the main problem, at $M = 1$ the full Hamiltonian is

$$H_1 = -\frac{d^2}{dx^2} + x^2 + \frac{\lambda^2 - \frac{1}{4}}{x^2} - \alpha\,. \tag{5.8.8}$$

With the given boundary conditions, $H_1$ has eigenfunctions

$$\phi_n^{\pm}(x) = \frac{\sqrt{2}\sqrt{n!}}{\sqrt{(1-e^{\mp 2\pi i\lambda})\Gamma(\pm\lambda+n+1)}} x^{1/2\pm\lambda} e^{-\frac{x^2}{2}} L_n^{\pm\lambda}(x^2)\,, \quad n = 0, 1, \ldots\,. \tag{5.8.9}$$

where $L_n^{\beta}$ are the Laguerre polynomials, and the normalisation prefactor is taken from [137]. The corresponding eigenvalues are

$$E_n^{\pm} = -\alpha + 4n + 2 \pm 2\lambda\,. \tag{5.8.10}$$

A degenerate eigenvalue requires $E_n^{+} = E_m^{-}$ for some $n$ and $m$, which amounts to

$$m - n = \lambda\,. \tag{5.8.11}$$

Thus the spectrum has degeneracies on the vertical lines $\lambda \in \mathbb{Z}$ in the $(2\lambda, \alpha)$ plane, and for these values of $\lambda$ infinitely-many pairs of eigenfunctions, $\phi_n^{+}$ and $\phi_m^{-}$, are proportional to one other. For $\lambda = q$, where $q$ is a non-negative integer, the normalisation in (5.8.9) is singular. Removing the singular term $(1 - e^{\pm 2\pi i q})$ and writing the Laguerre polynomials in terms of gamma functions

$$L_n^{\beta}(x) = \sum_{k=0}^{n} (-1)^k \frac{\Gamma(n+\beta+1)}{\Gamma(\beta+k+1)\Gamma(n-k+1)\Gamma(k+1)} x^k\,. \tag{5.8.12}$$

it is easily shown that $\phi_{p+q}^{-} = (-1)^q \phi_p^{+}$, for $p$ any other non-negative integer. Since $\phi_n^{+} \to \phi_n^{-}$ when $\lambda \to -\lambda$, it also follows that $\phi_{p+q}^{+} \propto \phi_p^{-}$ when $\lambda = -q$.

In order to find the eigenvalues of $H_M$ for $M = 1 + \epsilon$, the method of [123] is followed and $H_M = H_{1+\epsilon}$ is treated in the basis of eigenfunctions of $H_1$ by writing it as

$$H_{1+\epsilon} = H_1 + V_\epsilon \tag{5.8.13}$$

where $H_1$ is given in (5.8.8) and

$$V_\epsilon = -x^2 - (ix)^{2+2\epsilon} - \alpha(ix)^\epsilon . \tag{5.8.14}$$

The matrix elements of $V_\epsilon$ in the truncated basis of $H_1$ eigenfunctions were found exactly by Millican-Slater [137]. The results of his calculation are recorded here: The matrix element $\langle \phi_n^+ | (ix)^{2M} | \phi_m^+ \rangle$ is given by

$$\begin{aligned} &\langle \phi_n^+ | (ix)^{2M} | \phi_m^+(x) \rangle = \\ &(\cos(M\pi) + \sin(M\pi)\cot(\lambda\pi)) \frac{(-M)_n(\lambda+1)_m}{\sqrt{n!m!\Gamma(\lambda+m+1)\Gamma(\lambda+n+1)}} \times \\ &\Gamma(\lambda+M+1)\,{}_3F_2(-m, \lambda+M+1, 1+M; \lambda+1, 1+M-n; 1) \end{aligned} \tag{5.8.15}$$

in terms of the hypergeometric function ${}_3F_2$ and the Pochhammer symbol $(a)_n$, defined for positive integer $n$ as $(a)_n := a(a+1)(a+2)\ldots(a+n-1)$ and $(a)_0 := 1$. The corresponding matrix element for $\phi_n^-$ can be found by sending $\lambda \to -\lambda$. Note, when $M = 1$ this hypergeometric functions is not defined for all $n$ and $m$ so the result for $M = 1$ cannot be read off from the above. This becomes clear when the hypergeometric function ${}_AF_B(-m, a_2, \ldots, a_A; b_1, b_2, \ldots, b_B; z)$ is written in terms of the Pochhammer symbol

$${}_AF_B(-m, a_2, \ldots, a_A; b_1, \ldots, b_B; z) = \sum_{k=0}^{m} \frac{(-m)_k (a_2)_k \ldots (a_A)_k}{(b_1)_k (b_2)_k \ldots (b_B)_k} \frac{z^k}{k!} . \tag{5.8.16}$$

Note that if $a$ is a negative integer, $-n$, then

$$(a)_k = (-n)_k = \frac{(-1)^k n!}{(n-k)!} \quad \text{if } n \geq k \tag{5.8.17}$$

$$(a)_k = 0 \quad \text{if } n < k \tag{5.8.18}$$

so (5.8.16) is not well defined if one of the $b_i$ is negative and $-b_i < m$. Therefore, the hypergeometric function in (5.8.15) is undefined for $M = 1$ and $n - 2 < m$. However, for $|n - m| \geq 2$ the symmetry of the inner products in $n$ and $m$ can be used to avoid this problem. In these cases, when $M = 1$, the $(-M)_n$ term in the expressions above becomes $(-1)_n = 0$ so the inner products are zero. For $n = m$ and $n = m \pm 1$, by taking the limit $M \to 1$ in (5.8.15) it can be shown [137] that the only non-zero inner products for $M = 1$ are

$$\langle \phi_n^+(x) | x^2 | \phi_n^+(x) \rangle = 1 + \lambda + 2n \tag{5.8.19}$$

$$\langle \phi_n^-(x) | x^2 | \phi_n^-(x) \rangle = 1 - \lambda + 2n \tag{5.8.20}$$

and

$$\langle \phi^+_{n+1}(x)|x^2|\phi^+_n(x)\rangle = \sqrt{\frac{n+1}{n+\lambda+1}}\,(\lambda - n) \tag{5.8.21}$$

$$\langle \phi^-_{n+1}(x)|x^2|\phi^-_n(x)\rangle = \sqrt{\frac{n+1}{n-\lambda+1}}\,(-\lambda - n)\,. \tag{5.8.22}$$

The matrix element $\langle \phi^+_n(x)|(ix)^{2M}|\phi^-_m(x)\rangle$ is given by

$$\begin{aligned}\langle \phi^+_n(x)|(ix)^{2M}|\phi^-_m(x)\rangle = i\frac{\sin(M\pi)(1-\lambda)_m(\lambda - M)_n\Gamma(M+1)}{|\sin(\pi\lambda)|\sqrt{\Gamma(1-\lambda+m)\Gamma(1+\lambda+n)m!n!}} \\ \times {}_3F_2(-m, 1+M, M+1-\lambda; 1-\lambda, M+1-\lambda-n; 1).\end{aligned} \tag{5.8.23}$$

which, unlike (5.8.15), is always well defined at $M = 1$. Expanding the matrix elements to leading order and re-diagonalising the resulting $2 \times 2$ matrix of $H_{1+\epsilon}$ will then give the approximate energy levels.

### 5.8.2 Perturbative locations of the exceptional points

Now set $\lambda = q + \eta$ and $M = 1 + \epsilon$. It will also be assumed that $q \geq 0$, as results for negative $q$ are easily restored using the $\lambda \to -\lambda$ symmetry of the problem. For small values of $\eta$, the pairs of levels $\{\phi^+_p, \phi^-_{p+q}\}$, $p \geq 0$, are near degenerate, making the truncation of the Hamiltonian to the $2 \times 2$ blocks spanned by these two states a good approximation. To simplify the notation, fix the integer $p \geq 0$ and denote the corresponding basis by $\{\phi^+, \phi^-\} \equiv \{\phi^+_p, \phi^-_{p+q}\}$, with matrix elements $H_{ab} \equiv \langle \phi^a|H_M|\phi^b\rangle$, where $a, b \in \{+, -\}$. Recalling that $H_M = H_1 - x^2 - (ix)^{2+2\epsilon} - \alpha(ix)^\epsilon$ the matrix elements $H_{++}$, $H_{+-}$ and $H_{--}$ can be easily written down, using (5.8.15), (5.8.19), (5.8.20) and (5.8.23), and noting that

$$\langle \phi^+|H_1|\phi^+\rangle = 4p + 2q + 2\eta + 2 \tag{5.8.24}$$

$$\langle \phi^-|H_1|\phi^-\rangle = 4p + 2q - 2\eta + 2 \tag{5.8.25}$$

$$\langle \phi^+|H_1|\phi^-\rangle = \langle \phi^-|H_1|\phi^+\rangle = 0. \tag{5.8.26}$$

Expanding in $\epsilon$ and $\eta$ and keeping terms proportional to $\eta$, $\epsilon/\eta$, $\epsilon$ and $\epsilon^2/\eta$ yields

$$\begin{aligned} H_{++} \approx\ & 4p + 2q + 2 - \alpha + \left(2p + q + 1 - \frac{\alpha}{2}\right)\frac{\epsilon}{\eta} + 2\eta \\ +\ & \left(\left(2p + q + 1 - \frac{\alpha}{2}\right)\psi(p+q+1) + 2p + 2\right)\epsilon \\ +\ & \left(\left(2p + q + 1 - \frac{\alpha}{4}\right)\psi(p+q+1) + 2p + 1\right)\frac{\epsilon^2}{\eta}\,; \end{aligned} \tag{5.8.27}$$

$$\begin{aligned} H_{--} &\approx 4p+2q+2-\alpha-\left(2p+q+1-\frac{\alpha}{2}\right)\frac{\epsilon}{\eta}-2\eta \\ &+ \left(\left(2p+q+1-\frac{\alpha}{2}\right)\psi(p+1)+2p+2q+2\right)\epsilon \\ &- \left(\left(2p+q+1-\frac{\alpha}{4}\right)\psi(p+q+1)+2p+1\right)\frac{\epsilon^2}{\eta}; \end{aligned} \tag{5.8.28}$$

$$\begin{aligned} H_{+-} &\approx \frac{i}{|\eta|}\left[\left(2p+q+1-\frac{\alpha}{2}\right)\epsilon\right. \\ &+ \left(\frac{1}{2}\left(2p+q+1-\frac{\alpha}{2}\right)(\psi(p+q+1)-\psi(p+1))-q\right)\epsilon\eta \\ &+ \left.\left(\left(2p+q+1-\frac{\alpha}{4}\right)\psi(p+q+1)+2p+1\right)\epsilon^2\right] \end{aligned} \tag{5.8.29}$$

where $\psi(z) = \Gamma'(z)/\Gamma(z)$. Details of this expansion are given in appendix A. This matrix can now be diagonalised to find approximations to the eigenvalues $E_{\pm_{[\lambda=q+\eta]}}$:

$$\begin{aligned} E_{\pm_{[\lambda=q+\eta]}} &\approx 4p+2q+2-\alpha+\left(2p+q+2\right. \\ &+ \left.\frac{1}{4}(4p+2q+2-\alpha)(\psi(p+q+1)+\psi(p+1))\right)\epsilon \\ &\pm \left[(8p+4q+4-2\alpha)\epsilon+\left((8p+4q+4-\alpha)\psi(p+q+1)\right.\right. \\ &\quad \left.+8p+4\right)\epsilon^2+\left((4p+2q+2-\alpha)(\psi(p+q+1)-\psi(p+1))\right. \\ &\quad \left.\left.-4q\right)\epsilon\eta+4\eta^2\right]^{1/2} \end{aligned} \tag{5.8.30}$$

Having obtained the approximate energy levels, exceptional points can be identified as lines on the $(2\lambda, \alpha)$ plane where the argument of the square root in (5.8.30) vanishes. The approximations to these curves for both $E_{\pm_{\lambda=-q-\eta}}$ and $E_{\pm_{\lambda=q+\eta}}$ are plotted in figures 5.11, 5.12, 5.13, and 5.14, for $\epsilon = 0.005$, 0.01, 0.02 and 0.035 respectively. Each shows $\alpha$ against $2\lambda$ for fixed $\epsilon$, taking $q = 0, 1, 2$ in $E_{\pm_{\lambda=q+\eta}}$ and $E_{\pm_{\lambda=-q-\eta}}$ above, and $p = 0, 1$ and 2. (The lines of exceptional points for other values of $p$ and $q$ lie outside the regions shown on the plots.) The dotted lines are the $\alpha_\pm \in \mathbb{Z}^+$ lines, as previously.

As $M$ increases from 1, regions of complex eigenvalues open up from the lines $\lambda \in \mathbb{Z}$, starting near the bottom of the spectrum. While the cusps cannot be seen within this approximation (since the truncation is to just two levels), the pictures are consistent with the numerical evidence in the last section that the cusps should escape towards $\alpha = +\infty$ as $M$ decreases from 3 to 1.

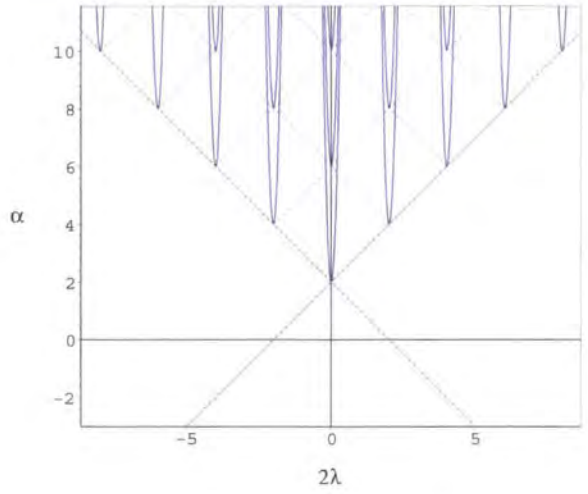


Figure 5.11: Perturbative $\mathcal{PT}$ boundary for $M = 1.005$.

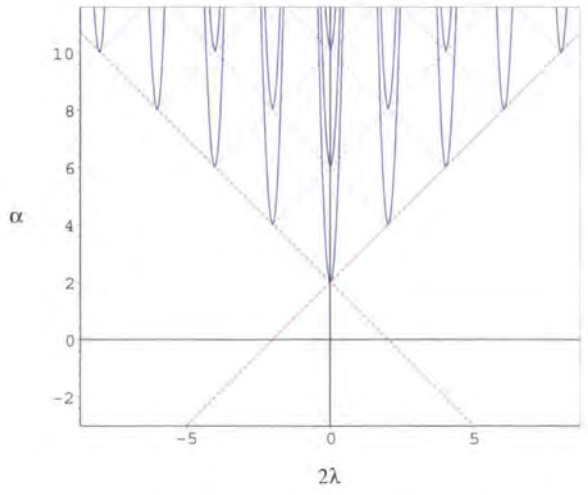


Figure 5.12: Perturbative $\mathcal{PT}$ boundary for $M = 1.01$.

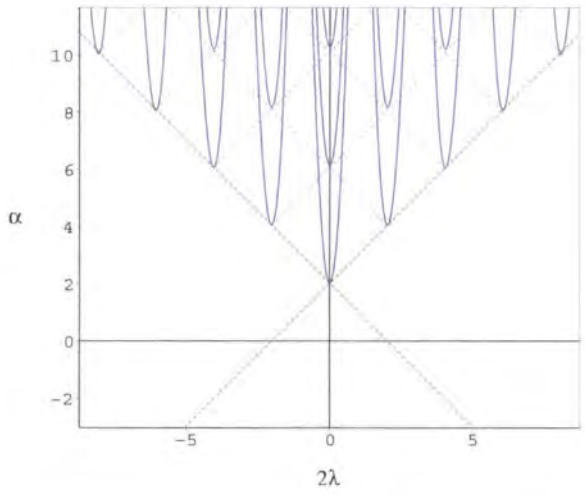


Figure 5.13: Perturbative $\mathcal{PT}$ boundary for $M = 1.02$.

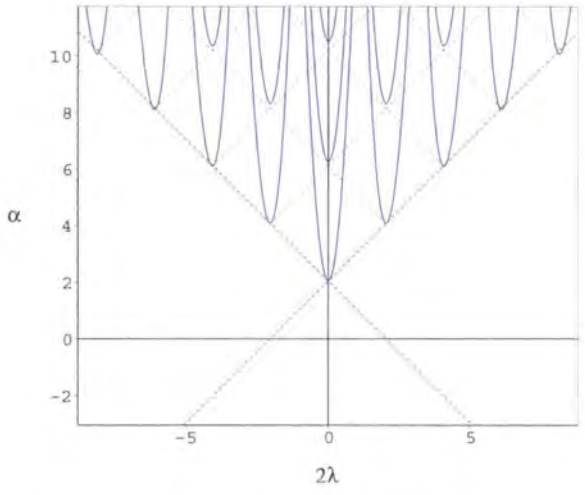


Figure 5.14: Perturbative $\mathcal{PT}$ boundary for $M = 1.035$.

A clearer insight into the transitions near $M = 1$ can be gained by retaining only the leading terms of the matrix elements for small $\eta$ and $\epsilon$, namely those proportional to $\eta$ and $\epsilon/\eta$. For $\lambda = q + \eta$ and $M = 1 + \epsilon$ as before, the matrix elements in the basis $\{\phi^+, \phi^-\} = \{\phi_p^+, \phi_{p+q}^-\}$ simplify to

$$\begin{pmatrix} H_{++} & H_{+-} \\ H_{-+} & H_{--} \end{pmatrix} = \begin{pmatrix} -2\kappa & 0 \\ 0 & -2\kappa \end{pmatrix} + \begin{pmatrix} 2\eta & 0 \\ 0 & -2\eta \end{pmatrix} + \begin{pmatrix} -\kappa\epsilon/\eta & -i\kappa\epsilon/\eta \\ -i\kappa\epsilon/\eta & \kappa\epsilon/\eta \end{pmatrix} \tag{5.8.31}$$

where

$$\kappa = \tfrac{1}{2}\alpha - 2p - q - 1\,. \tag{5.8.32}$$

The approximate eigenvalues are then

$$E_{approx} = -2\kappa \pm 2\sqrt{\eta^2 - \kappa\epsilon}\,. \tag{5.8.33}$$

Apart from the overall shift by $-2\kappa$ and the replacement of $\epsilon$ by $\kappa\epsilon$, (5.8.31) and (5.8.33) have exactly the same form as the toy example (5.8.5). Exceptional points occur when the argument of the square root vanishes. At fixed $\epsilon$, and using the $\lambda \to -\lambda$ symmetry, the curves of exceptional points form the parabolas

$$\alpha = 4p + 2q + 2 + \frac{1}{2\epsilon}(2\lambda \pm 2q)^2 \tag{5.8.34}$$

on the $(2\lambda, \alpha)$ plane, where $p$ and $q$ are non-negative integers. Note the significant difference between the situations for $\epsilon > 0$ ($M > 1$) and for $\epsilon < 0$ ($M < 1$): for given $\epsilon > 0$ the parabolas open upwards as in the figures above, and only a finite number of eigenvalues are predicted to be imaginary. On the other hand, for $\epsilon < 0$ the parabolas open downwards, and infinitely-many eigenvalues are imaginary. This provides an alternative understanding of the transition to infinitely-many complex eigenvalues as $M$ dips below 1, first observed by Bender and Boettcher [63] for $\alpha = 0$, $2\lambda = 1$.

Finally, in table 5.2 the various approximations used in this section are compared with numerical data obtained from a direct solution of the ordinary differential equation. The numerical eigenvalues are denoted by $E_{num}$ so it is against these values that the approximations are compared. The result using the truncation to two energy levels, but with no approximation of the matrix elements given in (5.8.15), (5.8.19), (5.8.20) and (5.8.23), is denoted by $E_f$ and, as shown in table 5.2, this truncation gives a very good approximation to the numerical result $E_{num}$. The initial approximation of this truncated result (including $\epsilon$ and $\epsilon^2/\eta$ terms), given in (5.8.30) from

which the figures 5.11-5.14 are plotted, is denoted by $E_{\pm}$ and the final approximation (omitting the $\epsilon$ and $\epsilon^2/\eta$ terms), as shown in (5.8.33), is given by $E_{approx}$. The table shows the comparison for various values of $\epsilon$, $\alpha$ and $\eta$, for $p = q = 0$ ($\lambda = \eta$) and $p = 0$, $q = 1$ (i.e. $\lambda = 1 + \eta$).

| $p = q = 0$ | | | | |
|---|---|---|---|---|
| | $\epsilon = 0.01$, $\alpha = 0.9$, $\eta = 0.3$ | | $\epsilon = 0.001$, $\alpha = 0.9$, $\eta = 0.01$ | |
| $E_{num}$ | 0.5012 | 1.727 | 1.15266823 | 1.05069482 |
| $E_f$ | 0.50122059 | 1.72733240 | 1.15266441 | 1.05069431 |
| $E_{\pm}$ | 0.49858501 | 1.73506561 | 1.15269439 | 1.05067066 |
| $E_{approx}$ | 0.48193851 | 1.71806148 | 1.15099019 | 1.04900980 |
| $p = 0$, $q = 1$ | | | | |
| | $\epsilon = 0.01$, $\alpha = 3.9$, $\eta = 0.01$ | | $\epsilon = 0.001$, $\alpha = 3.5$, $\eta = 0.01$ | |
| $E_{num}$ | 0.07899348 | 0.18089945 | 0.46597112 | 0.53999606 |
| $E_f$ | 0.07897778 | 0.18034086 | 0.46596643 | 0.53999457 |
| $E_{\pm}$ | 0.07913480 | 0.18078797 | 0.46595499 | 0.54000639 |
| $E_{approx}$ | 0.05101020 | 0.14898979 | 0.46258342 | 0.53741657 |

Table 5.2: Comparison of data

# Chapter 6

# Conclusion

For perturbed boundary conformal field theories, little is known about the link between the reflection factors and the corresponding conformal boundary conditions. In the bulk, this link can often be made with the TBA effective central charge, which allows the $S$ matrix to be matched with the perturbed CFT. It has been proposed that the boundary analogue for this is given by the exact off-critical $g$-function, and in Chapter 4, this was tested for the purely elastic scattering theories related to the $ADET$ Lie algebras. A special class of reflection factors was identified which, in the ultraviolet limit, were found to describe the reflection of massless particles off a wall with fixed boundary conditions $|i\rangle$, matching the low-temperature vacua.

A set of one-parameter families of reflection amplitudes was also proposed which, from the $g$-function calculations, appear to correspond to perturbations of Cardy boundary states, or of superpositions of such states, by relevant boundary operators, with each boundary flow ending at a fixed boundary condition $|i\rangle$.

While the results presented in Chapter 4 indicate that these models all have interesting interpretations as perturbed boundary conformal field theories, the checks performed so far should be considered as preliminary. In Section 4.10, the boundary bound-state spectrum was found for the three-state Potts model but it would be interesting to check this result using the boundary truncated conformal space approach [78]. It remains an open problem to determine the boundary spectrum for each of the remaining $ADET$ models and also to fix completely the boundary UV/IR relations proposed in Section 4.9.2. Finally, it would be interesting to extend this work to other models, in particular to the Virasoro minimal models perturbed by the

$\Phi_{13}$ operator. This perturbation leads to massless flows between the minimal models and knowledge of the exact $g$-function should allow conjectures to be made of the existence of flows between conformal boundary conditions of different minimal models. The exact $g$-function described in Section 3.4 must be modified for these models as they are not purely elastic scattering theories. An attempt at this has been made in [138], but this suffers from the same problems as the original off-critical $g$-function and must be modified by some boundary independent terms, as described in Section 3.4.

In Chapter 5, the phase diagram of the three-parameter family of $\mathcal{PT}$ symmetric Hamiltonians $H_{M,\alpha,l}$ was examined. At $M = 3$, this model is quasi-exactly solvable, which allowed the precise Jordan block structure, at the first quadratic and cubic points to be shown. The locations of the exceptional points were also explored away from $M = 3$, using both numerical and perturbative methods.

These curves of exceptional points, for the $M = 3$ case, have also been found using the complex WKB method by Sorrell [133]. It would be interesting to see if this method reproduces the same pictures for other values of $M$. It would also be interesting to investigate the phase diagram of this Hamiltonian when different lateral boundary conditions are imposed, i.e. when the quantisation contour tends to infinity in a different pair of Stokes sectors.

# Appendix A

# Perturbative expansion of the matrix elements

In this appendix, the matrix elements

$$
\begin{aligned}
H_{++} &= 2p+q+1+\eta+\frac{\sin((\epsilon+\eta+q)\pi)\Gamma(p-1-\epsilon)\Gamma(2+q+\eta+\epsilon)}{\sin((\eta+q)\pi)\Gamma(-1-\epsilon)\Gamma(1+q+\eta)p!} \\
&\quad \times {}_3F_2(-p,2+\epsilon,2+q+\eta+\epsilon;1+q+\eta,2+\epsilon-p;1) \qquad \text{(A.0.1)} \\
&- \alpha\frac{\sin((\eta+\frac{\epsilon}{2}+q)\pi)\Gamma(p-\frac{\epsilon}{2})\Gamma(1+q+\eta+\frac{\epsilon}{2})}{\sin((\eta+q)\pi)\Gamma(-\frac{\epsilon}{2})\Gamma(1+q+\eta)p!} \\
&\quad \times {}_3F_2\left(-p,1+\frac{\epsilon}{2},1+q+\eta+\frac{\epsilon}{2};1+q+\eta,1+\frac{\epsilon}{2}-p;1\right)
\end{aligned}
$$

$$
\begin{aligned}
H_{+-} &= i\frac{\Gamma(1-\eta+p)}{\Gamma(1-q-\eta)\sqrt{\Gamma(1-\eta+p)\Gamma(1+q+p+\eta)(p+q)!p!}}\times \\
&\quad \Bigg(\frac{\sin(\epsilon\pi)\Gamma(p+q-1+\eta-\epsilon)\Gamma(2+\epsilon)}{|\sin((\eta+q)\pi)|\Gamma(q-1+\eta-\epsilon)} \\
&\quad \times {}_3F_2(-p-q,2+\epsilon,2-q+\epsilon-\eta;1-q-\eta,2-q-p+\epsilon-\eta;1) \qquad \text{(A.0.2)} \\
&- \frac{\alpha\sin(\frac{\epsilon\pi}{2})\Gamma(p+q+\eta-\frac{\epsilon}{2})\Gamma(1+\frac{\epsilon}{2})}{|\sin((\eta+q)\pi)|\Gamma(q+\eta-\frac{\epsilon}{2})} \\
&\quad \times {}_3F_2\left(-p-q,1+\frac{\epsilon}{2},1-q+\frac{\epsilon}{2}-\eta;1-q-\eta,1-p-q+\frac{\epsilon}{2}-\eta;1\right)\Bigg)
\end{aligned}
$$

$$
\begin{aligned}
H_{--} &= 2p+q+1-\eta-\frac{\sin((\epsilon-\eta-q)\pi)\Gamma(p+q-1-\epsilon)\Gamma(2-q-\eta+\epsilon)}{\sin((\eta+q)\pi)\Gamma(-1-\epsilon)\Gamma(1-q-\eta)(p+q)!} \\
&\quad \times {}_3F_2(-p-q,2+\epsilon,2-q-\eta+\epsilon;1-q-\eta,2+\epsilon-p-q;1) \qquad \text{(A.0.3)} \\
&- \alpha\frac{\sin((\eta-\frac{\epsilon}{2}+q)\pi)\Gamma(p+q-\frac{\epsilon}{2})\Gamma(1-q-\eta+\frac{\epsilon}{2})}{\sin((\eta+q)\pi)\Gamma(-\frac{\epsilon}{2})\Gamma(1-q-\eta)(p+q)!} \\
&\quad \times {}_3F_2\left(-p-q,1+\frac{\epsilon}{2},1-q-\eta+\frac{\epsilon}{2};1-q-\eta,1+\frac{\epsilon}{2}-p-q;1\right)
\end{aligned}
$$

as described in section 5.8.2 are expanded in $\epsilon$ and $\eta$, including terms proportional to $\eta$, $\epsilon/\eta$, $\epsilon$ and $\epsilon^2/\eta$. The final results are quoted in (5.8.27), (5.8.28) and (5.8.29).

The first step, before expanding these matrix elements, is to simplify them. The hypergeometric functions, ${}_AF_B(-m, a_2, \ldots, a_A; b_1, \ldots, b_B; z)$ with $m$ a positive integer, are defined in terms of the Pochhammer symbol $(a)_n$

$$ {}_AF_B(-m, a_2, \ldots, a_A; b_1, \ldots, b_B; z) = \sum_{k=0}^{m} \frac{(-m)_k (a_2)_k \ldots (a_A)_k}{(b_1)_k (b_2)_k \ldots (b_B)_k} \frac{z^k}{k!}. \tag{A.0.4} $$

Note that when $a$ is not a negative integer or zero, $(a)_n$ can be written in terms of $\Gamma$ functions

$$ (a)_n = \frac{\Gamma(a+n)}{\Gamma(a)}. \tag{A.0.5} $$

Substituting this into (A.0.4) then gives:

$$ \begin{aligned} &{}_AF_B(-m, a_2, \ldots, a_A; b_1, b_2, \ldots, b_B; z) \\ &\quad = \frac{\Gamma(b_1)\Gamma(b_2)\ldots\Gamma(b_B)}{\Gamma(a_2)\ldots\Gamma(a_A)} \sum_{k=0}^{m} \frac{(-m)_k \Gamma(a_2+k)\ldots\Gamma(a_A+k)}{\Gamma(b_1+k)\ldots\Gamma(b_B+k)} \frac{z^k}{k!} \end{aligned} \tag{A.0.6} $$

Then using the recurrence relation of the $\Gamma$ function, $\Gamma(z+1) = z\Gamma(z)$, several times it is easy to see that

$$ \frac{\Gamma(p+z_1)}{\Gamma(z_1)} \frac{\Gamma(z_2-p)}{\Gamma(z_2)} = (-1)^p. \tag{A.0.7} $$

The matrix elements (A.0.1), (A.0.2) and (A.0.3), can now be rewritten using (A.0.6), (A.0.7) and (5.8.17) as

$$ \begin{aligned} H_{++} &= 2p+q+1+\eta \\ &+ \frac{\sin((\eta+\epsilon)\pi)}{\sin(\eta\pi)} \sum_{k=0}^{p} \frac{(-1)^{p+k}}{(p-k)!k!} \frac{\Gamma(2+\epsilon+k)\Gamma(2+q+\eta+\epsilon+k)}{\Gamma(1+q+\eta+k)\Gamma(2+\epsilon-p+k)} \\ &- \alpha \frac{\sin((\eta-\frac{\epsilon}{2})\pi)}{\sin(\eta\pi)} \sum_{k=0}^{p} \frac{(-1)^{p+k}}{(p-k)!k!} \frac{\Gamma(1+\frac{\epsilon}{2}+k)\Gamma(1+q+\eta+\frac{\epsilon}{2}+k)}{\Gamma(1+q+\eta+k)\Gamma(1+\frac{\epsilon}{2}-p+k)} \end{aligned} \tag{A.0.8} $$

$$ \begin{aligned} H_{+-} &= i \frac{\Gamma(1-\eta+p)}{\sqrt{\Gamma(1-\eta+p)\Gamma(1+q+p+\eta)(p+q)!p!}} \times \\ &\left( \frac{\sin(\epsilon\pi)}{|\sin(\eta\pi)|} \sum_{k=0}^{p+q} \frac{(-1)^{p+q+k}(p+q)!}{(p+q-k)!k!} \frac{\Gamma(2+\epsilon+k)\Gamma(2+\epsilon-\eta-q+k)}{\Gamma(1-q-\eta+k)\Gamma(2+\epsilon-\eta-q-p+k)} \right. \\ &- \left. \alpha \frac{\sin(\frac{\epsilon\pi}{2})}{|\sin(\eta\pi)|} \sum_{k=0}^{p+q} \frac{(-1)^{p+q+k}(p+q)!}{(p+q-k)!k!} \frac{\Gamma(1+\frac{\epsilon}{2}+k)\Gamma(1-q+\frac{\epsilon}{2}-\eta+k)}{\Gamma(1-q-\eta+k)\Gamma(1-q-p+\frac{\epsilon}{2}-\eta+k)} \right) \end{aligned} \tag{A.0.9} $$

$$
\begin{aligned}
H_{--} &= 2p+q+1-\eta \qquad\qquad (A.0.10)\\
&+ \frac{\sin((\eta-\epsilon)\pi)}{\sin(\eta\pi)}\sum_{k=0}^{p+q}\frac{(-1)^{p+q+k}}{(p+q-k)!k!}\frac{\Gamma(2-q+\eta+\epsilon+k)\Gamma(2+\epsilon+k)}{\Gamma(1-q+\eta+k)\Gamma(2-p-q+\epsilon+k)}\\
&- \alpha\frac{\sin((\eta-\frac{\epsilon}{2})\pi)}{\sin(\eta\pi)}\sum_{k=0}^{p+q}\frac{(-1)^{p+q+k}}{(p+q-k)!k!}\frac{\Gamma(1-q-\eta+\frac{\epsilon}{2}+k)\Gamma(1+\frac{\epsilon}{2}+k)}{\Gamma(1-q-\eta+k)\Gamma(1-p-q+\frac{\epsilon}{2}+k)}
\end{aligned}
$$

### A.0.3 Expanding $H_{++}$

Begin by expanding $H_{++}$ (A.0.8), including terms in $\eta$, $\epsilon/\eta$, $\epsilon$ and $\epsilon^2/\eta$. The Taylor expansion of $\Gamma(\epsilon+a)$ and $1/\Gamma(\epsilon+a)$ will be needed here:

$$
\begin{aligned}
\Gamma(\epsilon+a) &\approx \Gamma(a)(1+\psi(a)\epsilon)\\
\frac{1}{\Gamma(\epsilon+a)} &\approx \frac{1}{\Gamma(a)}(1-\psi(a)\epsilon)
\end{aligned}
\qquad (A.0.11)
$$

where $\psi(z)=\Gamma'(z)/\Gamma(z)$. It is useful to note that $\psi(1)=-\gamma$, where $\gamma\approx 0.5772$ is Euler's constant, and $\psi(z+1)=\psi(z)+1/z$. This is sufficient to expand most terms in (A.0.8), but more care must be taken over terms of the form $\Gamma(\epsilon+a+k)/\Gamma(\epsilon+a-p+k)$ for $k=0,\ldots,p$ and $a=1,\ldots,p$. Now, for $k=p+1-a,\ldots,p$ the expansion of these terms can be read off from (A.0.11) but for $k=0,\ldots,p-a$ this will not be well defined so a little more work is required. Let $j=k+a$, then

$$
\begin{aligned}
&\sum_{k=0}^{p-a}\frac{\Gamma(\epsilon+a+k)}{\Gamma(\epsilon+a+k-p)}=\sum_{j=a}^{p}\frac{\Gamma(\epsilon+j)}{\Gamma(\epsilon+j-p)}\\
&\approx\epsilon\sum_{j=a}^{p}((j-2)(j-3)\ldots(j-p)+(j-1)(j-3)\ldots(j-p)+\ldots\\
&\qquad +(j-1)(j-2)\ldots(j-p+1))\\
&\approx\epsilon\sum_{j=a}^{p}\left(\Gamma(p+1-j)\sum_{l=2}^{p+1}\prod_{i=1}^{l=2}(-1)^{p+1-k}\frac{j-i}{\Gamma(l-j)}\right).
\end{aligned}
\qquad (A.0.12)
$$

and using the fact that

$$
\prod_{i=1}^{l-2}\frac{j-i}{\Gamma(l-j)}=\begin{cases}(j-1)! & \text{for } j=l-1\\ 0 & \text{otherwise}\end{cases}
\qquad (A.0.13)
$$

gives

$$
\sum_{j=a}^{p}\frac{\Gamma(\epsilon+j)}{\Gamma(\epsilon+j-p)}\approx\epsilon\sum_{j=a}^{p}(-1)^{p-j}(j-1)!(p-j)!
\qquad (A.0.14)
$$

so, putting this all together, one finds

$$\begin{aligned}\sum_{k=0}^{p}\frac{\Gamma(\epsilon+a+k)}{\Gamma(\epsilon+a+k-p)} &\approx \epsilon\sum_{k=0}^{p-a}(-1)^{p-k-a}(k+a-1)!(p-k-a)! \\ &+ \sum_{k=p+1-a}^{p}\frac{(k+a-1)!}{(k+a-1-p)!}(1+(\psi(a+k)-\psi(a-p+k))\epsilon)\,.\end{aligned} \tag{A.0.15}$$

Substituting these results into (A.0.8) then gives

$$\begin{aligned}H_{++} \approx\ & 2p+q+1+\eta+\left(1+\frac{\epsilon}{\eta}\right)\Bigg[(p+1)(p+q+1)\Big(1+(\psi(2+p)+\gamma-1)\epsilon \\ &+ \psi(2+p+q)(\epsilon+\eta)-\psi(1+p+q)\eta\Big)-p(p+q)\Big(1+(\psi(1+p)+\gamma)\epsilon \\ &+ \psi(1+p+q)(\epsilon+\eta)-\psi(p+q)\eta\Big)+\sum_{k=0}^{p-2}\frac{(k+1)(1+q+k)}{(p-k)(p-k-1)}\Bigg] \\ &- \alpha\left(1+\frac{\epsilon}{2\eta}\right)\left[\left(1+\psi(1+p+q)\frac{\epsilon}{2}+(\psi(p+1)+\gamma)\frac{\epsilon}{2}\right)-\frac{\epsilon}{2}\sum_{k=0}^{p-1}\frac{1}{p-k}\right].\end{aligned} \tag{A.0.16}$$

Finally, replacing the sums above with the following

$$\sum_{k=0}^{p-1}\frac{1}{p-k} = \psi(p+1)+\gamma \tag{A.0.17}$$

$$\sum_{k=0}^{p-2}\frac{1}{(p-k)(p-k-1)} = 1-\frac{1}{p} \tag{A.0.18}$$

$$\sum_{k=0}^{p-2}\frac{k}{(p-k)(p-k-1)} = p-1-\psi(p)-\gamma \tag{A.0.19}$$

$$\sum_{k=0}^{p-2}\frac{k^2}{(p-k)(p-k-1)} = p^2-1+(1-2p)(\psi(p)+\gamma) \tag{A.0.20}$$

and keeping terms in $\eta$, $\epsilon/\eta$, $\epsilon$ and $\epsilon^2/\eta$ only, (A.0.16) reduces to

$$\begin{aligned}H_{++} \approx\ & 4p+2q+2-\alpha+\left(2p+q+1-\frac{\alpha}{2}\right)\frac{\epsilon}{\eta}+2\eta \\ &+ \left(\left(2p+q+1-\frac{\alpha}{2}\right)\psi(p+q+1)+2p+2\right)\epsilon \\ &+ \left(\left(2p+q+1-\frac{\alpha}{4}\right)\psi(p+q+1)+2p+1\right)\frac{\epsilon^2}{\eta}\end{aligned} \tag{A.0.21}$$

as advertised in (5.8.27).

### A.0.4 Expanding $H_{--}$

To expand the $H_{--}$ term (A.0.10), (A.0.11) and (A.0.15) are used, as above, but now more attention must also be paid to the $\Gamma(2-q-\eta+\epsilon+k)/\Gamma(1-q-\eta+k)$ and

$\Gamma(1-q-\eta+\frac{\epsilon}{2}+k)/\Gamma(1-q-\eta+k)$ terms. Taking the second of these, one would naively expand this, using (A.0.11), as

$$\frac{\Gamma(1-q-\eta+\frac{\epsilon}{2}+k)}{\Gamma(1-q-\eta+k)} \approx 1+\psi(1-q+k)\frac{\epsilon}{2} \tag{A.0.22}$$

however, this is not well defined for $k=0,\ldots,q-1$ so more care must be taken here. First, replace $k$ with $j=q-k$:

$$\sum_{k=0}^{q-1}\frac{\Gamma(1-q-\eta+\frac{\epsilon}{2}+k)}{\Gamma(1-q-\eta+k)} = \sum_{j=1}^{q}\frac{\Gamma(1-j-\eta+\frac{\epsilon}{2})}{\Gamma(1-j-\eta)} \tag{A.0.23}$$

then from the recurrence relation of the $\Gamma$ function, it can be shown that

$$\Gamma(1-\eta+\frac{\epsilon}{2}) = \Gamma(1-j-\eta+\frac{\epsilon}{2})\prod_{i=0}^{j-1}\left(\frac{\epsilon}{2}-\eta-i\right) \tag{A.0.24}$$

$$\Gamma(1-\eta) = \Gamma(1-j-\eta)\prod_{i=0}^{j-1}(-\eta-i). \tag{A.0.25}$$

Using this, (A.0.23) can be rewritten as

$$\begin{aligned}\sum_{k=0}^{q-1}\frac{\Gamma(1-q-\eta+\frac{\epsilon}{2}+k)}{\Gamma(1-q-\eta+k)} &= \frac{\Gamma(1-\eta+\frac{\epsilon}{2})}{\Gamma(1-\eta)}\sum_{j=1}^{q}\prod_{i=0}^{j-1}\frac{(-\eta-i)}{(\frac{\epsilon}{2}-\eta-i)} \\ &= \frac{\Gamma(1-\eta+\frac{\epsilon}{2})}{\Gamma(1-\eta)}\sum_{j=1}^{q}\left(\frac{\eta}{\eta-\frac{\epsilon}{2}}\right)\prod_{i=1}^{j-1}\left(\frac{\eta+i}{\eta-\frac{\epsilon}{2}+i}\right) \\ &\approx \frac{\Gamma(1-\eta+\frac{\epsilon}{2})}{\Gamma(1-\eta)}\left(\frac{\eta}{\eta-\frac{\epsilon}{2}}\right)\sum_{j=1}^{q}\prod_{i=1}^{j-1}\left(1+\frac{\epsilon}{2i}\right).\end{aligned} \tag{A.0.26}$$

Then, expanding the $\Gamma$ functions with (A.0.11), and noting that

$$\prod_{i=1}^{j-1}\left(1+\frac{\epsilon}{2i}\right) = \frac{\Gamma(\frac{\epsilon}{2}+j)}{\Gamma(j)\Gamma(1+\frac{\epsilon}{2})} \approx 1+\frac{\epsilon}{2}(\psi(j)+\gamma) \tag{A.0.27}$$

one finds that

$$\sum_{k=0}^{q-1}\frac{\Gamma(1-q-\eta+\frac{\epsilon}{2}+k)}{\Gamma(1-q-\eta+k)} \approx \frac{\eta}{\eta-\frac{\epsilon}{2}}\sum_{k=0}^{q}\left(1+\frac{\epsilon}{2}(\psi(q-k)+\gamma)\right). \tag{A.0.28}$$

Now, using the recurrence relation for the $\Gamma$ function on the $\Gamma(2-q-\eta-\epsilon+k)/\Gamma(1-q-\eta+k)$ term gives

$$\sum_{k=0}^{q-1}\frac{\Gamma(2-q-\eta+\epsilon+k)}{\Gamma(1-q-\eta+k)} = \sum_{k=0}^{q-1}(1-q-\eta+\epsilon+k)\frac{\Gamma(1-q-\eta+\epsilon+k)}{\Gamma(1-q-\eta+k)} \tag{A.0.29}$$

and now (A.0.28) can be used to expand this as

$$\sum_{k=0}^{q-1} \frac{\Gamma(2-q-\eta+\epsilon+k)}{\Gamma(1-q-\eta+k)} \approx \frac{\eta}{\eta-\epsilon} \sum_{k=0}^{q-1} (1-q+k-\eta+\epsilon)(1+(\psi(q-k)+\gamma)\epsilon)\,. \quad \text{(A.0.30)}$$

Putting all this together gives

$$\begin{aligned} H_{--} \approx\ & 2p+q+1-\eta+\epsilon \sum_{j=1}^{q} \frac{(q-j+1)(1-j)}{(p+j)(p+j-1)} \\ &+ \left(\epsilon - \frac{\epsilon^2}{\eta}\right) \sum_{k=q}^{p+q-2} \frac{(k+1)(1-q+k)}{(p+q-k)(p+q-k-1)} \\ &- \left(1-\frac{\epsilon}{\eta}\right) \Big[(p+q)(p-\eta+p(\psi(1+p+q)+\gamma+\psi(1+p))\epsilon) \\ &- (p+q+1)(1+p-\eta+(1+p)(\psi(2+p+q)+\psi(2+p)+\gamma-1)\epsilon)\Big] \\ &+ \alpha \left[\frac{\epsilon}{2} \sum_{j=1}^{q} \frac{1}{p+j} + \left(\frac{\epsilon}{2} - \frac{\epsilon^2}{2\eta}\right) \sum_{k=q}^{p+q-1} \frac{1}{p+q-k} \right. \\ &- \left. \left(1-\frac{\epsilon}{2\eta}\right)\left(1+(\psi(1+p)+\psi(1+p+q)+\gamma)\frac{\epsilon}{2}\right)\right]. \end{aligned} \quad \text{(A.0.31)}$$

Now, the sums above are given by

$$\sum_{j=a}^{q} \frac{1}{p+j} = \psi(p+q+1) - \psi(p+a) \quad \text{(A.0.32)}$$

$$\sum_{j=a}^{q} \frac{1}{(p+j)(p+j-1)} = \frac{1}{p+a-1} - \frac{1}{p+q} \quad \text{(A.0.33)}$$

$$\begin{aligned} \sum_{j=a}^{q} \frac{j}{(p+j)(p+j-1)} =\ & \frac{p}{p+q} + \psi(p+q) - \frac{p}{p+a-1} \\ & -\psi(p+a-1) \end{aligned} \quad \text{(A.0.34)}$$

$$\begin{aligned} \sum_{j=a}^{q} \frac{j^2}{(p+j)(p+j-1)} =\ & q+1-a+\frac{p^2}{p+a-1} - \frac{p^2}{p+q} \\ & +(1-2p)(\psi(p+q)+\psi(p+a-1)) \end{aligned} \quad \text{(A.0.35)}$$

with $a = 1$, and those in (A.0.17) to (A.0.20). This gives the final result, as written in (5.8.28):

$$\begin{aligned} H_{--} \approx\ & 4p+2q+2-\alpha - \left(2p+q+1-\frac{\alpha}{2}\right)\frac{\epsilon}{\eta} - 2\eta \\ &+ \left(\left(2p+q+1-\frac{\alpha}{2}\right)\psi(p+1) + 2p+2q+2\right)\epsilon \\ &- \left(\left(2p+q+1-\frac{\alpha}{4}\right)\psi(p+q+1) + 2p+1\right)\frac{\epsilon^2}{\eta}. \end{aligned} \quad \text{(A.0.36)}$$

### A.0.5 Expanding $H_{+-}$

Finally, the $H_{+-}$ term (A.0.10) must be expanded. Here there are a couple of terms that need some attention. The first being of the form $\Gamma(a+\epsilon-\eta-q+k)/\Gamma(a+\epsilon-\eta-p-q+k)$, where $a=1,2$. When $k=p+q+1-a,\ldots,p+q$, the expansion of this can be read off easily from (A.0.11) so concentrate on $k=0,\ldots,p+q-a$. Take the case $k=0,\ldots,q-a$ first:

$$\begin{aligned}\sum_{k=0}^{q-a}\frac{\Gamma(\epsilon-\eta+a-q+k)}{\Gamma(\epsilon-\eta+a-p-q+k)} &= (-1)^p\sum_{k=0}^{q-a}\prod_{i=1}^{p}(-\epsilon+\eta-a+q-k+i)\\ &= (-1)^p\sum_{k=0}^{q-a}\frac{\Gamma(-\epsilon+\eta-a+p+q-k+1)}{\Gamma(-\epsilon+\eta-a+q-k+1)} \qquad \text{(A.0.37)}\\ &\approx (-1)^p\sum_{k=0}^{q-a}\frac{(p+q-a-k)!}{(q-a-k)!}\Big(1-(\psi(p+q-a-k+1)\\ &\qquad -\psi(q-a-k+1))(\epsilon-\eta)\Big).\end{aligned}$$

For $k=q+1-a,\ldots,p+q-a$, replace $k$ with $j=k+a-q$ and using (A.0.14):

$$\begin{aligned}\sum_{k=q+1-a}^{p+q-a}\frac{\Gamma(\epsilon-\eta+a-q+k)}{\Gamma(\epsilon-\eta+a-p-q+k)} &= \sum_{j=1}^{p}\frac{\Gamma(\epsilon-\eta+j)}{\Gamma(\epsilon-\eta+j-p)}\\ &\approx (\epsilon-\eta)\sum_{j=1}^{p}(-1)^{p-j}(j-1)!(p-j)! \qquad \text{(A.0.38)}\\ &\approx (\epsilon-\eta)\sum_{k=q+1-a}^{p+q-a}\Big[(-1)^{p+q-k-a}(k+a-q-1)!(p+q-k-a)!\Big].\end{aligned}$$

The next term to look at is $1/\Gamma(1-q-\eta+k)$. For $k=q,\ldots,p+q$, (A.0.11) gives the correct expansion so only $k=0,\ldots,q-1$ needs more consideration:

$$\sum_{k=0}^{q-1}\frac{1}{\Gamma(1-q-\eta+k)} = \sum_{k=0}^{q-1}\frac{1}{\Gamma(1-\eta+k)}\frac{\Gamma(1-\eta+k)}{\Gamma(1-q-\eta+k)}. \qquad \text{(A.0.39)}$$

Now the expansion of $1/\Gamma(1-\eta+k)$ is perfectly straightforward for $k=0,\ldots,q-1$, and using (A.0.15) with $a=1$ gives

$$\sum_{k=0}^{q-1}\frac{\Gamma(1-\eta+k)}{\Gamma(1-q-\eta+k)} \approx \eta\sum_{k=0}^{q-1}(-1)^{q-k}k!(q-k-1)!. \qquad \text{(A.0.40)}$$

Finally, the expansion of the prefactor of $H_{+-}$ is

$$\begin{aligned}&\frac{\Gamma(1-\eta+p)}{\sqrt{\Gamma(1-\eta+p)\Gamma(1+p+q+\eta)(p+q)!p!}}\\ &\qquad\approx \frac{1}{(p+q)!}(1-\frac{1}{2}(\psi(p+q+1)+\psi(p+1))\eta).\end{aligned} \qquad \text{(A.0.41)}$$

Gathering these terms together gives

$$\begin{aligned} H_{+-} \approx\ & i\frac{\epsilon}{|\eta|}(1-\frac{1}{2}(\psi(p+q+1)+\psi(p+1))\eta)\Big[(p+q+1)(p+1)\times \\ & \Big(1+(\psi(p+2)+\psi(p+q+2))\epsilon+(\psi(p+1)-\psi(p+2))\eta+(\gamma-1)(\epsilon-\eta)\Big) \\ & - p(p+q)\Big(1+(\psi(p+1)+\psi(p+q+1))\epsilon+(\psi(p)-\psi(p+1))\eta+\gamma(\epsilon-\eta)\Big) \\ & + \sum_{k=q}^{p+q-2}\frac{(k+1)(k-q+1)}{(p+q-k)(p+q-k-1)}(\epsilon-\eta)+\sum_{k=0}^{q-2}\frac{(k+1)(q-k-1)}{(p+q-k)(p+q-k-1)}\eta \\ & - \frac{\alpha}{2}\Big(1+\frac{1}{2}\psi(p+q+1)\epsilon+\psi(p+1)\eta+(\psi(p+1)+\gamma)(\frac{\epsilon}{2}-\eta)\Big) \\ & - \sum_{k=q}^{p+q-1}\frac{1}{(p+q-k)}\left(\frac{\epsilon}{2}-\eta\right)+\sum_{k=0}^{q-1}\frac{1}{p+q-k}\eta\Big]. \end{aligned} \tag{A.0.42}$$

By replacing $k$ with $j = k - q$ in the 1st and 3rd sums and $j = q - k$ in the 2nd and 4th above, their results can be read off from (A.0.17) to (A.0.20) and (A.0.32) to (A.0.35). This then simplifies to give

$$\begin{aligned} H_{+-} \approx\ & \frac{i}{|\eta|}\Big[\Big(2p+q+1-\frac{\alpha}{2}\Big)\epsilon \\ & + \left(\frac{1}{2}\left(2p+q+1-\frac{\alpha}{2}\right)(\psi(p+q+1)-\psi(p+1))-q\right)\epsilon\eta \\ & + \left(\left(2p+q+1-\frac{\alpha}{4}\right)\psi(p+q+1)+2p+1\right)\epsilon^2\Big] \end{aligned} \tag{A.0.43}$$

as written in (5.8.29).

# Bibliography


[1] P. Dorey, A. Lishman, C. Rim and R. Tateo, *'Reflection factors and exact g-functions for purely elastic scattering theories'*, Nucl. Phys. B **744** (2006) 239 [arXiv:hep-th/0512337].

[2] P. Dorey, C. Dunning, A. Lishman and R. Tateo, *'$\mathcal{PT}$ symmetry breaking and exceptional points for a class of inhomogeneous complex potentials'*, in preparation.

[3] I. Affleck and A.W.W. Ludwig, *'Universal noninteger 'ground state degeneracy' in critical quantum systems'*, Phys. Rev. Lett. **67** (1991) 161.

[4] P. Dorey, D. Fioravanti, C. Rim and R. Tateo, *'Integrable quantum field theory with boundaries: the exact g-function'*, Nucl. Phys. B **696** (2004) 445 [arXiv:hep-th/0404014].

[5] P. Di Francesco, P. Mathieu and D. Senechal, *'Conformal field theory'*, Springer, 1997.

[6] J. Cardy, *'Scaling and Renormalisation in Statistical Physics'*, Cambridge University Press 1996.

[7] A. M. Polyakov, *'Conformal Symmetry Of Critical Fluctuations'*, JETP Lett. **12** (1970) 381 [Pisma Zh. Eksp. Teor. Fiz. **12** (1970) 538].

[8] A. A. Belavin, A. M. Polyakov and A. B. Zamolodchikov, *'Infinite conformal symmetry in two-dimensional quantum field theory'*, Nucl. Phys. B **241** (1984) 333.

[9] P. H. Ginsparg, *'Applied Conformal Field Theory'*, In *Les Houches XLIX - Fields, Strings and Critical Phenomena*, Elsevier 1989 [arXiv:hep-th/9108028].

[10] J. L. Cardy, *'Conformal Invariance and Statistical Mechanics'*, In *Les Houches XLIX - Fields, Strings and Critical Phenomena*, Elsevier 1989

[11] V.G.Kac, *'Contravariant form for infinite dimensional Lie algebras and superalgebras'*, Lecture Notes in Physics, vol. 94, Springer-Verlag, Berlin, 1979.

[12] B. L. Feigin and D. B. Fuchs, *'Invariant skew symmetric differential operators on the line and verma modules over the Virasoro algebra'*, Funct. Anal. Appl. **16** (1982) 114 [Funkt. Anal. Pril. **16** (1982) 47].

[13] J. L. Cardy, *'Operator Content Of Two-Dimensional Conformally Invariant Theories'*, Nucl. Phys. B **270** (1986) 186.

[14] C. Itzykson and J. B. Zuber, *'Two-Dimensional Conformal Invariant Theories On A Torus'*, Nucl. Phys. B **275** (1986) 580.

[15] A. Cappelli, C. Itzykson and J. B. Zuber, *'Modular Invariant Partition Functions in Two-Dimensions'*, Nucl. Phys. B **280** (1987) 445.

[16] A. Cappelli, C. Itzykson and J. B. Zuber, *'The ADE Classification of Minimal and A1(1) Conformal Invariant Theories'*, Commun. Math. Phys. **113** (1987) 1.

[17] A. Kato, *'Classification of Modular Invariant Partition Functions in Two-Dimensions'*, Mod. Phys. Lett. A **2** (1987) 585.

[18] E. P. Verlinde, *'Fusion Rules And Modular Transformations In 2d Conformal Field Theory'*, Nucl. Phys. B **300** (1988) 360.

[19] G. W. Moore and N. Seiberg, *'Polynomial Equations for Rational Conformal Field Theories'*, Phys. Lett. B **212** (1988) 451.

[20] R. Dijkgraaf and E. P. Verlinde, *'Modular Invariance And The Fusion Algebra'*, Nucl. Phys. Proc. Suppl. **5B** (1988) 87.

[21] A. B. Zamolodchikov, *'Integrable field theory from conformal field theory'*, Adv. Stud. Pure Math. **19** (1989) 641.

[22] A. B. Zamolodchikov and A. B. Zamolodchikov, *'Factorized S-matrices in two dimensions as the exact solutions of certain relativistic quantum field models'*, Annals Phys. **120** (1979) 253.

[23] P. Dorey, *'Exact S matrices'*, in the proceedings of the 1996 Eötvös Graduate School [arXiv:hep-th/9810026].

[24] S. J. Parke, *'Absence of Particle Production and Factorization of the S Matrix in (1+1)-Dimensional Models'*, Nucl. Phys. B **174** (1980) 166.

[25] S. R. Coleman and J. Mandula, *'All Possible Symmetries of the S Matrix'*, Phys. Rev. **159** (1967) 1251.

[26] S. R. Coleman and H. J. Thun, *'On The Prosaic Origin Of The Double Poles In The Sine-Gordon S Matrix'*, Commun. Math. Phys. **61** (1978) 31.

[27] P. A. Mattsson, *'Integrable quantum field theories, in the bulk and with a boundary'*, arXiv:hep-th/0111261.

[28] A.B. Zamolodchikov, *'Integrals of motion and S matrix of the (scaled) T = T(C) Ising model with magnetic field'*, Int. J. Mod. Phys. A **4**, 4235 (1989).

[29] A. B. Zamolodchikov, *'Irreversibility of the Flux of the Renormalization Group in a 2D Field Theory'*, JETP Lett. **43** (1986) 730 [Pisma Zh. Eksp. Teor. Fiz. **43** (1986) 565].

[30] Al.B. Zamolodchikov, *'Thermodynamic Bethe ansatz in relativistic models. Scaling three state Potts and Lee-Yang models'*, Nucl. Phys. B **342**, 695 (1990).

[31] N. Goldenfeld, *'Lectures on phase transitions and the renormalization group'*, Addison-Wesley, Advanced Book Program, 1992.

[32] T.R. Klassen and E. Melzer, *'Purely elastic scattering theories and their ultraviolet limits'*, Nucl. Phys. B **338** (1990) 485.

[33] T. R. Klassen and E. Melzer, *'The Thermodynamics of purely elastic scattering theories and conformal perturbation theory'*, Nucl. Phys. B **350** (1991) 635.

[34] Al.B. Zamolodchikov, *'On the thermodynamic Bethe ansatz equations for reflectionless ADE scattering theories'*, Phys. Lett. B **253** (1991) 391.

[35] F. Gliozzi and R. Tateo, *'Thermodynamic Bethe ansatz and threefold triangulations'*, Int. J. Mod. Phys. A **11** (1996) 4051 [arXiv:hep-th/9505102].

[36] E. Frenkel and A. Szenes, *'Thermodynamics bethe ansatz and dilogarithm identities. 1'*, arXiv:hep-th/9506215.

[37] R. Caracciolo, F. Gliozzi and R. Tateo, *'A topological invariant of RG flows in 2D integrable quantum field theories'*, Int. J. Mod. Phys. B **13** (1999) 2927 [arXiv:hep-th/9902094].

[38] S. Fomin and A. Zelevinsky, *'Y-systems and generalized associahedra'*, arXiv:hep-th/0111053.

[39] A. Y. Volkov, *'On Zamolodchikov's periodicity conjecture for Y-systems'*, arXiv:hep-th/0606094.

[40] A.Szenes, *'Periodicity of Y-systems and flat connections'*, math.RT/0606337.

[41] A. B. Zamolodchikov, *'From tricritical Ising to critical Ising by thermodynamic Bethe ansatz'*, Nucl. Phys. B **358** (1991) 524.

[42] A. B. Zamolodchikov, *'Thermodynamic Bethe ansatz for RSOS scattering theories'*, Nucl. Phys. B **358** (1991) 497.

[43] A. B. Zamolodchikov, *'TBA equations for integrable perturbed SU(2)-k x SU(2)-l / SU(2)-k+ l coset models'*, Nucl. Phys. B **366** (1991) 122.

[44] A. B. Zamolodchikov, *'Resonance factorized scattering and roaming trajectories'*, J. Phys. A **39** (2006) 12847. Preprint ENS-LPS-335, 1991

[45] P. Dorey and F. Ravanini, *'Staircase models from affine Toda field theory'*, Int. J. Mod. Phys. A **8** (1993) 873 [arXiv:hep-th/9206052].

[46] M. J. Martins, *'Exact resonance A-D-E S matrices and their renormalization group trajectories'*, Nucl. Phys. B **394** (1993) 339 [arXiv:hep-th/9208011].

[47] M. J. Martins, *'Renormalization group trajectories from resonance factorized S matrices'*, Phys. Rev. Lett. **69** (1992) 2461 [arXiv:hep-th/9205024].

[48] P. Dorey and R. Tateo, *'Anharmonic oscillators, the thermodynamic Bethe ansatz, and nonlinear integral equations'*, J. Phys. A **32** (1999) L419 [arXiv:hep-th/9812211].

[49] V.V. Bazhanov, S.L. Lukyanov and A.B. Zamolodchikov, *'Integrable structure of conformal field theory, quantum KdV theory and thermodynamic Bethe ansatz'*, Commun. Math. Phys. **177**, (1996) 381 [arXiv:hep-th/9412229].

[50] P. Dorey, C. Dunning and R. Tateo, *'The ODE/IM Correspondence'*, J. Phys. A **40** (2007) R205 [arXiv:hep-th/0703066].

[51] E. H. Lieb, *'Exact solution of the problem of the entropy of two-dimensional ice'*, Phys. Rev. Lett. **18** (1967) 692;
- *'Residual entropy of square ice'*, Phys. Rev. **162** (1967) 162;
- *'Exact solution of the F model of an antiferroelectric'*, Phys. Rev. Lett. **18** (1967) 1046;
- *'Exact solution of the two-dimensional Slater KDP model of a ferroelectric'*, Phys. Rev. Lett. **19** (1967) 108.

[52] B. Sutherland, *'Exact solution of a two-dimensional model for hydrogen-bonded crystals'*, Phys. Rev. Lett. **19** (1967) 103.

[53] R. J. Baxter, *'Exactly solved models in statistical mechanics'*, (Academic Press 1982)

[54] A. Klümper, M. T. Batchelor and P. A. Pearce, *'Central charges of the 6- and 19-vertex models with twisted boundary conditions'*, J. Phys. A **24** (1991) 13.

[55] F. C. Alcaraz, M. N. Barber and M. T. Batchelor, *'Conformal invariance, the $XXZ$ chain and the operator content of two-dimensional critical systems'*, Annals Phys. **182** (1988) 280.

[56] C. Korff, *'Auxiliary matrices for the six-vertex model and the algebraic Bethe ansatz'*, J. Phys. A **37** (2004) 7227 [arXiv:math-ph/0404028].

[57] R. J. Baxter, *'Eight-Vertex Model in Lattice Statistics'*, Phys. Rev. Lett. **26** (1971) 832.

[58] R. J. Baxter, *'Partition function of the eight-vertex lattice model'*, Annals Phys. **70** (1972) 193 [Annals Phys. **281** (2000) 187].

[59] V. V. Bazhanov, S. L. Lukyanov and A. B. Zamolodchikov, *'Integrable Structure of Conformal Field Theory II. Q-operator and DDV equation'*, Commun. Math. Phys. **190** (1997) 247 [arXiv:hep-th/9604044].

[60] V. V. Bazhanov, S. L. Lukyanov and A. B. Zamolodchikov, *'Integrable structure of conformal field theory. III: The Yang-Baxter relation'*, Commun. Math. Phys. **200** (1999) 297 [arXiv:hep-th/9805008].

[61] Y. Sibuya, *'Global theory of a second-order linear ordinary differential equation with polynomial coefficient'*, (Amsterdam: North-Holland 1975).

[62] C. M. Bender and A. Turbiner, *'Analytic Continuation Of Eigenvalue Problems'*, Phys. Lett. A **173** (1993) 442.

[63] C.M. Bender and S. Boettcher, *'Real spectra in non-hermitian Hamiltonians having $\mathcal{PT}$ symmetry'*, Phys. Rev. Lett. 80 (1998) 4243, `physics/9712001`

[64] V. V. Bazhanov, S. L. Lukyanov and A. B. Zamolodchikov, *'Spectral determinants for Schrödinger equation and Q-operators of conformal field theory'*, J. Statist. Phys. **102** (2001) 567 [arXiv:hep-th/9812247].

[65] P. Dorey and R. Tateo, *'On the relation between Stokes multipliers and the T-Q systems of conformal field theory'*, Nucl. Phys. B563 (1999) 573, [arXiv:hep-th/9906219].

[66] P. Dorey, C. Dunning and R. Tateo, *'Spectral equivalences, Bethe Ansatz equations, and reality properties in $\mathcal{PT}$-symmetric quantum mechanics'*, J. Phys. A34 (2001) 5679, `hep-th/0103051`

[67] J.L. Cardy, *'Conformal invariance and surface critical behavior'*, Nucl. Phys. B **240** (1984) 514.

[68] J.L. Cardy, *'Boundary conditions, fusion rules and the Verlinde formula'*, Nucl. Phys. B **324** (1989) 581.

[69] J. L. Cardy, *'Effect Of Boundary Conditions On The Operator Content Of Two-Dimensional Conformally Invariant Theories'*, Nucl. Phys. B **275** (1986) 200.

[70] J. L. Cardy, *'Boundary conformal field theory'*, arXiv:hep-th/0411189.

[71] D. Friedan and A. Konechny, *'On the boundary entropy of one-dimensional quantum systems at low temperature'*, Phys. Rev. Lett. **93** (2004) 030402 [arXiv:hep-th/0312197].

[72] S. Ghoshal and A.B. Zamolodchikov, *'Boundary S matrix and boundary state in two-dimensional integrable quantum field theory'*, Int. J. Mod. Phys. A **9** (1994) 3841 [Erratum-ibid. A **9** (1994) 4353] [arXiv:hep-th/9306002].

[73] A. Fring and R. Koberle, *'Factorized scattering in the presence of reflecting boundaries'*, Nucl. Phys. B **421** (1994) 159 [arXiv:hep-th/9304141].

[74] P. Dorey, R. Tateo and G. Watts, *'Generalisations of the Coleman-Thun mechanism and boundary reflection factors'*, Phys. Lett. B **448** (1999) 249 [arXiv:hep-th/9810098].

[75] R. Sasaki, *'Reflection bootstrap equations for Toda field theory'*, in the proceedings of the conference, Interface between physics and mathematics, eds. W. Nahm and J.-M. Shen [arXiv:hep-th/9311027].

[76] A. LeClair, G. Mussardo, H. Saleur and S. Skorik, *'Boundary energy and boundary states in integrable quantum field theories'*, Nucl. Phys. B **453** (1995) 581 [arXiv:hep-th/9503227].

[77] P. Fendley and H. Saleur, *'Deriving Boundary S Matrices'*, Nucl. Phys. B **428** (1994) 681 [arXiv:hep-th/9402045].

[78] P. Dorey, A. Pocklington, R. Tateo and G.M.T. Watts, *'TBA and TCSA with boundaries and excited states'*, Nucl. Phys. B **525** (1998) 641 [arXiv:hep-th/9712197].

[79] P. Dorey, I. Runkel, R. Tateo and G.M.T. Watts, *'g-function flow in perturbed boundary conformal field theories'*, Nucl. Phys. B **578** (2000) 85 [arXiv:hep-th/9909216].

[80] J.L. Cardy and G. Mussardo, *'S matrix of the Yang-Lee edge singularity in two-dimensions'*, Phys. Lett. B **225** (1989) 275.

[81] P. Dorey and R. Tateo, *'Excited states by analytic continuation of TBA equations'*, Nucl. Phys. B **482** (1996) 639 [arXiv:hep-th/9607167].

[82] F. Woynarovich, *'O(1) contribution of saddle point fluctuations to the free energy of Bethe Ansatz systems'*, Nucl. Phys. B **700** (2004) 331 [arXiv:cond-mat/0402129].

[83] H.W. Braden, E. Corrigan, P. Dorey and R. Sasaki, *'Affine Toda field theory and exact S matrices'*, Nucl. Phys. B **338** (1990) 689.

[84] V.A. Fateev and A.B. Zamolodchikov, *'Conformal field theory and purely elastic S matrices'*, Int. J. Mod. Phys. A **5**, 1025 (1990).

[85] P. Dorey, *'Root systems and purely elastic S matrices'*, Nucl. Phys. B **358** (1991) 654.

[86] P. Dorey, *'Root systems and purely elastic S matrices. 2'*, Nucl. Phys. B **374** (1992) 741 [arXiv:hep-th/9110058].

[87] A. Fring and D.I. Olive, *'The fusing rule and the scattering matrix of affine Toda theory'*, Nucl. Phys. B **379** (1992) 429.

[88] F. Ravanini, R. Tateo and A. Valleriani, *'Dynkin TBAs'*, Int. J. Mod. Phys. A **8** (1993) 1707 [arXiv:hep-th/9207040].

[89] F.A. Smirnov, *'The perturbated $c < 1$ conformal field theories as reductions of sine-Gordon model'*, Int. J. Mod. Phys. A **4** (1989) 4213.

[90] P.G.O. Freund, T.R. Klassen and E. Melzer, *'S matrices for perturbations of certain conformal field theories'*, Phys. Lett. B **229**, 243 (1989).

[91] P. Dorey and R. Tateo, *'Excited states in some simple perturbed conformal field theories'*, Nucl. Phys. B **515** (1998) 575 [arXiv:hep-th/9706140].

[92] P. Goddard and D. I. Olive, *'Kac-Moody And Virasoro Algebras In Relation To Quantum Physics'*, Int. J. Mod. Phys. A **1** (1986) 303. (Also in Goddard,

P. (ed.), Olive, D. (ed.): Kac-Moody and Virasoro algebras, World Scientific Publishing Co. 1988)

[93] V.G. Kac, *'Infinite dimensional Lie algebras'*, Cambridge University Press, 1990.

[94] E. Witten, *'Nonabelian bosonization in two dimensions'*, Commun. Math. Phys. **92** (1984) 455. (Also in Goddard, P. (ed.), Olive, D. (ed.): Kac-Moody and Virasoro algebras, World Scientific Publishing Co. 1988)

[95] D. Gepner, *'Field identification in coset conformal field theories'*, Phys. Lett. B **222** (1989) 207.

[96] A.N. Schellekens and S. Yankielowicz, *'Field identification fixed points in the coset construction'*, Nucl. Phys. B **334** (1990) 67.

[97] C.R. Ahn and M.A. Walton, *'Field identifications in coset conformal theories from projection matrices'*, Phys. Rev. D **41** (1990) 2558.

[98] P. Dorey, unpublished.

[99] E. Corrigan, P. Dorey, R.H. Rietdijk and R. Sasaki, *'Affine Toda field theory on a half line'*, Phys. Lett. B **333** (1994) 83 [arXiv:hep-th/9404108].

[100] E. Corrigan, P. Dorey and R.H. Rietdijk, *'Aspects of affine Toda field theory on a half line'*, Prog. Theor. Phys. Suppl. **118** (1995) 143 [arXiv:hep-th/9407148].

[101] V.A. Fateev, *'Normalization factors, reflection amplitudes and integrable systems'*, [arXiv:hep-th/0103014].

[102] C. Zambon, York PhD Thesis 2004, unpublished.

[103] S. Ghoshal, *'Bound state boundary S matrix of the sine-Gordon model'*, Int. J. Mod. Phys. A **9** (1994) 4801 [arXiv:hep-th/9310188].

[104] H.J. de Vega and A. Gonzalez Ruiz, *'Boundary K matrices for the six vertex and the n(2n-1) A(n-1) vertex models'*, J. Phys. A **26** (1993) L519 [arXiv:hep-th/9211114].

[105] F.A. Smirnov, *'Reductions of the sine-Gordon model as a perturbation of minimal models of conformal field theory'*, Nucl. Phys. B **337** (1990) 156.

[106] R. Chatterjee, *'Exact partition function and boundary state of 2-D massive Ising field theory with boundary magnetic field'*, Nucl. Phys. B **468** (1996) 439 [arXiv:hep-th/9509071].

[107] P. Fendley, H. Saleur and N.P. Warner, *'Exact solution of a massless scalar field with a relevant boundary interaction'*, Nucl. Phys. B **430**, (1994) 577 [arXiv:hep-th/9406125].

[108] V.V. Bazhanov, A.N. Hibberd and S.M. Khoroshkin, *'Integrable structure of W(3) conformal field theory, quantum Boussinesq theory and boundary affine Toda theory'*, Nucl. Phys. B **622**, (2002)475 [arXiv:hep-th/0105177].

[109] P. Goddard, A. Kent and D.I. Olive, *'Virasoro algebras and coset space models'*, Phys. Lett. B **152** (1985) 88.

[110] I.B. Frenkel and V.G. Kac, *'Basic representations of affine Lie algebras and dual resonance models'*, Invent. Math. **62** (1980) 23.

[111] V.G. Kac and D.H. Peterson, *'Infinite dimensional Lie algebras, theta functions and modular forms'*, Adv. Math. **53** (1984) 125.

[112] D. Bernard, *'String characters from Kac-Moody automorphisms'*, Nucl. Phys. B **288** (1987) 628.

[113] I. Affleck, M. Oshikawa and H. Saleur, *'Boundary critical phenomena in the three-state Potts model'*, [arXiv:cond-mat/9804117].

[114] L. Chim, *'Boundary S-matrix for the tricritical Ising model'*, Int. J. Mod. Phys. A **11** (1996) 4491 [arXiv:hep-th/9510008].

[115] J. Fuchs, *'Simple WZW currents'*, Commun. Math. Phys. **136** (1991) 345.

[116] T. Gannon, *'Algorithms for affine Kac-Moody algebras'*, [arXiv:hep-th/0106123].

[117] B. Schellekens, *http://www.nikhef.nl/~t58/kac.html.*

[118] H. Saleur and M. Bauer, *'On some relations between local height probabilities and conformal invariance'*, Nucl. Phys. B **320** (1989) 591.

[119] V.A. Fateev, *'The exact relations between the coupling constants and the masses of particles for the integrable perturbed conformal field theories'*, Phys. Lett. B **324** (1994) 45.

[120] S. Fredenhagen, *'Organizing boundary RG flows'*, Nucl. Phys. B **660** (2003) 436 [arXiv:hep-th/0301229].

[121] I. Affleck, *'Edge critical behaviour of the 2-dimensional tri-critical Ising model'*, J. Phys. A **33** (2000) 6473 [arXiv:cond-mat/0005286].

[122] K. Graham, *'On perturbations of unitary minimal models by boundary condition changing operators'*, JHEP **0203**, 028 (2002) [arXiv:hep-th/0111205].

[123] C. M. Bender, S. Boettcher and P. Meisinger, *'PT-Symmetric Quantum Mechanics'*, J. Math. Phys. **40** (1999) 2201 [arXiv:quant-ph/9809072].

[124] P. Dorey, C. Dunning and R. Tateo, *'Supersymmetry and the spontaneous breakdown of PT symmetry'*, J. Phys. A **34** (2001) L391 [arXiv:hep-th/0104119].

[125] R.E. Langer, *'On the connection formulas and the solutions of the wave equation'*, Phys. Rev. 51 (1937) 669.

[126] M. Abramowitz M. and I.A. Stegun eds, *'Handbook of Mathematical Functions'*, (National Bureau of Standards 1964)

[127] T. Kato, *Perturbation theory of linear operators* (Springer, Berlin, 1966).

[128] W.D. Heiss, *'Exceptional points of non-Hermitian operators'*, [arXiv:quant-ph/0304152].

[129] A. V. Sokolov, A. A. Andrianov and F. Cannata, *'Non-Hermitian Quantum Mechanics of Non-diagonalizable Hamiltonians: puzzles with self-orthogonal states'*, [arXiv:quant-ph/0602207].

[130] U. Guenther, I. Rotter and B.F. Samsonov, *'Projective Hilbert space structures at exceptional points'*, arXiv:0704.1291v3 [math-ph].

[131] A.V. Turbiner, *'Quasiexactly Solvable Problems and SL(2) Group'*, Commun. Math. Phys. **118** (1988) 467.

[132] C. M. Bender and G. V. Dunne, *'Quasi-Exactly Solvable Systems and Orthogonal Polynomials'*, J. Math. Phys. **37** (1996) 6 [arXiv:hep-th/9511138].

[133] M. Sorrell, *'Complex WKB analysis of a PT symmetric eigenvalue problem'*, arXiv:math-ph/0703030.

[134] H. Whitney, *'On singularities of mappings of Euclidean spaces. I. Mappings of the plane into the plane'*, Ann. Math. **62** (1955) 374

[135] M. Znojil, *'$\mathcal{PT}$-symmetric harmonic oscillators'*, Phys. Lett. A259 (1999) 220, [arXiv:quant-ph/9905020].

[136] P. Dorey, A. Millican-Slater and R. Tateo, *'Beyond the WKB approximation in PT-symmetric quantum mechanics'*, J. Phys. A **38**, 1305 (2005) [arXiv:hep-th/0410013].

[137] A. Millican-Slater *'Aspects of PT-Symmetric Quantum Mechanics'*, Ph.D. Thesis 2004.

[138] F. Lesage, H. Saleur and P. Simonetti, *'Boundary flows in minimal models'*, Phys. Lett. B **427** (1998) 85 [arXiv:hep-th/9802061].